STRUCTURAL AND METAMORPHIC EVOLUTION OF AN AREA AROUND KAKAMAS AND KEIMOES, CAPE PROVINCE, SOUTH AFRICA

by

JOHANNES MARINUS VAN BEVER DONKER

Thesis submitted in fulfillment of the requirements for the degree of Doctor of Philosophy in the Faculty of Science at the University of Cape Town

February 1979

ABSTRACT

The area investigated is underlain by metasedimentary rocks, deposited onto a granitic basement and intruded by granitic rocks. Situated in the northwestern Cape Province, it comprises some 1800 km^2 along the Orange River, west of Upington.

Several shear zones divide the area into a number of blocks; from west to east these are the Kakamas Shear Zone, the Duivelsnek Shear Zone, the Neusspruit Lineament, the Brakfontein Shear Zone and the Cnydas Shear Zone.

Three folding phases were recognised, the first of which (D_{n+1}) resulted in the formation of the main penetrative foliation and isoclinal folds. Some large D_{n+1} structures are described. The main deformational event was the second phase of folding, characterised by strong flattening in the vicinity of the major shear zones. Axial planes of this generation of structures generally dip to the northeast. The dip varies between 30° and 50° and increases to about 60° in the vicinity of the Cnydas Shear Zone. Foliations deformed by this event have been processed with the aid of a packet of computer programmes called Vecstaplot, in order to construct a fabric shape ellipsoid. These ellipsoids appear to become more prolate near the shear zones, representing S-tectonites.

The final folding phase was prominent in the part west of the Neusspruit lineament, where major interference patterns between the D_{n+2} and the northeast-trending D_{n+3} folds were formed. No significant D_{n+3} folds have been observed to the east of the lineament. The main metamorphism M_1 reached high-medium to high grade conditions and is shown to coincide with D_{n+2}, possibly even persisting from D_{n+1} onwards. A second metamorphic event M_2 is characterised by contact metamorphic assemblages as a result of the emplacement of hyperstene bearing granitoids. These intrusions undoubtedly postdate D_{n+2}, but appear to have suffered from some shearing.

Vertical displacement along the two main shear zones (Neusspruit Lineament and Cnydas Shear Zone) was between 5 and 10 km, where the former is thought to have accommodated considerably more displacement than the latter.

Horizontal displacement between the Cnydas and Brakfontein Shear Zones amounted to some 16 km sinistral. No evidence is available for horizontal movement along the Neusspruit Lineament. Dextral movement, amounting to some 2 km (post D_{n+3}) took place between the Kakamas and Duivelsnek Shear Zones.

A dynamic model consisting of a combination of block faulting and wrench-fault tectonics explains the kinematics of the structures mentioned above.

TABLE OF CONTENTS

List of Tables

List of Figures

List of Plates

1. INTRODUCTION

The area described in this report is situated along the Orange River in the northern part of the Cape Province, South Africa. It comprises about 1800 km^2 and stretches from south-west of Kakamas (29°00'S, 20°30'E) to Upington in the north-east (28°30'S, 21°15'E). (Figs. 1.1 and 1.2).

1.1 Previous work

The earliest publication concerning the geology of this area dates from 1949 when Poldervaart and Von Backström published their "Study of an area at Kakamas" (Poldervaart and Von Backström, 1949), followed by a report on the "charnockitic adamellite porphyry", of the area between the Neusberg range and Keimoes (Von Backström and Poldervaart, 1953). Three additional, specialised papers concerning the "charnockitic adamellite porphyry" have also appeared in print: one describing deuteric alteration on Tweelingkop (Von Backström, 1965) and another completed by Von Backström after the untimely end of Poldervaart (Poldervaart, 1966). In the third paper the results of a petrographical and geochemical investigation into the origin and mode of emplacement of these rocks are presented (R. Schultz, in press). This study was undertaken while the investigations for the present report were being conducted.

A tungsten-tin deposit on the farm Dyasons Klip in the north-eastern part of the area is described by Von Backström in 1950. In his study of the pegmatite belt Hugo (1969) describes most of the important pegmatites in the western part of the area.

Several other reports have been published on the geology of the surrounding areas. Von Backström (1966) describes the geology and mineral deposits of the Riemvasmaak area, situated along the Orange River west of Kakamas, following an earlier account of the geology along the lower part of the Molopo River (Von Backström, 1962). Geringer (1973) reports on the geology of "an area west of Upington", followed by a publication by Geringer and Botha (1977) dealing with the structural geology of the same area. Botha *et al.*, (1976, 1977) published two reports concerning the geology of an area east and south of the study strip (Fig. 1.2). An important publication dealing with the geology east of the area under consideration is a description by Vajner (1974) of the geology of the Marydale-Buchuberg area in which he redefines the formations of the Kheis Group. Cornell (1975) gave an account of the Marydale metabasites.

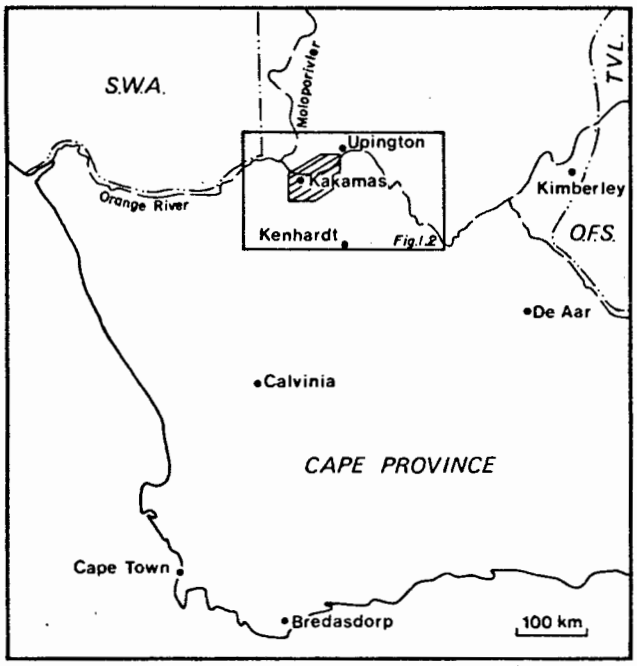

Fig. 1.1 Locality Map

Fig. 1.2 Areas covered by various investigations

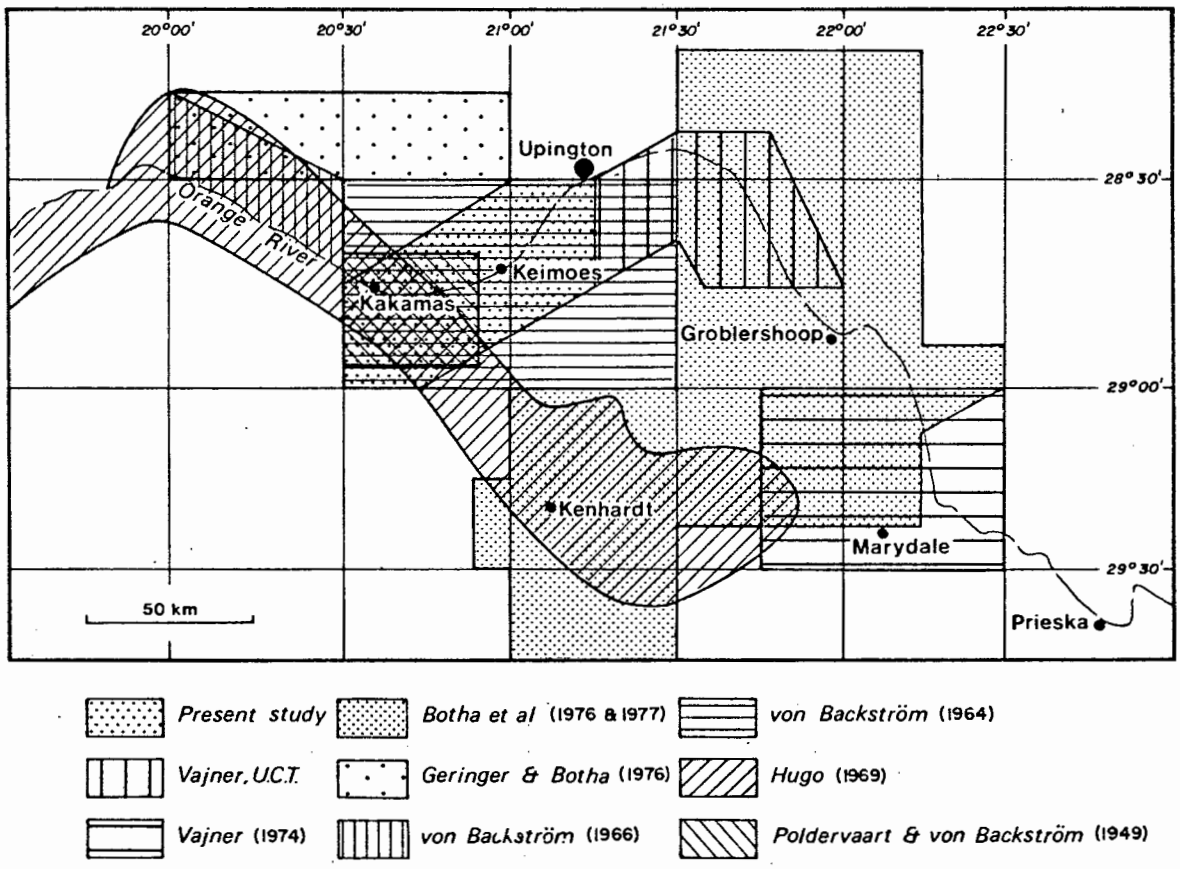

The area under consideration (Fig. 1.2) covers a strip across the existing official geological map (Keimoes-Louisvale; 2820D and 2821C) and that of the earlier publication by Poldervaart and Von Backström (Fig. 1.2). The adjacent strip to the east of the area is presently also under investigation as part of the National Geodynamics Project.

1.2 Purpose of this study

In 1974 the National Geodynamics Project (NGP) commenced under the auspices of S.A.C.U.G.S. (South African National Committee for the International Union of Geological Sciences) and the Upington Geotraverse (U.G.T.) as part of this project was allocated to the Precambrian Research Unit with Dr. Vajner as supervisor. The aims were to contribute to the understanding of processes taking place along the juncture of the Craton (Kaapvaal Craton) and Mobile Belt (Namaqualand Metamorphic Complex, N.M.C.) and to establish the character and locality of this boundary in the U.G.T. Vajner and Jackson (1974) suggested that the juncture might run along the Neusberg and put forward the name Neusspruit Lineament for this boundary.

The U.G.T. was divided into two parts: the eastern portion to be investigated by Dr. Vajner, the western part by the present writer.

1.3 Methods employed

To solve the problems mentioned above, detailed structural-metamorphic investigation was required. A pilot study proved the existing geological map to be reliable, later also confirmed by the results of remapping by a geologist from the Geological Survey, so that it became possible to concentrate on the area on both sides of the Neusberg where the chances were highest of finding sufficient information to solve the problems (Fig. 1.3). This area was mapped in detail (scale 1:25000) whereas the remainder of the strip was covered in a conventional reconnaissance-style 1:50000 scale mapping. In both cases extensive use was made of aerial photographs, both on a scale of 1:65000 and 1:25000, where available.

The laboratory work was carried out along conventional lines. Statistical analyses were conducted with the aid of a packet of computer programmes developed by Hartnady (1978). Transmission Electron Microscopy was performed with the object of obtaining an insight into the mechanical processes active during the last deformational event. The Electron Microprobe was used to a limited extent in the metamorphic analysis.

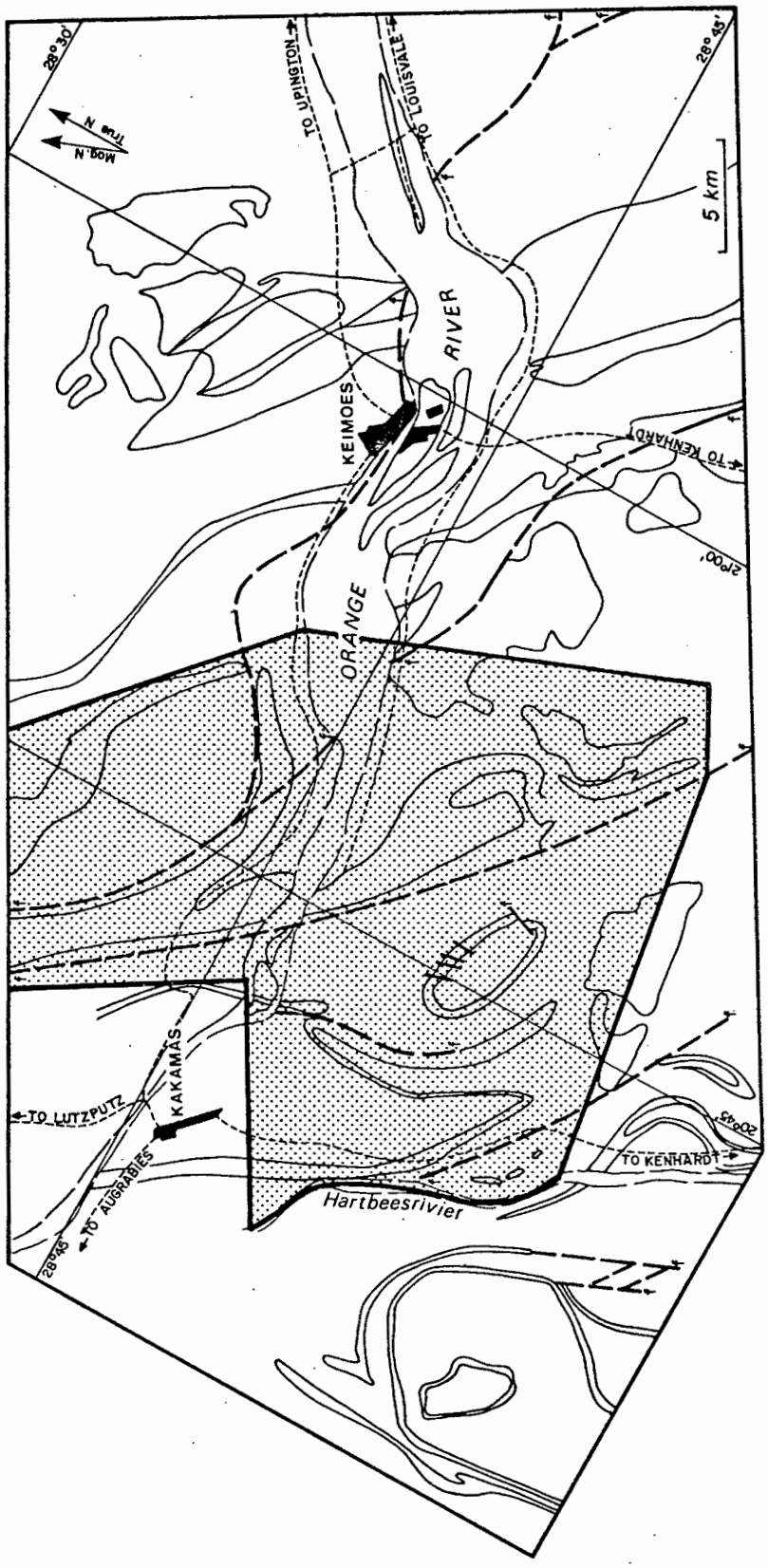

Fig. 1.3 Shaded area mapped at 1:25000

1.4 Acknowledgements

I would like to express my gratitude to Dr. A. Kröner, who arranged the project and who, together with the late Dr. Vajner, undertook the initial supervision. Thanks are due to their inspiration during the first period of the study. In 1976 Prof. P. Joubert took over supervision and I am indebted to him for his continuous interest and challenging criticism in all stages of the project. Thanks are also due to him for obtaining financial support during the final months of the project. I would like to thank Professors A. O. Fuller and A. M. Reid for providing research facilities in the Department of Geology and Prof. A. M. Reid and Dr. D. L. Reid for their assistance with the geochemical problems and analyses. Special thanks go to Dr. A. R. Newton, who spent considerable time discussing diverse problems and who read the first draft of the report. The discussions with other staff members of the department are gratefully acknowledged.

It is with pleasure that I acknowledge the financial support of the C.S.I.R. who funded the project. The many discussions in the field with several members of S.A.C.U.G.S. contributed greatly to the results obtained.

I owe thanks to representatives of the various mining houses that supported the project in many ways, both material and scientific. The project greatly benefited from many discussions with geologists of the Upington Branch of the Geological Survey and the various mining houses.

The many discussions and comments from the other members of the P.R.U. have been invaluable. A special word of thanks goes to Miss P. Eloff who drafted the maps and diagrams and to Mrs. J. Elliott who did the final typing of the manuscript. Mr B. Lawrence assisted in many ways.

Thanks are due to some of the members of the Bernard Price Institute of the University of the Witwatersrand and especially Mrs. E. Barton and Prof. L. O. Nicolaysen for providing the age dating for this study.

The Electron Microscopy work would have been impossible without the facilities of the Department of Materials Science, kindly made available by Prof. A. Ball, whose help and interest in the project are gratefully acknowledged.

Dr. D. Crawford, Director of the Electron Microscope Unit, spent many hours instructing and assisting me on the Electron Microscope, which proved to be invaluable.

The cooperation of the municipalities of Kakamas and Keimoes, in providing camping facilities and help in many other ways is gratefully acknowledged. This study would have been impossible without the cooperation of the many farmers in the area, who allowed me on their grounds and a special

word of thanks goes to Mr. and Mrs. Davies of "Dyasons Klip" and Mr. and Mrs. Kok of "Geluk" for providing camping facilities.

Finally I would like to thank my wife Fieke for her support and patience throughout the study and for typing the initial draft of the manuscript.

2. PETROGRAPHY

2.1 Introduction

In this section the characteristics of the main lithologic units outcropping in the area are described as comprehensively as possible to serve as a basis for the metamorphic analysis. The rocks can be divided into two groups: those where sedimentary features are preserved and those that are completely reworked by metamorphism. The first group has been described along the lines recommended by the I.U.G.S. Subcommission of Stratigraphic Nomenclature (Hedberg, 1970) and the South African Code of Stratigraphic Terminology and Nomenclature (1971). Because of the problems involved in correlating existing Formations to mappable units in metamorphic terrains (Etheridge, 1977; Jackson, 1976), the more strongly reworked rocks are described according to the guidelines for the Stratigraphic Nomenclature of Metamorphic Rocks (Etheridge, *op. cit.)*. This had the additional advantage of not adding to the already existing multitude of official formation names for identical rock types. As a result one formal Formation, according to the stratigraphic code, is proposed and for the metamorphic and intrusive rocks of the area the method, as outlined by Etheridge (*op. cit.)* has been followed. Where correlation is indisputable, existing rock names were used, otherwise the equivalent unit(s) or part of a unit is given.

The rock types described in the following sections may be divided into two groups: those of sedimentary and those of igneous origin. The term igneous, used here in the sense defined by Hyndeman (1972, p.33), includes "all igneous-looking rocks, regardless of their origin. They may have been formed by magmatic, metamorphic or metasomatic crystallization."

In the following sections the rocks of sedimentary origin will be described first, in stratigraphic order from bottom to top.

2.2 Kakamas Suid Leucogneiss (GnK)

Distribution. The Kakamas Suid Leucogneiss has its type locality on the farm Kakamas Suid II, where it forms the core of the dome structure, surrounded by a band of the Venterskop Kinzigite (Section 2.3). In previous publications this unit is referred to as the "Granite-gneiss of the Central Dome" (Poldervaart & Von Backström, 1949; Von Backström, 1964). This rock type has not been observed elsewhere in the area (Fig. 2.1).

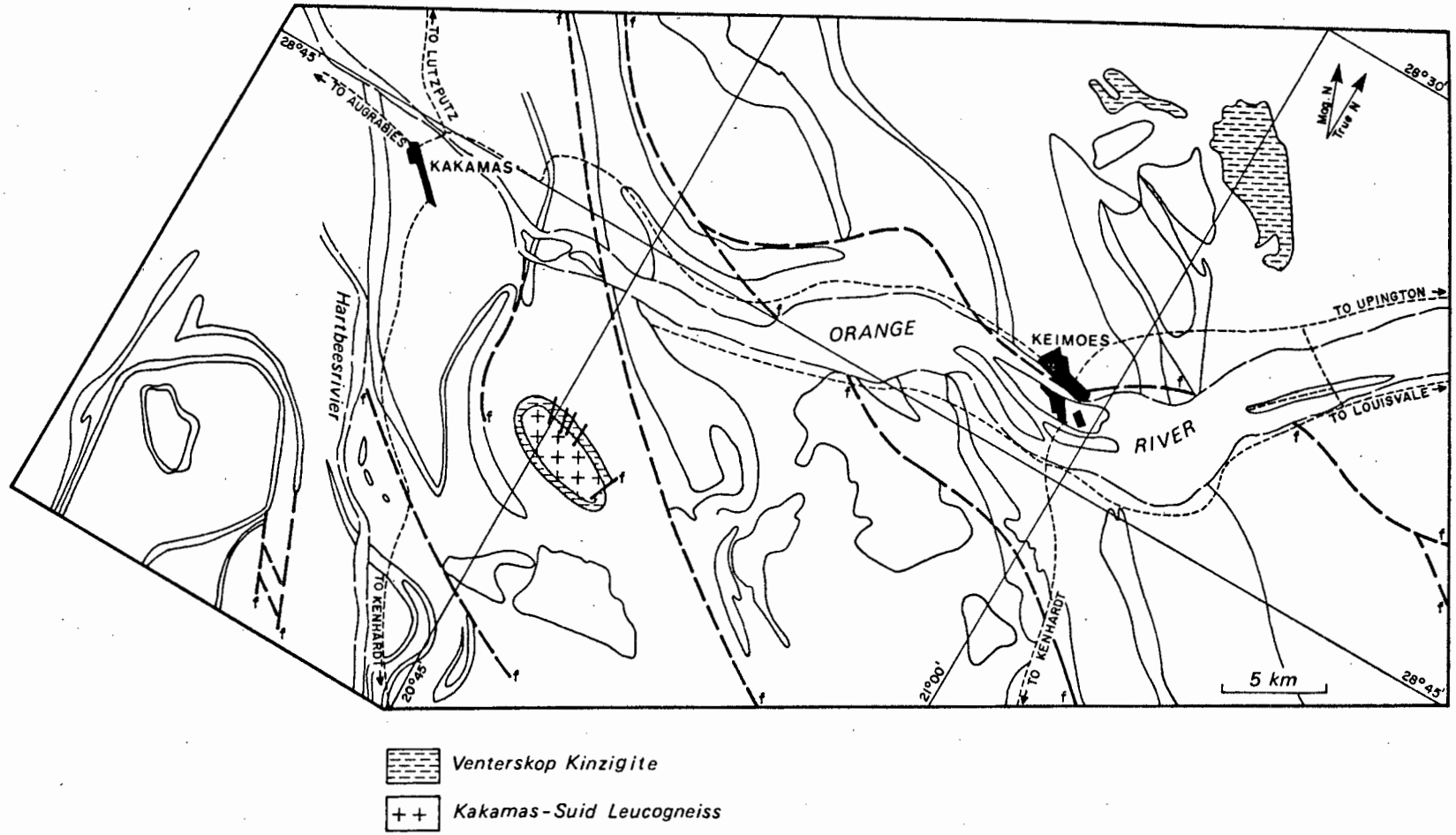

Fig. 2.1 Distribution of Kakamas Suid Leucogneiss and Venterskop Kinzigite

Petrography. In hand specimen it is a leucocratic banded gneiss, with 1-4 mm thick bands formed by alternating quartz-rich and feldspar-rich layers. Concentrations of mafic minerals give the rock a slightly spotted appearance and these gradually become more streaky as zones of more intense deformation are approached. Under the microscope the rock is very much like its appearance in hand specimen in that there is an alternation of quartzitic and feldspathic bands several mm in thickness. Different stages of recrystallization can be observed in the *quartz*: small, strain-free, virtually equant grains contrast with the large blebs of quartz, the latter resulting from an early stage of recrystallisation with numerous equant subgrains. The other bands are composed of *K-feldspar* and *plagioclase*, strongly intergrown and with many exsolution features.

The mafic spots are composed of *biotite* and *amphiboles*, with a preponderance of biotite. It appears that the biotite (reddish-brown) grew around the amphibole (brown) as the latter is surrounded by biotite. The biotite defines a foliation, which in places suggests remnants of an older foliation, as relics of a crenulation cleavage are present. *Chlorite* and *prehnite* grow as secondary products of biotite (Table 2.1).

QUARTZ	FELDSPAR	BIOTITE	PREHNITE	CHLORITE	AMPHIBOLE
40	55-60	5-10	+	± 2	acc

Table 2.1 Estimated modes of Kakamas Suid Leucogneiss

Contact relations. As this rock type constitutes the lowest unit of the range of rocks described in this report and occurs only in one locality, it is only seen in contact with the overlying Venterskop Kinzigite. Where exposed, it can be seen that some movement took place along the otherwise straight contact.

Origin. In the description to the official geological map, Von Backström (1964) refers to this rock as a granite gneiss, representing an "ultrametamorphosed equivalent of a rock, of a composition similar to the Aasvogelkop Granulite" (compare Tables 2.1 and 2.4). Another possibility is that the rock represents metamorphosed basement and originated from a granite or similar acid rock type.

As the present texture is that of a metamorphic rock, it is virtually impossible to identify the origin with certainty, but as this rock is at the base of the succession described here and in some hand specimens does resemble the Nababeep-type gneiss (Benedict *et al.*, 1964; Joubert, 1971) it could very likely be metamorphosed basement.

2.3 Venterskop Kinzigite (GnV)

Distribution. The type locality for the Venterskop Kinzigite is on the farm Kakamas Suid II, where it forms a marked dark ridge around the domal structure east of the Uitspankop. Typical outcrops of the rock can be observed on one of the highest "koppies" of this ridge locally known as "Venterskop". A second typical occurrence is in the north-east of the area on the farms Keimoes, Bloemsmond, Dyasons Klip, Geelkop and Keboes (Appendix A).

In earlier publications the former is referred to as a "dark granulite band in the Central Dome" (Poldervaart & Von Backström, 1949) and the "Sillimanite-garnet Granulite" (Von Backström, 1964). The latter is described as a "Kinzigite" (Von Backström, 1964).

Apart from single small outcrops, all the occurrences of this rock are limited to the farms listed above, with the bulk of the rock outcropping in the north-east of the area (Fig. 2.1).

Petrography. Typically the rock is a black, fine to medium-grained garnet-sillimanite-biotite gneiss. Conspicuous garnets is the common characteristic of the two varieties. At the type locality the rock is strongly foliated and the foliation wraps around the garnets and feldspar porphyroblasts. Some garnets, however, obviously grew after formation of the foliation as they cut across it. In the north-east outcrop however, the foliation is weakly developed. The major minerals of this rock are garnet, cordierite, sillimanite and biotite (Table 2.2).

In both types the *cordierite* is clearly in contact with the garnet, sillimanite and biotite and in the type area, cordierite can be seen to rim the garnets. Alteration of cordierite to pinite is a very common feature (Fig. 2.2). In the north-east, large grains of cordierite contain numerous inclusions of green spinel (hercynite).

Spinel is a rather common mineral in the north-eastern outcrops of the rock, usually as equant, almost euhedral grains, but only occurs sporadically in the type locality.

Sillimanite occurs mainly in needles, usually defining a foliation together with biotite. Less frequently larger, randomly oriented grains are present.

Station number / Minerals	TYPE - LOCALITY						N.E. VARIETY		
	23-A	96-1	96-2A	96-2	127-3	127-5	208	977-6	967
QUARTZ		+			40	15	10	5	19
FELDSPAR	15		20	20	20	20	5	5	15
BIOTITE	13	+	15	15	15-20	15-20	10	10-15	25
SILLIMANITE	14	+	20	15	2-5	20		20	25
GARNET	40	+	30-40	30	10-15	20	2	20	10
SPINEL				2			20	acc	acc
CORDIERITE	5-10	+	2-5	5-10			60	20	20
OPAQUE	10		5	5	2-9	15		10	
CHLORITE								5	

Table 2.2 Estimated modes of Venterskop Kinzigite

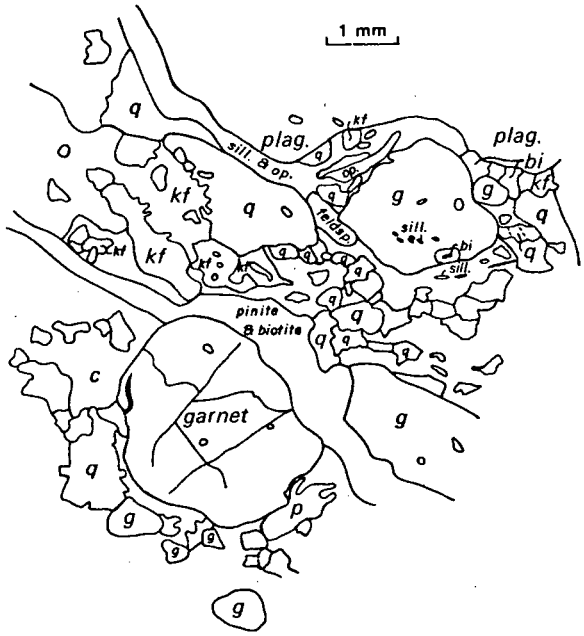

Fig. 2.2

Garnets rimmed by pinitised cordierite.

q = quartz
kf = k-feldspar
g = garnet
c = cordierite
sill = sillimanite
op = opaque
bi = biotite

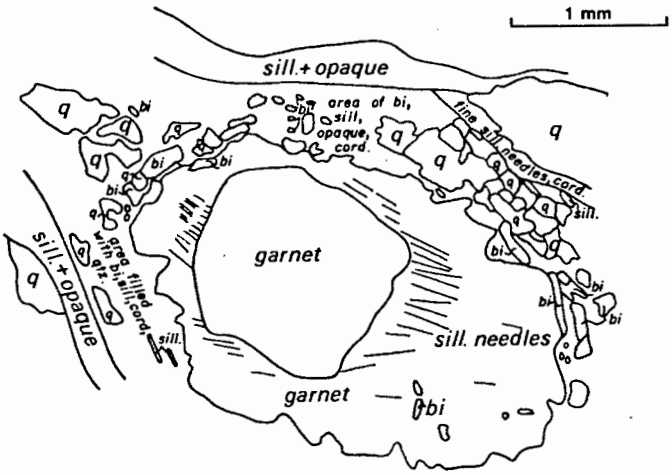

Fig. 2.3 Two generations of garnet, sillimanite needles grown on the first, and subsequently both overgrown by a secondary generation of garnet.
(for key see Fig. 2.2)

In Fig. 2.3 two generations of *garnet* are shown : sillimanite grew around the euhedral crystals of garnet, mainly in patches, presumably in pressure shadows and subsequently this configuration was overgrown by a second generation of garnet. The second growth presumably took place after formation of the foliation, in places generating entirely new garnets overgrowing the foliation and elsewhere expanding the existing garnets at the expense of the surrounding minerals. The garnet is usually colourless to pink.

Biotite in both localities is of the brown to red-brown variety and can be seen to have grown at the expense of garnet in pressure shadows. In combination with sillimanite, it defines the foliation in the type locality where, in some instances, vague relics of a crenulation cleavage have been observed.

Opaque minerals appear in both varieties of the rock. In the north-east they form scattered inclusions in the garnet and are often in contact with sillimanite, whereas in the type locality they are related to the biotite.

Quartz usually shows recrystallization features and in the *feldspars* exsolution lamellae is a common feature. *Plagioclase* falls in the oligoclase-andesine range. Secondary *chlorite* was found in cracks in the garnet.

Contact relations. Contacts between the Venterskop Kinzigite and its underlying and overlying units are sharp and in the case of the type locality, the relations appear to be conformable, though sheared. Of the north-eastern variety only the contact with the overlying rocks is exposed. Most probably this contact is conformable too, but because it has been strongly folded, the exact nature of the contact is difficult to assess.

Origin. The mineral composition of this formation is characteristic for a metapelite, because of its large aluminous-mineral content. A sediment containing clay minerals can be deposited in either a shallow water fluviatile environment or a deep water marine environment. Thus it is impossible to determine the environment in which the original sediment was deposited.

2.4 Kakamas Metamorphic Complex

The Kakamas Metamorphic Complex consists of several gneisses and an amphibolite. The gneisses vary in composition mainly in the amount of biotite and amphibole. Rocks similar to the gneisses belonging to the complex occur throughout Namaqualand and have been given different names by the various authors (Table 2.3). A common factor in the description of all these rocks is the use of the term "pink gneiss", but it is by no means certain that the same rock is referred to in every case.

Table 2.3 Nomenclature of gneisses occurring in Namaqualand and resembling gneisses of the Kakamas Metamorphic Complex.

REFERENCE	NAME
Poldervaart & von Backström (1949)	Pink Gneiss
von Backström (1964)	Aasvogelkop Granulite
	Central Dome granite gneiss
Jansen (1960)	Pink Gneiss and granulite
von Backström (1967)	Pink Gneiss
Kröner (1968, 1971)	Pink Gneiss
Joubert (1971)	Pink Gneiss
Beukes (1973)	Houms-revier Formation
Geringer (1973)	Riemvasmaak Formation
Toogood (1976)	Austerlitz Formation
Botha *et al.* (1976)	Kokerberg Formation
Moore (1977)	Pink Gneiss

The primary mappable units, grouped together in the Kakamas Metamorphic Complex are:-

The Wolfskop Biotite Gneiss, mainly cropping out on the farms Kakamas Suid and Omkyk and constituting the centre of the Warm Zand Structure.

The Maraisrivier Amphibolite, cropping out on the farms Omkyk, Boesmansrivier and Kakamas Suid.

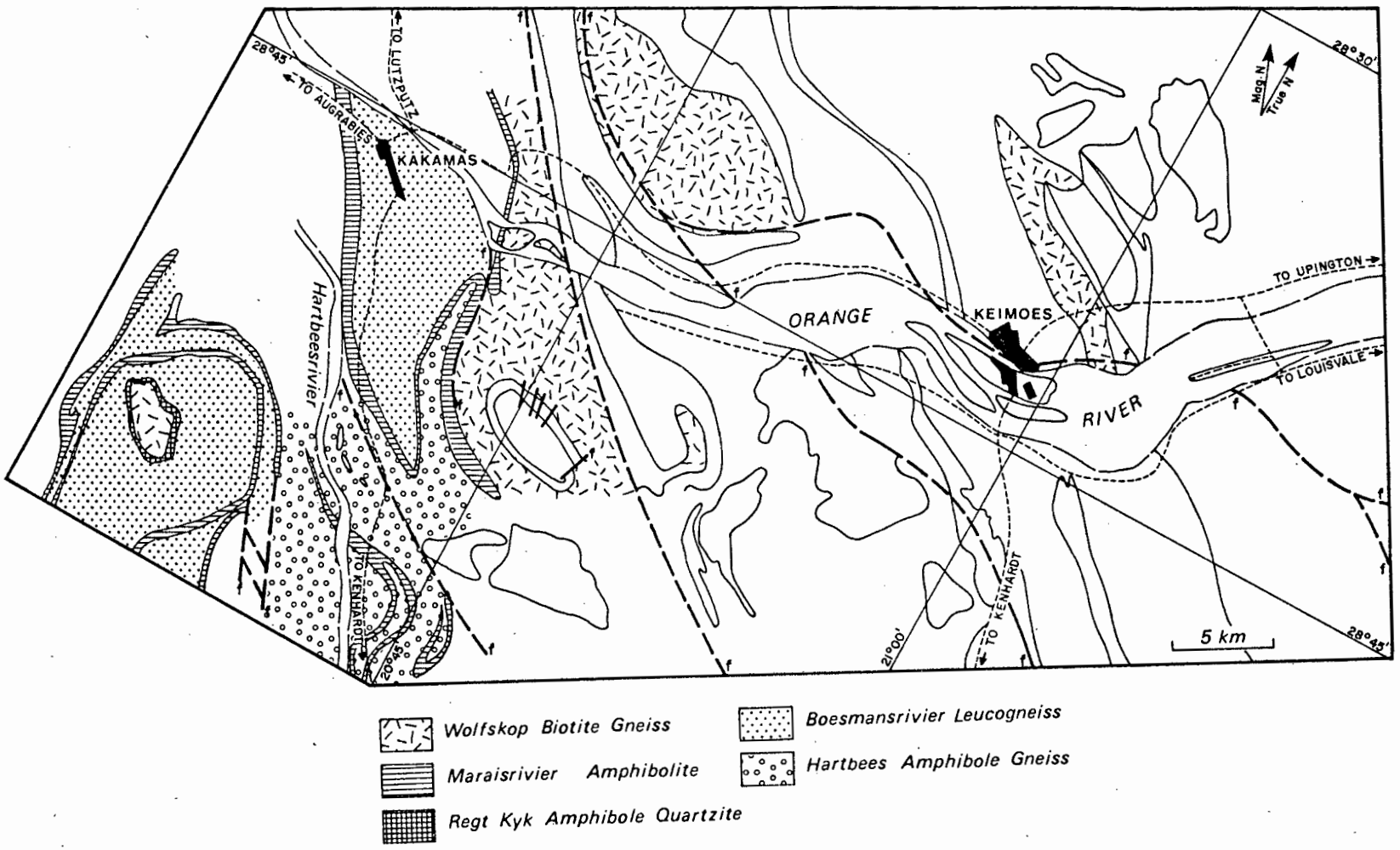

Fig. 2.4. Distribution of rock types constituting the Kakamas Metamorphic Complex.

The Hartbees Porphyroblastic Amphibole Gneiss, cropping out along the Hartbeesrivier on the farms Koegab, Klein Koegab, Middel Post and Nieuwe Post Oos.

The Regt Kyk Banded Amphibole Quartzite, cropping out on the farm Regt Kyk (Fig. 2.4).

2.4.1 Wolfskop Biotite Gneiss (GnW)

Distribution. The Wolfskop Biotite Gneiss may be studied in good outcrops on the farm Kakamas Suid II in the vicinity of a hill, locally known as the "Wolfskop", and in outcrops along the two major tracks leading onto this farm.

On the farm Omkyk many outcrops are available and especially on the northern part of the farm, the variations of this rock type may be observed. It should be mentioned here that on the official geological map of the area, a distinction was made between "Pink Gneiss" and "Aasvogelkop Granulite", here grouped together as the differences between the two rock types have been found to be too subtle to distinguish with certainty at all outcrops. Poldervaart and von Backström (1949) and later also von Backström (1964) point out that in many cases the "Pink Gneiss" and "Aasvogelkop Granulite" can be seen to grade into one another and especially in the northern parts of the area it becomes increasingly difficult to differentiate between them. On the southern boundary of the official geological map of the area however, the rocks are definitely different, but always occur together. The difference in appearance in the field can be ascribed to minor variations in the dark-mineral content resulting in dissimilar aspect on weathering. These small variations in dark mineral content are thought to be the result of slight facies changes and are in the writer's opinion, too small to justify classification into two separate rock types. In Table 2.4 the mineral composition of each type has been added.

Petrography. In hand specimen this unit has the appearance of a fine to medium-grained biotite gneiss, locally developing feldspar augen of about 1 x 4 mm in size and developing into porphyroblastic gneiss in places, the porphyroblasts reaching sizes up to 1 x 1,5 cm. As can be seen in Table 2.4, there is a considerable variation in the amount of quartz and total feldspar, the former ranging from 20 to 50 volume percent and the latter from 80 to 10 volume percent.

Whilst biotite is a normal constituent of the rock, amphibole has been observed only locally, giving the rock a more mafic appearance. Garnet, like amphibole, is only observed locally. The garnets seem to have grown at a late stage in the history of the rock, as no snowball garnets or pressure shadows around them have been observed.

A distinguishing characteristic of this unit in the field is the appearance of amphibolite bands near the overlying calc-silicate rocks. These amphibolites are a few metres thick and some tens of metres long.

It can be seen in Table 2.4 that this rock is leucocratic and judging by the mineral content, the rock is most adequately described as biotite gneiss.

The *biotites* are mainly light brown, sometimes reddish brown and have often broken down into *chlorite* or *prehnite*.

	Q	kf	plg	bi	chl	pr	op	A	car	px	G	Z	ep	msc
265.B	20	70		3			acc	5					S	
269.1	40	50		5-10			2-5	acc						
362	25	40		5			10						S	5
363	40	55		acc				2-5	acc	2				
364	20	60						20S						
365	50			15										
402	30	60		<10	S	S	S							
404A	50	25	5	20								acc		
404H	50	25	5	20								acc		
411A	20	75		5										
411B	20	80		acc										
412	20	60	5	10				5						
413	50	30		15				5-10						
421-1	48	50		2			2-5							
451-1	20	40		15-20				15-10						
451-2/1	30	35		15			2-5	10			5			
451-2/2	35	40		10			5	10			5			
474	30	40		5			5	15-20						
478-1	30	40		5			acc	15			5-10	acc		
478-2	30	45		10			5	10			S			
514	25-30	70			5			5						
Pink Gneiss	X	X	X	acc			acc							acc
Aasvogel-kop gran.	X	X		acc			acc	acc		acc				

Table 2.4 Estimated modes in volume percent of the Wolfskop Biotite Gneiss. Compare the mode for Pink Gneiss (PG) and Aasvogel-kop Granulite (AG).

X = major acc = accessory S = secondary

The *amphiboles*, if present, are usually green and are often replaced by biotite. If sufficient amphibole and biotite are present the rock assumes the appearance of a banded gneiss, the bands defined by an alternation of leucocratic and mafic minerals. Where the gneisses developed feldspar augen, the foliation is usually seen to wrap around them. This has been observed in both the rock with the small augen and those with the large augen, notwithstanding the fact that the bigger porphyroblasts are angular in some cases, suggesting a late growth.

A frequently recurring feature seen in the thin sections is the relationship between *opaque minerals* and biotite, suggesting an iron-rich composition for the biotites (Fig. 2.5).

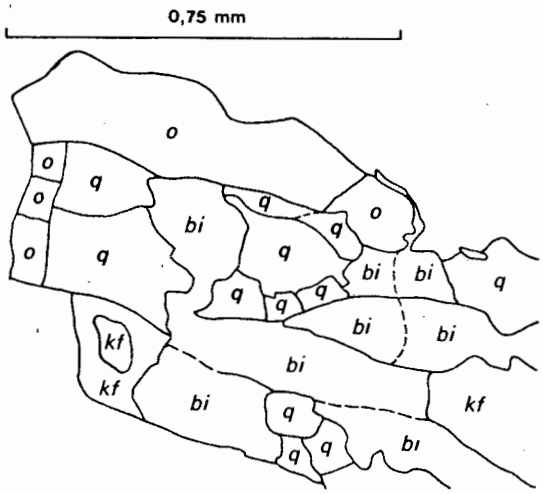

Fig. 2.5 Opaque mineral in contact with biotite.

o = opaque
q = quartz
bi= biotite
kf= k-feldspar

Another characteristic of the opaque minerals is that, like the garnets, they usually occur in the more mafic bands. The *garnets* (up to 5 mm ∅) are usually poikiloblastic and appear to be growing at the expense of the amphibole and biotite.

In virtually all the thin sections *quartz* shows features that suggest recrystallisation, such as lobate grain boundaries and intergrowth of grains. In addition, most of those quartz grains show undulatory extinction, indicating some degree of deformation during or after recrystallisation. (See also the section on electron microscopy, (chapter IV)).

Feldspar is often altered to sericite and perthitic exsolution is a common feature. Plagioclase generally has an extinction angle of +17-18° (⊥a) which places them within the andesine range.

The amphibolites consist of green amphibole, plagioclase and K-feldspar, the two latter minerals considerably altered, most probably

to sericite. The texture is that of an intrusive rock.

Micaceous Quartz-feldspar Schist occurs as in layers in the Wolfskop Biotite Gneiss (Station 92). The rock consists of recrystallised and subsequently deformed quartz (40 percent), microcline (50 percent), flakes of white mica (5 percent) and opaque minerals (3 percent).

2.4.2 The Regt Kyk Banded Amphibole Quartzite (GnR)

Distribution. The Regt Kyk Banded Amphibole Quartzite is a very small unit cropping out on the farm Boesmansrivier, where the type locality is some six km west of the homestead. It was previously referred to as "light weathering quartz-rich granulite" (von Backström, 1964) and has not been observed elsewhere in the area (Fig. 2.4). Stratigraphically it overlies the Wolfskop Biotite Gneiss and underlies the Boesmansrivier Leucogneiss.

Petrography. In the field it is an easily recognisable unit due to its distinct light colour and forms a circular ridge, separating the Boesmansrivier Leucogneiss on the outside from the Wolfskop Biotite Gneiss on the inside.

In hand specimen the rock is made up of thin bands of mafic minerals (5-7 mm thick) separated by quartzo-feldspathic bands of ± 1 cm thick, containing some scattered mafic minerals.

The constituent minerals of this formation are listed in Table 2.5. The *amphibole* crystals are generally small and rounded, forming impure amphibolite bands or they are scattered throughout the rock.

QUARTZ	FELDSPAR	PLAGIOCLASE	MUSCOVITE	AMPHIBOLE	PYROXENE	GARNET	PIEDMONTITE	SPHENE	OPAQUE
20-30	30	20-30	acc	15-20	cpx acc	acc	acc	± 5	2-5

Table 2.5 Estimated modes of Regt Kyk Banded Amphibole Quartzite

Biotite appears in some bent flakes and has a light-brown colour. *Opaque minerals,* which are most probably iron-oxides, are enclosed by biotite. *Chlorite* occurs in small amounts in contact with the biotite.

Another aspect of the opaque minerals mentioned above, is that they are often in contact with *sphene*, and both minerals are often enclosed by amphiboles. The remainder of the sphene crystals (often euhedral) are scattered throughout the rock.

Garnet and *pyroxene* are not to be considered as common constituents of this rock, as only one or two grains of each have been observed.

From the appearance of the *feldspar*, *plagioclase* and *quartz* it is clear that the rock recrystallised to a certain extent, as all these minerals show lobate grain boundaries. Exsolution features in the feldspars are rather common, as well as alteration to sericite, mainly along the grain boundaries.

Contact relations. The contacts are most probably of sedimentary origin, usually rather sharp and may have accommodated some movement, which is indicated by silicification and the appearance of piedmontite. As with epidote, the formation of piedmontite is favoured by shearing stress and low temperature (Deer, Howie and Zussman, 1966; Heinrich, 1965) and hence can be found in shear zones in manganese-bearing rocks. Good examples of its characteristic growth in clusters of needles can be observed in the rocks immediately adjacent to the Duivelsnek Shear Zone (Station 17).

2.4.3 The Boesmansrivier Leucogneiss (GnBL)

The type area for this rock is on the farm Boesmansrivier, where it overlies the Regt Kyk Banded Amphibole Quartzite (Fig. 2.4). The main difference between the Wolfskop Biotite Gneiss and this leucogneiss is that it resembles a coarse sandstone, with remarkably large quartz and feldspar grains and a marked absence of mafic minerals. It has a limited occurrence as it has only been observed on Boesmansrivier between the Maraisrivier Amphibolite and the Regt Kyk Banded Amphibole Quartzite. An unusual feature of the rock seen in thin section is feldspars with altered cores and unaltered rims. The biotites are mainly green-brown, sometimes red-brown.

2.4.4 Maraisrivier Amphibolite (GnM)

Distribution. On the farm Omkyk, to the east of the road between Kakamas and Kenhardt, runs a low ridge, composed mainly of the amphibolite constituting the Maraisrivier Amphibolite. The type locality is situated where the ridge is cut by the Maraisrivier. The rock

is not very widespread and has been observed west of the Neusberg range only, where it served as a useful aid to unravel the structures of this part of the area (Fig. 2.4).

In the two previous publications covering this part of the area, the unit has been described as a "dark-weathering, often garnetiferous quartzo-feldspathic rock" (Poldervaart & von Backström, 1949) and "dark-weathering quartz-rich granulite" (von Backström, 1964). On the farm Regt Kyk/Boesmansrivier, this unit overlies the Boesmansrivier Leucogneiss.

Petrography. The rock is usually a fine-grained amphibolite although some coarse-grained outcrops have been observed (e.g. Station 721). The rock is often foliated, sometimes becoming schistose when contacts are sheared. When both massive and schistose amphibolites occur in one outcrop, the massive one is boudinaged, with individual boundins surrounded by the more biotite-rich schistose variety (Station 589).

The unit varies in thickness from about 30 cm up to several tens of metres and is often in contact with a quartzo-feldspathic rock or a porphyroblastic biotite gneiss. On the farm Omkyk it bounds the zone of intense deformation described in Chapter 3.

The mineral content includes *amphibole*, *quartz*, *feldspar*, *garnet*, *pyroxene* and *biotite*. Feldspar porphyroblasts are a common feature of the rock. They are usually orientated parallel to the foliation, which can often be seen to wrap around them. Garnets occur in about half the number of outcrops, but this cannot be said for pyroxene, as this mineral has been observed in a few outcrops only (e.g. 1606 and 1607). To the south of the type locality, the unit contains a number of carbonate layers associated with magnetite-rich bands, e.g. 200 m north of the Middle Post homestead.

Amphibole is the main mineral of the rock (Table 2.6) and is usually of the bluish-green variety. It can often be seen to break down to *biotite* which rims the amphibole. Other minerals in contact with amphibole are biotite, *tourmaline* and *opaque minerals*. In most thin sections some kind of foliation can be observed, defined by amphibole, opaque minerals and tourmaline.

Minerals of the *feldspar* group are of secondary importance. They are usually strongly altered to sericite and often show exsolution features. Feldspars occur as inclusions in amphiboles and constitute the matrix around the amphiboles, while bigger aggregates are situated in the fabric as small porphyroblasts.

The micas are usually related to one another : *muscovite* and *biotite* often show parallel intergrowth, whilst the latter breaks down to chlorite, occurring as inclusions. Parallel intergrowth between biotite and *prehnite* can be observed as well.

Station number / Minerals	173-2	174-2	174-4	323	416.B	524.B	724	746.2	747.1
QUARTZ	20	25	20	15	5		5-10	2	
FELDSPAR GROUP	60-70	40	60	25	33		70	25	30
BIOTITE	2-5		4			2-5			
PREHNITE		2							- 20
CHLORITE		acc					2		
AMPHIBOLE	10-15	25	5	60	60	50	20	70	50
PYROXENE				acc		5-10			
ZIRCON	acc	acc	acc						
TOURMALINE		acc	5						
CHLORITOID							acc		
EPIDOTE			acc			acc		acc	2
SPHENE	acc	1-2		2					
OPAQUE		10			2-5			2	acc

Table 2.6 Estimated modes of Maraisrivier Amphibolite

2.4.5 Hartbees Porphyroblastic Amphibole-Biotite Gneiss (GnH)

This unit crops out at the farms Omkyk and Middel Post, west of the road between Kakamas and Kenhardt, and differs from the Wolfskop Biotite Gneiss in containing a markedly lower percentage of feldspar, in the absence of biotite and in the presence of pyroxene (Fig. 2.4).

In the field this rock, like the Wolfskop Biotite Gneiss, is a banded gneiss with the distinction that amphibolite bands frequently make their appearance. This feature, together with porphyroblasts becomes the normal appearance further to the south on the farms Middel Post, Nieuwe Post, Koegab and Klein Koegab.

Similar occurrences of an amphibole-biotite gneiss, with intercalated bands of amphibolite have been recorded in the eastern parts of the area on the farms Blauwskop and Vaalputs south of the river, as well as on the northern side of the river, to the east of the "Warm Zand structure".

2.4.6 Contact relations of the Kakamas Metamorphic Complex

Two types of contact relations can be distinguished: contacts between the different rocks of the Kakamas Metamorphic Complex and those between the K.M.C. and the over- and underlying rocks.

Internal contacts between the Regt Kyk Amphibole Quartzite and the Wolfskop Biotite Gneiss and between the Boesmansrivier Leucogneiss and the Regt Kyk Amphibole Quartzite are most probably of sedimentary origin, because neither discordances nor intrusive relations are apparent. Likewise the contacts between the Maraisrivier Amphibolite and the over and underlying rocks are concordant and here too no intrusive features have been observed. It is not correct however, to conclude that it is a sedimentary contact, as geochemistry indicates a strong possibility of this rock being of intrusive origin (see section 2.4.7.). As the rocks passed through several metamorphic and deformational events, the original contacts will most probably have been reworked entirely. Virtually all contacts within the K.M.C. have accommodated some shearing. The contact between this Amphibolite and the Biotite Gneiss at Omkyk is a strongly sheared contact, characterised by silicification and a considerable piedmontite enrichment. Significant vertical movement has taken place at this contact (Chapter 3).

External contacts are of two different kinds. On the farm Kakamas Suid the Wolfskop Biotite Gneiss conformably overlies the Venterskop Kinzigite. The contact is sharp and only slightly sheared. The contact with the overlying Baviaans Krantz Calc-silicate rocks is exposed on Baviaans Krantz and Zwart Boois Berg in the north and on Kakamas Suid in the south. It is a gradual change: bands of amphibolite in the Biotite Gneiss become gradually more abundant when approaching the Calc-silicate Quartzite until Calc-silicate rocks begin to appear and become the major rock type, together with the amphibolite.

2.4.7 Mode of origin of the Kakamas Metamorphic Complex

Previous workers (Poldervaart & von Backström, 1949; von Backström, 1964) concluded that the "Pink Gneiss" is a sedimentary rock, most probably a meta arkose. Botha *et al.* (1976) suggest that acid volcanics as original source for similar rocks is a possibility worth considering. In the area under investigation it is not possible to decide conclusively, without adequate geochemical data. Also the field appearance does not yield any clues. A preliminary study of the trace element content of several amphibolites occurring in the gneisses and in the calc-silicate rocks, revealed a high vanadium and varying Cr and Ni contents, thus suggesting a high volcanogenic component. As this is also indicated by the

texture some of the amphibolites show in thin section (such as pyroxene rimmed by amphibolite, feldspar growth in randomly oriented laths), it is likely that the amphibolites are ortho-amphibolites. However, considerably more geochemical work is required before a definite conclusion can be drawn. In summary, it is not possible to specify the mode of origin of the Kakamas Metamorphic Complex conclusively, but it seems likely that the rocks were originally deposited in a basin, where sediments, interspersed by deposits of volcanic origin, accumulated. These deposits were intruded by basic rocks during a late stage in the pretectonic history.

2.5 The Baviaans Krantz Banded Calc-silicate Quartzite (GnBc)

Distribution. The Baviaans Krantz Banded Calc-silicate Quartzite consists of quartzites with bands of calc-silicate rocks and has two characteristic aspects in the field, the difference being the abundance of amphibolite layers. The type locality of the first variety, with many bands of amphibolites is in the Neusberg, on the farm Zwart Boois Berg, where it underlies the Neusberg Formation and overlies the Wolfskop Biotite Gneiss (Fig.2.6). It can be traced around the southern Neusberg closure onto the farm Koekoeb (where many good outcrops can be found) and subsequently onto the farms Koms and Gif Berg. In previous publications the rocks constituting this unit were called "cafemic rocks" by Poldervaart and von Backström (1949) and the unit as a whole called "Granulite, containing lenses of calc-silicate rocks" by von Backström (1964), who used the calc-silicate rocks as markers to solve the structural geology of the area. On the farms Eksteens Kuil, T'Kabies, Loxton's Vale and Friersdale a pronounced ridge is formed by rocks of this type. Botha *et al.* (1976) describe a similar unit called the N'Rougas Formation. In the Warmbad area of South West Africa, Beukes (1973) grouped the calc-silicate rocks with the Umeis Formation while Geringer (1973), in an area around Lutzputz, named the calc-silicate rocks the Biesiepoort Formation. The type locality of the second type is situated on the southern ridge of the Warm Zand Structure and can be found on the farm Friersdale (Fig.2.6). Only few amphibolite layers are encountered here, hence on the first impression one would map this rock as a separate unit. Its stratigraphic position however, correlates it undoubtedly with the amphibole-richer variety : both are overlain by the feldspathic quartzites. More evidence for correlation is supplied by the petrographical records.

Petrography (Neusberg). The quartzite, rich in calc-silicate minerals, is basically a banded rock, where the individual bands are defined by variations in the content of epidote and amphibole. It is mainly dark weathering and usually has a dense, fine-grained appearance. Although the thickness of the individual bands ranges from about 10 cm to 30 m, thinner bands appear more frequently. Bands of mica-rich quartzite, grading into amphibole-rich quartz-mica schist are sometimes found, as well

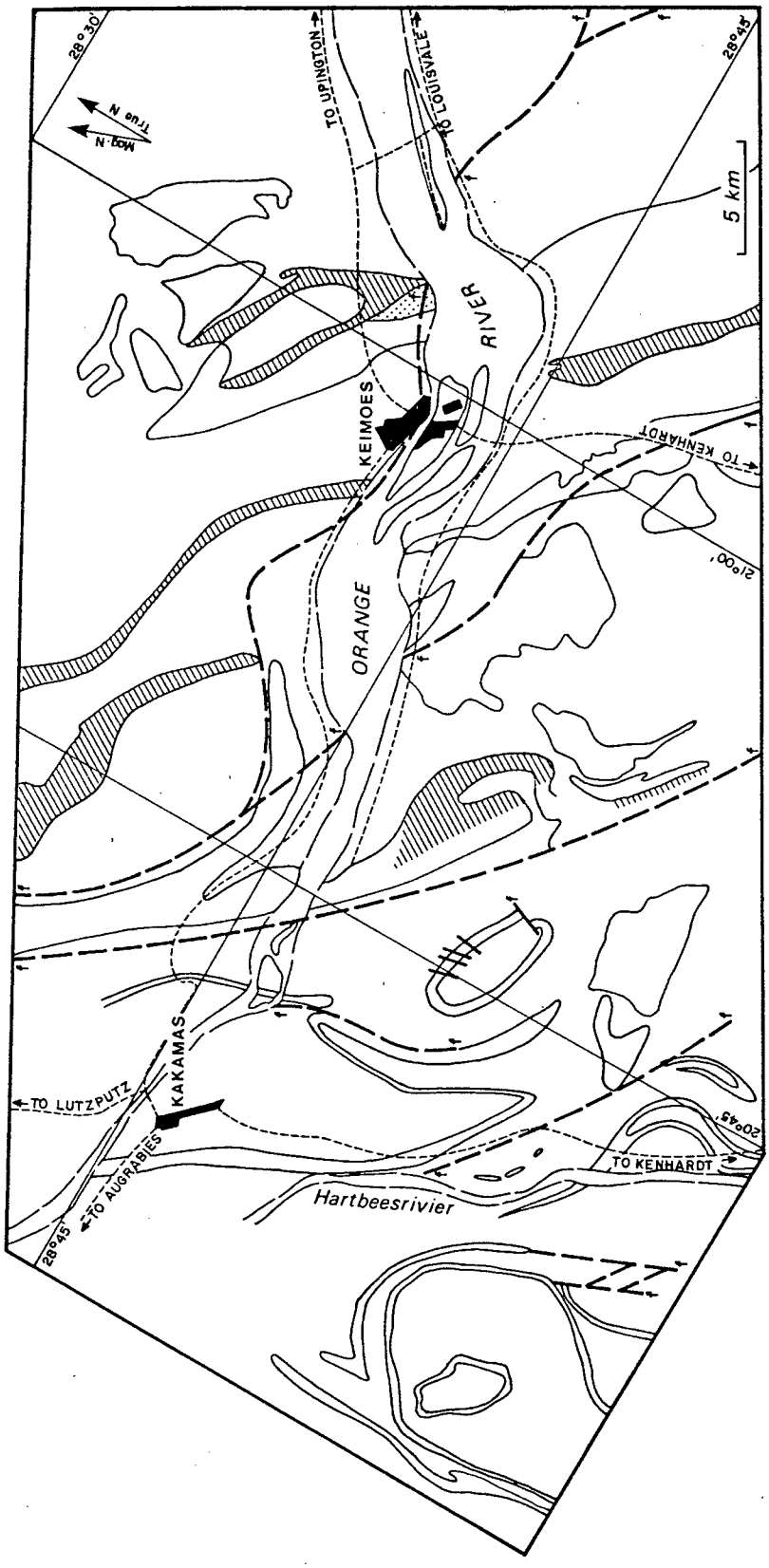

Fig. 2.6 Distribution of Baviaans Krantz Banded Calc-silicate Quartzite and Zoovoorby Staurolite-tourmaline schist.

as mylonitic quartzites containing layers of about 2 mm thick, consisting of amphiboles and biotite. Iron oxides, tourmaline and some malachite occur as accessory minerals.

Sedimentary structures have not been observed in this rock in contrast with the overlying feldspathic quartzites and generally the rock is moderately foliated, sometimes displaying a parting at irregularly spaced intervals, parallel to foliation. Wollastonite appears mainly south of the Orange River at distances of 100-3000 m from the nearest outcropping intrusive rock. The field appearance of the wollastonite bands is very characteristic. Bands varying in thickness from some millimetres to about 4 m invariably contain fold structures of thin layers of the surrounding amphibole-epidote rich rocks, which in places strongly resemble flow structures (Plate 1). Normally the bands of wollastonite are of limited length.

On the southern ridge of the Warm Zand Structure, dark, usually elliptical inclusions, consisting mainly of mafic minerals, characterise the second variety of the Baviaans Krantz Banded Calc-silicate Quartzite, besides the fact that amphibolite layers are considerably less abundant than in the first variety. The rock can vary laterally to a schistose dark quartzite and is in such cases extremely fine grained (e.g. Station 437).

Wollastonite is not as abundant in the Warm Zand area as on Koekoeb. Only one outcrop has been encountered on the farm Warm Zand (Station 483, Appendix A). It consists of several bands of maximum length of some 10 m, where the thickness varies between 40 and 100 cm. Here too, flow structures have been observed.

Petrography

The similarity between the two varieties of this rock unit becomes clear from the petrography when such bands characterising the difference in the field are not taken into account (Table 2.7). The major constituents are *quartz* (30-70%) and *K-feldspar + plagioclase* (up to 90%). *Quartz* is sometimes seen to have a preferred orientation and shows strain features such as undulatory extinction, but almost strain-free grains with triple-point junctions are also present. The latter variety occurs mainly in the surroundings of the intrusive rocks. In several cases growth inhibition of the quartz by micas has been observed.

Microcline and *plagioclase* have often been altered to sericite and in some cases exsolution of the feldspars occurs. Plagioclase has been established to be of the oligoclase/andesine range.

Epidote, with an estimated percentage of up to 30 percent, is the third most abundant mineral after quartz and feldspar. In one thin section it is the major constituent with an estimated volume percentage of 80. In some slides it can be seen to be an original mineral whereas in others it is clearly of a late growth as euhedral grains overgrow the other minerals in the rock (Station 437; Appendix A). Early epidote is rimmed by chlorite

Minerals \ slide numbers	Neusberg and Koekoeb area																								
	179	201	202	290	141	144	144-2	146-1	146-2	143	156	157-1	158-2	159	237	240	241-2	241-3	245-1	245-2	252	255	258-1	258-2
QUARTZ	18	50		40	65	40			47		40	40		60	45	10		30		70			30	
PLAGIOCLASE					215															20				
K-FELDSPAR	80	30	20	40		40		15	47	20	55	30	25	5	45		20	40	70		40	30	60	30
BIOTITE	2		acc	15							2-5		15					25					2-5	
MUSCOVITE															5-10					10				acc
AMPHIBOLE	acc		75			acc		80					60									30		40
TOURMALINE	2-5	2								acc				acc	2-5					1-2				
EPIDOTE		10		2-5	25	20	2-5		2	10				30		80			30	acc	30	10		acc
ZIRCON	acc																			acc				
SPHENE					5	acc	2-5		2					5							5-10	10		5
OPAQUE		5	5	2-5	5-10			5			1-2					8		acc	acc		5-10	20	2-9	20
SILLIMANITE		acc	acc		acc					acc								acc		1-2		2-5		
GARNET							5-10	acc	2								70	acc						
CARBONATE					acc		acc									2					acc	acc		
WOLLASTONITE							80					30												
CLINOPYROXENE							2-5										10							
PREHNITE													acc											
VESUVIANITE										60														

Table 2.7 Estimated modes of Baviaans Krantz banded Calc-silicate Quartzite

	S-ridge Warm Zand Structure															N+E ridge Warm Zand Structure					
slide numbers / Minerals	120-1	120-3	120-4	120-5	120-A	120-C	401-1	437-1	464	483-2	483-3	487-1	496-2	497-2	497	487-1	825	370-2	431	458	830
QUARTZ			10	20	50	60		90		5	30	30	10	35	30	30		10		50	
PLAGIOCLASE										5	5						10	10			
K-FELDSPAR	85	60/70	60	10	45	37	85		90		20	35	50	35	30	35	15		35	40	40
BIOTITE					1-2							10	5	2	20	10		a	20	10	
CHLORITE					1-2				10												
AMPHIBOLE		10	10				10				acc		20				60	50			25
EPIDOTE		5	2-5	acc			5						acc	2							2
ZIRCON					acc						acc										
SPHENE	acc	5			acc		1-2			acc	5		5	2	10			10			
OPAQUE		10											10		10		15		15		15
SILLIMANITE					2-5		acc	acc											25	2-5	
GARNET				70			1-2			50											
CARBONATE				acc						acc				2			acc				
WOLLASTONITE										30	5										
ORTHOPYROXENE												25				25					
CLINOPYROXENE	10	20								10	40							15			20
CORDIERITE																			5		
SCAPOLITE	acc																	5			
ZOISITE	acc																				
PIEDMONTITE								10													

Table 2.7 (continued)

and amphibole and associated with carbonate.

The *mica-group minerals* are next in importance and biotite is the more abundant (up to 25%). Normally the biotite is of the brown variety, but near the adamellite a reddish-brown biotite appears. Quite a normal feature of the rock is the replacement of biotite by chlorite and prehnite, which together with muscovite may reach abundances of up to 10 volume percent. Usually the micas define a foliation, but in some cases they appear to have grown in random orientation.

Spinel is often confined to specific locations, e.g. a boundary between quartz and feldspar.

Garnet, when present, is mainly the pink grossular, in some cases with carbonate inclusions. The garnet is normally poikiloblastic and is usually an accessory mineral apart from two outcrops, where the rocks were found to contain up to 70 percent garnet. Finally sillimanite and tourmaline should be mentioned, as they have been observed as accessory minerals whilst sphene appears more frequently (up to 10%).

The bands of amphibolites have as their major constituent mineral green-brown *amphibole*, varying between 30 and 80 volume percent. Green and brown amphiboles are seen next to each other and where pyroxenes have been encountered (Warm Zand area), amphiboles grew at the expense of the pyroxenes and thus represent metamorphic downgrading. In the Neusberg bottle-green amphiboles can be observed, often with a distinct shape orientation.

The leucocratic minerals form up to 30 volume percent of the rocks, followed by *opaque minerals* (5-20%) and *biotite* (0-15%).

The bands of *wollastonite* obviously consist mainly of wollastonite (up to 80%) followed by garnet (in one case up to 50%) and the leucocratic minerals (5-30%).

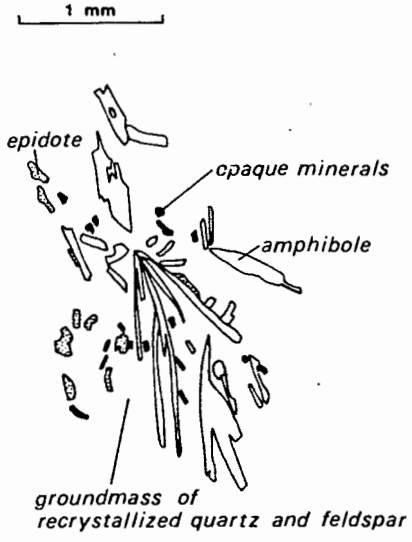

Fig. 2.7. Sheaf-like growth of amphiboles in fine-grained quartzo-feldspathic groundmass.

Contact relations. The contact with the overlying feldspathic quartzites is invariably sharp and has often been sheared due to competence differences. Such shearing appears to be minor, however, and the contact is evidently an original sedimentary one and probably reflects a sudden change of depositional environment - maybe even an unconformity.

Contacts with the underlying rocks may be divided into two types. On the farms Zwart Boois Berg and Baviaans Krantz the boundary with the biotite-gneiss is of a transitional character, in that the gneiss becomes gradually more rich in amphibole, with bands of amphibolite appearing more frequently. Hence, this contact can be considered to represent gradual change of depositional environment. In the other cases intrusive relations prevail at the contacts with the adamellite and the Straussburg granite (Station Nos. 497 and 456 respectively). Xenoliths of the calc-silicate rocks can be observed at Station 456 at the contact with the amphibole-biotite orthogneiss (Plate 2). Most of the contacts with the adamellite, however, appear to have been sheared after the emplacement of the intrusive, developing a foliation which varies in intensity between a fracture cleavage and a schistosity. Fairly often enrichment in epidote has been noted.

A rock type similar in its field appearance to the calc-silicates as outcropping on Baviaans Krantz, appears on Curries Camp and Zoovoorby, in a similar stratigraphic position as in the Neusberg: underlying the Neusberg Formation and overlying Wolfskop Biotite Gneiss. In one feature its appearance is different however from the two varieties described above, in that close to the contact with the feldspathic quartzite an epidote-amphibole quartzite crops out with randomly oriented amphibole needles. The needles vary in size from 1 mm length and 0,05 mm width up to 10 mm length and 2 mm width and invariably they grow in sheaf-like fashion. Other minerals that can be recognised in hand specimen are quartz and epidote.

In thin section the rock is made up of a fine-grained, recrystallised quartzo-feldspathic groundmass and small, late-grown grains of epidote. The amphibole sheafs are made up out of blue-green amphiboles (Fig. 2.7).

2.6 The Zoovoorby Staurolite-tourmaline Schist (GnZ)

Distribution. This unit has previously been described as "Staurolite schist" by von Backström (1964) and has its sole occurrence on the farms Zoovoorby and Curries Camp, south of the main road between Keimoes and Upington, just under 6 km from Keimoes. (Fig. 2.6). At its maximum width it stretches from the railway line for some 1,75 km to the east, while at its maximum length it stretches from about the Trigonometrical Beacon no.10 some 5 km to the southeast where it terminates at a fracture.

Petrography. In hand specimen the Zoovoorby Staurolite-tourmaline Schist is an almost phyllitic, schistose rock, mainly composed of two micas. Staurolite porphyroblasts are most conspicuous and crystals of about 1 x 2 cm are often euhedral, usually showing the monoclinic (or pseudo-orthorhombic) class of the crystals. Garnets appear in some specimens whereas tourmaline occurs in all those collected. All porphyroblastic minerals grew at a late stage of the rocks history, as they overgrow the foliation. However, in some cases rotation of staurolite porphyroblasts and formation of pressure shadows have been observed. These two conflicting observations can be explained by a syn- to post-tectonic growth.

As is shown in Table 2.8 *staurolite* is one of the most important minerals and grows in large, often euhedral crystals. The crystals are always poikiloblastic and remnants of the foliation can be seen in it (Fig. 2.8).

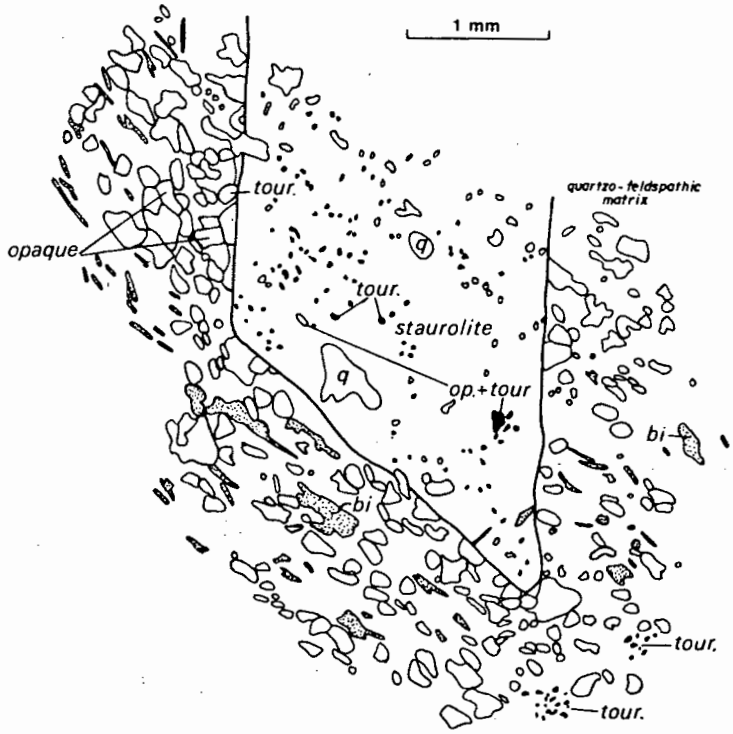

Fig. 2.8 Poikiloblastic, euhedral staurolite crystal in the schist from Zoovoorby.

Staurolite crystals poikiloblastically enclose *opaque minerals, tourmaline, quartz and feldspar.*

The schistosity in all the slides is defined by green-brown *biotite and muscovite*. The minerals often show parallel intergrowth and at some places it can be seen that the schistosity developed from a crenulation cleavage, as remnants of an older foliation are present. Most of the micas are responsible for growth inhibition of the quartz grains. In

QUARTZ	FELDSPAR	BIOTITE	CHLORITE	MUSCOVITE	STAUROLITE	SILLIMANITE	GARNET	TOURMALINE	OPAQUE
10-30	30	15	2-5	30-40	24-40	acc	5	2-5	2-5

Table 2.8 Estimated modes of Zoovoorby Staurolite-Tourmaline Schist

some thin sections biotite breaks down to *chlorite*. The *opaque minerals* also seem to be related to biotite, in that they too grew in contact with it.

Garnet and tourmaline both occur in rather small amounts in the rock and have a late growth in common. Both appear as sub- to euhedral crystals and seem to have opposite relations to the staurolite in that tourmaline is only an accessory mineral when staurolite is present whereas the garnet has been observed to grow in the direct vicinity of staurolite. In the samples where staurolite is not abundant, tourmaline reaches somewhat higher concentrations. In a case like this tourmaline has been seen to grow in trains of small grains along lines at a fairly high angle to the foliation.

Sillimanite is a minor mineral in this unit and has only been observed in one thin section, where it occurs as fibrolite. *Quartz* is a normal constituent of the rock and occurs in equant strain-free grains, often bounded by micas at one or more sides, demonstrating the growth inhibition of the recrystallising grain exercised on it by the existing micas. *Feldspar* is, like quartz, a common mineral in this rock and often appears to be altered, most probably to sericite.

Contact relations. At Station 1202 the Zoovoorby Staurolite-tourmaline Schist and biotite-gneiss are separated by a $\pm$ 1.5 m thick spotted, amphibole-rich rock. The amount of amphibole is variable to such an extent that the rock looks like an amphibolite in places. The contact with the Straussburg granite is not exposed.

2.7 The Neusberg Formation

This formation consists of two characteristic members, both having their type locality in the Neusberg range, which forms a very

prominent ridge in the area. Its western side is marked by the presence of a major shear zone, named the "Neusspruit Lineament" by Vajner and Jackson (1974).

The two members are the Zwart Boois Berg Member and the Neuspoort Member; a feldspathic quartzite and a platy quartz-mica schist respectively.

2.7.1 The Neuspoort Member (NM)

Distribution. The type locality of this platy quartz-mica schist is in the combined railway-roadcutting through the Neusberg on the main road from Kakamas to Keimoes, some 12 km east of Kakamas, recorded as Neuspoort on the topographical map (2820 DA) (Fig. 2.9). The schist constitutes a major part of the tight Neusberg fold (see Section 3.6) and has not been encountered elsewhere in the area.

In previous publications this rock was called quartz-sericite schist (Poldervaart and von Backström, 1949) and mica schist (von Backström, 1964).

Petrography. At the type locality the Neuspoort Member is a platy quartzitic rock with conspicuous flakes of mica on the cleavage planes. Its platy appearance is of tectonic origin as can be seen on the farm Zwart Boois Berg-Annex. Between the ruins of the old homestead "Die Poort" and the main road, the parallel joints in the Zwart Boois Berg Member gradually become more closely spaced until the rock has developed into the platy quartz-mica schist. Minerals visible in hand specimen are quartz, feldspar and micas. In some places remnants of sedimentary structures such as graded bedding, have been seen, but this is not a common feature of the rock and when present, it is usually poorly developed.

Quartz is the major constituent of the rock, reaching up to 80 volume percent. Generally the grains show clear features of recrystallisation such as intergrowth and lobate boundaries. Another indication of the recrystallisation is the frequent appearance of inclusions of small mica flakes in the quartz, and grain boundary growth inhibition caused by micas. In virtually all thin sections shape orientation and undulose extinction can be observed.

Micas are the second important mineral group of the rock, averaging between 10 and 30 volume percent. Mainly white micas have been observed and only in some thin sections do biotite and chlorite occur. Where biotite is present, it often encloses prehnite. Micas invariably cause growth inhibition of quartz grains and have virtually everywhere been seen to be in contact with opaque minerals. Another common characteristic of the

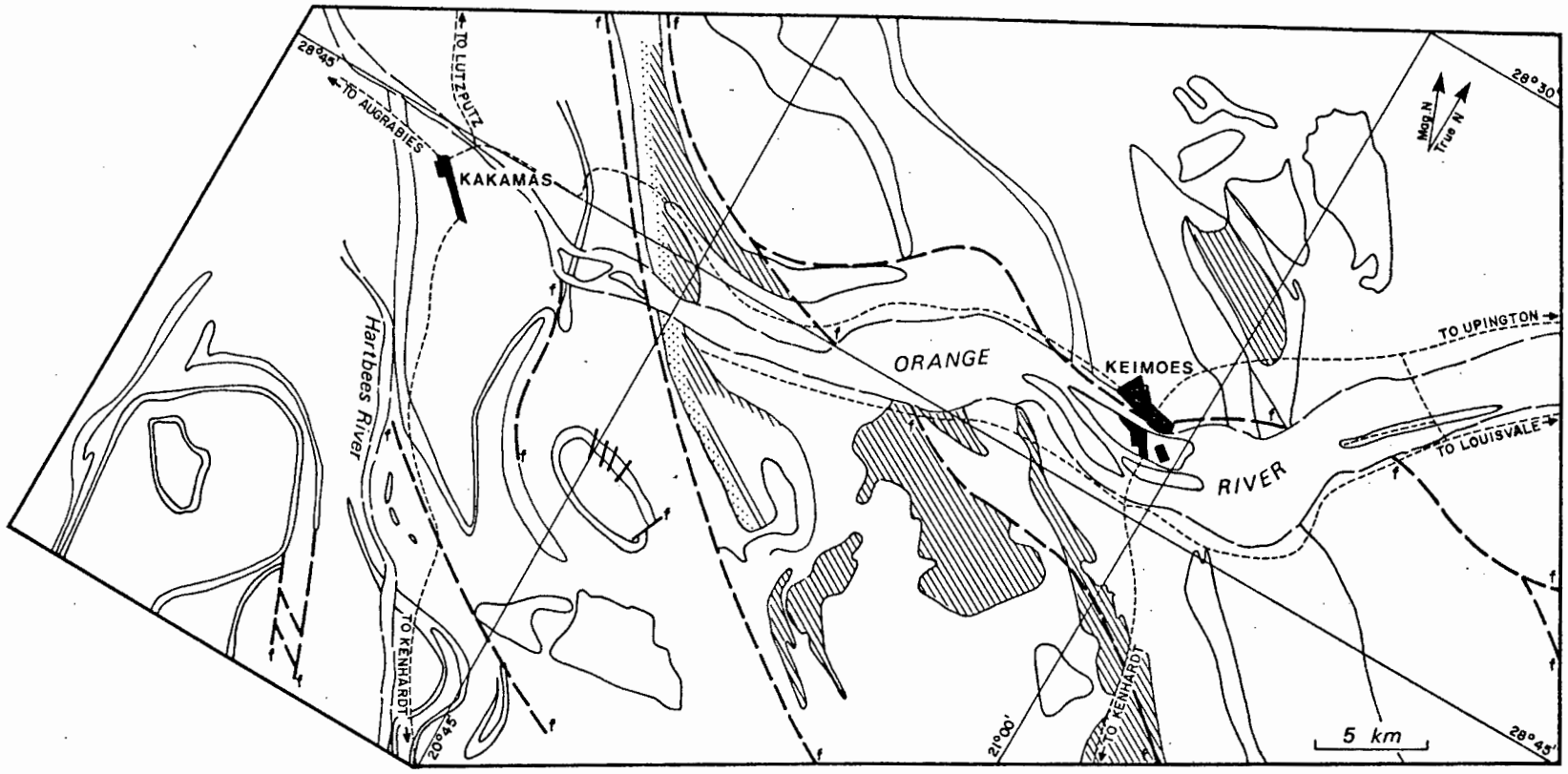

Fig. 2.9 Distribution of Neusberg Formation

mica is that in all slides it defines a foliation. In a few cases bent micas have been observed, but more often they have been broken and subsequently healed.

Feldspar is usually not one of the major constituents and only reaches percentages of up to 15 volume percent, apart from one thin section of a specimen, collected close to the adamellite (Station no. 86), where it is a major component. Usually the feldspars have been altered to sericite and about 50 percent of the feldspars consist of microcline.

The *opaque-mineral* content reaches the 5 percent level in some thin sections, but otherwise can be regarded as an accessory mineral. The minerals *sphene, tourmaline* and *epidote* have only been observed in some thin sections, while some of the rocks are iron stained. (Table 2.9).

Contact relations. Contacts with the overlying quartz-feldspar rocks are, as will be described in the following section, of a gradual character and of a tectonic origin. Contacts with underlying calc-silicate quartzite are usually sharp and also sheared. In the Neusberg, just to the north of the northern closure, the contact with the underlying calc-silicate rocks is marked by extremely mica-rich pegmatite (Station. no. 1802).

2.7.2 The Zwart Boois Berg Member (NZ)

Distribution. The type locality for this feldspathic quartzite is on the farms Zwart Boois Berg and Baviaans Krantz (Appendix A) in the Neusberg range, where the quartzite is found to be overlying a platy quartz-mica schist. Elsewhere a series of rocks, rich in calc-silicate minerals, is found at its base. No rocks have been observed overlying this quartzite. Not only is the type locality situated in the Neusberg range, but the range also forms the western boundary of this rock type (Fig. 2.9).

Other major occurrences are situated on the farms Koekoeb, Koms, Gif Berg and Neilers Drift; on the latter farm the quartzite is found to be intruded by adamellite and amphibole-biotite gneiss. Farther to the east on the farms Curries Camp and Zoovoorby, the feldspathic quartzite constitutes the core of a synformal structure.

In previous publications the feldspathic quartzite and platy quartz-mica schist were named "quartzites and quartz-sericite schists of the Neusberg" by Poldervaart and von Backström (1949) and in his later publication von Backström (1964) labelled these rocks as "quartzite and quartz-sericite schist" (occasionally containing bands of "metamorphosed conglomerate") and "mica-schist" respectively. A similar unit has been described by Geringer (1973) from the Lutzputz area, named the Goede Hoop Formation.

	NEUSPOORT MEMBER							ZWART BOOIS BERG MEMBER										
Slide number / Mineral	86-1	86-2	87A	87B	88	90-2A	214	10-A	10	191-1	288-5	293-3	833-1	856	1000	1016	1500	1512
QUARTZ	60	40	60	65	70	80	70-80	80	99	60	95	95	80	80	50	75	85	85
K-FELDSPAR	20	50	30	15	2-5	2-5	5-10	10		20	acc	2-5	5-10	10	30	20	5	5
BIOTITE		5-10	10	10				2		10						2	2	
CHLORITE	20													acc				
WHITE MICA					20-25	20	20-30		acc		2		10	10			10	5
PLAGIOCLASE			+					7							20			
OPAQUE	2	5-10	acc	acc	2-5	1-2		2	acc	10			1-2			1-2		3-5
SPHENE	acc							acc					acc		acc			
TOURMALINE					acc													
EPIDOTE							acc								acc			
ZIRCON											acc							

Table 2.9 Estimated modes of Neusberg Formation

Petrography. Due to the abundance of quartz in this rock, the resistance to weathering is high so that pronounced ridges and hills formed by this unit, are easily recognisable in the field and on the aerial photographs. The rock weathers to a whitish colour and sometimes has a glitter in hand specimen due to the presence of mica. The minerals recognisable in hand specimen are quartz (rounded, elongate grains up to 1 x 2 mm), feldspar, mica and ocassionally some tourmaline. Epidote occurs in late vein fillings.

One of its most striking characteristics is the presence of primary sedimentary structures such as cross-bedding and layers containing quartz pebbles. The cross-bedding is generally well developed (Plate 3) throughout the unit and could be used as a top-bottom criterion at several places. Judging from the grain size and the dimensions of the cross-beds, these structures may be classified as trough-crossbedded sand deposits (Miall, 1977, p 26) with mutually cross-cutting troughs. The set thickness ranges from 55-180 mm and the width from about 275 to about 1300 mm. The bases of the troughs consist of erosional surfaces and are mainly filled with grains of uniform size, up to 2 mm long and 1 mm wide. The series of sets together reach a considerable thickness up to about 150 m.

Most of the ovoidal-shaped grains appear to have a shape orientation with their longest axes parallel to the strike of the bedding. Assuming the fabric is primary, such an orientation would be typical of beach environments, but in a beach environment, the type of cross-stratification observed here, does not occur (Miall, 1977). It is therefore justifiable to infer that this mineral lineation is of tectonic origin.

The appearance of pebble beds differs from place to place. In some places they form a single string of pebbles, up to one metre in length and with separate quartz pebbles. In other cases the term conglomerate could be applied with pebbles almost touching each other and containing about 10 percent of rounded fragments larger than 2 mm. In the latter case the pebble shapes could be classified as flattened ellipsoids.

Microscopically the bulk of the rock consists of *quartz*. The grain size varies from 0,5 x 0,5 mm up to 5 x 10 mm. Lobate grain boundaries and mutual intergrowth of the grains are common features, as well as the ubiquity of deformation lamellae. Different types of inclusions have been observed : zircons, usually rounded, are common in the rock. Other inclusions are flakes of mica and rounded feldspar grains.

Feldspar amounts to less than five percent of the volume of the rock and includes plagioclase and microcline, usually as equant grains of about 0,25 mm across. Mica is present in amounts of between two and five volume percent with the sizes of flakes up to 0.1 x 0.8 mm. The *mica* flakes do not define a tectonic fabric, but are mostly arranged around the quartz grains. Locally grain boundary inhibition of recrystallised quartz grains is observed, characterised by a straight mica-quartz boundary, whereas the quartz-quartz boundary is lobate. Accessory minerals include *tourmaline, zircon and iron ore* (Table 2.9).

Contact relations. Contacts with the underlying rocks are often sheared. On the farm Friersdale, west of the Trigonometrical Beacon of the same name (Station no. 1788, Appendix A), the concordant contact between the feldspathic quartzite and the underlying calc-silicate rocks is well exposed. Apparently contradicting this observation is the occurrence of abundant small D_{n+1} -type folds in the basal calc-silicate rocks, which are completely lacking in the overlying quartzite, suggesting a discontinuity in the deposition. The following observations exclude this possibility however:

(a) elsewhere in the feldspathic quartzite, a small number of D_{n+1} -type folds in quartz veins have been observed.

(b) a considerable number of planar and linear features measured within 100 m of the contact, and taken in both rock-types, reveals no difference in the orientation of these structures.

It is thought that the lack of D_{n+1} folds in the feldspathic quartzites can be ascribed to the difference in competency of the rock types.

In the Neusberg range, the contact with the platy quartz-mica schist can be seen to be gradational going from east to west and consists of an increase in frequency of parallel joints in the same direction, until a fracture cleavage is developed giving the rock a platy appearance.

On the farm Koekoeb-D (Annex. A) several outcrops have been found (Station no. 327 Appendix A), showing intrusion by the adamellite, with blocks of the feldspathic quartzite enclosed by the intrusive rocks. An apparently concordant contact between these two rock types is located on Koekoeb-A, where up to five percent sillimanite occurs in the quartzite. Under the microscope it can be seen that these late-growing random needles of sillimanite are undeformed.

Environment of Deposition. The grain size of the rock is indicative of a high-energy environment, as fine-grained material is virtually lacking. Such a high-energy environment can be produced by a braided river system where intermittent streamflow occurs. "Where bedload is coarse (coarse sand and gravel) the stream spreads laterally and is typically braided. Hence the resulting sediment is predominantly well sorted and consists of reasonably well-bedded gravel or coarse sand" (Verhoogen *et. al.*, 1970, pp 414-428).

2.8 Intrusive rocks

Several intrusive rock types occur in the area, in some cases intruding into one another. They are

- The Warm Zand Charnockitic Adamellite
- The Straussberg Granite
- The Middel Post mafic rocks
- pegmatites and dolerite dykes

2.8.1 Warm Zand Charnockitic Adamellite (GrA)

Distribution. The type locality for this rock type is situated on one of the subdivisions of the farm Warm Zand, called Geluk. In a quarry north of the national road from Kakamas to Keimoes the rock can be observed in a fresh and undeformed state. The major occurrence of the rock is in the area bounded by the Warm Zand Structure in the north, Neusberg in the west and Koekoeb-Koms in the south. As can be seen in Fig. 2.10, this area forms the largest single body of this rock. Smaller bodies are observed on Kakamas Suid, Neilers Drift, Curries Camp and Blauws Kop. Generally low "koppies" are found with exfoliation, but on Curries Camp and Blauwskop, high hills consisting of charnockitic adamellite only have been encountered. Previously this rock has been described as a charnockitic adamellite porphyry (Poldervaart & von Backström, 1949; von Backström, 1964, 1965; Poldervaart, 1966) and as a charnockitic granolite (Schultz, in press).

Petrography. In the field the rock has a rather characteristic appearance. Granitic weathering in the form of exfoliation of low "koppies" is the normal appearance, but occasionally some larger hills occur. In one case a dyke of adamellite has been mapped on Koms (Station 1502). Minerals seen in hand specimen are opalescent, blue quartz, biotite, pyroxene, amphibole and dark feldspar. The latter gives the rock a a considerably darker appearance than its name would suggest. Late epidote growth and formation of feldspar porphyroblasts are common in the sheared variety of the rock. Inclusions consist of mafic and leucocratic lenses of varying shapes and sizes, and blocks of feldspathic quartzite complete with preserved crossbedding. Intrusive relations have been established between this rock and the Straussburg Granite, each rock intruding the other.

The mineralogy of the rock has been described very extensively in the four different publications that deal mainly with the adamellite (von Backström, 1964, 1965; Poldervaart, 1966; Schultz, in press).

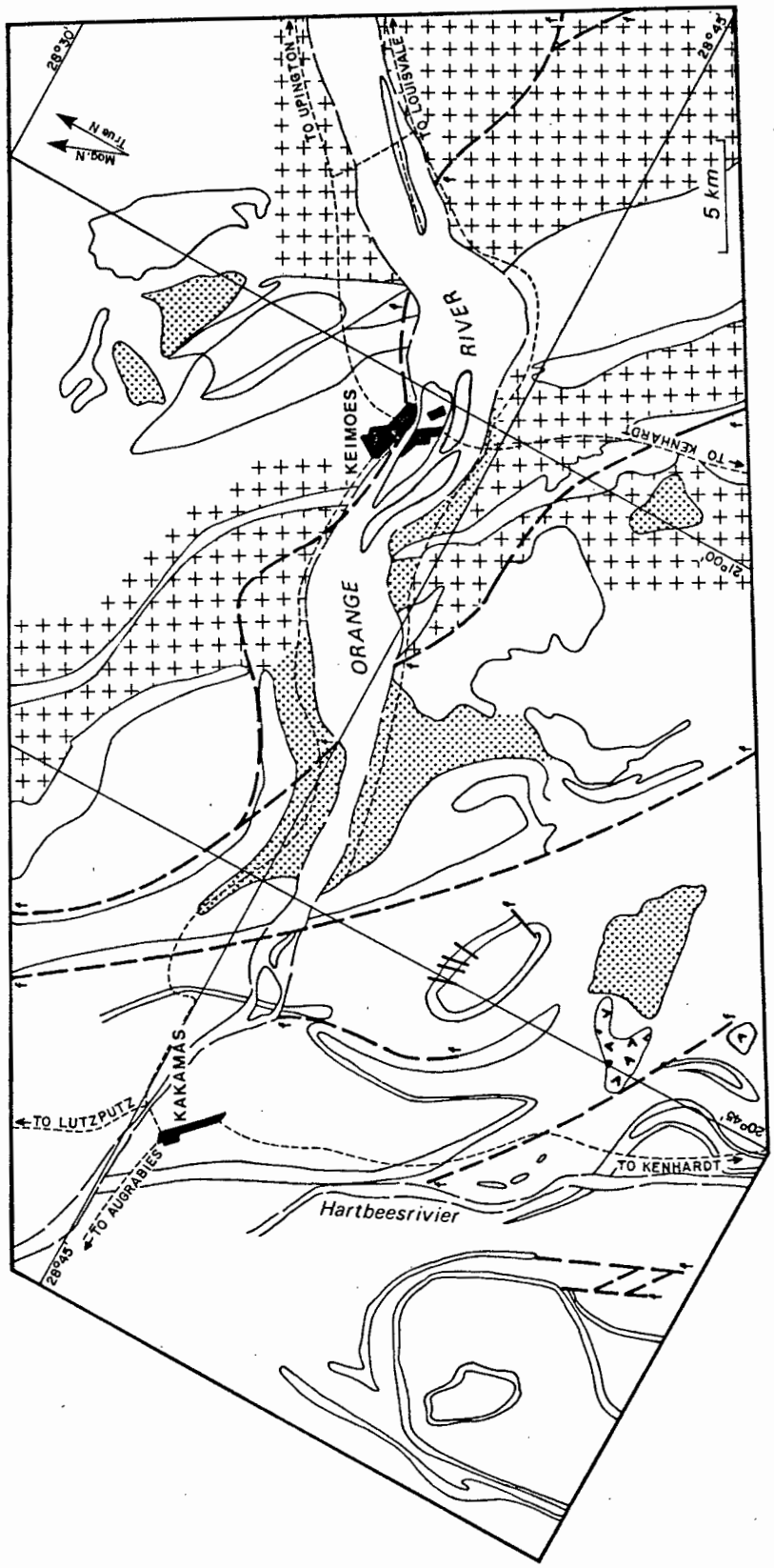

Fig. 2.10 Distribution of Igneous rocks

Mineral	Poldervaart (counted)	Schultz (estimated)	This study (estimated)
qtz	26, 6-29,1	10 - 30	35
plag	26, 4-34,7	20 - 35	20 - 30
K-feldsp	17,3-23,6	17 - 30	
biotite	5, 7-6, 1	4 - 10	5 - 10
opx	0, 1-0, 2	0 - 5	8
cpx	0, 2-3, 6	0 - 8	
amph	5, 0-9, 3	0 - 10	5
sphene	a	a	a
opaque	a	a	a
zircon	a	a	a

Table 2.10 Modes of Warm Zand Charnockitic Adamellite

Some of the major characteristics of the rock's microscopic appearance are the zoned and rounded plagioclase megacrysts, rounded quartz megacrysts and the poikiloblastic hypersthene armoured by amphibole and occasionally clinopyroxene. Amphibole breaks down to biotite, which itself grows as large poikiloblastic brown flakes. Megacrysts are often rounded, but in some cases partly euhedral grains appear. Intergrowth between the groundmass and the megacrysts appears frequently. Biotite (red brown) and opaque minerals are often related, in that biotite rims the opaque crystal, sometimes in radiating aggregates. Where the rock has been sheared a biotite (light brown) foliation is developed, together with alterations of the feldspar, so that the rock has a different appearance from its normal character.

Contact relations. Intrusive relations with the Straussburg Granite are often of a gradual character, resulting in severe difficulties when the exact boundary between the two rocks has to be established, as they can look very much alike. In places the adamellite is clearly different from the Straussburg Granite, however, and it is on such occasions that xenoliths of the one in the other have been encountered (The difference lies mainly in the darker appearance of the adamellite).

Contacts with the country rocks, where exposed, show the intrusive character of the adamellite: xenoliths of feldspathic quartzite and of calc-silicate rocks are encountered frequently. At Station 802 the feldspathic quartzite is altered. The main characteristic is the appearance of clear, recrystallised quartz grains between flattened pebbles, giving the rock almost the appearance of a mortar texture. Contact metamorphic effects have been observed on Koekoeb and Vaal Hoek, where wollastonite formed in the calc-silicate rocks. At several outcrops the contact with the country rock has been sheared, for example at the base of a hill named Vuurkop on the farm Koekoeb, where both adamellite and calc-silicate

developed a schistosity several tens of meters wide, becoming less penetrative away from the contact. Elsewhere minor shear zones appear to form the boundary with the Straussburg Granite.

Origin. Different opinions have been expressed as to the origin and mode of emplacement of the charnockitic adamellite. Von Backström in his major work on the rock type (1964) states "The adamellite magma seems to have evolved through contamination of basaltic magma by siliceous rocks before emplacement at its present level." Further in his text nine points are listed (pp 110,111) to prove that the rock is of magmatic origin, i.e. "a tholeiitic magma situated at depth and partly contaminated by the assimilation of xenoliths of country rock." Schultz (in press) in the final report of his investigation into the origin and mechanism of emplacement of the rock states that the "hypersthene-bearing rock is possibly not of an igneous origin. The scatter of element ratios, the lack of clear trends in variation diagrams, the iron, zirconium and phosphorus enrichment and the very low Mg content point to a sedimentary origin of these rocks of charnockitic affinities. The investigation of element correlations in the igneous and sedimentary environments reveals distinct differences in both and the application of this method has clearly shown correlations not in accord with an igneous derivation neither by way of anataxis and subsequent intrusion nor by differentiation from a parental magma." He concludes then that the adamellite is probably a metamorphosed carbonaceous argillite.

This last conclusion has to be rejected, on basis of field evidence (intrusive relations) and structural grounds (Section 3.6). An explanation remains to be found for the spread shown by the geochemical data. The author is of the opinion that the key is given by Von Backström, when he speaks of contamination by assimilation of xenoliths. When the geological map of the area is studied, it can be seen that the adamellite occupies the space between several major structures that consist of feldspathic quartzite and calc-silicate rocks. Two of these structures (Warm Zand and Koms) are thought to have been connected to one another (Section 3.6). If the whole area between Warm Zand on the one side and Koekoeb and Koms on the other side, originally consisted of feldspathic quartzites and calc-silicate rocks, an appreciable amount of country rock (varying in thickness due to local structural thickening) has been assimilated in the magma, producing its characteristic chemical composition. Such a mechanism also provides a solution for the different rocks exposed on T'Kabies and Tweelingkop, described as special variants of the charnockitic adamellite (Schultz, in press; Von Backstrom, 1965). Assimilation of large amounts of calc-silicate rocks produced the more CaO-rich rocks as described by Schultz (*op.cit.*). This interpretation is supported by the appearance on Tweelingkop of rocks that very much resemble the calc-silicate rocks. The fact that near the top more quartzo-feldspathic rocks occur can be explained by the assimilation of feldspathic quartzite (normally overlying the calc-silicate rocks) and subsequent weathering rather than by deuteric alteration.

2.8.2 The Straussburg Granite (GrS)

Distribution. The Straussburg Granite has its type locality in a quarry near Straussburg some 6 km east of Upington. It has positively been identified on the farm Dyasons Klip and from here further west, as far as Friersdale, gradually changing into the Warm Zand Charnockitic Adamellite. South of the Orange River it has been observed as far west as Gif Berg. This rock does not appear west of the Neusspruit Lineament. In his description of the geology of the area Von Backström (1964) referred to this rock as the Grey Gneiss. Geringer and Botha (1977a) correlate this rock with the Colston Granite.

Petrography. In the field the rock shows a remarkable resemblance to the charnockitic adamellite in that it contains dark and leucocratic inclusions and has a rather dark appearance. The inclusions vary in size from 10x3 cm up to 50x40 cm and are usually oriented parallel to a weak biotite mineral foliation. Other inclusions that have been observed are pieces of adamellite and blocks of the country rocks, for example at Station 1144 (Appendix A). The rock in hand specimen varies from porphyroblastic with porphyroblasts of about 1 cm long to a fine-grained rock. Minerals recognisable in hand specimen are quartz, feldspars and biotite. Epidote and piedmontite have been encountered only where the rock is sheared. On such occasions it closely resembles the Wolfskop Biotite Gneiss. Silicification and epidote and piedmontite enrichment are normal features of the sheared rock.

In the northeastern part of the area a sheared variety of the rock crops out and has been mapped as separate units because of its characteristic appearance and possible tectonic importance (related to Cnydas Shear Zone). Its main characteristics are large porphyroblasts (up to 7 cm long) and a multitude of minor shear zones, recognisable by silicification, porphyroblastesis and migmatisation. This is expressed in the appearance of porphyroblastic gneiss and biotite schist.

Under the microscope the rock appears to be a biotite gneiss (Table 2.11). The *biotite* is only statistically oriented. This is not the case in the mafic inclusions which appear to be made up of 50 percent small oriented biotite flakes. Secondary minerals, grown at the expense of the biotite, are *chlorite* and *prehnite*, the latter always in parallel intergrowth with biotite. The same applies to *allanite* and *pumpellyite*. Unfortunately, pumpellyite and prehnite have never been found together, so that no conclusions with respect to the prehnite-pumpellyite facies of metamorphism can be drawn.

As in the Wolfskop Biotite Gneiss, a relation between the *opaque* minerals and biotite is apparent. One of the characteristics this rock has in common with the adamellite is the appearance of rounded feldspar and quartz megacrysts. The *feldspars* often show perthitic exsolution and an intergrowth with the quartzo-feldspathic groundmass is

not uncommon. A dimensional orientation more or less parallel to the biotite orientation has been observed. Many of the megacrysts have been altered to sericite, where in several cases orientation of the mica needles along the cross-hatched microcline pattern is observed. *Quartz*, like feldspar, is often shape-oriented. In the groundmass, grains show the angular outlines of recrystallisation products, sometimes showing an early stage of recrystallisation by lobate grain boundaries. Undulose extinction is a normal feature of the quartz grains.

	1045	1041	1034	1030	1023	990	989
q	40	30	-	25	40	50	20
felds	40	60	70	60	50	30	40
bi	15	10	-	15	7	15	10
chl	-	-	10	-	-	a	a
prehnite	a	-	a	-	-	a	-
allanite	-	-	-	-	a	a	-
opaque	1	a	a	a	a	5	a
white mica	5	-	5	a	a	a	a
sphene	-	a	5	-	-	a	-
ep	-	-	5	a	-	-	-
tourm	-	-	a	-	-	-	-
pumpellyite	-	-	-	-	a	-	-
apatite	-	-	-	-	-	a	-

Table 2.11 Estimated modes of Straussburg Granite

Origin. Chemical analyses by Von Backström (1964) and more recently by Geringer and Botha (1977a) show a marked resemblance between this rock and the adamellite. The major difference between them is the absence of hypersthene from the Straussburg Granite. It is this difference that suggests a lower pressure-temperature regime or a higher P_{H_2O} for the conditions of formation of the Straussburg Granite. The similar chemistry suggests a similar source of origin of the magma.

2.8.3 Middel Post Mafic Rocks (M)
Dolerite Dykes (D)
Pegmatites

Distribution. *Mafic* rocks have their main occurrence in the western part of the study strip, in the close vicinity of the Kakamas Shear Zone (Fig. 2.10). A V-shaped body on Middel Post is the major outcrop of this rock type. Another large body exists on Koegab, further to the south. On Swartpad a band of mafic intrusives is bounded by amphibole-biotite gneiss. Little plugs of mafic rocks occur frequently on Kakamas Suid along the Hartbeesrivier and in the Maraisrivier Amphibolite, along the Duivelsnek Shear Zone.

Pegmatites, like the mafic rocks, have their main occurrence in the west of the area. Hugo (1969) in his study of the pegmatite belt of the Gordonia and Kenhardt districts mentions the existence of at least 30 beryl-bearing pegmatites on Middel Post alone. Two major pegmatites, both situated in the major mafic body, have been described in detail (Hugo, *op.cit.*). These bodies have been mined to produce beryl.

More to the northeast, on Baviaans Krantz, another major pegmatite is described by Hugo. Not described by him is the zone of extremely mica-rich pegmatites in the Neusberg, separating two calc-silicate layers. Elsewhere in the area occasional pegmatites occur.

Dolerite dykes have been mapped on Dyasons Klip, Bloemsmond and Keimoes, where one long dolerite dyke can be traced for several kilometers.

Petrography. In the field the V-shaped body at Middel Post stands out as an easily recognisable hill, formed by an alteration of noritic rocks, pegmatitic rocks and fine-grained quartzite. As on the smaller body on Koegab, pegmatites occur very frequently. A slight amphibole foliation has been developed in the norite. The smaller plugs are different in that they are not strongly foliated and not intruded by pegmatites. Pyroxenes are usually randomly oriented, except at Station 1631 (Appendix A).

Under the microscope it appears that *amphiboles* are the major constituent (Table 2.12). They are greenish-brown or brown and always rimming the pyroxenes. In a thin section of a dolerite dyke the amphiboles occur as inclusions in the pyroxenes (Station 708). A weak foliation is defined by amphiboles in sample 699 (Appendix A). Green amphiboles have been found rimming opaque minerals.

Clinopyroxene is the second most important mineral reaching up to 50 volume percent (estimated) in some thin sections. Poikiloblastic inclusion of amphibole has been observed.

Feldspars form rounded megacrysts, often altered to sericite. In sample 879 intergrowth at the edges of megacrysts with the fine-grained quartzo-feldspathic groundmass gives the rock an appearance similar to the charnockitic adamellite. *Microcline* (up to 20 volume percent) also alters to sericite and in addition, perthitic exsolution is observed.

Plagioclase reaches up to 40 volume percent of the rock and occurs mainly as randomly oriented laths. Anorthite percentage varies between 30 and 45 percent and hence the plagioclase always falls within the andesine range. The laths are often slightly bent.

Biotite is brown to red-brown and occupies up to 20 volume percent of the rock. Poikiloblastic grains are no exception and generally the mineral is of a secondary origin. Parallel intergrowth with muscovite and chlorite is observed in several thin sections. Clusters approximately 2x2 mm, of opaque minerals rimmed by amphibole and biotite, give the rock a spotted appearance (Station 879).

Accessory minerals are *chlorite, muscovite, orthopyroxene* and *opaque minerals*.

Contact relations with the surrounding rocks are generally not exposed, apart from a single site (Station 740) where a sheared contact, marked by silicification, crops out. In the biotite gneiss in the immediate vicinity of the larger body, garnets developed. The smaller bodies that crop out at places like station 1871 (Appendix A) are in fact boudins.

2.9 Kakamas Oos Porphyroblastic Gneiss (GnO) (Nababeep type)

Distribution. The Kakamas Oos Porphyroblastic Gneiss has a very limited occurrence. Outcrops of the rock occur on Kakamas Oos, Kakamas Noord and Kakamas Suid. The type locality is in a quarry on the farm Kakamas Suid (as this farm name is already used in the name of another rock type it could not be used for this one), just south of Kakamas. The extension north of the Orange River could not be established beyond doubt, because in weathered outcrops, e.g. near the German war graves, Lutzberg, the gneiss strongly resembles a slightly porphyroblastic version of the biotite gneisses of the Kakamas Metamorphic Complex.

Petrography. In fresh specimens the rock is a porphyroblastic amphibole-biotite gneiss. Porphyroblasts usually consist of feldspars with some mafic inclusions and vary in size from 1,5 x 4 cm to 0,5 x 3 cm in more flattened zones. Usually the megacrysts are rounded

and flattened, with the foliation wrapping around them. The major differences as compared with the Hartbees Porphyroblastic Gneiss (section 2.4.5) are the presence of biotite and amphibole and the "old" porphyroblasts, which also distinguish the rock from the porphyroblastic variety of the Wolfskop Biotite Gneiss. Under the microscope quartz and *feldspar* are the major components of the rock; the feldspar includes microcline and plagioclase (together about 60 volume percent). *K-feldspars* exhibit perthitic exsolution and are often altered to sericite. *Quartz* (about 30 volume percent) forms grains as small as 0,25 mm across up to 0,25 x 1 mm (feldspars range up to 1,5 x 4 cm). Equant grains with straight grain boundaries and grains with lobate grain boundaries both occur and both display undulose extinction. A shape orientation of the quartz grains is not uncommon. *Biotite* comprises about 6 volume percent of the rock. It generally defines a foliation which wraps around the porphyroblasts. The biotites are of the brown variety.

Green *amphiboles* make up approximately 4 percent of the rock by volume and are generally poikiloblastic. Most of the amphiboles appear to break down to biotite. *Sphene* is an accessory mineral.

Contact relations. Where exposed, they are of a distinctly tectonic character with silicification and piedmontite enrichment and are mainly exposed near the type locality.

	728	747/1	777	778	672	699	634	Dol. 708	D.A. 879
amph	20	50	20	25	95	30	20	8	a
bi	1-2	20	10	a	-	-	-	-	5
chl	-	a	-	-	2	-	-	-	-
cpx	20	-	40	50	1	30	40	60	a
feldsp	60	30	-	5	a	40	-	-	80%
microcl	20	ne	ne	ne	ne	ne	ne	ne	ne
plag	40	ne	30	20	ne	ne	40	30	10
opaque	-	a	25	-	-	-	a	-	-
opx	-	-	a	-	2	1-2	-	2	-

Dol. = dolerite dyke
D.A. = dyke of adamellite

Table 2.12 Estimated modes of mafic intrusive rocks and dykes. Feldspar is total feldspar, including microcline and plagioclase. ne = not estimated separately.

2.10 Summary

From the previous Sections it follows that the Kakamas Suid Leucogneiss is situated at the base of the sequence and probably represents metamorphosed basement. Conformably overlying this gneiss is the Venterskop Kinzigite, a highly metamorphosed pelite, deposited either in a fluviatile (overbank) or a marine deep-water environment (both low energy environments). Overlying the kinzigites is the Kakamas Metamorphic Complex which is shown to have been a series of sedimentary rocks containing ortho-amphibolites with a high volcanogenic component. The internal stratigraphy of the complex is not clear as large sections are separated and relatively displaced by the Duivelsnek and Kakamas Shear Zones. Towards the end of the deposition of the sediments, the environment of deposition changed towards a more calcareous type of environment, as at the top of the sequence a gradual change to the Baviaans Krantz Calc-silicate-rich quartzite is recorded.

The sedimentary cycle was completed with the deposition of the Neusberg Formation, probably in a braided river system as shown by grain size and crossbeds. The sudden termination of this unit against the Neusspruit Lineament suggests deposition in a fracture-bound basin.

After the sedimentation ceased, folding occurred and following the main folding phases (section 3) the Warm Zand Charnockitic Adamellite and the Straussburg Granite were emplaced. They probably originated from similar magmas, with the major difference being the depth of penetration of the shear zones along which these rocks migrated upwards: the adamellite is thought to have originated at greater depth than the Straussburg Granite, which is expressed in the presence of hypersthene in the former. Noritic rocks were emplaced at different stages in the history of the area : the Middel Post Mafic complex is thought to have been intruded during D_{n+3} folding,whereas dykes and small plugs are clearly posttectonic.

3. STRUCTURE

3.1 Introduction

3.1.1 General description of structures and division into geometrically homogeneous areas

The geological map of the study-strip is dominated by several megascopic structures and a number of major shear zones (Annex. 1). It appears that these shear zones in some cases separate homogeneous areas from each other and in other cases transsect large structures. The division into homogeneous areas has been made on basis of geometrical characteristics of the large structures.

Area I in the west of the area comprises the area to the west of Hartbeesrivier and consists of the subareas 1 and 2. Major feature in this area is the Regt Kyk Structure, an interference pattern of the last two deformational events D_{n+2} and D_{n+3}.

Area II to the east of the Hartbeesrivier is bounded in the east by the Duivelsnek Shear Zone and transected by the Kakamas Shear Zone. It comprises the Swartpad Structure and the Omkyk Structure. The similarity between these structures lies in the fact that they both have a steeply dipping axial plane with the fold axis plunging close to the direction of dip of the axial plane. Also is the influence of D_{n+3} on these structures of a similar character : a slight flexure of the axial plane and no development into a dome or basin. The Omkyk Structure

---

* *Annotation* of the different phases of deformation is in the form D_{n+a}, where a is the number valid for the area under consideration only. This system has been chosen to enable correlation of the present investigation with investigations done elsewhere in Namaqualand/Bushmanland. Also it is thought that this annotation avoids confusion likely to arise by using the more familiar F_1, etc. system, as this automatically suggests a correlation with similarly labelled deformation phases from other areas. Additionally, n reflects the unknown factor. If a=1 this refers to the oldest visible event in this area. It is possible that this event can be correlated to another event in another area, which need not be the oldest event there.

has been divided into three subareas:
Duivelsnek synform (6), where the eastern limb of the Omkyk Structure is drawn into the Duivelsnek Shear Zone;
Omkyk-nose (4), as a virtually undisturbed D_{n+2} neutral to anti-formal structure; and
Omkyk-N (5), describing the D_{n+3} flexure.
The Swartpad Structure too has been divided, but here the differences between the synformal closure in the south and the remainder of the structure were too subtle to justify the definition of two separate subareas and hence the structure is presented as one subarea (3) on the structural map (Annex. 2). In the Swartpad Structure considerable shearing and fracturing took place as a result of the Kakamas Shear Zone passing between the Omkyk Structure and the Swartpad Structure.

Area III is bounded by the Duivelsnek Shear Zone in the west and the Neusspruit Lineament in the east. Apart from the Skurweberg Structure (D_{n+3}), this area is made up out of the Central Dome (subarea 8) and related structures to the north. The Central Dome is an interference pattern of a D_{n+2} antiform and a D_{n+3} antiform and the three structures north of the dome (subarea 7) yield information of all three phases of deformation. *The Neusspruit Lineament* is an important structural entity, as it separates an area of predominantly right-lateral shearing (Duivelsnek and Kakamas Shear Zones) from an area of left-lateral shearing (Brakfontein Shear Zone). The lineament itself could not be placed in either of these groups, but appears to have accommodated vertical movement.

Area IV, to the east of the Lineament, comprises the two isoclinal synforms of the Neusberg (subareas 10 and 11) and the Koekoeb Structure (subarea 14). The latter is composed of two antiforms, flanking a synform. No strong influence of the last deformational event is evident, but the structures do reflect the strong crustal shortening along the lineament.

Area V contains the large structures of Koms (subareas 15, 16 and 17) and Warm Zand (subareas 12 and 13). The Koms Structure is a large synformal structure. It is transsected by the Brakfontein Shear Zone along which adamellite and Straussburg Granite intruded. On the western limb two parasitic structures formed and are treated here as individual subareas (16 and 17).

The Warm Zand Structure resulted from interference between a D_{n+3} antiform and synform (with easterly trending axial-plane trace), with a D_{n+2} antiform with northeasterly dipping axial plane. During D_{n+2} considerable shortening took place, resulting in an imbricated structure, indicating that the shortening took place in northeast-southwesterly direction against the Neusspruit Lineament. As the D_{n+2} axial plane is inclined with respect to this lineament, the resulting interference structures are rather different: a domal structure in the south and a synformal structure in the north.

Subarea 18 in the east of the area (Curries Camp Structure)

stands alone as it can actually not be grouped with the structures in Area V on basis of its geometry: a rather closed, synformal structure. D_{n+3} has not effected the structure.

3.1.2 Methods used

For the description of the folds the method outlined by Ramsay (1967) has been utilised both for mesoscopic and megascopic structures. In the latter case the only photographs available are aerial ones, not necessarily perpendicular to the fold axis. To obtain a proper section the structures were orthogonally projected onto a plane at right angles to the fold axis. This was done in two steps:

1° projection onto a plane perpendicular to the axial plane and chosen such that the line of intersection between the two planes is parallel to the line of intersection between axial plane and surface (axial planar trace)

2° projection onto a plane perpendicular to the fold axis.

The orientation of the fold axis was arrived at by means of a package of statistical computer programmes called VECSTAPLOT, which is part of the P.R.U. Tectonic Database management routines, written and compiled by Hartnady (1978). Strike and dip of the axial plane was subsequently found by combining trend and plunge of the fold axis with the trend of the axial planar trace on a stereo net. Another feature of VECSTAPLOT is that it calculates the shape and orientation of the fabric ellipsoid. The axial ratios are subsequently plotted on a fabric which is analogous to a Flinn diagram (Flinn, 1962), onto which lines of equal fabric strength $\overline{E}_s$ have been added. The Fabric Shape Parameter $\overline{E}_s$ is analogous to the amount of strain ($\overline{\varepsilon}_s$) which is related to the natural octahedral shear ($\overline{\gamma}_o$) as defined by Nadai (1963) by $\overline{\varepsilon}_s = \left(\frac{\sqrt{3}}{2}\right)\overline{\gamma}_o$ (Nadai, 1963; Hossack, 1968) so that

$$\overline{E}_s = \frac{\sqrt{3}}{2} \times \frac{2}{3} \left[(\mathrm{Ln}\lambda_1 - \mathrm{Ln}\lambda_2)^2 + (\mathrm{Ln}\lambda_2 - \mathrm{Ln}\lambda_3)^2 + (\mathrm{Ln}\lambda_3 - \mathrm{Ln}\lambda_1)^2\right]^{\frac{1}{2}}$$

where Ln is ^{e}Log and $\lambda_1 \geq \lambda_2 \geq \lambda_3$ are the principal axes of the fabric ellipsoid, which is derived from the orientation tensor as described by Woodcock (1977) and Watson (1966). Also indicated are the types of distribution of points on the orientation diagram, by means of the fabric shape parameter, which is analogous to the k-value. The divisions on basis of these two parameters are summarised in Table 3.1. The information obtained with VECSTAPLOT is used to obtain trend/plunge of fold axis and subsequently strike/dip of axial plane and hence to describe the major folds in an accurate manner and to monitor changes in the fabric, according to the method described by Lisle (1977), who was able to record changes from a L-tectonite to a S-tectonite. Based on the information thus obtained and the variety in orientation of other fabric elements is the kinematic interpretation in the final section of this chapter.

Fabric strength parameter		Fabric shape parameter	
value	fabric strength class	k-value	fabric shape class
$0 < E_s < 1$	random	0,2 - 0,5	girdle (G)
$1 < E_s < 2$	diffuse	0,5 - 1	girdle-cluster (G-C)
$2 < E_s < 3$	weak	1 - 2	cluster-girdle (C-G)
$3 < E_s < 4$	moderate	2 - 5	cluster (C)
$4 < E_s < 5$	strong		
$5 < E_s < 7,5$	very strong		
$7,5 < E_s$	severe		

Table 3.1 Limits of the fabric shape and fabric strength classes

The relative age of the structures has been determined on the basis of interference features. Correlation on basis of fold style and orientation of axial plane and fold axis has been avoided, as heterogeneous and non-cylindrical deformation can produce a variety of styles in a small area (Williams, 1970).

Transmission Electron Microscopy has been applied in an attempt to gain information on the strain rate of the last deformational event.

3.2 Fractures and shear zones

Fractures and shear zones in the study-strip can be divided into three different types, each with a different structural significance: those that can only be recognised in the field, those that can also be recognised on the aerial photographs and those that also show up on the airborne magnetic records (Fig. 3.1).

3.2.1 Kakamas Shear Zone

The Kakamas Shear Zone is visible on the airborne magnetic map as a "quiet-low", bounded in the east by the trace of the Duivelsnek

Fig. 3.1

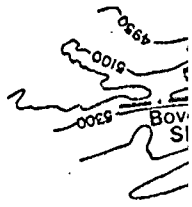

Ge

3.2.2 Duivelsnek Shear Zone

The Duivelsnek Shear Zone (Annex. 2), which appears to be the eastern termination of the magnetic low mentioned earlier, joins up with the Kakamas Shear Zone on the north bank of the Orange River. This has been inferred from the ERTS-images, as migmatisation, sand, calcrete cover and the buildup area of Kakamas, obliterate the northern continuation of the Kakamas Shear Zone (Fig. 3.1, 3.2). This zone is best observed on both sides of the road from Kakamas to Neilersdrift, just where it has cut through the Duivelsnek, some 6 km from the turn-off to Neilersdrift (Annex. 1, 2). Randomly oriented piedmontite needles occur on the fault planes and strong flattening and shearing are evident. Right-lateral movement took place, indicated by the Duivelsnek Structure in subarea 6 (Annex. 2). In addition, a considerable amount of vertical movement has taken place whereby the eastern block moved upwards with respect to the western block, as indicated by the appearance of high-grade metamorphic rocks in the Venterskop Kinzigite (Section 5, Annex. 3).

3.2.3 Neusspruit Lineament

The Neusspruit Lineament is characterised by two features: its pronounced topographic expression due to the hard platy quartz-mica schist and the termination of the feldspathic quartzite. The structures on both sides of the lineament show severe flattening in the area directly adjacent to the lineament. Farther away they tend to become more open. On the eastern side this is best illustrated in the Koekoeb area, comprising the isoclinal southern closure of the Neusberg Structure and the open fold of the Komsberg Structure. On the western side the severe flattening is not expressed in significant megascopic and mesoscopic structural features. Microscopically however, there is some evidence: over a zone of about 1,5 km wide in the Wolfskop Biotite Gneiss, quartz is strongly deformed and recrystallised, plagioclase twins are bent and the fabric is rather linear, sometimes approaching a ribbon mylonite. Hand specimens of the Micaceous Feldspathic Quartzite may look like mylonites with strong flattening around feldspar megacrysts. On the airborne magnetic map the lineament is very pronounced and can be traced further south and north. From the structures adjacent to the zone, it does not appear that left-lateral or right-lateral movement took place. Overthrusting from east to west and vertical movement, in that the western part moved upwards with respect to the eastern part, have certainly taken place. The pronounced appearance on airborne magnetics is

probably due to shortening and hence thickening of the crust on the eastern side of the lineament (Annex. 3). The fact that the charnockitic adamellite appears on both sides of the lineament is an important piece of evidence for the interpretation of the tectonic history of the area. It is certainly an indication of the depth of the discontinuity.

3.2.4 Brakfontein Shear Zone

The Brakfontein Shear Zone is best observed where the road from Keimoes to Kenhardt cuts through the feldspathic quartzite of the Neusberg Formation, near the homestead Brakfontein on the farm Neilers Drift. Here the zone consists of several parallel, narrow shear zones (60 cm wide), about 1,5 m apart with no apparent vertical displacement (Plate 5). The horizontal displacement at each of these zones is about 60 cm. (This figure is obtained from outcrops as shown in Plate 5). Unfortunately no strong schistosity developed so that no estimation of the shear strain of the zone can be obtained. Further north the shear zone becomes less easily recognisable because of the emplacement of the later granites. However, on the farm Koms the feldspathic quartzites of the Neusberg Formation are cut off by the shear zone. Piedmontite enrichment, brecciation and silicification are the main characteristics here. The actual shear zone here is some 200 m wide and consists of a number of parallel smaller shear zones. The course of the shear zone further north as shown on the maps is mainly inferred : its course in the river is indicated by topographic evidence such as rapids and sudden termination of islands. Due to the late intrusion of the charnockitic adamellite, the shear is obscured north of the river, although a relatively large number of parallel, widely spaced small shear zones have been mapped (Annex. 1). The lithological sequence of the west part of the Warm Zand Structure can only be explained as an imbricate structure in which the Brakfontein Shear Zone plays an important role. Uncertainty still exists about the point where the shear enters the Warm Zand Structure, mainly due to the abundance of sand dunes. The position on the map is based on airborne magnetic evidence and ERTS-images (Figs. 3.1, 3.2). Also based on airborne magnetic evidence in combination with ERTS-images is the conclusion that the Brakfontein Shear Zone continues to the south into the Boven Rugzeer Shear Zone (Botha *et al.*, 1977). Unfortunately not all of the characteristics of the two shear zones are in agreement : the Brakfontein Shear is syn- to late-tectonic (syntectonic in Warm Zand and late tectonic further south), whereas the Boven Rugzeer Shear Zone is entirely posttectonic. The mismatch of structure across the shear zone is of a dramatic nature in Warm Zand: isoclinal folding to the west compared to close to open folding to the east. Further south the mismatch becomes less pronounced (eg. Koms-Koekoeb area), whilst south of 29°S a significant mismatch again exists (Botha *et al.*, *op.cit.*). These factors are all dependent on the local geological history of the rocks cut by the shear zones, as deformation phases need not continue over vast areas. A more independent and hence more significant indication is the sense of movement of the shear

zones; both are left-lateral (Botha *et al.*, 1977, Plate 5). It is concluded therefore that the Boven Rugzeer is the southern continuation of the Brakfontein Shear Zone. This conclusion contradicts the suggestion that the Cnydas and Boven Rugzeer Shear Zones should join (Botha *et al.*, 1977). It is more likely that the Cnydas Shear Zone trends approximately in the same direction as the Keboes Line (Vajner, 1974; Geringer & Botha, 1977). This is based on ERTS image and airborne magnetic interpretation (Figs. 3.1, 3.2), as the shear zone itself is covered by recent deposits. Further to the southeast, poor outcrop conditions make it almost impossible to follow the trace of the shear zone. A strong indication for its presence however, is the sheared Straussburg Granite on the farm Kalksloot (Annex. 1). Here too outcrop conditions obstruct the investigations, but the variation in strike suggests a left-lateral movement, which is in good agreement with the description by Geringer & Botha (1977).On the southern bank of the Orange River on the farms Keboes and Bethesda a massive shear zone occurs, apparently the southern continuation of the Cnydas Shear Zone.

3.2.5 Fractures and shear zones of lower order

Fractures and shear zones of lower order than the three major discontinuities described above, are often characterised by piedmontite enrichment, silicification and porphyroblastesis. These properties are an important aid in the recognition of the structures; they often stand out as slightly redder and more brittle zones in the otherwise pinkish gneisses of the area and thus are easily discernable on aerial photographs. Good examples are the shear zones on Kakamas Suid just west of the Duivelsnek. The major fracture here is prominent on aerial photographs and in the field and is probably related to the Omkyk Structure. Several smaller faults branch out to the northwest, each of them with piedmontite enrichment and silicification. It is difficult to assess the structural significance of this system of faults. It is very likely that these are low-angle thrusts as a slice of porphyroblastic Nababeep-type gneiss (Kakamas Oos Porphyroblastic Gneiss) is bounded by these zones and not recognised on airborne magnetics. Such structures are usually not recognisable on airborne magnetics (Gay, 1972). In some cases mylonitisation gives the rock a dark appearance which may lead to errors in mapping, as the rock on first observation looks like a fine-grained amphibolite; a good example is the shear zones on the southeastern side of the Regt Kyk Structure.

A brecciated, silicified shear zone runs from Blauws Kop via Curries Camp to Vaal Hoek in the Warm Zand structure, where it terminates. Where the zone runs through adamellite, it is characterised by a marked increase in epidote. Displacement is difficult to assess because the displaced marker of quartz-mica schist on Blauws Kop and Curries Camp has partly been obliterated by the emplacement of the Straussburg Granite. Maximum displacement however, is estimated to be 2,5 km, and the sense of movement left-lateral. It is likely that some vertical movement also took place,

as the staurolite-tourmaline schist on Zoovoorby is cut out by this shear zone. In the Warm Zand Structure no significant displacement has been observed.

The shear zones and fractures that have only been observed in the field are of local significance only and are mainly associated with D_{n+2} structures.

Piedmontite and tourmaline crystals appear as late growths in many shear zones. The presence of piedmontite is not surprising, as it is mainly found in stressed areas (Deer, Howie & Zussman, 1966). Tourmaline however, indicates boron metasomatism (Parker, 1961; Fitch, 1932; Hyndman, 1972), which is thought to have occurred under conditions similar to pegmatite formation, i.e. enriched residual fluids from granitic crystallisation (in all cases either charnockitic adamellite or Straussburg Granite is present nearby), thus producing the necessary boron for tourmaline formation. In addition many rocks of sedimentary origin contain boron (Ethier & Campbell, 1977), which will form tourmaline when the rock undergoes metamorphism. These crystals have probably grown syntectonically and not posttectonically, as explained in Section 2.6.

3.3 Area I

This part of the study strip is divided into two subareas: the Regt Kyk Structure in the south (subarea 2) and the Vaalgras area (subarea 1) encompassing the remainder of the area.

3.3.1 Vaalgras Area (subarea 1)

The Vaalgras area is the area immediately to the north of the Regt Kyk Structure (Annex. 2) and is underlain mainly by gneisses, subjected to a reasonable degree of remobilisation as a result of which porphyroblastesis is a common feature. This is the main reason why the Kakamas Shear Zone as described in Section 3.2 could not be traced to the area north of the river. For the same reason, no other major structures than that of the last event are visible in the subarea. However, the stereogram of this area (Fig. 3.3a) displays a crossed-girdle pattern of poles to foliation due to interference of the last two deformational events : D_{n+2} and D_{n+3}. Figs. 3.3b and 3.3c show the stereograms of the readings of the respective deformational events. The separation of the two events has been done from the stereogram, as no major structures representing the two phases have been observed. The diagram for D_{n+2} has a computed value for the pole to the girdle of a 2^{o} plunge towards 129^{o}. In Fig. 3.3a a second girdle is drawn, fitted by hand, with a plunge of 10^{o} towards 310^{o}. The difference is accounted for by the fact that the former is a computer-derived diagram, representing the mathematically correct girdle (λ_2 - λ_3 of fabric ellipsoid), whereas the latter is a best-fit

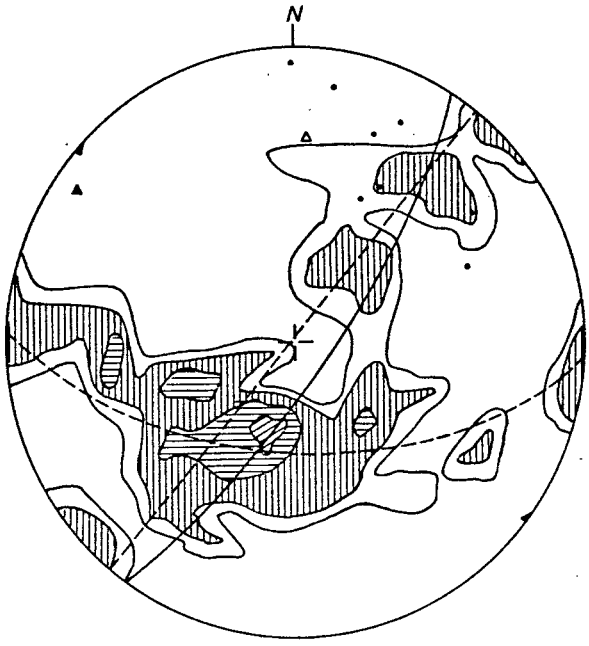

Fig. 3.3

Equal area projection of poles to foliation (S_{n+1})
subarea 1 - contours at 1, 2, 5, 10% of points per % area.

- ▵ pole to girdle
- • mineral lineation
- a All data available. N_s=53.
- b Girdle representing D_{n+2} only. N_s=31.
- c Girdle representing D_{n+3} only. N_s=39.

Fig. 3.3a

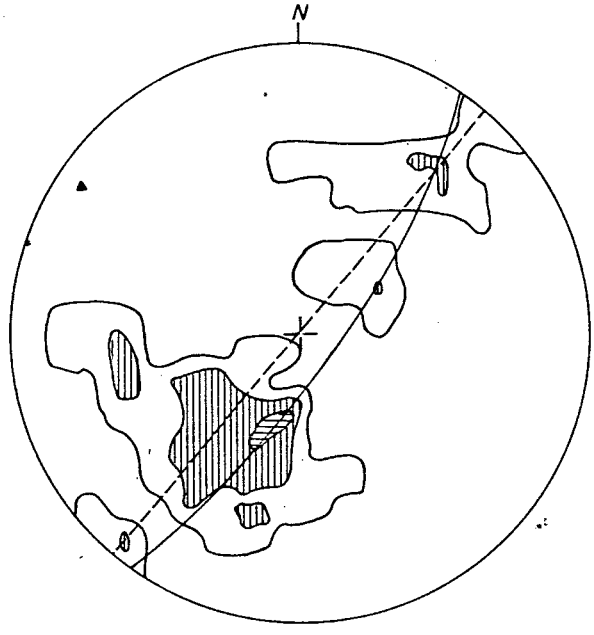

Fig. 3.3b

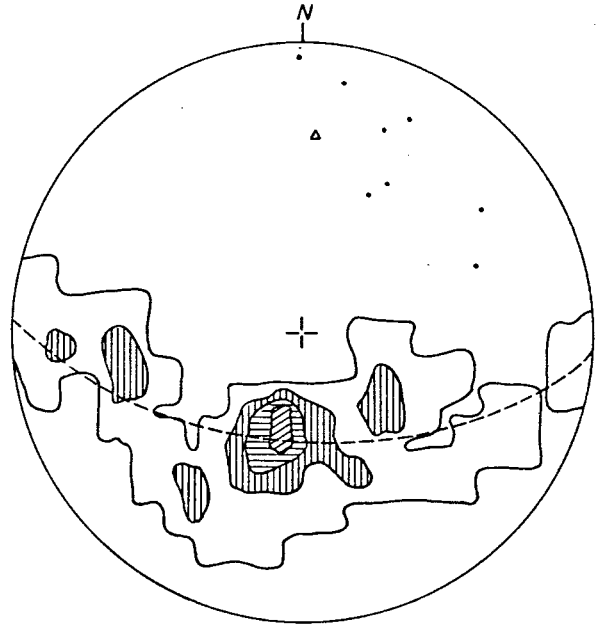

Fig. 3.3c

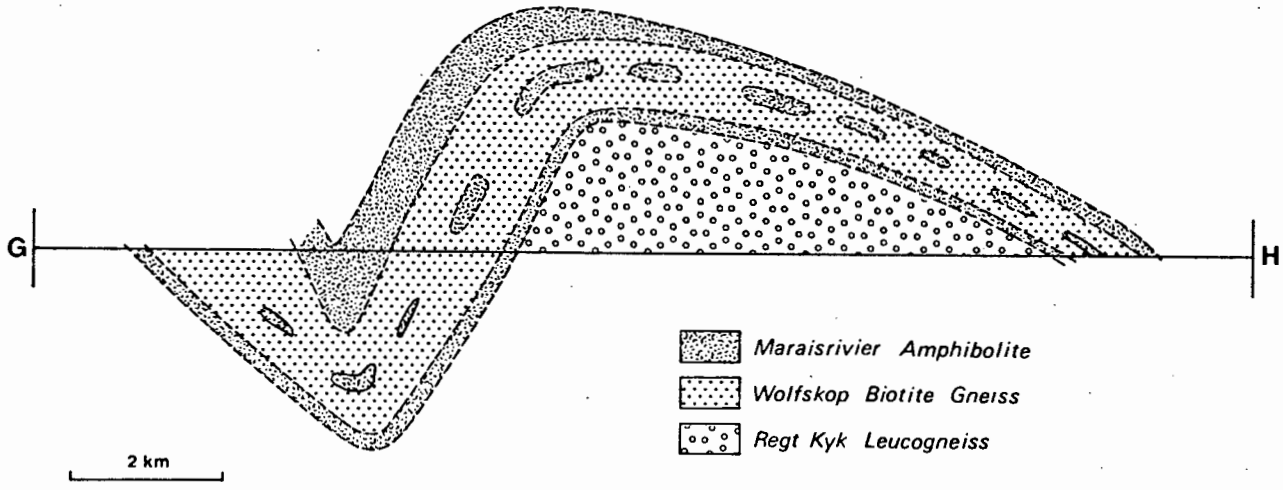

Fig. 3.4 Section through the Regt Kyk Structure.
The synform on the lefthand side continues in the Vaalgras area.

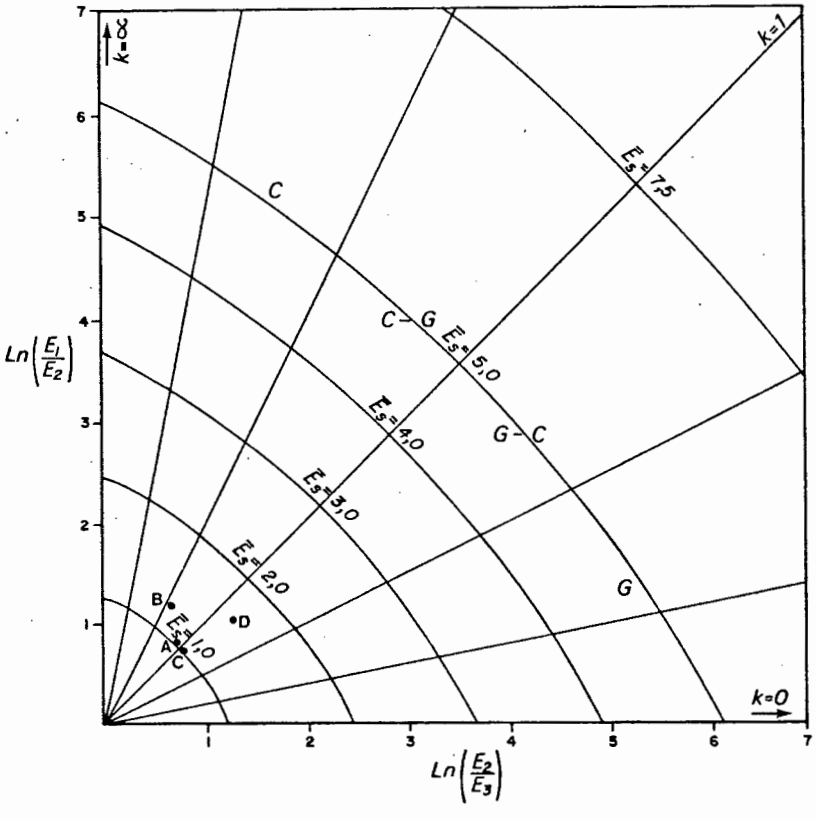

Fig. 3.5
Fabric diagram of Area I.
A = subarea I (Vaalgras)
B = subarea 2 (Regt Kyk)
C = Vaalgras D_{n+3} only
D = Vaalgras D_{n+2} only

girdle, based on the maxima of the contoured stereogram. Similarly, the diagram for subarea 1 on Annex. 2. is the mathematical average of all data, whereas Fig. 3.3 is based on the maxima on the contoured diagram. This trend and plunge agree reasonably well with the D_{n+2} trend and plunge of the Regt Kyk Structure. The last event is better documented. In Fig. 3.3c, a girdle with a pole plunging 33° towards 3° is shown. In combination with the trace of the axial plane this yields a strike and dip of 210/54 for the axial plane of the structure, which agrees well with the general strike of D_{n+3} fold axial planes throughout the area. A section through this structure is presented in profile G-H (Fig. 3.4).

On the fabric diagram (Section 3.1.2., Fig. 3.5) point D reflects the fabric shape ellipsoid of the D_{n+3} deformational event and is an oblate-type ellipsoid. Point C represents D_{n+2} and is close to the k = 1 line, but also in the oblate field of the diagram. Both ellipsoids plot close to the origin, which is a reflection of the strength of the fabric. The points seem to lie on a straight line, thus indicating no notable difference in fabric shape.

Mesoscopic structures. Several folds in the order of magnitude of one metre (total limb length) may be observed in this subarea. Tight to isoclinal folds show that the main foliation is in fact an axial-plane foliation. Elsewhere the gneissic banding has been deformed into sigmoidal structures : small parallel shear zones at about 15 cm intervals give the appearance of coarse crenulation cleavage. This is however, a local feature (Station 1573) and has been partly obscured in later migmatisation. A small (3 m total limb length), probably parasitic, D_{n+2} fold crops out at station 1596. It is a tight fold with an interlimb angle of approximately 20° and almost horizontal fold axis (8°) plunging toward 293°. This isolated structure has been classified as a D_{n+2} structure because of its orientation: at right angles to the axis of the D_{n+3} deformation and because the S_{n+1} foliation has been deformed.

3.3.2 Regt Kyk Structure (subarea 2)

The outlines of this complex interference structure are defined by the Maraisrivier Amphibolite (Annex. 1 and 2). Three phases of deformation can be recognised in this subarea. D_{n+1} resulted in an isoclinal fold, probably recumbent, with a northerly plunging axis. No direct field evidence such as fold closures have been recorded, but the structure can be inferred from profile G-H (Fig. 3.4, Annex. 2). This seems to be supported by petrographic evidence, as no marked difference has been observed in texture and composition of samples taken from the inner and outer amphibolite layer. Fig. 3.6 shows the airborne magnetic record of the area with superposed on it the geology. There appears to be some indication for a fold closure, but rather from the gneisses north of the amphibolite than from the amphibolite itself.

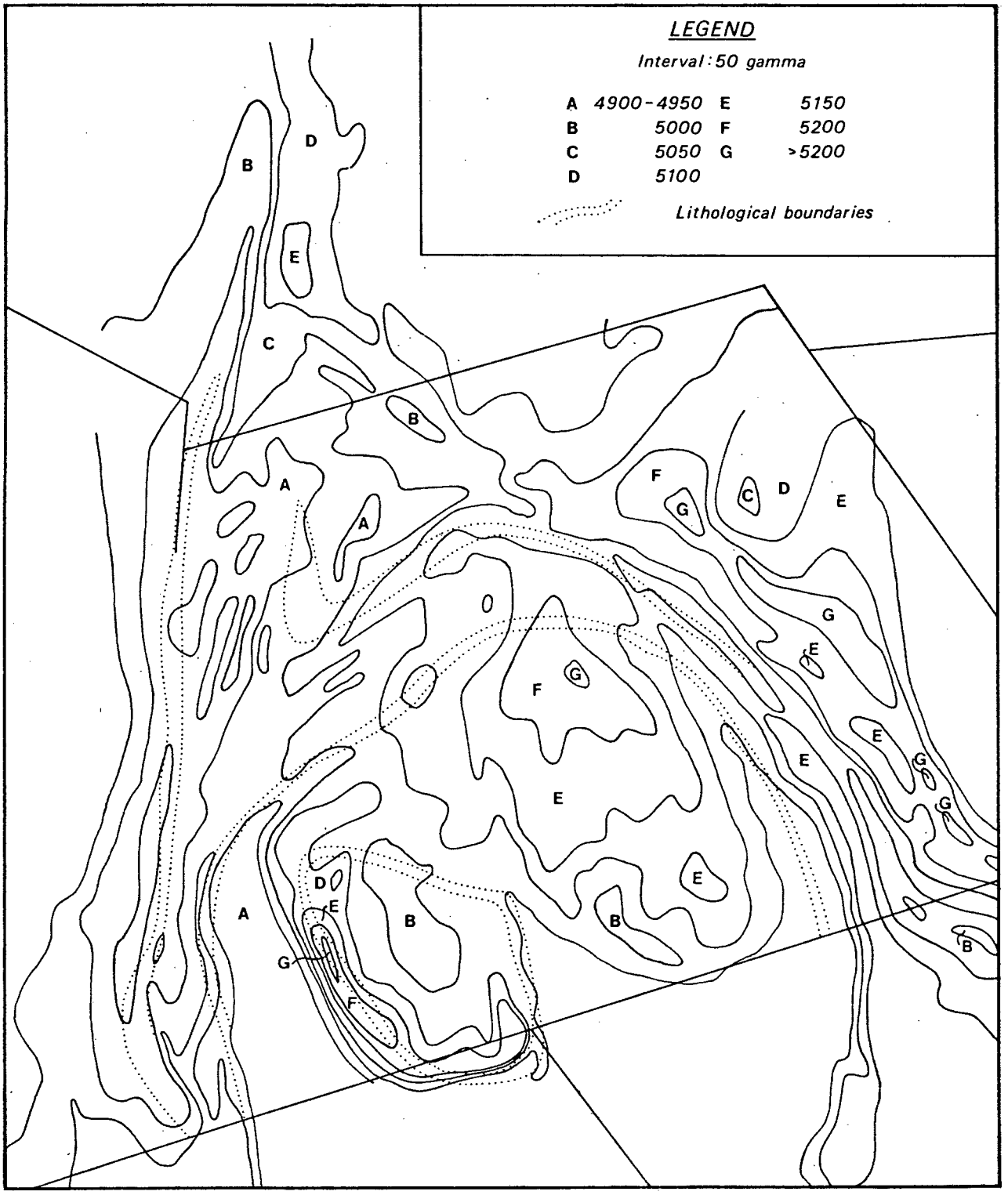

Fig. 3.6 Airborne magnetic map of Regt Kyk Area. Contour intervals at 50 gamma.

In summary it must be concluded that the evidence for this early structure is weak. What seems to be the strongest evidence, the petrography, is not conclusive as due to variation in composition, samples of a positively continuing geological entity can look entirely different. Likewise separate rock units can look identical.

The last two deformational events produced the actual interference structure. The axial planes of D_{n+2} dip 35° towards 30°. The diagram in Fig. 3.7 represents the structure as a whole and therefore reflects the total fabric ellipsoid of this structure. It is an oblate ellipsoid (point B, Fig. 3.5) . At station 1590 boudins have been observed with the long axes in the foliation plane, dipping 50° towards 64°, indicating that

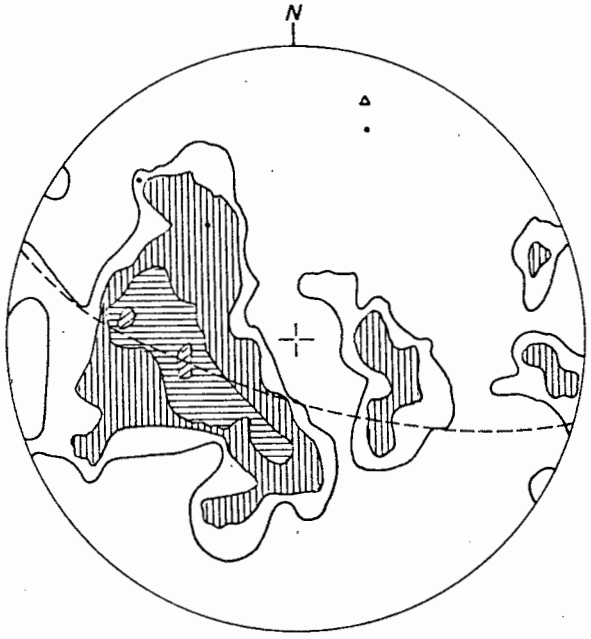

Fig. 3.7 Equal area projection for Regt Kyk Structure (subarea 2) of poles to S_{n+1}. N=77 Contour lines at 1, 2, 5 and 10% of points per percent area.

▵ = pole to girdle

• = mineral lineation

the foliation is parallel to the xy plane of the strain ellipsoid. It should be emphasized that the finite strain ellipsoid on a specific point in a structure need not be similarly oriented as the finite strain ellipsoid of the total structure as it represents the local state of strain, which need not be the same as the finite strain for the entire structure.

Mesoscopic structures. In Fig. 3.8 refraction of the main foliation at a quartz vein is illustrated. Situations like this are difficult to interpret as there is no real control as to the origin of the competent layer: it may be an original depositional difference or it may be a quartz vein, developed in an early stage of the history of the rock, or it may be some sort of metamorphic banding, formed during early metamorphism.

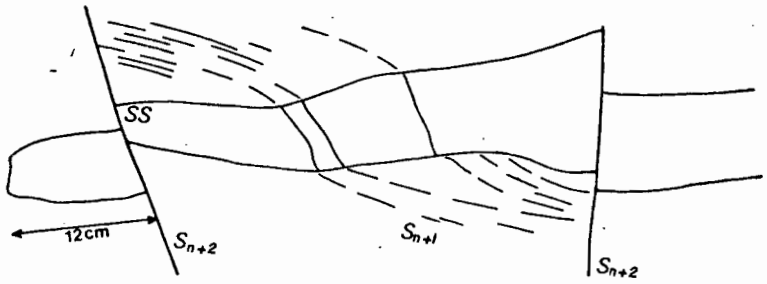

Fig. 3.8. Refraction of main foliation at a quartz vein

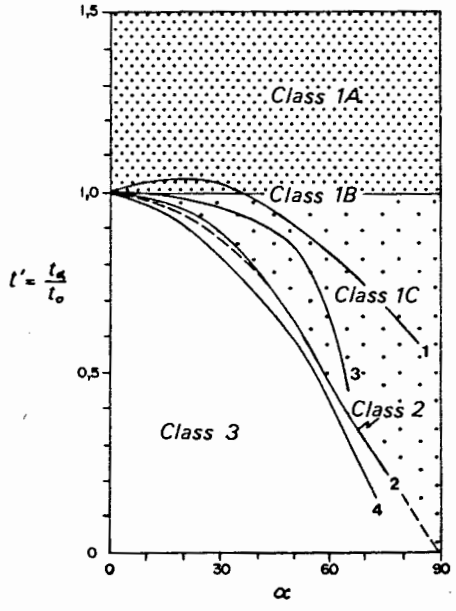

Fig. 3.9. Heterogeneity of strain on a small scale: from top to bottom the folds classified are : class 1C, 2, 1C, 3.

In Fig. 3.9 the heterogeneity of the strain in the area is shown. The folds have been classified using the method as outlined by Ramsay (1967). They belong to the D_{n+1} deformational event and their axial-plane foliation is the main foliation measured in the area.

Boudins, as mentioned earlier, occur mainly in the amphibolite. They form in the competent, more massive amphibolite layers and are surrounded by the more schistose variety (eg. Station 1590). The longest axis most often lies in the foliation plane at right angles to the strike. The other two axes vary in length, but usually do not exceed the 50 cm.

3.4 Area II

Bounded by the Duivelsnek Shear Zone in the east and the Kakamas Shear Zone and Hartbeesrivier in the west, Area II contains two major structures : the Omkyk Structure and the Swartpad Structure.

3.4.1 The Swartpad Structure

The Swartpad Structure is situated to the east of the Regt Kyk Structure, between the Hartbeesrivier and the Kakamas Shear Zone. In previous publications the structure is referred to as the Southern Basin (Poldervaart & von Backström, 1949; von Backström, 1964). Like most of the other major structures in the area it reflects the last two deformational events.

The fold closure of the D_{n+2} structure is situated in the eastern part of the area (Fig. 3.10). It is a tight fold with a fold axis plunging 47° towards 3°. As the axial plane dips 48° towards 28° this structure is to be classified as an inclined plunging, tight fold. The fabric ellipsoid (point E in Fig. 3.12) has an oblate shape, which means an L–type fabric. Suitable markers to compare the orientation of the fabric ellipsoid with that of the strain ellipsoid are not available. Interpretation of this fold closure as a D_{n+2} structure is based on the fact that it is defined by deformation of the main foliation, which proved to be a S_{n+1} (see Mesoscopic structures). As a result of the extensive shearing in this part of the area the actual fold closure is not preserved, but is cut by a fault (Fig. 3.10). In the northwestern part of the area no indications of a D_{n+2} fold closure exist and for this reason the deformation of this area is ascribed to the D_{n+3} deformational event. It proved to be impossible to determine the trace of the axial plane of the D_{n+3} accurately as fractures influenced the trend of the foliation, especially in the northwestern part of the area. It appears however from the data that the trend will conform to the general trend in the area: northeasterly. Combining this information with the mathematically derived fold axis, yields an axial plane that plunges

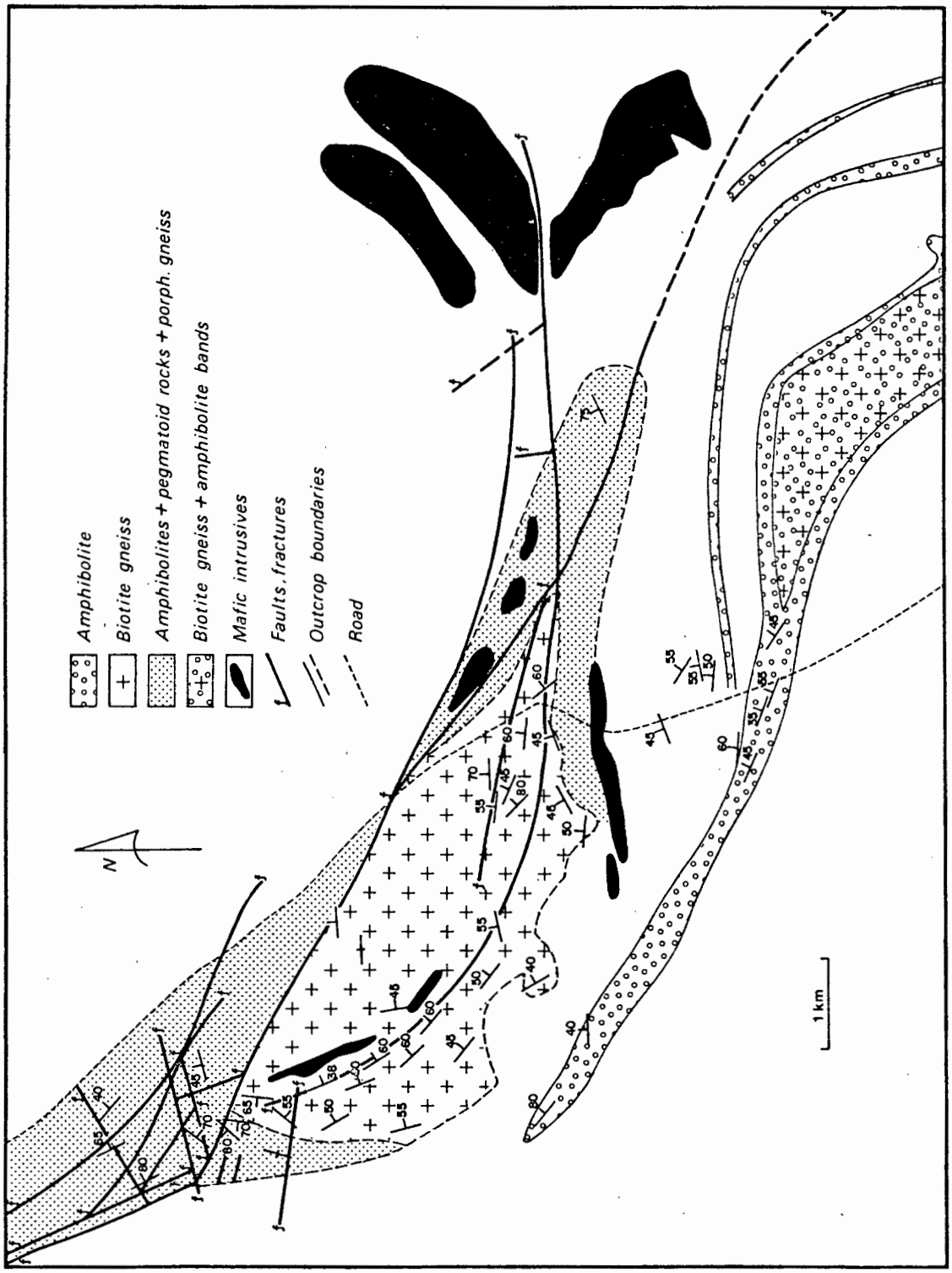

Fig. 3.10 Sketch map of Swartpad Structure

68° towards 310°. As the interlimb angle is approximately 130°, this D_{n+3} structure is an inclined plunging, gentle fold. Point F in Fig. 3.12 represents this part of the Swartpad Structure and its position indicates that the fabric ellipsoid is of a slightly more oblate type than the ellipsoid of the fold closure. This is not surprising as the former part of the subarea contains the limbs of the D_{n+2} structure so that the foliations may be expected to have been parallel to a higher extent than in the fold hinge. Hence the resulting ellipsoid is of a more oblate character than the ellipsoid of the fold hinge.

When comparing the stereograms presented in Fig. 3.11 with those in Fig. 3.20, it is clear that the structure under consideration is by no means a basin-type structure, as there is no evidence for two synformal fold hinges. Obviously it can be argued that the Kakamas Shear Zone obliterated important evidence and that it is logical to expect a basin between two domes (Regt Kyk and Central Dome), but then there is the Omkyk Structure that clearly does not follow this pattern either (Section 3.4.2). It is not abnormal to find a synformal structure as the Swartpad Structure adjacent to the neutral-to-antiformal Omkyk Structure.

Mesoscopic structures. In the Swartpad Structure these support the interpretation that the fold closure in the southeast is a D_{n+2} structure, as mesoscopic folds are generally tight to isoclinal and have developed an axial plane foliation parallel to the main foliation. It is important to note that the mafic rocks in this subarea predate D_{n+2}, as a foliation is developed in them. Shearing, accompanied by silicification and piedmontite enrichment, is a common feature in the area and on several occasions elongated feldspar augen (up to 1 cm long axis) have been encountered. Likewise do streaks of quartz (20 x 3 mm) appear. Development of pressure shadows too can be observed frequently.

Microscopic features of significance are rare, but the few that are worth mentioning are in full support of the previous section in that microscopically it could be confirmed that the main foliation plane is in fact an axial planar foliation of close folds (observed in the quartzites at station 667). This same foliation can be found in the thin sections of the intrusive rocks. Here the minerals are more or less oriented, indicating that they formed late- or syntectonically, as only a weak foliation formed, whereas in pretectonically emplaced rocks a more penetrative foliation, better defined on the microscopic scale, would be expected to have formed.

3.4.2 The Omkyk Structure

The Omkyk Structure contains three subareas : Duivelsnek (6), Omkyk-N (5) and Omkyk-nose (4). These subareas shall be treated

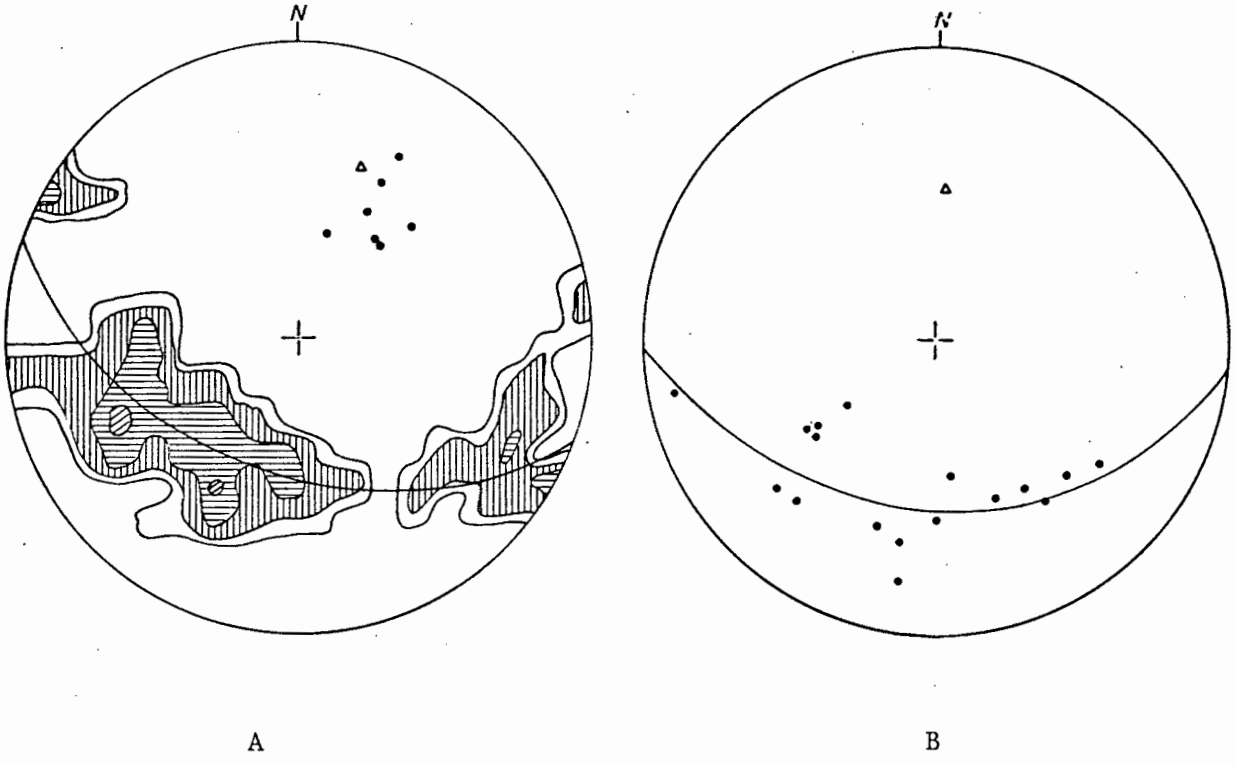

A B

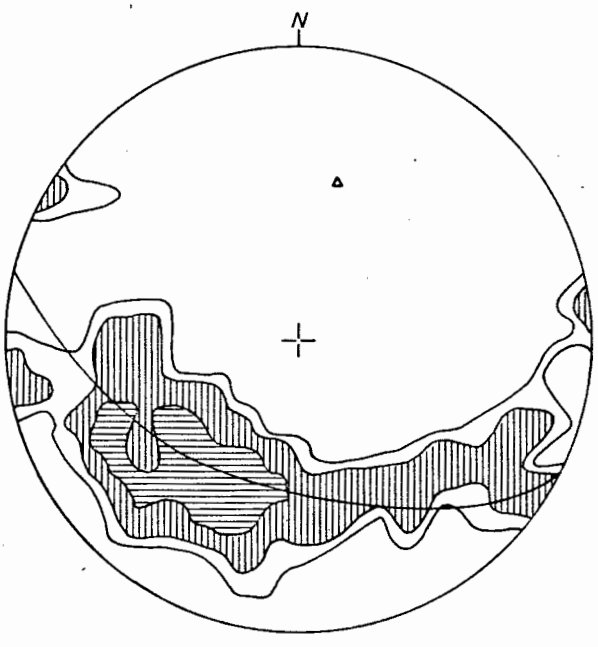

C

Fig. 3.11

Equal area projection of poles to S_{n+1} in Swartpad Structure. Contour lines at 1, 2, 5 and 10% of points per percent area.

A = northern part of subarea N_s=49
B = southern closure N_s=16
C = Total subarea N_s=75
▵ = Pole to girdle
• = Mineral lineation

in two groups because of the character of the D_{n+3} fold in this part of the area. The point of maximum curvature of this gentle fold is situated between the subareas 5 and 6 and although the effect of D_{n+3} on these structures is very small, the non-parallellism of their axial planes is a direct result of D_{n+3}. As a result the information gained from the stereogram and statistical data of subarea 5 (Fig. 3.15) is related to the last deformational event (D_{n+3}) and the information from the subareas 4 and 6 related to the previous phase of deformation, D_{n+2}.

The structures of the subareas 4 and 6 are complementary and both can be classified as plunging inclined folds (Turner and Weiss, 1963): in subarea 4 (Figs. 3.13 and 3.14) the axial plane dips towards 63° and the fold axis plunges 39° towards 76° and in subarea 6 the axial plane dips towards 80° and the fold axis plunges 43° towards 63°. The trend and plunge of the two axes seem to be in good agreement (a difference of 14° and 15° respectively), but the lineations do not always conform so well. In subarea 4 the fold axis lies between the lineations (Fig. 3.14), whereas in subarea 6 the fold axis lies at the edge of the field of the lineations. The explanation of this feature can be found by studying the field data producing this last stereogram. Stereogram 6 on Annex.2 represents the larger

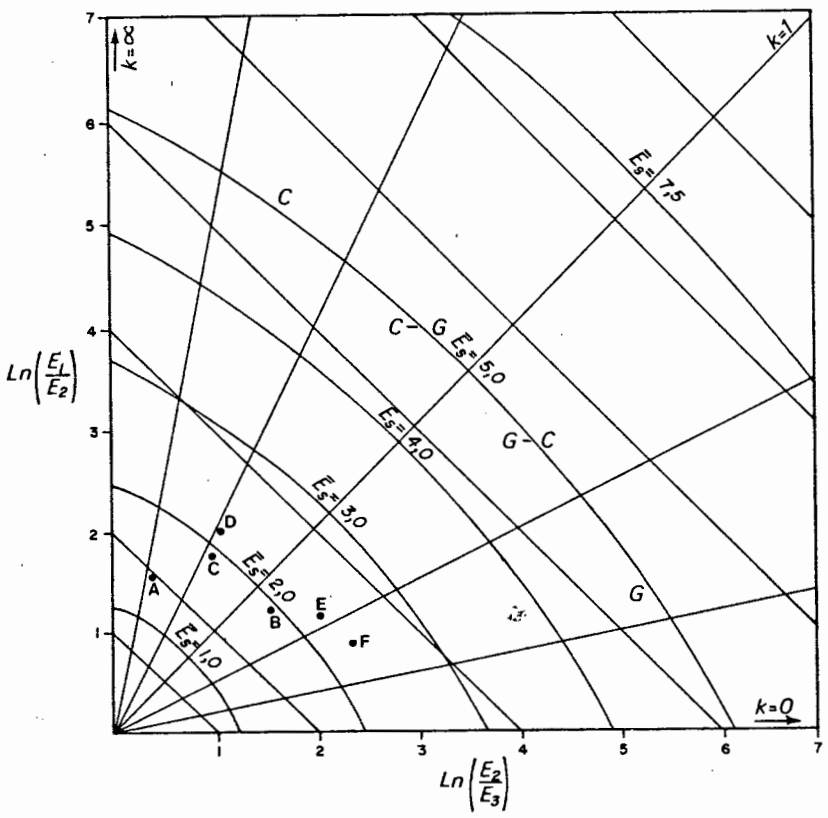

Fig. 3.12 Fabric diagram of area II

A Subarea 6 total
B Subarea 6 excluding Duivelsnek Shear Zone
C Subarea 5
D Subarea 4
E Swartpad south closure
F Swartpad northern part

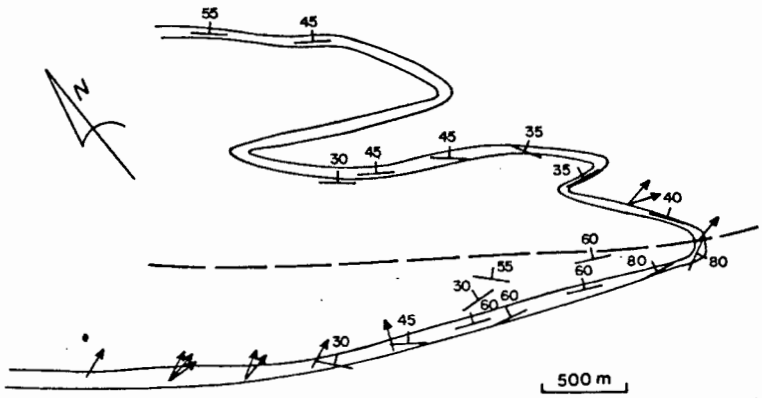

Fig. 3.13 Sketch map of subarea 4 (hinge zone of Omkyk Structure)

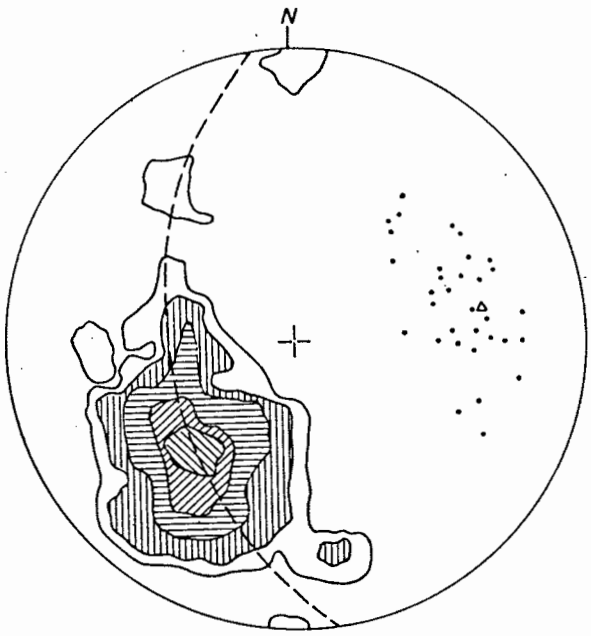

Fig. 3.14 Equal area projection of poles to S_{n+1} of subarea 4. N_S=174. Contour lines at 1,2,5,10, 15% of points per percent area.
▵ = pole to girdle
• = mineral lineation

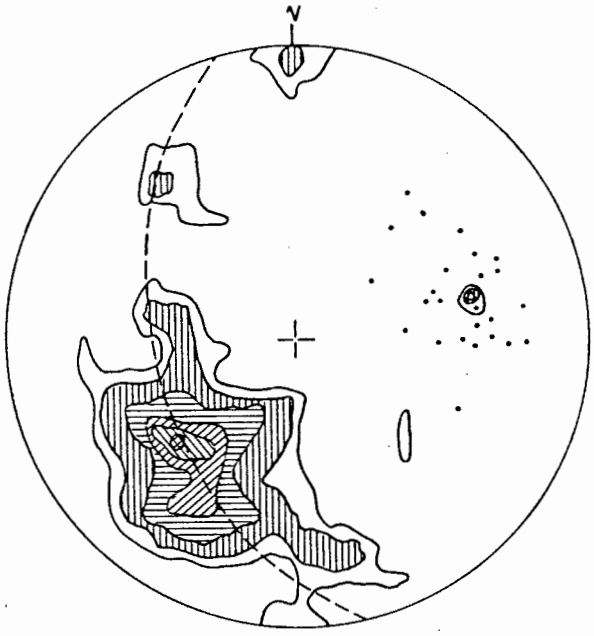

Fig. 3.15 Equal area projection of poles to S_{n+1} for subarea 5. N_S=78. Contour lines at 1,2,5,10,15,20% of points per percent area.
▵ = pole to girdle
• = mineral lineation

Duivelsnek area, including the Duivelsnek Shear Zone itself and some of the minor fractures in that area. It is some of these readings outside the Marais rivier Amphibolite that plot on the right-hand side of the stereogram (Fig. 3.16a). When these are removed, the poles to foliation of this structure plot as shown in Figure 3.16b. The two areas on the lower side of the stereogram represent readings taken from fold hinges of parasitic folds and the hinge of the major structure itself. If more data had been available on these parts of the structure, the maximum of the girdle should have shifted towards the lower part of the diagram and consequently the axis to the π circle moves towards the top and hence should have been situated among the lineations. The conclusion is therefore that the fold axes of subareas 5 and 6 are not parallel. This may be explained by the presence of the Duivelsnek Shear Zone into which existing directions have been forced by drag (right-lateral movement) and by the folding due to D_{n+3}, as mentioned earlier.

In Fig. 3.12 the shapes of fabric ellipsoids of the three subareas of the Omkyk Structure have been plotted (points A-D). Note that the two fabric ellipsoids of subarea 6 differ considerably. Point A is a strongly prolate shape, whereas B plots in the oblate field. This indicates that the fabric, developed in a shear zone is an S-type fabric compared with the L-type fabric of the subareas B, E and F. It is concluded therefore that the S-type fabric of subareas 5 and 4 indicates that considerable shearing took place in the direct vicinity of these structures. The outline of the fold closure of the Omkyk Structure has been projected onto a plane perpendicular to the fold axis, according to the technique described in section 3.1.2. As a result this structure may be described as a class 3 fold according to the classification of Ramsay (1967).

The last deformational phase affecting the Omkyk structure resulted in a gentle fold, with a fold axis plunging 36^{o} towards 83^{o} and an axial plane dipping 42^{o} towards 150^{o} (Fig. 3.15), hence the structure may be classified as a gentle, plunging inclined fold. In order to be able to construct a profile of this D_{n+3} fold, the average strike and dip on both sides of the axial plane were calculated. This was achieved by processing the data with the program VECSTAPLOT (Section 3.1.2.) as was done for all the other subareas. Both groups of data yielded a cluster on the stereogram thus indicating a rather homogeneous distribution (D_{n+2} fold hinges excluded). The stereogram of the total structure (subarea 5) is a cluster as well, with fabric strength parameter = 2.08, indicating that it is a weak cluster. This is not surprising as the structure concerned is a very gentle fold indeed, but the position where it plots on the fabric diagram (Fig. 3.12 point D) is interesting as this indicates, like for the hinge zone, a prolate fabric ellipsoid, attesting some elongation into the direction of the principal axis (221/45): an S-type fabric.

Mesoscopic folds in the Omkyk Structure are usually tight folds, approaching the isoclinal. The degree of weathering of the gneisses on the one hand, and the relative homogeneity of the rocks on mesoscopic scale on the other, considerably diminish the chances of finding a section plane perpendicular to the fold axis. For these reasons, only very few mesoscopic

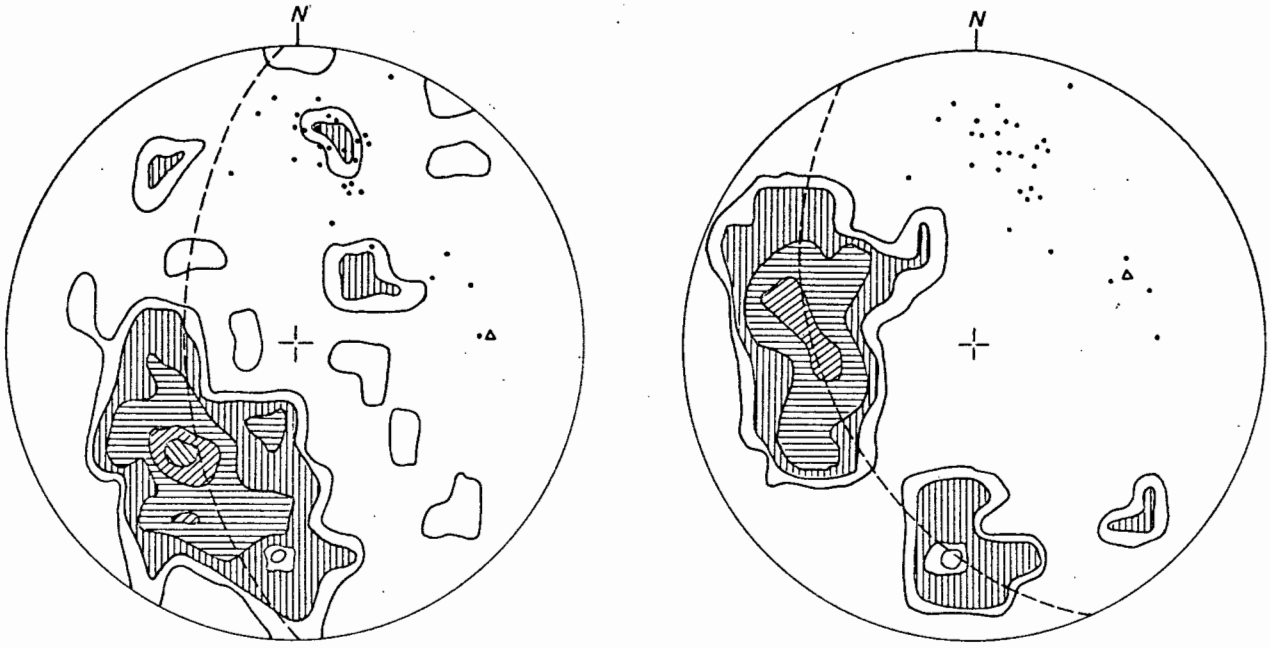

A B

Fig. 3.16 Equal area projection of poles to S_{n+1} of subarea 6
Contour lines at 1, 2, 5, 10 and 15% per percent area.

▵ = Pole to girdle
· = Mineral lineation

A = Duivelsnek area including shear zone as on Annex 2. N_s= 66

B = Duivelsnek fold only. N_s = 41

folds suitable for classification as described by Ramsay (1967) are available. The few that were used proved to fall in class IC and some in class IB and class 2, which is in contrast to the fold style of the major structure, illustrating the different finite strains in different parts of the area.

Other mesoscopic features observed in this subarea are isoclinal D_{n+1} folds and small, asymmetrical D_{n+2} folds on the major structure. The tight mesoscopic folds are the oldest structures observed and their axial plane is the main foliation generally observed in the area. Microscopically there is no evidence whatsoever that this foliation, which in some thin sections proved to be a crenulation cleavage, deforms anything else but lithological banding. Hence these small structures are thought to be D_{n+1} structures and their axial-plane foliation S_{n+1}.

Boudins occur in the Maraisrivier Amphibolite (Station 524). They are oriented with their long axes plunging down the dip of the foliation and the intermediate axes parallel to strike. The foliation plane is thus parallel to the xy plane of the strain ellipsoid and dips 45° towards 10°.

3.5 Area III

Like the Omkyk Structure, the area of the Central Dome and surrounding structures has been divided into three subareas : Central Dome (8), Skurweberg (9) and the structures to the north of the Central Dome (7). This last subarea in turn has been divided into three separate structures. In this manner information is obtained of all three major deformational events : D_{n+1} (7B), D_{n+2} (7C,8) and D_{n+3}(7A,9) and this section is therefore divided into three sections, each describing the megastructures, developed during one of the deformational events.

The earliest event

In this part of the area one large structure, belonging to the earliest deformation phase can be distinguished (subarea 7B, Annex. 2, Fig. 3.17). It has been constructed on the basis of the profiles A-B and I-J (Annex. 2). The outline of the structure has been projected onto a plane perpendicular to the fold axis, according to the method set out in section 3.1.2. As a result it has been classified as a class 1C fold (Ramsay, 1967). The fold axis plunges 33° towards 40°, which in combination with the trace of the axial plane yields an axial plane dipping 35° towards 20°, so that the structure can be classified as a moderately plunging inclined, neutral to antiformal fold. The axial plane of the Dome strikes 300° (measured in the centre), but the D_{n+2} axis plunges towards 110° in the northern closure, a considerable difference when compared with subarea 7B. This difference in trend cannot be accounted for by folding during the last deformational event as this phase produces very gentle folds. Hence this

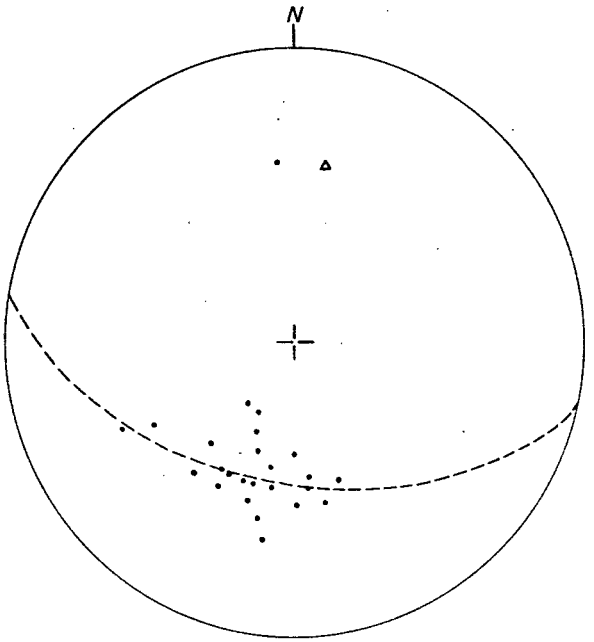

Fig. 3.17 Equal area projection of poles to S_{n+1} of subarea 7B, reflecting a D_{n+1} structure. N_s=11

▵ = pole to girdle
• = pole to S_{n+1}

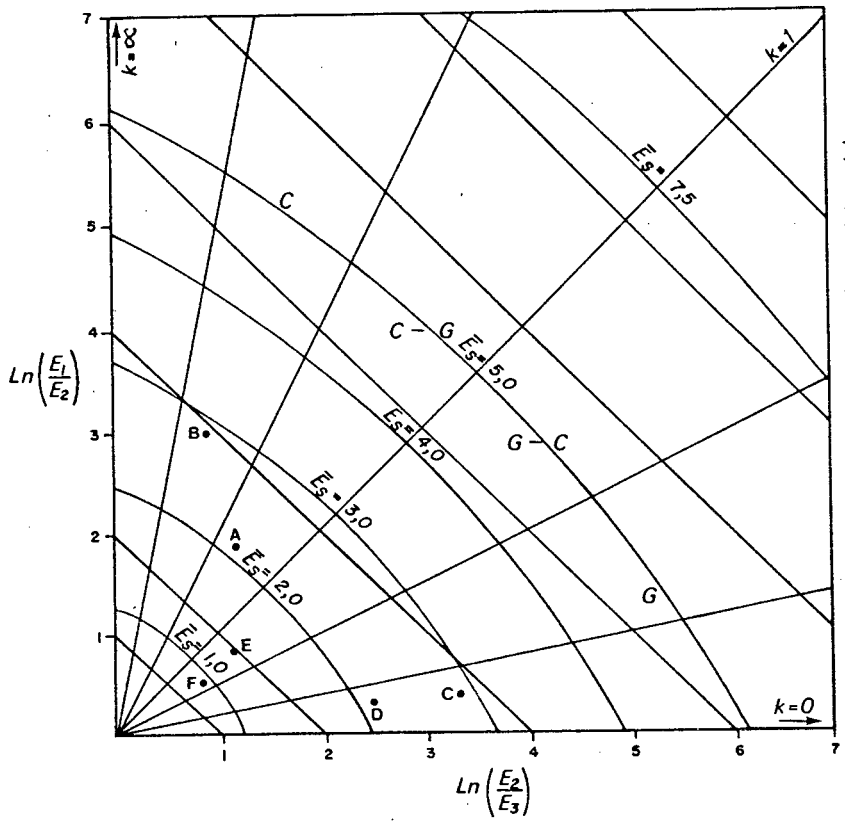

Fig. 3.18

Fabric diagram of Area III.

A = subarea 7A
B = subarea 7B
C = subarea 7C
D = subarea 8 (north)
E = subarea 8 (south)
F = subarea 9

structure can neither be a D_{n+2} nor a D_{n+3} structure and the discrepancies mentioned earlier, can only be explained when this fold is a D_{n+1} structure.

This interpretation is supported by the data shown in the fabric diagram (Fig. 3.18). Subarea 7B is represented by point B and when compared with the position of point D (northern part of the Dome) and point A (subarea 7A), it is clear that the fabric ellipsoids of B and A are both prolate, but that B has a considerably stronger planar fabric than A. Point D on the other hand, is very much an oblate fabric ellipsoid, where no constrictional element is evident. On the contrary, considerable flattening is likely to have occurred. It is unlikely that these three entirely different types of tectonite in such a small area should be brought about by the same deformational event, as the different parts of the area inevitably influence each other during deformation. Hence the variation in fabric should be more gradual. It is therefore very likely that the three types of fabric represent three phases of deformation.

The number of data has a direct influence on the statistics produced by VECSTAPLOT. If on a total of 100 data, two points plot out of the general area where the other points plot, the final conclusion will not be much influenced. If however, two out of ten data are out of line, this will obviously have effect on the shape of the calculated fabric ellipsoid. It is thus obvious that the data from subarea 7C are not very reliable.

The second event

Large structures formed during the second event occur in subareas 7C and 8 (Figs. 3.19 and 3.20) represented by the points C, D and E on the fabric diagram (Fig. 3.18). All three show an oblate fabric ellipsoid, with a marked similarity between the points C and D, as both types of tectonites are strongly flattened. This is in contrast with the less pronounced oblate type of fabric of the southern part of the Dome (Point E). However, it should be noted that the latter plots in the next to lowest fabric strength field indicating a sub-random fabric in a girdle to cluster type distribution. This is a direct result of the low number of data available in this area (8).

The fold in subarea 7C is an antiformal structure with the axis plunging 37° towards 354°. As the axial plane dips 72° towards 70°, it is a plunging inclined close fold (interlimb angle 55°), that plots in class 1A, after correction.

The northern closure of the Dome is very much a similar type of structure. The fold axis plunges 33° towards 293° and the axial plane dips 80° towards 30°. It is thus a plunging inclined fold. The mineral lineations belonging to this generation plot around the fold axis (Fig. 3.20B).

The southern closure is a plunging inclined structure as well, since the axial plane dips 88° towards 20° and the axis plunges 26° towards 110°. It is important to note that the plunging axes are due

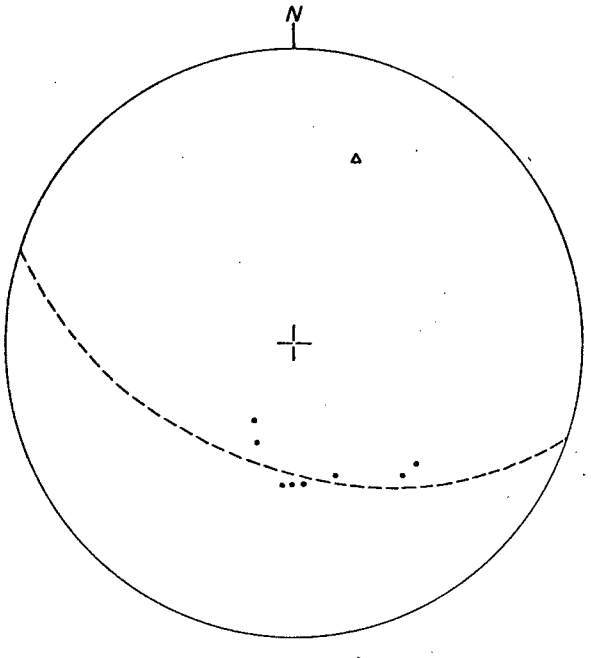

Fig. 3.19 Equal area projection of poles to S_{n+1} of subarea 7C. N_s=13

▵ - pole to girdle
• - pole to S_{n+1}

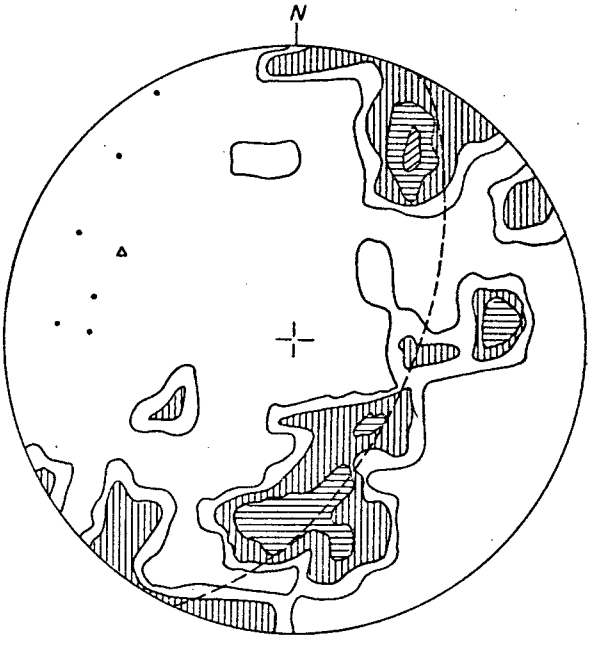

Fig. 3.20 A

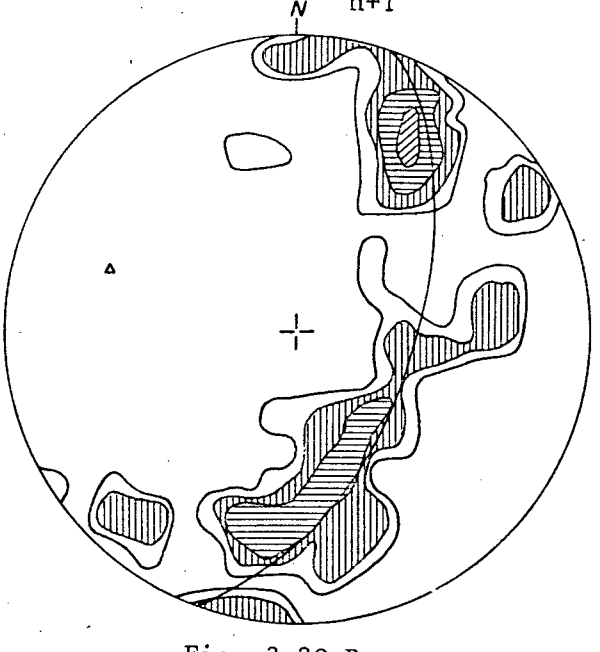

Fig. 3.20 B

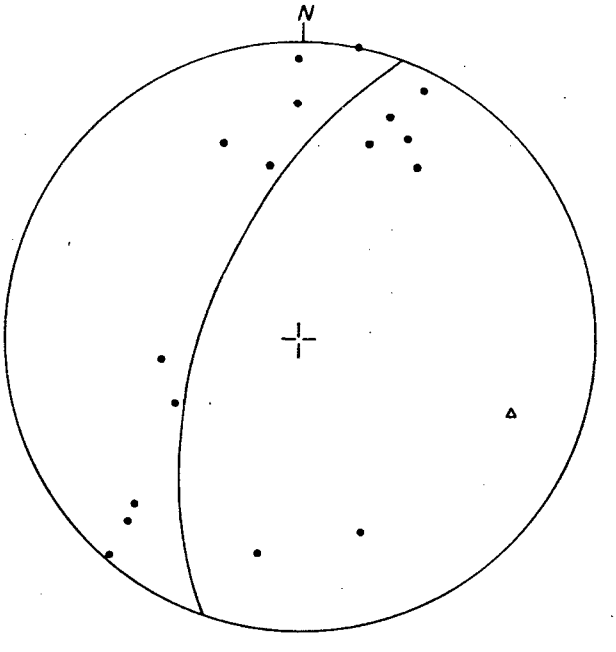

Fig. 3.20 C

Fig. 3.20 Equal area projection of poles to S_{n+1} of subarea 8. Contour lines at 1, 2, 5 and 10% per percent area.
A : total subarea N_s=51, B : northern closure N_s=46
C : southern closure N_s=18
▵ : pole to girdle
• : mineral lineation

to the latest event and that the original D_{n+2} structure was most probably a horizontal-normal or plunging-normal fold with fold limbs that now form the long sides of the Dome Structure.

The last event

The structure in subarea 7A has been classified as a D_{n+3} structure because of the attitudes of the axial plane and axis and because of the fold style: the axial plane dips 80° towards 335°(Fig.3.21) and the trend and plunge of the fold axis are 040/33, so the structure is an inclined plunging fold with an interlimb angle of 120°. On the fabric diagram (Fig. 3.18, point A) it plots in the field between k=1 and k=2, close to k=2 and hence has a prolate fabric ellipsoid representing an S-type of tectonite. When considering the late structure in Skurweberg (subarea 9, Fig. 3.22), the type of structure here is also a gentle, plunging inclined fold. The fabric ellipsoid here, however, is more of an oblate type, indicating an S-type tectonite. This is especially remarkable as this structure is situated in close vicinity of the Duivelsnek Shear Zone. As in the discussion of subarea 6, it has been concluded that this shear zone supplied an element of elongation, the lesser amount of elongation and the consequent shift towards a more oblate type of fabric may be evidence for a lack of continuation in southerly direction of this shear zone.

The major significance of D_{n+3} is in the interference patterns it produced with D_{n+2} structures, resulting in features such as the dome (Annex. 2 and 3).

Proof that the dome is a D_{n+2} -D_{n+3} interference pattern is supplied by the statistics of the two halves of the structure, and in particular the trend and plunge of the fold axes to the best fit girdle to pole dispersion: the axis of the southern part plunges 26° towards 110° and the axis of the northern part plunges 33° towards 293°. A pattern like that can be produced by an antiformal structure with a vertical or subvertical axial plane. The distribution of the data makes it impossible to arrive at a computed value for the trend and plunge of the D_{n+3} fold axis, since outcrop conditions allowed measurement of considerably more data of the northern closure than of the southern closure, hence the calculations performed on the entire structure tend to be overshadowed by the data of the northern closure.

When comparing the result of the D_{n+3} deformation on this part of the area with the Omkyk Structure, it appears that no significant flexure in the D_{n+2} axial plane of the Dome has been produced. This may be explained in terms of ductility contrast, as the leucogneiss in the core of the structure may be expected to be rather competent in comparison to the biotite gneiss of the surrounding areas. Another explanation may be that this part of the area is bounded by two fractures : the Neusspruit Lineament and the Duivelsnek Shear Zone, hence expansion in easterly and westerly direction is very difficult indeed and as a result the only possible direction of expansion is in vertical direction, thus resulting in a dome-like structure.

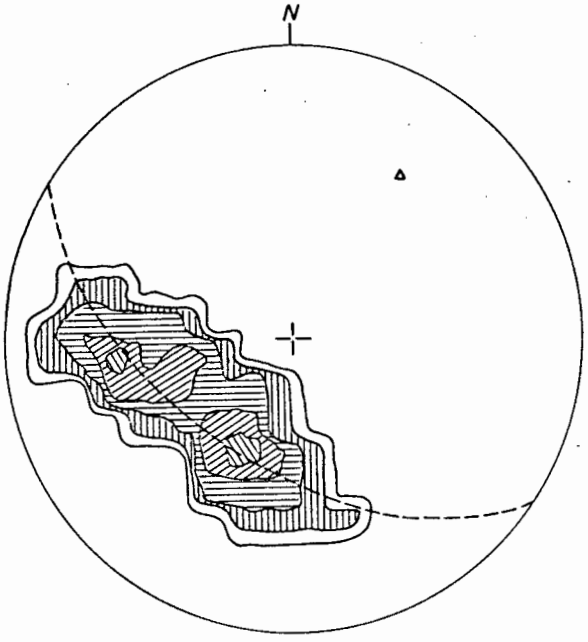

Fig. 3.21 Equal area projection of poles to S_{n+1} of subarea 7A. N_s=34
Contour lines at 1, 2, 5, 10 and 15% per percent area.

▵ = pole to girdle

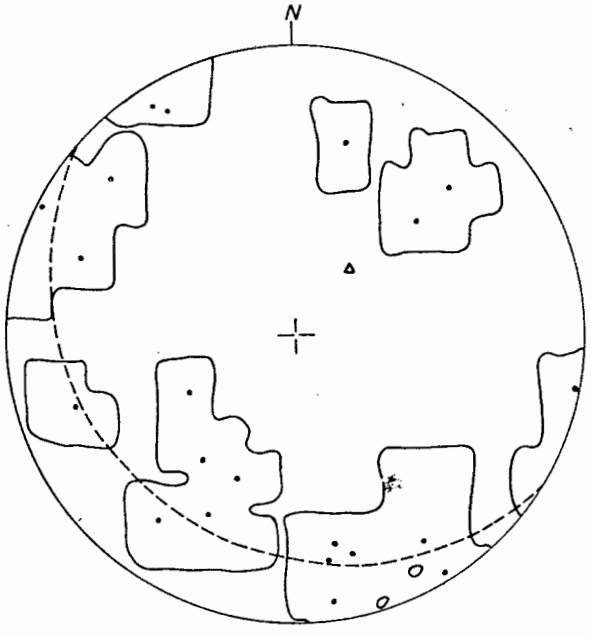

Fig. 3.22 Equal area projection of poles to S_{n+1} of subarea 9 (Skurweberg).
N_s=22
1% contour line shown.

• = pole to S_{n+1}

▵ = pole to girdle

Fig. 3.23a Intrafolial folds in leucogneiss (Station 444)

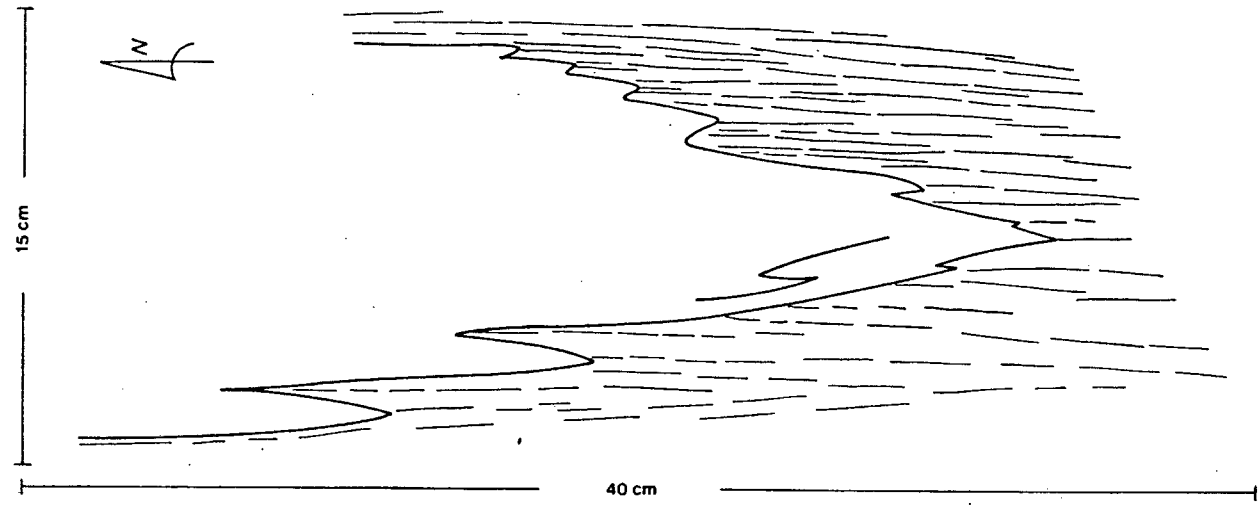

Fig. 3.23b Tight fold where the axial plane foliation is the main foliation of the region (Station 449)

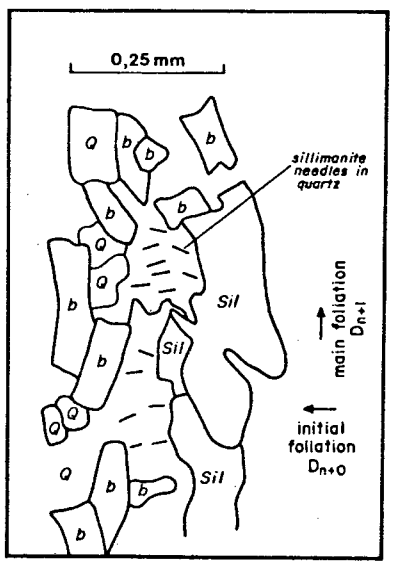

Fig. 3.24 Relics of S_{n+o} overprinted by S_{n+1} in kinzigite

Mesoscopic structures. In this part of the area, as in the Omkyk Structure, many tight and isoclinal folds have been observed in the gneisses. The folds usually have a limb-length of about 40 cm and an axial-planar foliation which is the main foliation observed in the region (Fig. 3.23b). Intrafolial folds also occur (Fig. 3.23a). These two types of folds, which are thought to be of the same generation, show different degrees of transposition, independent of their position in the area, suggesting a heterogeneous deformation pattern.

In the Venterskop Kinzigite on Venterskop, boudins occur with their long axes in the plane striking 114°, thus indicating the direction of the XY plane of the strain ellipsoid. Small minor shear zones have also been observed.

Microstructures. Due to the high grade of metamorphism this rock was subjected to during the existence of the D_{n+2} stress field, most of the pre-D_{n+2} features have been completely transposed. The only microscopic indication for the existence of an earlier foliation exists in the Venterskop kinzigite where the presence of small sillimanite needles lying perpendicular to the larger sillimanite grains orientated parallel to the main foliation, suggests that the latter is probably a crenulation cleavage (Fig. 3.24). The fact that the foliation wraps around the garnets (Figs. 2.2 and 2.3) indicates that the flattening of the fabric took place after formation of the garnets. A similar feature is recorded at several outcrops in the Wolfskop Biotite Gneiss, where small (up to 2 mm long) feldspar porphyroblasts predate the deformation of the foliation as the latter wraps around them.

3.6 Area IV

This area is bounded by the Neusspruit Lineament in the west and the Brakfontein Shear Zone in the east. It comprises three subareas, each representing an individual structure. Both closures of the Neusberg Structure are included (subareas 10 & 11) and the Koekoeb structure (subarea 14).

3.6.1 Neusberg Structure

The southern closure

The southern closure of the Neusberg Structure (subarea 11) is an isoclinal fold, easily recognisable as such in the field and outlined by a deformed contact between the calc-silicate rocks and the platy quartz-mica schist. As the axial plane dips towards 40° and the fold axis plunges towards 22° the structure is to be classified as an inclined plunging

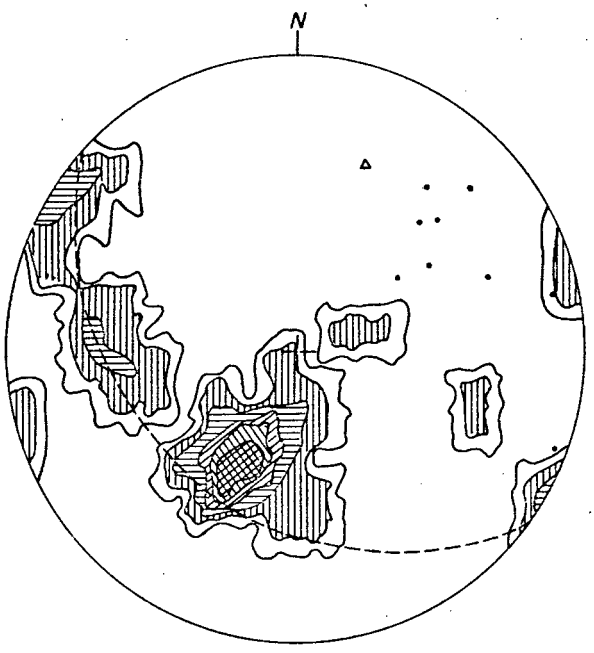

Fig. 3.25 Equal area projection of poles to S_{n+1}, subarea 11. N_s=29.
Contour lines at 1, 2, 5, 10, 15 and 20% of the points per percent area.
▵ pole to girdle. • mineral lineation.

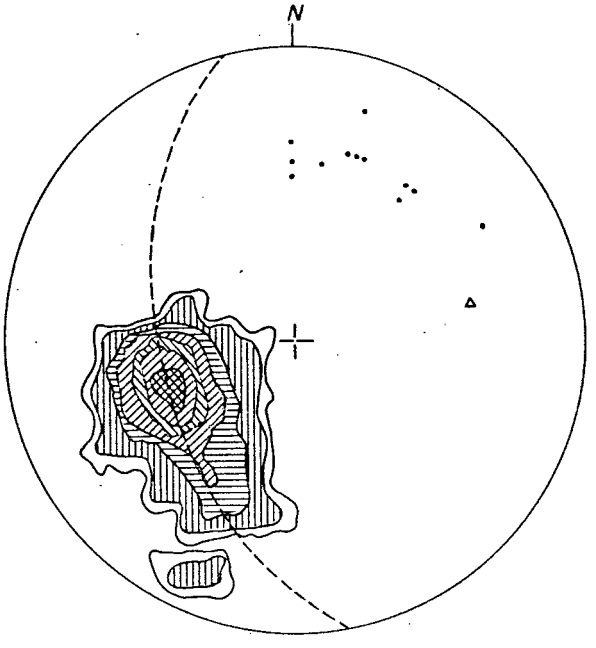

Fig. 3.28 Equal area projection of poles to S_{n+1}, subarea 10. N_s=34.
Contour lines at 1, 2, 5, 10, 20 and 25% of points per percent area.
▵ pole to girdle. • mineral lineation.

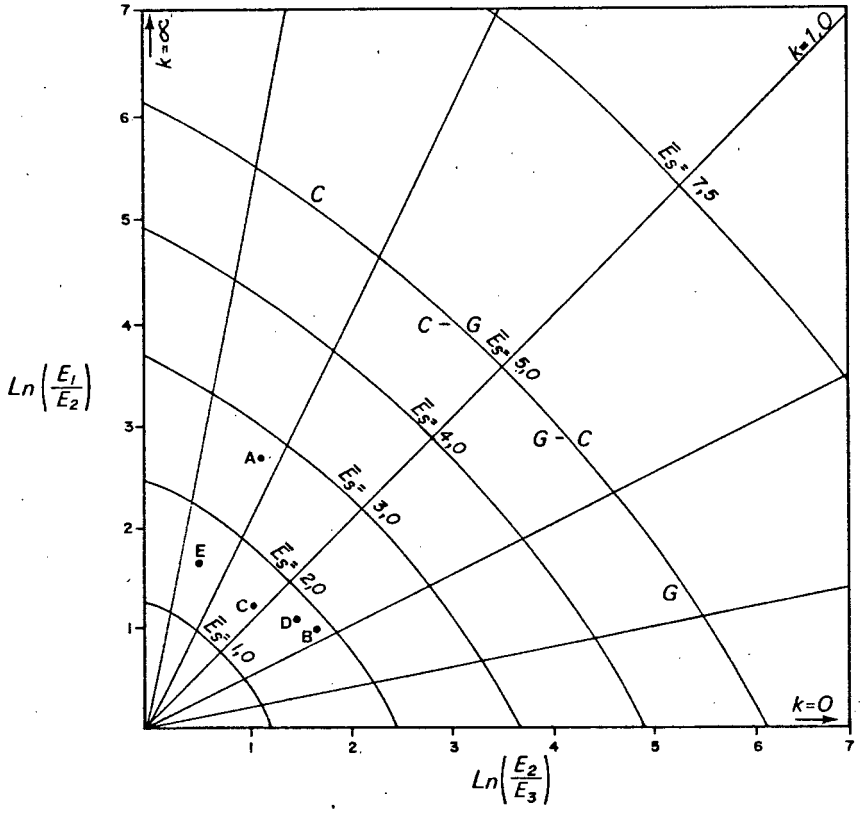

Fig. 3.27 Fabric diagram of Area IV.
A = subarea 10 (N closure).
B = subarea 11 (S closure).
C = subarea 14 (total).
D = subarea 14 (W antiform).
E = subarea 14 (E antiform).

fold. The stereogram of this structure (Fig. 3.25) is not as homogeneous as might be expected of an isoclinal structure. The main cluster (maximum of 25 percent of points per percent area) is strong enough for an isoclinal structure, but the total fabric strength parameter (1.86) falls short of the cluster criterion (fabric strength parameter = 2.0). The points outside the main cluster represent fold hinges and flexures of parasitic folds on the major structure. The total number of points on the diagram is rather low, so that the low percentage areas are not very reliable.

From field evidence it could be established that the structure is a synform, although the average mineral lineation, if interpreted as being parallel to the fold axis, instead indicates a neutral or antiformal structure. It is important to realise therefore that the mineral lineation tends to align itself parallel to the direction of maximum extension (X) of the strain ellipsoid, whereas the fold axis usually parallels the Y direction (in the ideal case) (Thaker, 1976; Schwerdtner, 1970, 1971, 1973).

On the fabric diagram (Fig. 3.27) this fold is plotted in the field between k=0,5 and k=1, indicating an oblate-type of ellipsoid.

Mesoscopic structures in this very small subarea consist of tight to isoclinal folds in the calc-silicate rocks (Station 810) demonstrating that the main foliation plane here is in fact an axial plane foliation and therefore belongs to D_{n+1}. This automatically classifies the Neusberg fold as a D_{n+2} structure, which is in good agreement with the general orientation of D_{n+2} structures throughout the area.

Boudins lie with their long and intermediate axes in the foliation plane, approximately parallel to the direction of dip. Hence the foliation here is parallel to the XY plane of the strain ellipsoid.

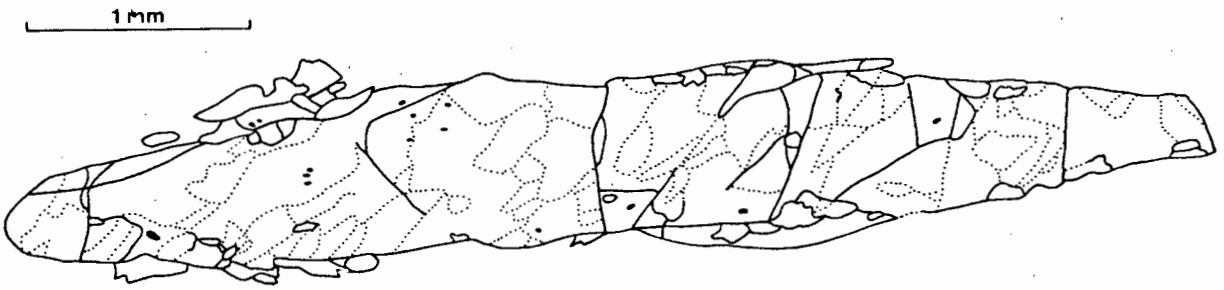

Fig. 3.26 Strongly flattened pebble with subgrains (stippled) developing at 45° to maximum direction of shortening. Section is parallel to intermediate axis of the pebble and perpendicular to long axis. m=mica; black ticks are rutile needles.

Microscopic features with a bearing on stress orientation have been observed to the north of this subarea, where a thin quartz conglomerate crops out, with the long axes of the pebbles down the dip of the foliation. A thin section cut at right angles to the long axis of one of these pebbles reveals subgrains at an angle of about 45° to the long sides of the pebble (Fig. 3.26). Because of the orientation of the pebble with respect to the foliation, these subgrains developed at approximately 45° to the main foliation and might therefore reflect the direction of the maximum shear stress in the rock. To state this with certainty, a three dimensional reconstruction of the subgrains, combined with extensive electron microscopy would be required, as at present the research concerning stress controlled preferred orientation in recrystallisation has not yet supplied a simple straight-forward model for the problem.

Neusberg Northern Closure (subarea 10)

Like the southern closure of the Neusberg this structure is an isoclinal fold as its limbs are parallel. The subarea chosen is small, but sufficient to describe the structure adequately. The stereogram of poles to foliation contains 34 points with a weak cluster distribution (Fig. 3.28). The pole to the girdle plunges 38° towards 79°, which together with the trace of the axial plane was used to find the orientation of the axial plane: dipping 42° towards 50°. Following Turner and Weiss (1963) this structure can be classified as an inclined plunging isoclinal synform. When projected onto a plane at right angles to the fold axis, according to the method described in section 3.1.2 , the fold can be classified as a class 2 structure (Ramsay, 1967). Mineral lineations, mainly defined by amphiboles and micas , are not oriented parallel to the fold axis,but plunge in north-northeasterly directions and all plot close to the axial plane. Additionally,a conglomerate layer has been found where the pebbles are oriented with their long axes down the dip of the foliation and their intermediate axes in the foliation. This implies that the main foliation in this structure is parallel to the XY plane of the strain ellipsoid. As the mineral lineations plot around this plane it is very likely that their orientation reflects the direction of maximum extension of the strain ellipsoid, so that the orientation of the strain ellipsoid is fully described. When plotted on the fabric diagram (point A, Fig. 3.27) the axial ratios indicate a pronounced prolate shape of the fabric ellipsoid, which is characteristic for an S-tectonite.

Mesoscopic structures in this subarea indicate that the main foliation, used to describe the fold, is in fact an axial planar foliation of tight to isoclinal folds (Fig. 3.29). Parasitic folds on the major structure are present as well and they invariably indicate a fold closure in a northern direction (Fig. 3.30). Fold axes plunge 30° towards 100° thus indicating that the major structure is a synformal structure.

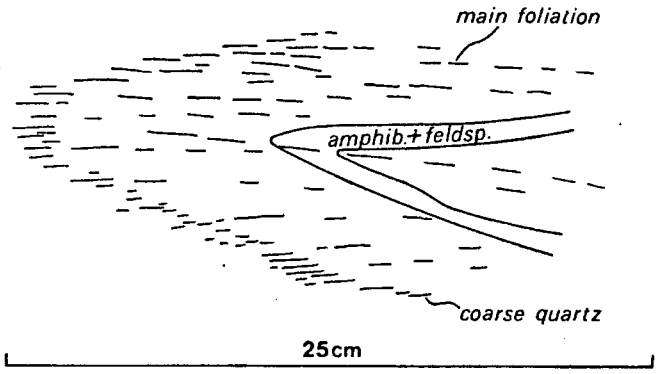

Fig. 3.29 D_{n+1} fold in Neusberg, subarea 10.

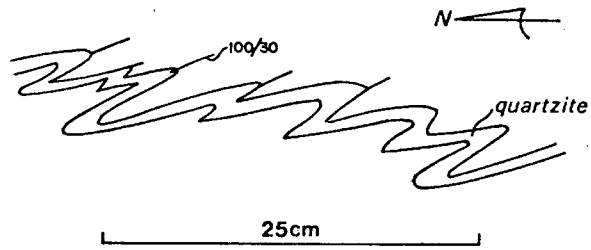

Fig. 3.30 Parasitic D_{n+2} folds in Neusberg, subarea 10.

In summary it appears that the Neusberg Structure consists of two isoclinal synforms. The traces of the axial planes of these folds together form one continuous line. This leads to the conclusion that the Neusberg Structure is in fact a strongly flattened basin, formed due to crustal shortening in the area immediately adjacent to the Neusspruit Lineament.

3.6.2 Koekoeb Structure

Situated east of the Neusberg is the Koekoeb area (subarea 14), mainly underlain by strongly deformed calc-silicate rocks. All three deformation phases are represented in this subarea. The earliest event D_{n+1} is preserved in mesoscopic features such as fold hinges.

The main event in this subarea is D_{n+2}, reflected by two antiforms flanking a synform (Fig. 3.31). Both antiforms are plunging inclined structures. Strike/dip of the axial plane of the western antiform is 307/54 whereas the trend/plunge of the fold axis is 328/28, so that it is a plunging inclined structure. The interlimb angle is 20° and some shearing took place parallel to the axial plane, characterised in the field by silicification. The fabric ellipsoid of this tight structure is oblate. Figure 3.32a is the stereogram of this structure and it is a rather diffuse pattern for such a tight fold. This is mainly due to many smaller structures as a result of competence differences in the calc silicate rocks, especially in the

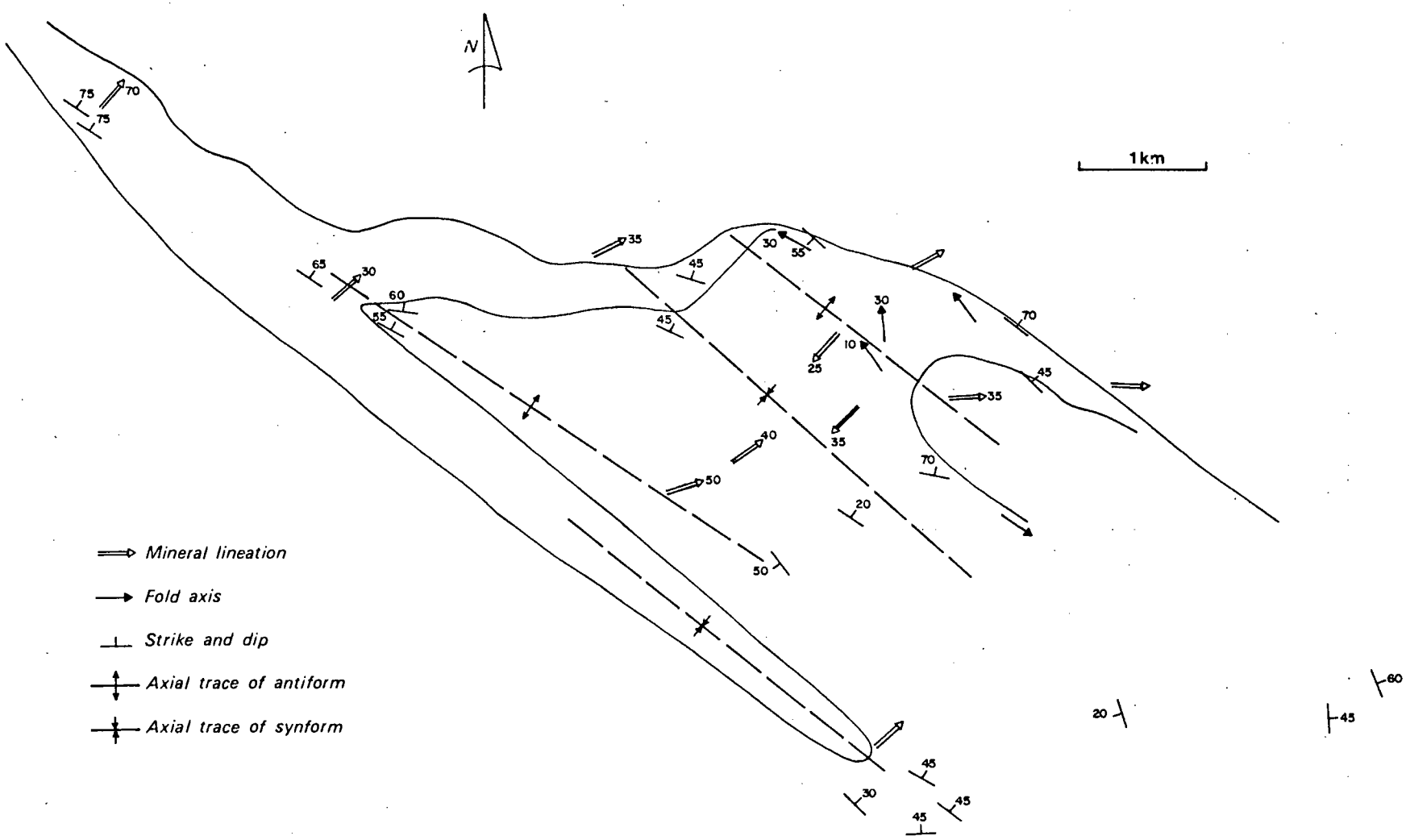

Fig. 3.31 Map of Koekoeb Structure and Neusberg-South closure.

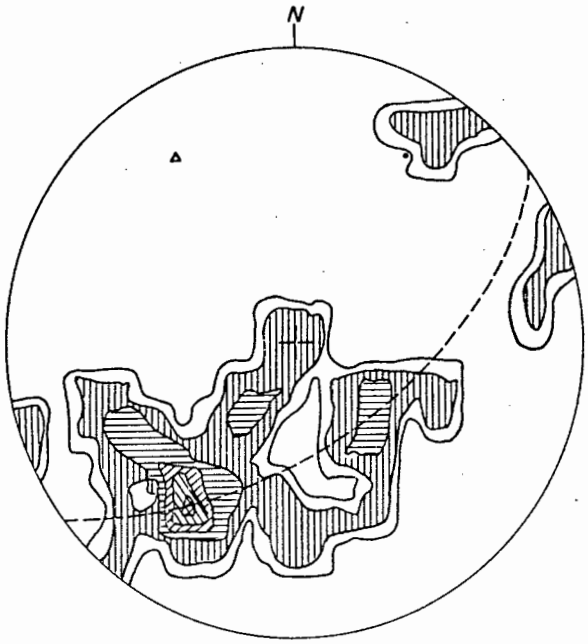

Fig. 3.32 A

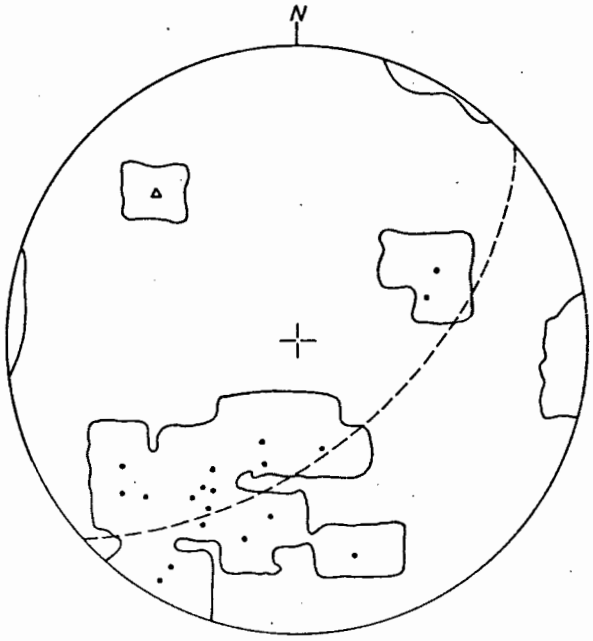

Fig. 3.32 B

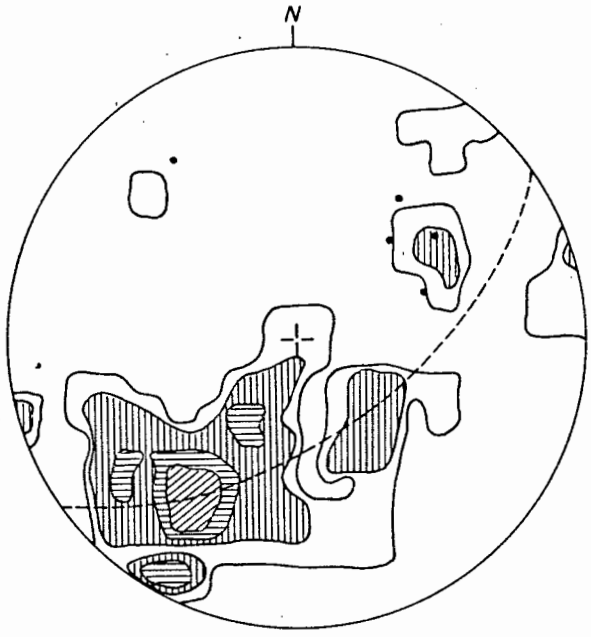

Fig. 3.32 C

Fig. 3.32 Equal area projection of poles to S_{n+1} in Koekoeb area. Contour lines at 1, 2, 5, 10 and 15% of points per percent area.

▵	=	poles to girdle
A	=	Western antiform N_s = 37
B	=	Eastern antiform N_s = 23
		1% contour line shown
.	=	poles to foliation
C	=	Total area N_s = 60
•	=	mineral lineations

vicinity of the bands of wollastonite. Other factors are the emplacement of the charnockitic adamellite and the influence of D_{n+3}.

The eastern antiform is a similar structure. This too is an inclined plunging tight antiform (str/dip of axial plane 291/52, trend/plunge of axis 319/30). The fabric ellipsoid is markedly different from the former ellipsoid, as it plots well in the prolate field of the fabric diagram, thus showing a strongly constrictive fabric. Unfortunately the data on which this diagram is based are very few (Fig. 3.32b) so that it is not very reliable.

The synform, flanked by the two previously mentioned structures is mainly reflected by the outcrop pattern (Fig. 3.31) and the trend of the foliation.

The extent of these three structures is of a local character only, as the structures in the subareas 16 and 17 do not seem to be related to the Koekoeb folds. Because of the limited information available on the last two structures described, the stereogram on Annex. 2 (Fig. 3.32c) includes all three folds, in order to obtain a more reliable fabric ellipsoid.

Mesoscopic structures in the Koekoeb area are mainly ptygmatic folds, generally parasitic to the main D_{n+2} structure and themselves possessing parasitic folds. An example of such a situation can be found at Station 159.

Otherwise mesoscopic structures are generally tight folds with an axial planar foliation, thus supporting the interpretation that the major structures in this subarea are D_{n+2} structures, as these mesoscopic folds deform the oldest recognisable fabric element in the area: S_{n+0} and their axial plane (S_{n+1}) is deformed to form the larger structures.

The fold as shown in Plate 1 is a good representation of the type of structure occurring in and close to the wollastonite bands. They are isoclinal folds and some of them could be described as elasticas. When analysed according to the method outlined in section 3.1.2 they appear to be class 1C folds.

Microscopic structures are very scarce in this area. However, where they have been observed it could be confirmed that the main foliation in the area is the axial planar foliation to D_{n+1} folds. The fabric element that is deformed is the oldest observed and can be an original lithological banding. Obviously it is not possible to exclude the possibility that this deformed foliation is in fact a metamorphic or tectonic banding, but clear microstructural indications to back such a supposition are not available in the thin sections studied.

3.7 Area V

This area contains the Koms Structure south of the Orange River and the Warm Zand Structure to the north of the Orange River.

3.7.1 Koms Structure

The Koms Structure as a whole is represented by diagram 15 on Annex. 2 (Fig. 3.33). It is a large synformal structure, severely disrupted by large intrusions of adamellite and Straussburg Granite along the Brakfontein Shear Zone. As a result this structure is not completely preserved and no closure could be established. This explains the position of the girdle to cluster distribution on the orientation diagram : the entire structure should have yielded a stronger concentration of poles in the northern area of the diagram, representing the southerly dipping readings of the expected closure. The interpretation that it is a synform with its closure in the north is based on the following :

In the feldspathic quartzite on the Komsberg-Gifberg range crossbedding is preserved, providing indications that the sequence is younging upwards. In the Neilers Drift range however, the same criteria indicate that the rocks here are younging downwards. These overturned rocks can be explained by an overturned synform with a shallow, easterly dipping axial plane. Alternatively, one can propose an antiform with an easterly dipping axial plane, but the parasitic fold on the western limb of the structure indicates a synform as both the fold axes plunge in easterly directions, away from the fold closure. The position of the closure is inferred from structures further south, a possible connection with the Warm Zand Structure and the fact that the feldspathic quartzite gets thinner towards the south. An additional feature is that the crossbedding indicates a return to the top normal situation around Station 1149 (Appendix A). This can only be explained in a synformal structure.

From the directions of the axes of the parasitic folds it can be concluded that the calculated orientation of the axis for the total Koms Structure is more or less correct : plunging 44^{o} towards 73^{o}. As the axial plane dips towards 55^{o} and the axis plunges towards 73^{o} this structure is to be classified as an inclined, plunging syncline. The tightness of the fold is difficult to assess because the closure has not been preserved. The fabric ellipsoid is oblate and plots close to the k=1 line on the fabric diagram (Fig. 3.34). Structures such as boudins have not been encountered in the Koms Structure, so that no indications on the orientation of the XY plane of the strain ellipsoid are available. However, mineral lineations with an average trend and plunge of 053/59 indicate the direction of maximum extension, most probably of the D_{n+1} strain ellipsoid.

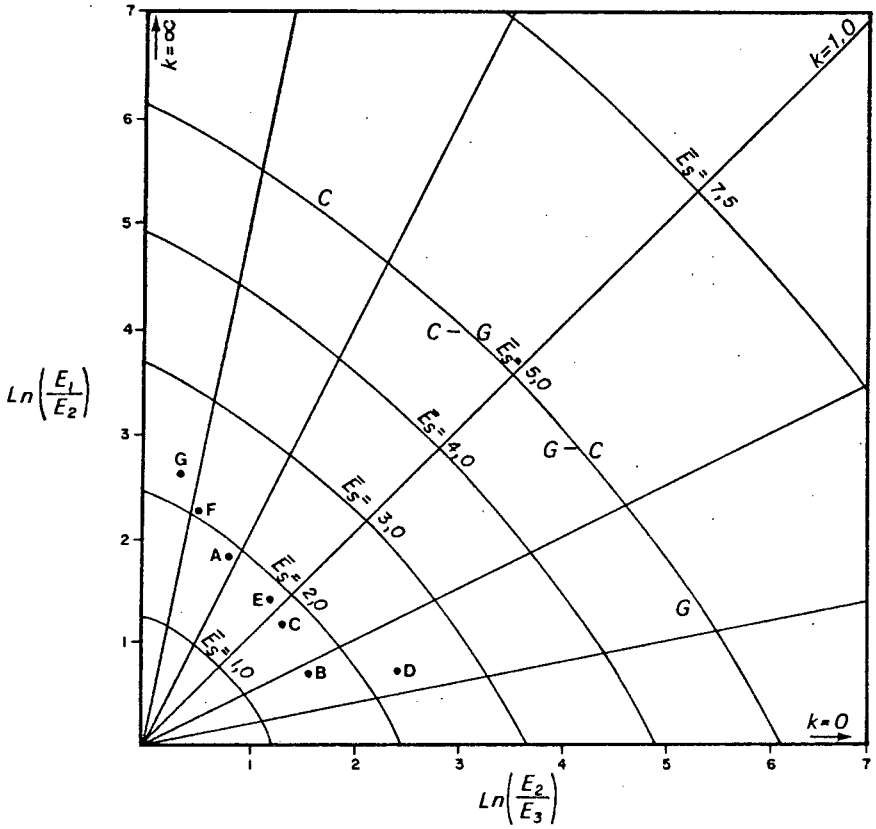

Fig. 3.34 Fabric diagram of Area V plus Curries Camp.

A = subarea 12 (Warm Zand North)
B = subarea 13 (Warm Zand South)
C = subarea 15 (Koms Total)
D = subarea 16 (Koms North)
E = subarea 17 (Koms South)
F = subarea 18 (Curries Camp)
G = east ridge of subarea 13 only.

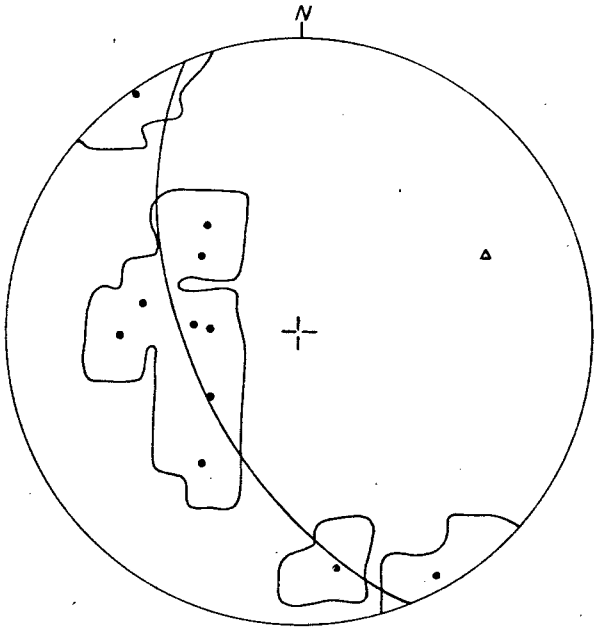

Fig. 3.35 Equal area projection of poles to S_{n+1} of Northern parasitic fold of Koms Structure. N_s=11
1% contour line shown.
▵ = pole to girdle
• = poles to foliation

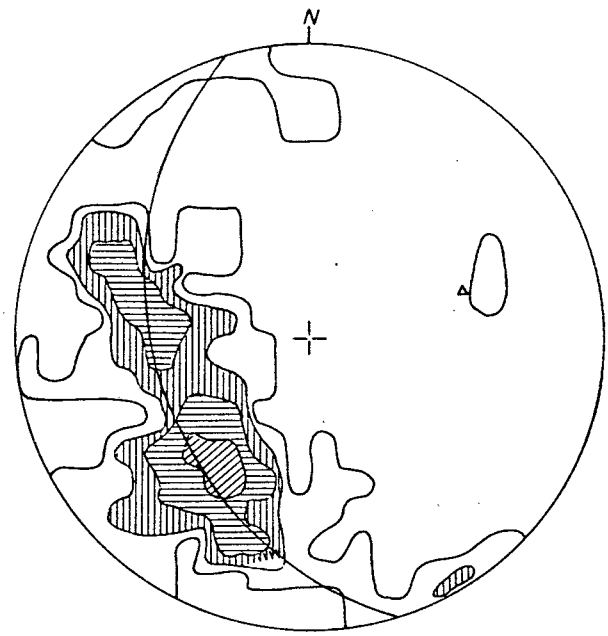

Fig. 3.33 Equal area projection of poles to S_{n+1} of total Koms Structure. N_s=66. Contour lines at 1, 2, 5 and 10% of points per percent area.
▵ = pole to girdle

Mesoscopic and microscopic structures have not been found outside the subareas 16 and 17.

Subarea 16 contains the northern flexure of the structure parasitic on the larger Koms Structure. It is an anticlinal structure, with its fold axis plunging 30° towards 65°. As the axial plane dips 42° towards 15° this structure is a plunging inclined open fold (interlimb angle approximately 90°). A classification on fold profile could not be made as no lithological contacts other than of intrusive character are available. Fig. 3.35 shows that the stereogram of the poles to the foliation is a weak girdle. Due to the low number of points (11) the statistically derived classifications are not very reliable and this applies to the position of point D in Fig. 3.34 as well, where the fabric ellipsoid is shown to have a strongly oblate shape.

Mesoscopic structures are scarce, which is mainly due to the fact that the feldspathic quartzite is a rather competent rock. Boudins have been observed (Station 30) with their long axis down the dip of the main foliation (S_{n+1}) and the intermediate axis in the foliation, thus giving an indication of the orientation of the XY plane of the strain ellipsoid. Added to this is the orientation of a mineral lineation of 54/40, so that the position of the strain ellipsoid at this point is fully described.

Microscopic structures have not been observed in this subarea.

Subarea 17 is the southern flexure of the structure parasitic on the Koms Structure. From the trend and plunge of the fold axis and axial planar trace, the strike and dip of the axial plane have been calculated to be 269/90, so that with a fold axis plunging 39° towards 89° the structure is to be classified as a plunging upright, open syncline (interlimb angle about 90°). In Fig. 3.36 the stereogram of this structure shows a diffuse cluster to girdle pattern. On the fabric diagram (point E, Fig. 3.34) this fold plots just above the k=1 line in the field of prolate ellipsoid shapes.

Mesoscopic structures indicate that the foliation in this subarea developed during the oldest recognisable event. In the calc-silicate rocks at Station 1490 (Appendix A) isoclinal folds are observed. The main foliation in the subarea is parallel to the axial-planar foliation. It appears that in the direct surroundings of this particular station severe flattening took place as transposition of the foliation has taken place, producing intrafolial folds. The strong flattening is not surprising as this station is situated on the Neusspruit Lineament.

In the feldspathic quartzite some pebbles have been observed with their long axis down the dip of the foliation and intermediate

axis in the foliation. No conclusion may be drawn in this case concerning the orientation of the strain ellipsoid, as in this obviously sedimentary rock an original random orientation of the pebbles cannot be assumed to have occurred.

Microscopic Structures have not been observed in this subarea.

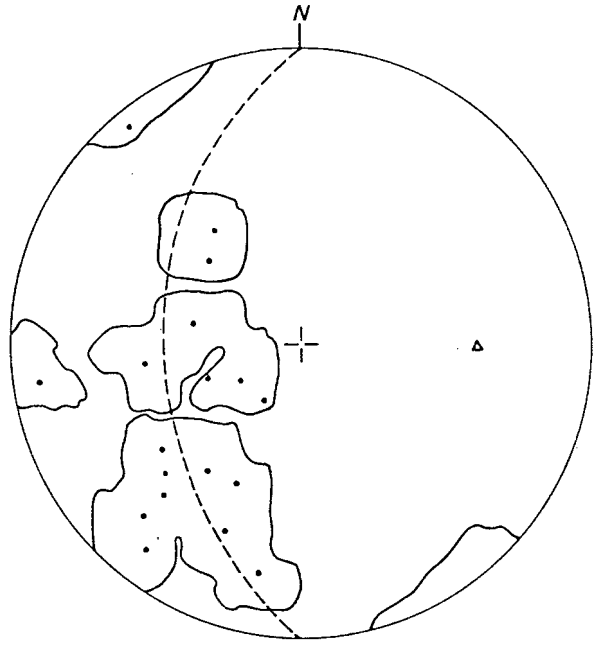

Fig. 3.36 Equal area projection of poles to S_{n+1} of southern parasitic fold on Koms Structure (Subarea 17). N_s = 18. 1% contour line shown. • = poles to foliation
▵ = pole to girdle

3.7.2 Warm Zand Structure

The Warm Zand Structure is a domal structure, partly the result of interference of the last two deformational events. It has been divided into two subareas, on the basis of the D_{n+3} structures.

The northern part (subarea 12) is a synformal D_{n+3} structure, expressed by the deformation of a D_{n+2} fold limb. The stereogram of the structure shows a diffuse cluster (Fig. 3.37) with a pole plunging 29° towards 323°. Combining this orientation with the trace of the axial plane yields an axial plane dipping 30° towards 298°, a near-reclined fold. On the fabric diagram the fabric ellipsoid of this fold plots in the prolate field (point A, Fig. 3.34), which means that it is a S-type fabric.

The reason that only one limb of the D_{n+2} structure is preserved lies in the oblique position the axial plane has with respect to the Neusspruit Lineament and the Brakfontein Shear Zone, so that in a northerly direction an increasing part of the D_{n+2} structure is being cut off. This also explains why the southern part of the Warm Zand Structure is more completely preserved.

Mesoscopic structures in subarea 12 invariably confirm the hypothesis that the main foliation is in fact the axial plane of D_{n+1} folds. These folds are generally isoclinal and observed in the calc-silicate rocks only. The lack of folds in the gneiss can be explained by competence differences between the gneisses and the calc-silicate rocks : because the Wolfskop Gneiss is here rather leucocratic it may be expected to be more competent than the more biotite-rich variety, exposed in the Omkyk-Central Dome area. No boudins have been observed in this area, but a few mineral lineations, plunging approximately 40° towards 60° could be measured, so that the X-direction of the D_{n+1} strain ellipsoid for this area could be established.

Microscopic structures in this subarea are rare, a fact that can very well be due to recrystallisation as a result of the intrusion of granites so close by (Annex. 1). In some cases relics of a crenulation cleavage have been observed, supporting the mesoscopic evidence that the main foliation is of tectonic origin, most probably a crenulation cleavage, partly transposing the older foliation.

Subarea 13, the southern part of the Warm Zand Structure, is an interference structure, resulting from D_{n+2} and D_{n+3} folding on near orthogonal axes supplying mainly information on the D_{n+2} deformational event for the major structure. This can be seen from a comparison of the stereogram representing this part of the structure (Fig. 3.38) and the traces of the D_{n+2} and D_{n+3} axial planes (Annex. 2). The distribution in Fig. 3.38 is a diffuse girdle with a fold axis plunging 29° towards 100°. Combined with the

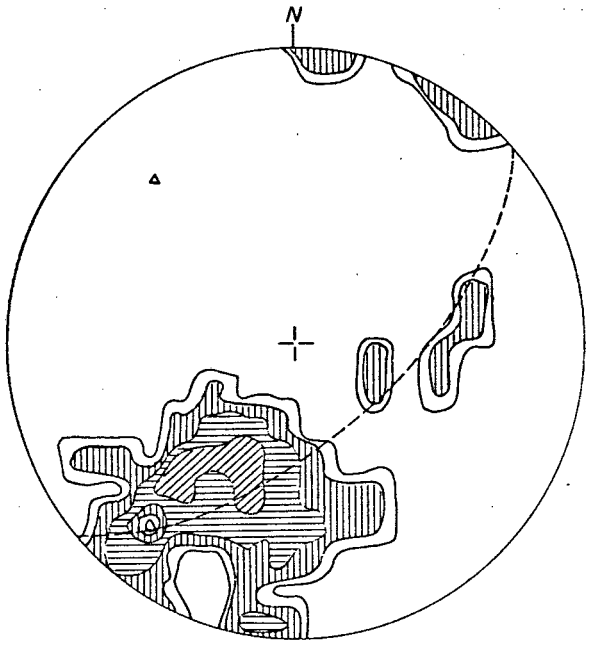

Fig. 3.37 Equal area projection of poles to S_{n+1} of northern part of Warm Zand Structure (subarea 12) N_s=40 Contour lines at 1, 2, 5 and 10% of points per percent area.
▵ = pole to girdle

Fig. 3.38 Equal area projection of poles to S_{n+1} of southern part of Warm Zand Structure (subarea 13)

▵ = pole to girdle

A Total structure, N_s= 94
Contour lines at 1, 2, 5 and 10% of points per percent area

B Eastern ridge of subarea 13 only.
N_s=22 1% contour line shown
• = pole to S_{n+1}

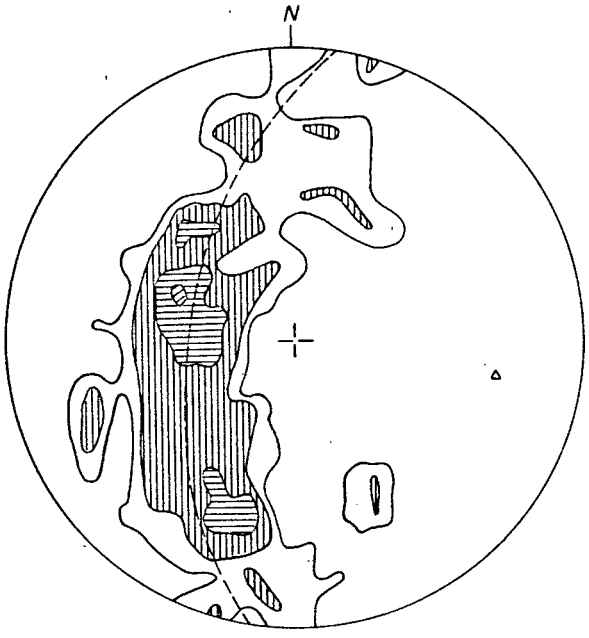

Fig. 3.38 A

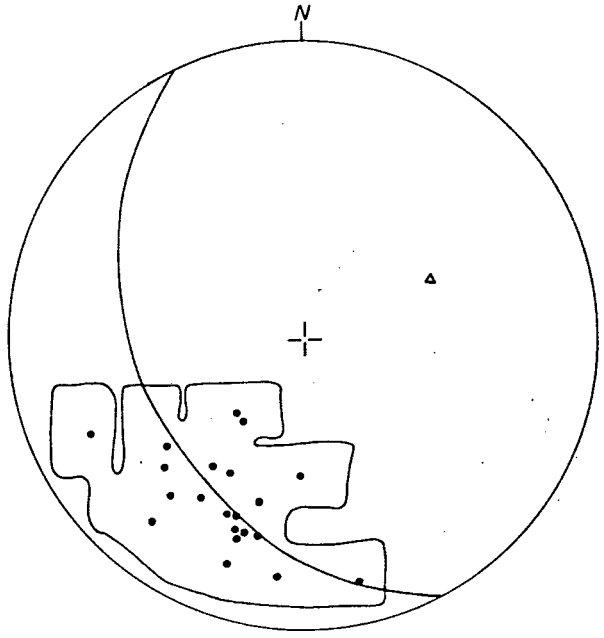

Fig. 3.38 B

trace of the axial plane this yields an axial plane dipping 53° towards 165°. The fabric ellipsoid for this structure has a rather oblate shape (point B, Fig. 3.34) and the total fabric of this structure can be classified as that of an S-tectonite. The fold itself is classified as a plunging inclined, open antiformal fold. This structure has been modified by D_{n+3} but this last deformational event is considerably weaker than on the western side of the Neusspruit Lineament. Because the Warm Zand Structure and the Koms Structure are related and their axial planes at some stage probably continued into one another, the plunging D_{n+2} fold axis is probably mainly the result of the transition from antiform to synform and to a far lesser extent the result of D_{n+3} deformation. The effect of D_{n+3} on this subarea is best reflected by the flexure in the eastern ridge of the structure. (Fig. 3.38b shows that the influence of D_{n+3} is not very strong, as the diagram hardly shows any deviation from the D_{n+2} pattern (Fig. 3.38a)). The fabric is a very strong S-tectonite, as the fabric ellipsoid plots quite close to the k= ∞line (point G, Fig. 3.34).

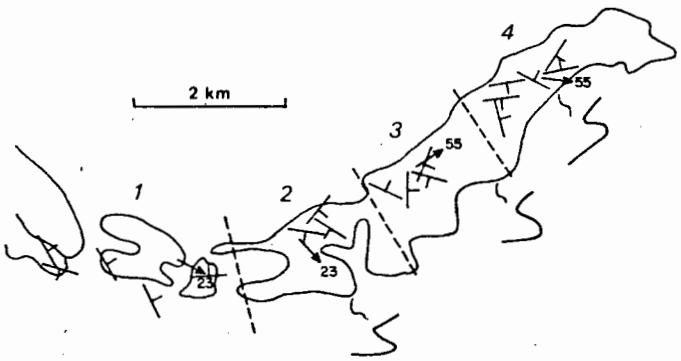

Fig. 3.39 Sketch map of the southern ridge of the Warm Zand Structure. The division into four groups of structures is shown, together with their asymmetry.

Mesoscopic structures in subarea 13 exist mainly in the calc-silicate rocks and folds of both D_{n+1} and D_{n+2} are present. On the southern ridge of the structure four groups of folds have been mapped, together forming a series of S-shaped parasitic folds (Fig. 3.39). These structures were of great value in determining the position and character of the major fold closure. Processing these groups of data with VECSTA-PLOT revealed that all four folds fall in the group of L-S to S-L tectonites, with plots on the fabric diagram around the line k=1. Another result of the application of the programme is that it can be shown that all four folds have axes plunging in easterly directions. This feature, combined with their S-shape undoubtedly leads to the conclusion that the Warm Zand Structure is an anticlinal structure. Parasitic folds occur frequently on the limbs of the structures described above. These D_{n+2} folds are generally small with wavelength of 4 to 7 cm.

D_{n+1} structures are usually isoclinal with an axial planar foliation (S_{n+1}). At some places this D_{n+1} foliation reached a high degree of transposition, with intrafolial folds as a result, as shown in Figure 3.40.

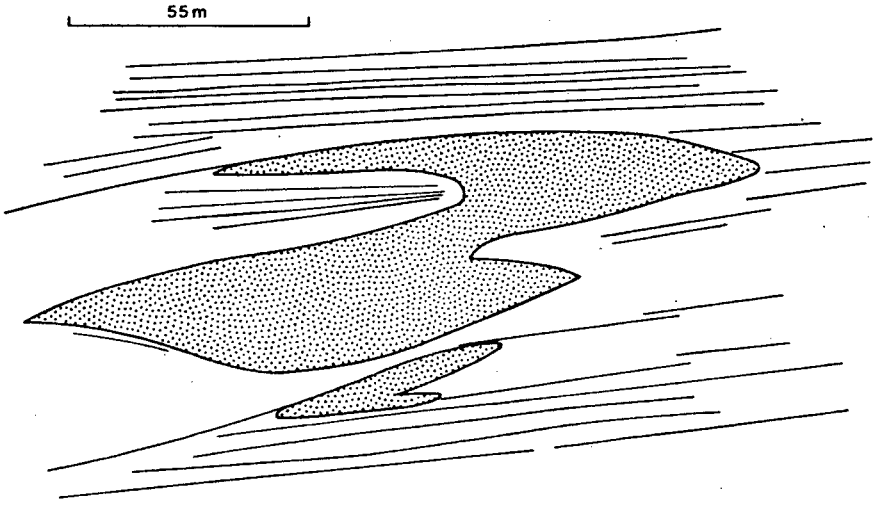

Fig. 3.40 Intrafolial fold in calc-silicate rocks at Friersdale.

The planar structure of the eastern ridge does not supply any information on the type of strain. The presence of structures as shown in Figure 3.41 suggest that elongation took place. As this feature lies in the main foliation plane, this is most probably the orientation of the XY plane of the strain ellipsoid. Another possibility is that this kind of structure resulted from the emplacement of intrusive rocks in the vicinity, maybe by stoping.

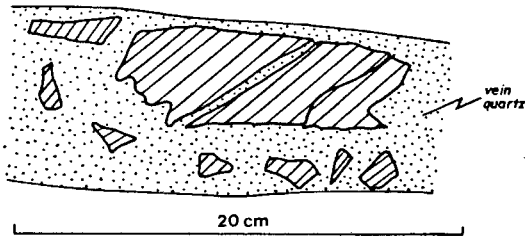

Fig. 3.41 Broken calc-silicate rocks at Friersdale.

A type of mesoscopic structure, different from that described above, consists of ptygmatic flows folding in the calc-silicate rocks. Invariably they developed in the vicinity of and most probably due to, the adamellite and Straussburg Granite.

Microscopic structures are rare, but when found generally support the foregoing interpretation. Only one thin section from the many studied from this area shows microfolding, which is defined by a band of quartz and feldspar deformed into close folds with a sharp hinge and penetrative axial plane : D_{n+1}

3.7.3 The relationship of the Warm Zand Structure to the Neusberg Structure

The relationship of the Warm Zand Structure to the Neusberg Structure is shown in the three dimensional diagram on Annex. 3. The cross-bedding in the feldspathic quartzite as described in section 2.7.2 indicates that the direction of younging is in westerly direction, so that it could be established that the rocks forming the eastern slope of the Neusberg are most probably overturned and thus represent the overturned western limb of the Warm Zand Structure. The repetition in the sequence in the Neusberg is due to imbrication : in the north the hinge of the Warm Zand antiform is cut by the Brakfontein Shear Zone. The overturned western limb of the Warm Zand antiform became detached from the eastern limb of the Neusberg synform and subsequently either the Neusberg synform moved upwards or the western limb of the Warm Zand Structure moved downwards. No significant cutting out or repetition of units along the Brakfontein Shear Zone has been noted and as the presence of calc-silicate rocks between the gneiss and the feldspathic quartzite suggests the contrary, it is concluded that the imbrication as shown in Annex. 3 is only of limited importance.

3.8 Curries Camp Structure (Area VI, subarea 18)

The easternmost structure in the area is situated at the farms Curries Camp and Zoovoorby. The structure is not directly connected with the other structures described, as it is separated from them by intrusive rocks and no post D_{n+2} structures occur. It is a synclinal structure (Annex. 1,3), which is obvious from aerial photographs and field observations. A total of 29 poles to S_{n+1} are plotted in Fig. 3.42, which shows a weak cluster around a pole plunging 42° towards 87°. Combination of the pole and the trace of the axial plane yields an axial plane dipping 56° towards 36°. The structure is therefore to be classified as an inclined plunging syncline. On the fabric diagram (Fig. 3.34, point F) the fabric plots as a S-tectonite with a strongly prolate fabric ellipsoid.

Mesoscopic structures are scarce in this structure and have only been observed in the calc-silicate-rich rocks, where closed D_{n+1} folds indicate that the main foliation is S_{n+1}. In this foliation plane $^{n+1}$boudins are oriented with their long axis down the dip and intermediate axis in the foliation and hence the XY plane of the strain ellipsoid is parallel to the main foliation. Mica and quartz mineral lineations in the feldspathic quartzite (Station 1197) plunge 40° towards 46° and most probably indicate the direction of maximum extension of the strain ellipsoid, which, combined with the evidence of the boudins, is thus fully described.

Microscopic structures indicate that the main foliation is a crenulation cleavage, deforming original lithological banding, as polygonal outlines of relic crenulation cleavages have been observed. In most thin sections these features do not occur, indicating complete transposition of the original features.

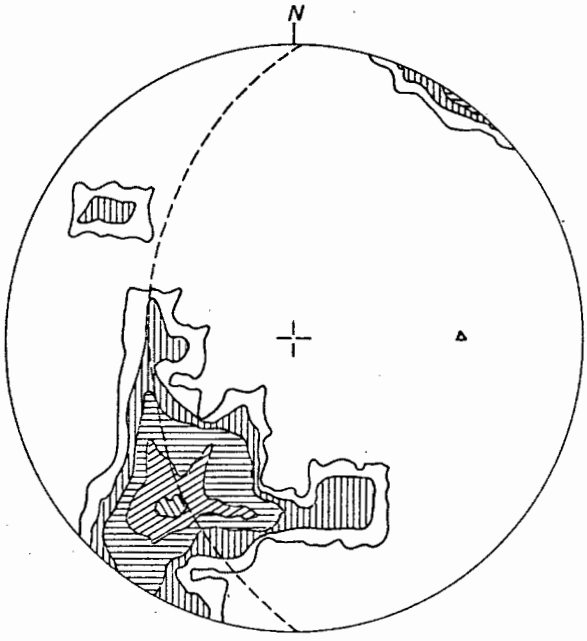

Fig. 3.42 Equal area projection of poles to S_{n+1} of Curries Camp Structure.
N_S = 29 Contour lines at 1, 2, 5, 10 and 15% of points per percent area.
▵ = pole to girdle

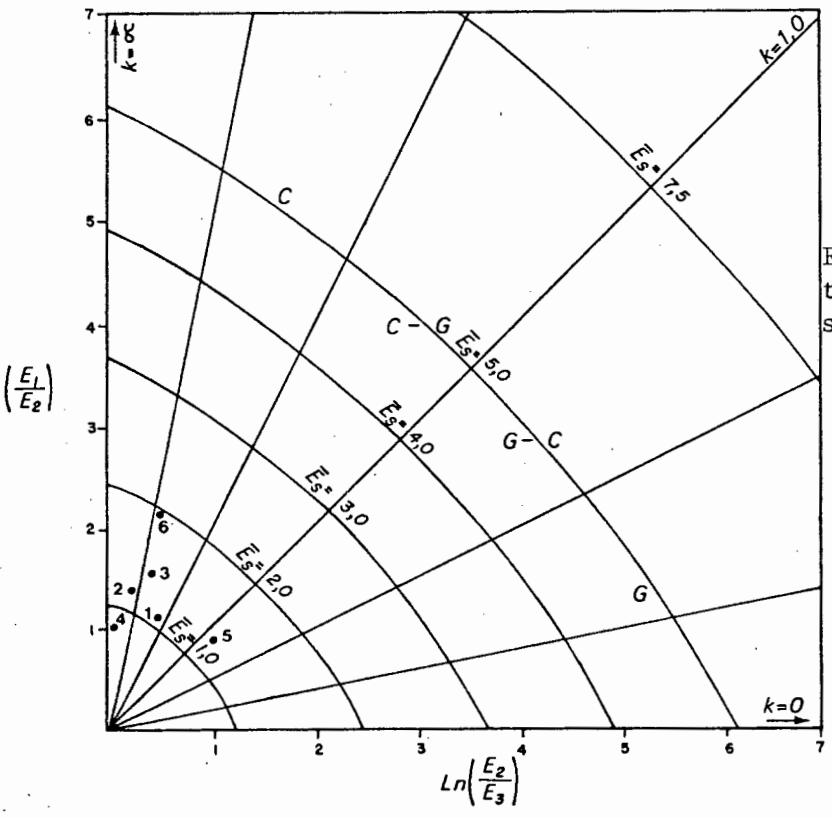

Fig. 3.43 Fabric diagram showing the fabric ellipsoid plots of the six areas.

3.9 Variation of strain through the area

When interpretation of the variation of the fabric shape through the area is attempted, it is important to realise that the k-parameter used in the fabric diagram is analogous to, but certainly not the same as the k-value of Flinn (1962, 1978; Woodcock, 1977). When poles to planes are plotted on a stereogram, a girdle is interpreted as an L-tectonite (Lisle, 1977), which has a strain ellipsoid where $\infty > k > 1$ (Sander, 1970; Flinn, 1962; Ramsay, 1967). On the fabric diagram however (section 3.2), a girdle plots in the field where $0 < k_f < 1$.

If the descriptions of the previous sections are regarded with this in mind, the following conclusions can be drawn with respect to the distribution of bulk strain through the area. Pronounced clusters of poles occur in the direct vicinity of the Neusspruit Lineament, (Annex.2) indicating S-tectonites (points 2,3 and 4 in Fig. 3.43). Note that point 4 (Area IV) is closest to the $k_{fabric} = \infty$line and that point three of these three is the furthest away. In terms of total bulk strain this means that the strain ellipsoid of Area IV is extremely oblate, the strain ellipsoid of Area II less oblate and the ellipsoid of Area III the least oblate of the three. This agrees very well indeed with the structures described in this chapter: very strong flattening along the Neusspruit Lineament resulted in a very planar fabric. Area II contains the Kakamas Shear Zone and here too the fabric is rather planar, especially in the shear zone itself. The reason that the ellipsoid is slightly different lies in the style of the folds: they are not as tight as in the Neusberg and hence yield a more linear fabric ellipsoid. Although Area III is not transected by a shear zone, considerable flattening occurred, which is reflected in the total strain. Away from this central part of the area the fold characteristics are those of more open folding and this too is reflected in the strain ellipsoid. As in previously mentioned areas, the rocks of area I constitute an S tectonite, but to a lesser extent than the central three areas. This may be a reflection of the fact that fold hinges have not been documented all that well, so that the orientation diagram does not reflect the structure to the same degree as is the case in the central block. It may therefore be expected that the strain ellipsoid of this area is less oblate than it appears to be from the available data.

Area V plots in the girdle-cluster field and hence is an L-S-tectonite with a slightly prolate ellipsoid. Note that the presence of the Brakfontein Shear Zone apparently has no influence on the strain ellipsoid.

Area VI again is a pronounced S-tectonite with a rather strong oblate strain ellipsoid. This can be explained by the presence of the southern continuation of the Cnydas Shear Zone.

In summary, the bulk strain over the study strip reflects the presence of major shear zones. From west to east the strain ellipsoid becomes more flattened, slightly less oblate between Neusspruit Lineament and

Kakamas Shear Zone, extremely oblate along the lineament, then suddenly changes to slightly prolate in the Koms-Warm Zand area and back again to oblate when the Cnydas Shear Zone is approached.

Two important conclusions are drawn from this pattern:

- The Kakamas Shear Zone and the Neusspruit Lineament (Fig. 3.2) are of similar importance with respect to the total bulk strain, whereas the Brakfontein Shear Zone appears to be a minor event, in terms of total bulk strain.
- D_{n+3} did not have any significant influence on the distribution of the bulk strains throughout the area (compare Area III and Area VI)

It is important to know what the reliability is of the strain markers used and what folding phase they exactly represent. Additionally it should be investigated what the initial state of orientation of the fabric elements was, as the method used to correlate fabric shape with strain type depends on the assumption of an initially uniform or random state of orientation of the fabric elements.

Boudins are an expression of layer parallel extension and form at right angles to the direction of maximum shortening (Ramsay, 1967; Hobbs *et al.*, 1976). This means that whenever boudins are encountered, the orientation of the XY plane of the strain ellipsoid is known. Throughout the area boudins have been shown to be oriented with the plain defined by long and intermediate axis parallel to the main foliation and hence the main foliation in those places is parallel to the XY plane of the D_{n+1} strain ellipsoid. As a result, the variation in orientation of the main foliation is a measure of the post-D_{n+1} deformation. Of D_{n+2} and D_{n+3} the latter played a subordinate role in the formation of the distribution of total bulk strains. This is based on the following.

Cloos (1947) states that in limestones a foliation first appears at 20% shortening and Wood (1973) shows that strain in slates from Wales and Vermont exceeds 60% shortening. This suggests that a relation exists between the total amount of strain and the development of a foliation. Obviously, a foliation is more easily developed in a micaceous than in a quartzo-feldspathic rock. In experiments on plasticine-plasticine and plasticine-painters putty models conducted by the author (Van Bever Donker, 1974) along the lines of the theories of Ramberg (1970, a & b, 1971) and Biot (1961, a & b, 1965) it was demonstrated that when shortening exceeded 23%, amplification and flattening of the folds takes place (limbs move into parallel position and become parallel to $\sigma_2 - \sigma_3$ plane). When applying these values to the structures in the area under consideration the following conclusions can be drawn with respect to the three folding phases.

- The observation that D_{n+1} folds have almost completely been transposed can indicate that a considerable amount of shortening took place syn- or post D_{n+1} (these two possibilities can, without markers, not be distinguished). How much shortening took place cannot be established.

The fact that a considerable amount of shortening and transposition took place suggests that after D_{n+1} a rather uniform orientation of the foliation existed. This means that correlation of the post D_{n+1} fabric shape with this type of strain is possible.

- Shortening in D_{n+2} exceeded 23% as flattening obviously took place but probably did not reach values significantly high to produce a penetrative foliation, apart from the Neusberg area, where shortening probably exceeded 60%.
- Shortening during D_{n+3} did not reach the threshold value for flattening (23%) as no flattened structures appear to exist.

It is possible to calculate the maximum shortening by assuming layer parallel shortening and initially flat lying strata. To achieve this, the ratio between the surface distance between two points on the profile and the length of the folded layer between the same two points is calculated (Fig. 3.44).

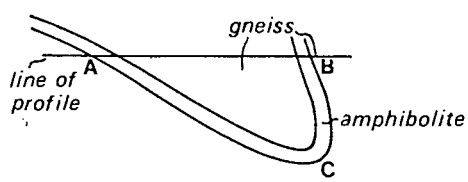

Fig. 3.44 Method to calculate layer parallel shortening: profile of Omkyk Structure taken from profile A-B (Annex. 1).

$$\text{Shortening} = \frac{ACB-AB}{ACB} \times 100\%$$

The results of the calculations made for the individual structures in the area (Table 3.2) support the conclusions regarding the shortening during the respective deformation phases mentioned above. As the D_{n+3} shortening is relatively little and took place in a different direction (almost orthogonal D_{n+2} and D_{n+3} axial planes), the main foliation has mainly been deformed in D_{n+2}. Hence the variation in total bulk strain mentioned above is a result of the D_{n+2} deformation.

Two more conclusions can be drawn on basis of the distribution of the bulk strains and the shortening percentages throughout the area:

- The importance of the major shear zones in the area is reaffirmed (74% and 66% shortening near the Neusspruit Lineament and the Cnydas Shear Zone)
- a relation exists between the type of tectonite and total shortening: large shortening yields S-tectonites, little shortening L-tectonites

and intermediate shortening L-S or S-L tectonites.

Structure	Type of Tectonite	Shortening %
Regt Kyk	S-L	30
Omkyk	S-L	42
Central Dome	L	20
Neusberg N	S	74
Warm Zand N	S	50
Koekoeb	S-L	58
Curries Camp	S	66

Table 3.2 Relation between shortening and type of tectonite of the various structures

This last conclusion means that the shape of the fabric ellipsoid through the area is an indication of the variation in total bulk strain through the area.

When taking a closer look at the values listed in Table 3.2, it appears that the results do not always meet the predictions: from their setting between or next to shear zones it is expected that Omkyk and Koekoeb would have been S-tectonites, rather than S-L-tectonites. In Omkyk it is thought that the linear component is the result of the D_{n+3} deformation (8% shortening; calculated on basis of the deformation of the eastern limb) resulting in the slightly bent axial plane and limbs of the structure. In Koekoeb the L-component is thought to be of a different origin, as the structures are probably slightly distorted by the emplacement of the adamellite. The amount of shortening in D_{n+3} is calculated on a bent limb of the Omkyk Structure, subarea 7A and the eastern ridge of the Warm Zand Structure and never exceeds 8%. This small amount of shortening is accompanied by the slow strain rates obtained for D_{n+3} on basis of deformation structures in the quartz crystal lattice in and east of Neusberg (Section 4). The values in the order of 2-7 x $10^{-12}sec^{-1}$ at $800^{o}K$ and $10^{-14}sec^{-1}$ at $550^{o}K$ with 20 kcal/mole activation energy and 5-6 x $10^{-19}sec^{-1}$ at $800^{o}K$ and 6-11 x $10^{-25}sec^{-1}$ at $550^{o}K$ with 55 kcal/mole activation energy suggests slow to very slow strain rates, the latter even suggesting a "standstill" (Price, 1975).

3.10 Conclusions

The area has been deformed by three folding phases. Of D_{n+1} very little is known except that it formed the regional foliation and in places tight to isoclinal and intrafolial folds. Two large D_{n+1} structures are still discernable.

The second event was the major event, during which the major structures formed. Shortening due to this event ranged from 30% in the west to 74% in the Neusberg, with a "low" of 20% in the Central Dome and 66% in the east. The structures that formed during D_{n+2} are plunging inclined structures, with axial planes dipping towards the northeast. These dips vary between 30^{o} and 50^{o}, but increase to 60^{o} in the east (Curries Camp). In the area where shortening was most severe, an imbricated structure developed (the northern part of the Warm Zand Structure) with possible overthrusting from northeast to southwest.

Both the fold pattern and the total bulk strain distribution appear to be strongly affected by a number of major shear zones of which the Kakamas Shear Zone, Neusspruit Lineament and Cnydas Shear Zone are the most important. Of these three the Neusspruit Lineament has the most outstanding appearance because of the associated platy quartz mica schist. It appears to be the oldest of the three as it has been shown to have been in existence before the deposition of the feldspathic quartzites of the Neusberg Formation and thus prior to D_{n+1} (Section 2.7).

The last deformational event yielded a small amount of deformation (7-8%) at slow to extremely slow strain rates. Interference of this D_{n+3} with D_{n+2} in some cases resulted in domal structures such as Regt Kyk and Central Dome. Further east, however, the influence of D_{n+3} decreased and it is not recorded at all in Curries Camp.

With regard to the orientation of the D_{n+1} and D_{n+2} structures, it was thought that D_{n+1} and D_{n+2} followed shortly after each other and together form a more or less continuous process with two distinct pulses, with possibly an angular difference. The interpretation that an appreciable time span lapsed before the last folding phase took place hinges on the fact that the intrusive rocks, belonging to the "1000 My event" suffered some deformation during D_{n+3}. This leads to the conclusion that D_{n+3} and this thermal event were related to each other and not to the older two deformation phases, as the intrusions took place after D_{n+2} was completed.

4. TRANSMISSION ELECTRON MICROSCOPY

4.1 Introduction

Transmission Electron Microscopy (T.E.M.) in geology is a still young and rapidly increasing field of research. In 1965 McLaren and Phakey describe the first application of T.E.M. on quartz samples, with the clear object of studying dislocation structures in the crystal lattice. The paramount problem then was the preparation of the required ultra-thin (~0,1 μm) samples. Crushing the rock and hoping for fragments with sufficiently thin edges was the common method. The introduction of the ion-beam thinner in the early seventies (Gillespie, McLaren and Boland, 1971; Heuer *et al.*, 1971) was a great leap forward. As a result, one now has the ability to thin large areas of a known orientation and one is able therefore, to compare quite accurately the optical features of the specimen such as deformation lamellae, with the observed defects in the crystal lattice (White, 1973 b, c). Presently it is possible to distinguish the type of recrystallisation that took place in the system (White, 1973a, 1977) which in turn supplies information that enables the observer to arrive at an estimate of the strain-rate under which the system has been deformed provided certain conditions are fulfilled.

The aim of the present electron microscopy programme carried out was twofold. Firstly it was intended to compare the results of the etching technique described by Ball & White (1977) with the results of electron microscopy, both performed on the same sample. Secondly it was intended to use the now available knowledge of the behaviour of quartz under deformation with the aim to develop a method to estimate the strain-rate of the deformation phase responsible for the development of the observable lattice defects in quartz.

4.2 Evaluation of plastic deformation on the scale of the crystal lattice

Ardell *et al.*, (1973) describe the dislocation substructures of experimentally deformed quartz rocks, which have been examined by Transmission Electron Microscopy. The tests were performed under well-known conditions, thus making it possible to arrive at a conclusion regarding the relation between strain-rate and the observed dislocation substructures. Two notable

facts were reported:-

- the dislocation density appears to be related to the strain-rate temperature combination
- there are no signs of recovery within the deformed original grains, but recrystallisation features did occur. This indicates that recrystallisation takes place easier than recovery (Ardell, *op.cit.*).

In order to explain the first of these findings it is important to have a good understanding of the different sources of dislocations.

One of the sources of dislocations is the occurrence of growth imperfections in the form of point defects, such as vacancies and impurities. For quartz this number may be taken as $10^3 cm^{-2}$ (Hobbs, *et al.*, 1976). The main source of dislocations however, is deformation. Gyulai and Hartly (1928) state that point defects are generated when a crystal is being deformed. In plastic deformation two parts of the crystal move with respect to each other. Should this shearing be brought about in one step, by simultaneous movement of all the atoms in a specific plane from one position of perfect registry to the next, disruption or at least local melting of the crystal would be expected (Christie and Ardell, 1974). The theoretical critical shear-stress required for this is :

$$T_{th} = \frac{d}{a}\frac{G}{2\pi} \qquad (4.1)$$

where G = the shear modulus
d = the spacing between atoms in the direction of the shear-stress
a = the spacing of the rows of atoms.

Calculated values for copper, silver and gold are in the range of about $T_{th} \sim \frac{G}{30}$ which is many orders of magnitude greater than the observed values of 10^{-4} to 10^{-6} G in well-annealed crystals. The difference between the calculated and the observed values is accounted for by the presence and movement of dislocations. The deformation moves through the crystal as a wave-like motion so that the actual lattice distortion at any moment is limited to a very narrow region (Hobbs *et al.*, 1976).

Von Mises (1928) and Taylor (1938) point out that the homogeneous deformation of an aggregate of randomly orientated grains without change of volume requires shear on five independent slip-systems. However, not all of these slip-systems have been verified experimentally in quartz, in fact, movement in the directions [a+c] yield severe difficulties and in contrast to the other systems, only becomes operational at temperatures over 750°C (Wilson, 1973; Ball & White, 1978). If quartz nevertheless deforms plastically at lower temperatures, it is the ability of dislocations to climb out of a specific plane that relaxes the von Mises criteria and enables quartz to deform plastically (Ball & White *op.cit.*). The presence of dislocations

will increase the total free energy of the system. In order to reduce the free energy several processes operate:

- Recovery
- Primary recrystallisation
- Normal grain growth
- Secondary recrystallisation is the growth of some grains unstable at elevated temperatures. The temperature should be sufficiently high for this to happen.

(for a more comprehensive outline of these processes, see Hull, 1965).

If the sample were to be annealed in the absence of the confining stress, the first three processes should produce a strain-free rock, with a grain size smaller than the original grain size. Normally such a situation will not take place in nature; it is normal that the confining stress still operates while the recovery, etc. start. Therefore the generation of new dislocations will continue; together with the processes to reduce the number of dislocations. This combination is called dynamic recrystallisation (White, 1973a).

Another source of dislocation generation is found in the grains themselves. When a crystal is bent, this deformation will be reflected by a wall of dislocations and a number of dislocations in the grain. During recrystallisation, eventually subgrains will form with an irregular shape. This shape can be explained by the mean free path of the dislocations, in other words, the distance a dislocation can move through the lattice until it meets more dislocations of the same sign, or one of the opposite sign. As all the grains together form a complex pattern, it is evident that the free path in the different cells will not be equally long. Thus irregular, interlocked grains will form. Because of this interlocking of the new grains, stresses will develop in the grains when the deformation of the lattice continues, and the recrystallisation process recommences (White, 1973a).

4.3 Dislocation movement and its controlling factors

Several factors are known to control the movement of dislocations. Of them the factor temperature is recurring in almost each formula. In dealing with the effect of temperature on dislocations Leibfried and Dietze (1951) and Dietze (1952) regard the atoms across the glide plane as regions of finite extent. Thermal vibration will cause an uncorrelated motion of neighbouring atoms, which makes the actual atomic position less exact. This in turn reduces the energy of misfit across the glide plane, since neither complete register nor complete disregister can be achieved. That is why the dislocation is wider at higher temperatures and hence more mobile (Nabarro, 1967).

The deformation maps (Fig. 4.1 .) constructed by White (1976) and Rutter (1976) are based on the assumption that the deformation mechanism in quartz is either by dislocation glide, dislocation creep, Coble creep (stress-induced grain boundary diffusion) or Nabarro-Herring creep (stress-induced lattice diffusion). Dislocation glide is so-called conservative motion in which the dislocation moves in the surface defined by its line and Burgers vector. The three other processes however are non-conservative motion in which the dislocation moves out of the glide plane. Climb is the mechanism that brings this about and in order to get climb operating, a minimum amount of energy is required, as the movement of the dislocation from one place to another happens by means of ion-diffusion. Data on diffusion in quartz are rather rare. From experimental work carried out by Tullis *et al.*, (1973), White (1976) calculates the diffusion rate at a specific temperature, by substituting a value of 5×10^{-14} cm^2s^{-1} for the absolute diffusity D_o into the Arhenius relation:

$$D_{v(T)} = D_o \exp (-Q_v/RT) \qquad (4.2)$$

where Q is the activation energy for volume diffusion, T the temperature in ^{o}K.

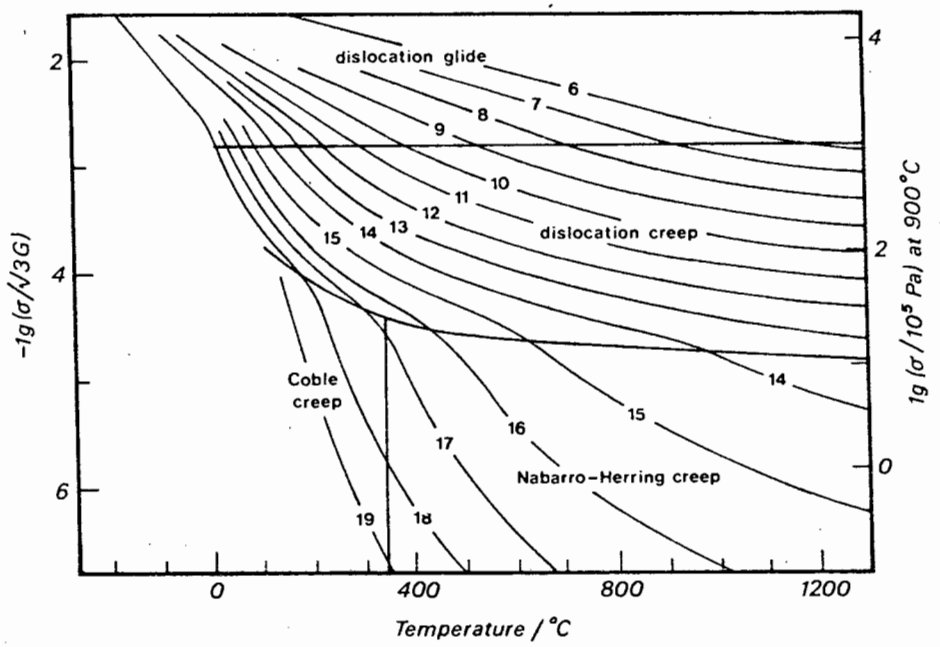

Fig. 4.1 Deformation map for quartz after Rutter, 1976.

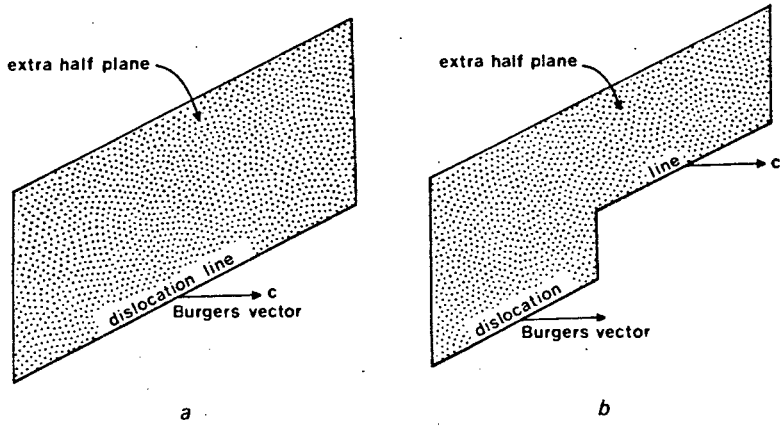

Fig. 4.2. Climb of an edge dislocation that has Burger's vector c. By changing the shape of the extra half plane, that is, by extending it or shortening it at any one place (b), the dislocation line moves out of one slip plane into a parallel, neighbouring one. This motion is called *climb* (after Hobbs *et al.*, 1972).

4.4 The effect of water on the mobility of dislocations

Two categories can be distinguished here:

1. The case where water is situated in the crystal lattice. This actually means that a number of Si-O-Si bonds have been changed into Si-OH bonds, which are less strong than the original bonds. As dislocation climb involves the breaking and subsequent healing of bonds when material diffuses through the crystal, it is self evident that the presence of water in the crystal lattice of quartz will ease the dislocation movement and therefore increase the plasticity of the crystal. This is called hydrolythic weakening (Hobbs, McLaren & Paterson, 1972; Hobbs, 1968; Griggs & Blacic, 1965; Griggs, 1967).

2. The case where water is located in bubbles, sitting in the crystal lattice as a kind of impurity, has exactly the opposite effect. Here the dislocations, when encountering one of those bubbles, are unable to progress and are trapped, or rather pinned. The result is that with the same stress and increasing strain more dislocations get pinned and thus the crystal hardens. This is called strain hardening (Hobbs, McLaren & Paterson, 1972; Knipe & White, 1978).

The activation energy for quartz varies from 15 kcal. mol^{-1} for OH^- diffusion (White, 1970, 1971) and 25 kcal. mol^{-1} for Na^+ (Frischat, 1970). What actually happens when climb takes place, is that material is diffusing towards or away from the dislocation core, so that the length of the extra half plane alters (see also Fig. 4.2). This is only possible when the rate of solid-state diffusion can keep pace with dislocation movement, i.e. at high temperatures or slow strain-rates. A highly probable mode of deformation in quartz is cross slip of screw $[c+a]\{10\bar{1}0\}$ dislocations on to $\{10\bar{1}1\}$ (Hobbs *et al.*, 1976).

In Plate 6 many dislocations, pinned by some kind of an impurity, are shown. In the centre of the picture some split dislocations (parallel lines) can be seen, these may be stacking faults, where one dislocation is decomposed into two partial vectors each having Burgers vectors enclosing an angle of 120°. If such a dislocation were to move by cross slip onto another plane the two parts should be merged first, which requires a certain amount of energy : the stacking fault energy (γ) :

$$\gamma \simeq G \frac{b_1 - b_2}{2 \pi d} \qquad (4.3)$$

(after Amelinckx, 1964 p.247)

where G = shear modulus
b_1 and b_2 the two Burgers vectors (estimated)
d = distance between the parts of the dislocation.
The lower the energy the more problematic cross-slip becomes :

γ < 20 dyne cm^{-2} gives work hardening
γ < 5 dyne cm^{-2} makes cross-slip very difficult

As $\gamma \simeq$ 1,166 dyne cm^{-2} in this case, cross-slip can not operate, hence climb must be the mechanism of dislocation movement. On this basis Ball & White (1978) use the formula

$$V = D\sigma b^2/kT \qquad (4.4)$$

for the velocity V with which dislocations move,
where D = the diffusion rate
σ = the differential stress
b = Burger's vector 5×10^{-8} cm
k = Boltzman's constant
T = absolute temperature

From the formulas for D and v it will be clear that T and σ are actually the only two variables. Therefore for each combination of σ and T, a value may be obtained that reflects the maximum speed at which a dislocation can move, expressed in cm/sec., when climb is the factual means of dislocation movement.

4.5 The reason why the dislocation substructures in quartz can act as a memory for the deformation history

When considering a quartzite under deformation it is evident that the individual grains are not free to move, as the fabric consists of mutually interlocked grains. In the previous paragraphs it has been explained that bending is accommodated by edge dislocations: an excess of dislocations of one sign develops, with undulous extinction as a result. In order to lower the total free energy of the system, dislocations start to move and are arranged into low-energy subgrain walls. Depending on σ and T they move to a steady state arrangement. If all this occurs at 500°K the subgrain structures are at a minimum energy for this temperature and are consequently very stable at lower temperatures. Furthermore, as the subgrain walls are constructed out of "necessary dislocations", they must remain for as long as the bending caused by the deformation remains, that is until recrystallisation or obliteration by a later deformation.

Thus subgrains in quartz may preserve a memory of the past deformation conditions and of the role of subgrains in the formation of strain-free grains during dynamic recrystallisation.

4.6 The relation strain-rate - dislocation density

A dislocation generated as a result of the deviatoric stress will begin to move to the boundary of the area. If this dislocation with a strength b reaches the boundary and subsequently moves out, the strain of the body (of a unit length measured in the direction of b) will equal b. When at a specific moment n dislocations with a length b move out of the crystal, the strain at that very moment will equal n.b. To express the strain rate, all one has to do is to express the amount of strain per unit time.

As the velocity v gives the maximum speeds at which a dislocation can travel by means of climb under specific conditions, a combination of the strain with the velocity v gives the maximum strain rate that can be taken up by dislocation climb at a specific combination of temperature and stress :

$$\dot{\varepsilon} = nbv \qquad (4.5)$$

4.7 Reliability

The reliability of the method is strongly dependent on the quality of the observations done for the individual calculations.

In formula (4.5) n represents the number of mobile dislocations and this factor of the three is the one that yields the highest number of possible errors. Factors that influence the ultimate number of dislocations may intervene as early as the preparation of the sample, where, unless very carefully handled indeed, dislocations may be generated in cutting the specimen. It is self evident therefore that only by treating the specimen with the utmost possible care, this factor can be minimized effectively and even eliminated as the polishing process removes the affected material.

During the second stage of sample preparation where the sample is being subjected to ion bombardment, the unavoidable risk of changing the orientation of the dislocations exists, e.g. a stable dislocation "confronted" with a thinning environment may have to rotate to find a new stable orientation, hence its intersection with the surface of the foil shall change (Hirsch *et al.*, 1965). Also dislocations may move out of and into the thin area, but these two movements shall probably balance each other.

It is known that the temperature in the ion-beam thinner increases considerably above room-temperature. This will affect the mobility of the dislocations, as has been pointed out previously. An exact figure for the temperature increase in the instrument used at U.C.T. is not known. A factor of uncertainty is not introduced in the accuracy of the dislocation density measurements as the number of dislocations moving out of the thin area is likely to be the same as the number that migrates into the thin area.

If the correct method of counting the dislocation density is applied, this re-orientation need not give any problems. Two methods are available:

- the length of dislocation line per cm^3 N_V
- the number of dislocation lines threading an area of 1 cm^2 (N_S)

The advantage of the latter method is that the thickness of the foil need not be known, thus eliminating a source of inaccuracy. Also the orientation of the dislocation and therefore the length between its intersections with the surfaces of the foil is not significant, thus eliminating possible errors due to the ion-bombardment. Nabarro (1967) gives the relation between the two methods : $N_V = 2N_S$

For obvious reasons it is important to make sure that all dislocations in a specific area are being observed. To achieve this, certain conditions have to be met in the electron microscopy, because some dislocations will not show up, unless several strong reflections are operating (Hirsch *et al.*, (1965). In order to meet this condition one has to tilt the sample with the goniometer stage until either two-beam condition (i.e. two points for which the Bragg condition is satisfied) is reached, or a zone-axis orientation has been achieved (i.e. until the observer looks along a crystallographic zone axis). The latter method is to be preferred over the former for several reasons : When a zone-axis orientation is reached, the electron diffraction pattern represents the highest possible number of points, for which the Bragg

condition is fulfilled. This means that there is a large area for which the special reflections mentioned above are in operation, hence the largest number of dislocations will be visible (compare Plates 7 & 8). The advantage of tilting the sample in this manner is that a large area can be studied at once, whereas in the case of two-beam condition, several smaller areas have to be studied before the same area of the sample is covered. As quartz is very sensitive for beam radiation the zone-axis method will yield better results, as the time a specific area is exposed to the beam is considerably shorter than when the two-beam method is used repeatedly.

To be sure all dislocations are registered in the area of observation, ideally one should tilt to all possible zone-axes, as obviously dislocations that are visible when looking along one zone-axis, need not be visible when looking along another zone-axis. On the other hand, there is a real risk that the same dislocation is observed several times and hence counted several times, thus influencing the accuracy of the figure obtained.

Another important factor is the reproducability. Because of the problems experienced in the sample preparation it was not possible to repeat the experiments on samples from similar locations in the time available for the project as a whole. It should be stressed however, that the reliability depends for a great deal on the reproducability of the experiments.

4.8 Geological factors influencing the accuracy of the method

The main problem area is the sensitivity of quartz for deformation and recrystallisation.

As has been stated earlier, the process of dislocation generation and subsequent annihilation continues as long as the same stress field is in operation and as long as sufficient energy is added to the rock to keep the recrystallisation going. If temperature and stress fall simultaneously below their critical values, it is obvious that the strain-rate of the deformation can safely be deduced from the preserved dislocation substructures. In the event where either of the two outlasts the other one however, complications do arise and specific dislocation patterns may be the result, as in both cases no steady-state conditions are in operation: When the temperature outlasts the deformation, movement of dislocations remains possible after the generation of new dislocations has ceased. This will result in features such as network structures of dislocations, which are regarded as being representative of recovery structures (Ardell *et al.*, 1973). Eventually a situation such as this one will in the ideal case result in strain-free grains of quartz with triple-point junctions and straight grain boundaries. In the other case generation of dislocations will continue, but the energy available is not sufficient to move the dislocations into more stable configurations and strain hardening follows. As a result the number

of dislocations increases rapidly, tangles of dislocations become increasingly abundant, the total free energy of the specimen increases considerably and ultimately brittle failure will take place. From these descriptions it will be clear that the two cases just described can actually be recognised in the electron microscope. What cannot be recognised however, is the case where a renewed rise in P/T conditions took place which is not reflected in the metamorphic mineral paragenesis. Although stable configurations such as subgrain boundaries are unlikely to move, mobile single dislocations that stopped moving due to lack of energy, will be reactivated and in addition new dislocations will be generated, so that effectively the entire cycle of dislocation generation and annihilation is in operation again. It is this restarting of the cycle at submetamorphic P/T conditions that forces the geologist into the assumption that the latest mineralogically observable event registered has been the last occurring event indeed, as no distinction can be made between mobile dislocations left behind by either of the deformation phases. The same applies to the formation of walls of dislocations : it is not possible to distinguish between walls formed at e.g. 800°K and 5 kbar and those formed at 500°K and 3 kbar.

4.9 Sample preparation

The basis for each T.E.M. sample in geological multimineralic samples is of necessity a thin section, as one of the purposes of T.E.M. is relating the submicroscopic features to the optical features. This thin section should be polished on both sides to at least 1 μm as experience teaches that even the smallest differences in section thickness are accentuated by the ion-beam thinning.

After completion of the optical microscopy a copper grid is glued onto the sample with a quick-setting epoxy resin in such a manner that the grain to be studied is in the centre of the grid. Subsequently grid and T.E.M. sample are separated from the thin section. To allow this the thin section must be prepared such that the removal of the rock from the substratum is possible.

Two methods have been tried to achieve this. Firstly a polished sample was mounted on unfrosted glass with lake-side (which will become fluid when heated). A major problem here was the lower bonding strength of the lake-side compared to araldite, as a result of which pitting occurred frequently when preparing the sample, to such an extent that in some instances the entire sample was destroyed. As a result samples could not be ground down to the correct thickness, which resulted in extremely long thinning periods (up to 100 hours) in addition to identification problems in optical microscopy. In an attempt to evade these problems polished thin sections were mounted with araldite on thin perspex, which, after grids were mounted and photography was performed, was dissolved in acetone. This was a very successful method as far as the separation of

sample and thin section is concerned : a highly polished (1 µm), rather thin (30 µm) sample was obtained. However, this method had to be abandoned for two reasons : firstly because perspex is not an optically neutral medium optical mineral identification was impossible and secondly because the araldite cannot be removed from the sample, it has to be thinned away in the ion-beam thinner. As araldite particles are deposited all over the interior of the ion-beam thinner, even into moving parts such as the gearbox, the performance of the machine decreases gradually, until it finally comes to a halt.

In the end the only method that yielded satisfactory results was to mount a less perfectly polished sample with lake-side onto frosted glass and grind it down to approximately 30 µm. This method allows optical work as well as the removal of the grid plus sample by heating up the thin section. Subsequently soaking in acetone cleans off the remnants of the lake-side.

Failure rate in sample preparation is fairly high, mainly due to bonding problems : about 50% of mounted copper grids will come off again. The reason is that the bond between the two rather smooth surfaces of polished thin section and copper grid must be heat and acetone resistant, as these are the two possibilities to remove the sample from the substratum. Additionally, it is preferable to use a quick-setting glue for technical reasons (e.g. accuracy of selected area).

Thinning was performed in a "ion-tech" ion-beam thinner under an angle of incidence of 10-15°. Argon gas is the active agent. With a total current of approximately 3 mA and at 5-6 KV it took between 15 and 100 hours (normal average is 24 hours), to thin through a sample. This considerable time difference is due to preferential thinning of the area within the grid. If a crack or grain boundary between two different minerals occurs in the sample, or if micas or iron oxides are present, preferential thinning will take place around these areas and only slowly shall the opening proceed into the selected grain.

Etching was done following the directions given by Ball & White (1977). The aim of this exercise was to make dislocations visible by means of a slow destruction process, as outlined by Ball & White (*op.cit.*). If such a method could be applied to multi-mineralic naturally deformed specimens the tedious process of sample preparation could be done away with. It was found however, that reactions between the feldspars and the HF "protected" the quartz against any etching. The results are in sharp contrast with the results described by Ball & White for Witwatersrand Quartzite and it must be concluded that etching to vizualize dislocations can only be used in monomineralic samples that do not react with HF.

4.10 Discussion of results

Three specimens were studied, all of them situated in

the feldspathic quartzite and its derivatives. Of these, two samples were taken from the direct vicinity of the Neusspruit Lineament: 891 from the feldspathic quartzite between Gifberg and Komsberg and 1775 from the platy quartz mica schist in the hinge area of the northern Neusberg Structure. The third specimen (1500) was taken from the feldspathic quartzite massif on Komsberg. These samples were selected because they represent two areas which are markedly different in total strain suffered: strong flattening along the Neusspruit and open folding in the Koms-Neilersdrift area. The dislocation density was derived by counting dislocations as shown in plate 9. Not all the dislocations shown in plates 6, 10 and 11 are considered to be mobile as they are pinned in some way or another. Apart from the situation shown in plate 6, the dislocations can be considered to be randomly oriented so that the $2N_s$ method, where N_s is the number of dislocations threading the surface, could be applied to calculate the dislocation density on each photograph. The average of all the micrographs of one sample was taken to be the dislocation density at that point. The velocity v was calculated for 800°K and 550°K, the expected maximum and minimum temperature at which the shearing took place, based on mineral paragenesis indicating low grade of metamorphism (Winkler, 1974). The differential stress is taken at 20 MPa and 100 MPa, the likely minimum and maximum values existing in the crust (Yuen *et al.*, 1978; Heard, 1976). For the Burgers vector the value 5×10^{-8} cm was used (Ball & White, 1978). The strain rates calculated on basis of these values are listed in Table 4.1. From the strain rates shown in the table it is clear that an activation energy (Q) for diffusion of 55 $Kcal.mole^{-1}$ results in extremely low strain rates ranging from "very slow" to "standstill" and slower (Price, 1975). For plastic deformation to take place with this high activation energy, a temperature and differential stress considerably higher than the maxima shown here are required. This is in contrast to the character of the features observed, as they reflect the last increment of the last deformational event and it is not feasible that such high temperature and differential stress should have existed at such a late stage of the rocks' deformation history.

The second conclusion one can draw from the values shown in Table 4.1 is that a difference in temperature of 250° (i.e. 550° and not 800°K) results in a strain rate which is two orders of magnitude lower.

Differences in differential stresses are directly reflected in the calculated strain rate. This follows from the formula used to calculate the velocity of dislocation movement (4.4), which is subsequently substituted into formula 4.5.

To calculate the differential stress σ from the dislocation density, Twiss (1977) uses the formula

$$\sigma = \alpha \frac{\mu}{1 - \nu} b\rho^{\frac{1}{2}} \qquad (4.6)$$

where μ is the shear modulus = 4.2×10^4 MPa
ν is Poissons ratio = 0.15
b is the Burgers vector = 5×10^{-8} cm
ρ is the dislocation density
α is an empirical parameter of order 1, correcting for the complexity of dislocation interactions.

When the obtained dislocation densities are substituted in formula 4.6, a differential stress between 17 and 34 MPa is obtained. This means that only the low stresses used in the calculations of the strain rates will yield realistic results for the strain rates.

			$\dot{\varepsilon}$ (sec^{-1})		
		Sample :	1775	891	1500
		N_s (cm^{-2}) :	$5{,}8132 \times 10^7$	$9{,}583 \times 10^7$	$20{,}513 \times 10^7$
T ^oK	J MPa	Q kcal.mole^{-1}			
800	20	20	$2{,}25 \times 10^{-12}$	$3{,}72 \times 10^{-12}$	$7{,}97 \times 10^{-12}$
800	20	55	$6{,}21 \times 10^{-19}$	$10{,}24 \times 10^{-19}$	$21{,}92 \times 10^{-19}$
800	100	20	$11{,}27 \times 10^{-12}$	$18{,}62 \times 10^{-12}$	$39{,}86 \times 10^{-12}$
800	100	55	$3{,}10 \times 10^{-18}$	$5{,}11 \times 10^{-18}$	$10{,}9 \times 10^{-18}$
550	20	20	$1{,}08 \times 10^{-14}$	$1{,}78 \times 10^{-14}$	$3{,}82 \times 10^{-14}$
550	20	55	$1{,}33 \times 10^{-25}$	$2{,}19 \times 10^{-25}$	$22{,}9 \times 10^{-25}$
550	100	20	$5{,}41 \times 10^{-14}$	$8{,}92 \times 10^{-14}$	$1{,}91 \times 10^{-13}$
550	100	55	$6{,}65 \times 10^{-25}$	$10{,}95 \times 10^{-25}$	$11{,}45 \times 10^{-25}$

Table 4.1 Strain rates calculated for 800°k, 550°k and activation energy of 20 kcal.mole^{-1} and 55 kcal.mole^{-1}.
Note the extreme low strain rates if Q = 55 kcal.mole^{-1}.

The observed dislocation pattern shows no indication of strain hardening (i.e. tangled dislocations). Whether such tangles were present and subsequently removed by posttectonic annealing or whether differential stress was relaxed at the same rate as the excess temperature was relaxed, cannot be inferred from the micrographs, unless like in specimen 1775, specific recovery features such as mats of dislocations are present (Plate 12). This indicates that the dislocation density in this sample is affected by annealing, removing a portion of the dislocations. There are two possible mechanisms to explain this feature: either a (probably general) posttectonic annealing due to some widespread thermal event, removed existing tangles of dislocations, or the excess heat generated during the shearing (Yuen *et al.*,1978) caused a sufficiently high temperature to achieve a local annealing after the stress relaxed.

These two possibilities result in two virtually opposite explanations as to what caused the obtained strain rates. In the first case, the conclusions are that the obtained values do not reflect the main deformational event in the area (D_{n+2}), as the trend is the opposite of what was expected on the basis of the total strain (i.e. highest in the Neusberg, lowest on Komsberg). This means that shearing along the Brakfontein Shear Zone continued, when movement along the Neusspruit lineament had ceased (that is if the degree of annealing was the same throughout the study strip).

In the second case it can be concluded that due to a stronger increase in the frictional heat in the Neusspruit lineament and particularly in the north (sample 1775), more energy was available to remove dislocations because of the higher temperature while stress relaxation occurred. This mechanism leads to the conclusion that shearing was strongest in the surroundings of the northern closure in the Neusberg, decreased towards the south and towards the east, which is in agreement with the total strain of the area.

Because of later annealing it is not necessarily true that the observed dislocation patterns indicate plastic deformation, as tangles of dislocations may have been removed. As field evidence does not suggest brittle deformation however, it is concluded therefore that plastic deformation did take place, as suggested by the dislocation patterns in the electron micrographs.

In summary it can be concluded that T.E.M. in naturally deformed rocks is a useful tool to provide additional information on the mechanism of deformation during the last increment of the last deformational event. Conditions for the application of the method are that comparisons are made on samples of the same rock type and that temperature limits and stress limits are known. In the case this last condition cannot be fullfilled, it is still possible to obtain valuable information that can assist in unravelling the kinematic history of the area studied, although reliable strain rate values cannot be obtained.

(Some of this work has been presented in an early stage of the project at the Cape Town conference of the Electron Microscopy Society of Southern Africa in 1977 (Van Bever Donker, 1977)).

5. METAMORPHISM

5.1 Introduction

Previous work

The metamorphism of the area has been described in three previous publications. Poldervaart and von Backström (1949) gave a detailed petrology of the area around Kakamas and concluded that increasing grades of metamorphism occurred towards the Central Dome, ranging from "chlorite zone" in the platy quartz-mica schist of the Neusberg (Annex. 1) via "biotite zone" in the micaceous quartz-feldspar schist and "garnet zone" in the "Aasvogelkop Granulite", to "sillimanite zone" in the Central Dome. Von Backström (1964) carefully described all the mineral assemblages significant in the determination of the grade of the metamorphism. Some of the results are summarised in Table 5.1.

Rock type	Facies of regional metamorphism	Subfacies
Kakamas Suid Leucogneiss Kinzigite	almandine-amphibolite	sillimanite-almandine
Staurolite schist	almandine-amphibolite	staurolite-quartz
porphyroblastic gneiss amphibolite	greenschist	quartz-albite-epidote-almandine
Wolfskop Biotite Gneiss	greenschist	quartz-albite-epidote-biotite
platy quartz-mica schist	greenschist	quartz-albite-muscovite-chlorite

Table 5.1 Metamorphic classification after Eskola (1915, p.143) used by von Backström (1964, Table 45).Rock names have been changed to names used in this report.

Schultz (in press) discussed the formation of the kinzigites outcropping in the northeastern parts of the area and concluded that these rocks were subjected to PT-conditions of about 690°-740°C and 4± 1 kbar. On the basis of the random distribution of sillimanite and garnets and the lack of a foliation, Schultz concludes that the highest temperatures have prevailed during a tectonically quiet period.

With respect to the origin of the charnockitic adamellite, his conclusion, based on geochemistry, is that these rocks represent carbonaceous argillites that underwent metamorphism of the regional hyperstene zone (Winkler, 1974).

Present study

In the present study three events, each resulting in a characteristic metamorphic assemblage, are shown to have taken place. Regional metamorphism (M_1) reached high-grade conditions ("muscovite out") and is preserved in the type-locality of the Venterskop Kinzigite, being the deepest rocks exposed in the area. This is due to tectonic reasons and elsewhere in the area rocks from a higher crustal level are exposed, displaying medium grade metamorphism (Fig. 5.1)

A second peak of high grade metamorphism (M_2) was reached in the direct vicinity of the charnockitic adamellite, the Straussburg Granite (granolite high grade) and the mafic intrusions on Middel Post. Good examples of this high grade contact metamorphism are the kinzigite assemblages in the northeast of the area and the wollastonite bands in the calc-silicate rocks (see also Fig. 5.1).

Low-grade metamorphism (M_3) has occurred throughout the area and is expressed by the late growth of minerals such as biotite, chlorite, prehnite and pumpellyite.

5.2 The first metamorphic event M_1

Assemblage and texture

At the type-locality of the Venterskop Kinzigite the assemblage cordierite + biotite + sillimanite + garnet + quartz + K-feldspar is present. The cordierite rims the garnet and is itself often altered to pinite. Biotite occurs in contact with garnet and has also been observed in the foliation, defined by sillimanite. As described in section 2.3, two distinct types of sillimanite have been distinguished: The first type consists of small needles of sillimanite, grown at right angles to the garnets, out-

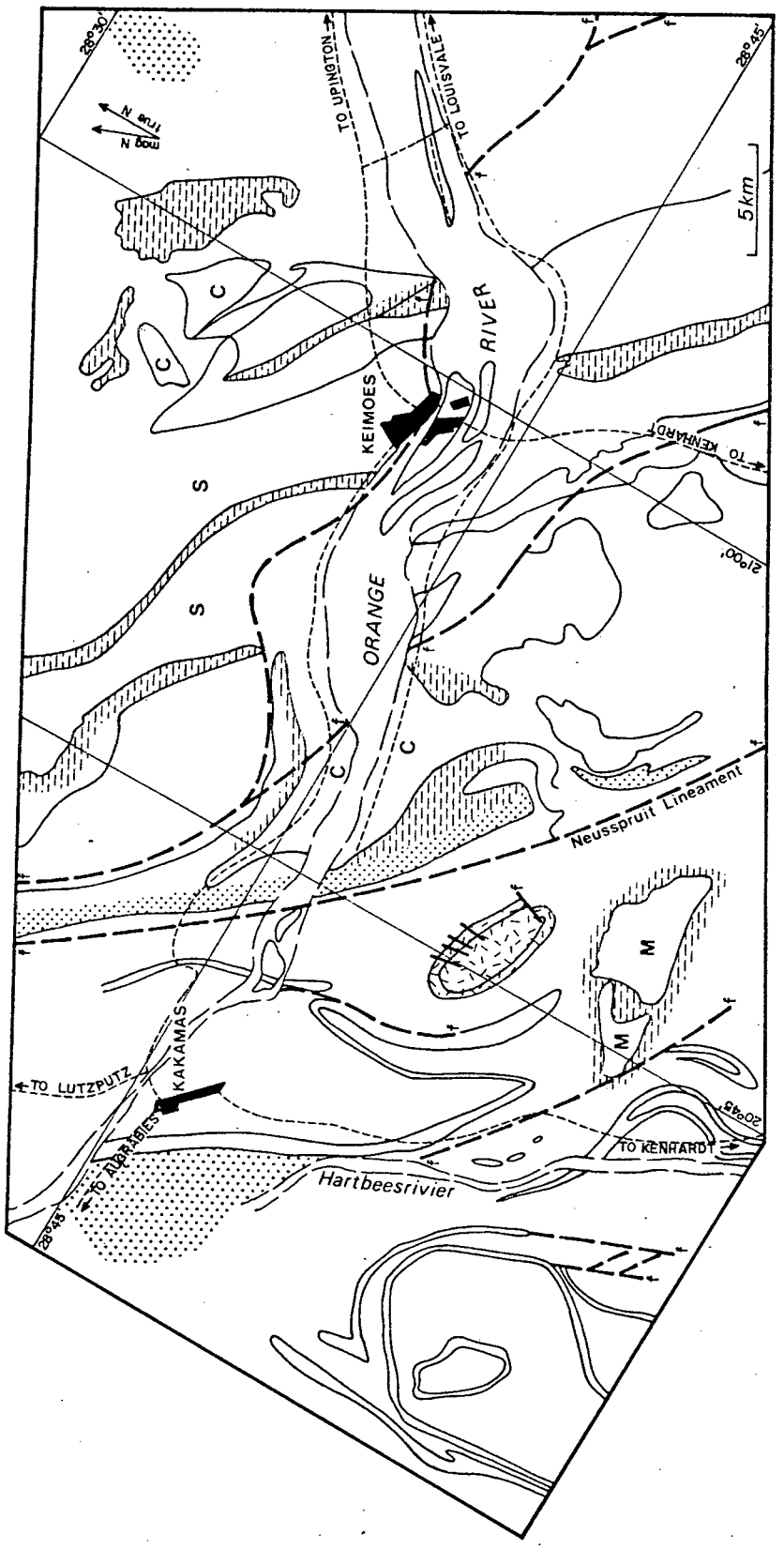

High grade metamorphism (M_1)

Rocks affected by contact metamorphism (M_2)

Area of retrogression (M_3)

Area where feldspar megacrysts appear

S *Straussburg granite*

C *Charnockitic adamellite*

M *Middelpost mafics*

Medium grade

Fig. 5.1 Areal distribution of the various grades of metamorphism

lining the euhedral shape of the latter. These garnet-sillimanite aggregates are invariably surrounded by a larger garnet. It is this garnet that is rimmed by (altered) cordierite.

The second type of sillimanite defines the foliation in this rock and is undoubtedly the more important variety. In the sillimanite foliation biotite and opaque minerals occur. Garnet and cordierite are both in contact with biotite.

Other assemblages that were formed as a result of M_1 occur in -

- The Regt Kyk Banded Amphibole Quartzite:

  quartz + feldspar + plagioclase + muscovite + amphibole

  sphene and opaque minerals occur quite regularly and garnet, clinopyroxene and piedmontite are accessory minerals

- The Maraisrivier Amphibolite:

  quartz + feldspar + biotite + amphibole

  plagioclase, where undeformed and unaltered, has been measured and ranges from low-oligoclase to high-andesine.

- The Baviaans Krantz Banded Calc-silicate Quartzite in the Neusberg, north of the Orange River:

  K-feldspar + biotite + amphibole + occasional sillimanite

  and

  quartz + K-feldspar + biotite + epidote + occasional amphibole + accessory tourmaline

- The Wolfskop Biotite Gneiss:

  quartz + K-feldspar + biotite + amphibole

Interpretation

From the mineral paragenesis it appears that the assemblage present in the kinzigite plots somewhere on the line A-B, (Fig. 5.2) depending on the Fe/Mg ratio. This assemblage is :

cordierite + biotite + garnet + sillimanite + K-feldspar + quartz (no muscovite)

This assemblage is a bivariant paragenesis and it is pointed out by Reinhardt (1968) that, though the assemblages garnet + cordierite + biotite

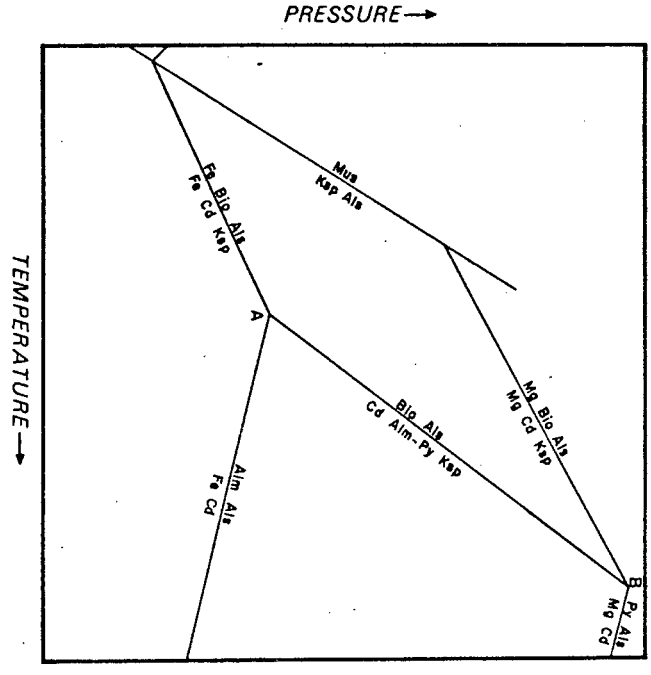

Fig. 5.2 Schematic pressure-temperature diagram for cordierite breakdown reactions in the presence of muscovite, K-feldspar and quartz (after Holdaway & Lee, 1977). Cd = cordierite; Alm = almandine; Py = pyrope; Bio= biotite; Als = Al-silicate; Ksp = K-feldspar.

and garnet + cordierite + sillimanite are stable parageneses (Fig. 5.3), it is important to establish very carefully which minerals have actually been formed progressively and which have formed retrogressively. In the case of the Venterskop Kinzigite as outcropping on Kakamas Suid, special care is necessary, as there appear to be two generations of biotite. The biotite in direct contact with the garnet grew at the expense of the garnet, whereas the biotite in the sillimanite foliation is most probably older and is in equilibrium with the opaque minerals. This becomes clear from the $X_{Fe(II)}$

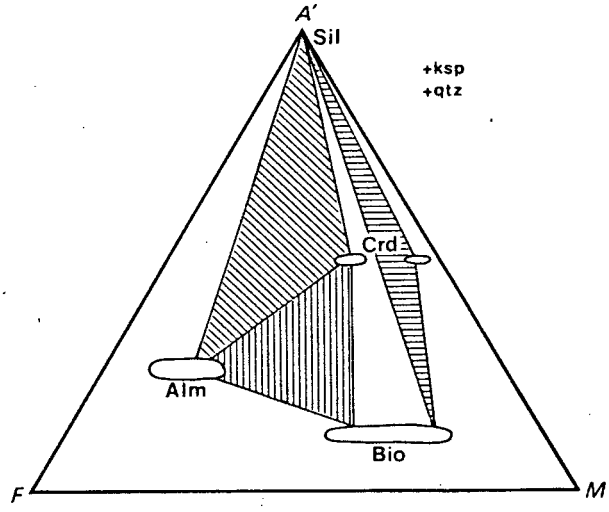

Fig. 5.3 A'FM diagram showing the two stable assemblages as described by Reinhardt (1968). (After Winkler, 1974).

ksp = K-feldspar
qtz = quartz

(FeO/FeO + MgO ratios) for garnet, biotite and cordierite and the K_D values for the garnet-biotite, garnet-cordierite and biotite-cordierite (Table 5.2).

	X_{FeO} 96 $(\frac{FeO}{FeO + MgO})$			X_{FeO} 944 $(\frac{FeO}{FeO + MgO})$		
Ga Co Bi	0.79 0.34 0.60			0.875 0.40 0.65		
	K_D (H)	K_D (T)	Lnk_D	k_D (H)	k_D (T)	Lnk_D
Ga-Co	0.13	7.3	2.0	0.09	11.11	2.4
Ga-Bi	0.39	2.56	0.935	0.26	3.84	1.34
Bi-Co	0.34	2.94	1.07	0.35	2.85	1.04

Table 5.2 X_{FeO} values for garnet (Ga), cordierite (Co) and biotite (Bi) and K_D values calculated according to Holdaway & Lee, 1975 (K_D(H)) and according to Thompson,1976 ,(K_D(T)) for Fe-Mg exchange between garnet and cordierite (Ga-Co), Garnet and biotite (Ga-Bi) and biotite-cordierite (Bi-Co)

Using Thompson's (1976) graphs, the garnet-biotite and garnet-cordierite LnK_D yield temperatures that lie some 100°C apart, with the garnet-biotite temperature the higher of the two (Fig. 5.4). When the K_D for cordierite-biotite is calculated, according to Holdaway & Lee (1977, equation (4)), the value obtained is too low to be indicative of equilibrium exchange of iron and magnesium between cordierite and biotite. (The value is about 0.3, whereas the values given by Holdaway & Lee (*op.cit.* Table 6) are in the range of 0.40 - 0.67, irrespective of temperature). As only a pilot study was performed into the feasibility of using the garnet-cordierite and garnet-biotite thermometers, few probe analyses on this sample were done and only biotite occurring in the sillimanite has been analysed, so that no reliable temperature can be obtained on basis of the exchange reaction of iron and magnesium between garnet and biotite. The temperature obtained from the exchange reaction garnet-cordierite is about 660 ± 15°C. Furthermore, on the basis of the X_{FeO} of cordierite (0.34) it is possible to arrive at a value for the total pressure, when using the graphs as given by Holdaway

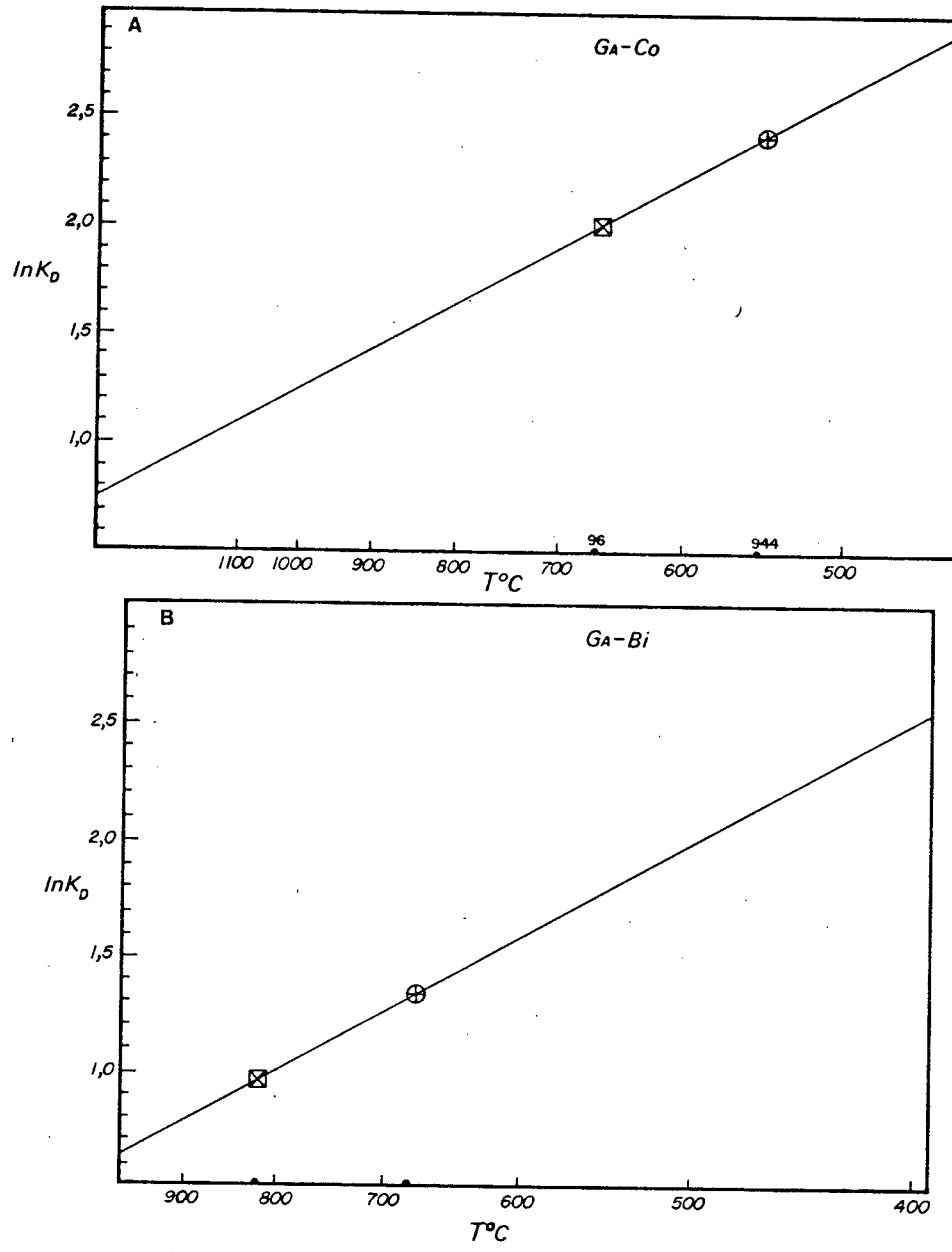

Fig. 5.4 Plots of Lnk_D versus temperature for garnet-cordierite (A) and garnet-biotite (B), after Thompson 1976.

and Lee (Fig. 7A and 7B, 1977). Fig. 5.5 shows that for cordierite with X_{FeO}=0.34 the line for Alm + Sil + Q + V versus Fe-cordierite shall intersect the curve Bio + Sil + Q/Crd + Alm - Py + Ksp + V for a temperature at about 700°C and a pressure of about 5 Kbar. These figures suggest that P_{H_2O} was slightly lower than 0.4 P_{tot}, as the temperature has been fixed at 660° ± 15°C.

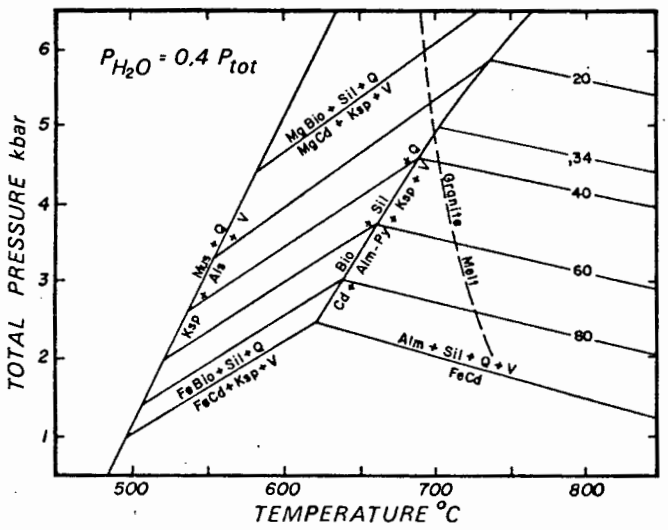

Fig. 5.5 Calculated PT curves from Holdaway and Lee (1977) for the univariant Fe-Mg reaction producing cordierite, garnet and K-feldspar. Abbreviations as in Fig. 5.1. See text for explanation.

In order to establish at what point of the history of the rock this P and T were active, or in other words, whether they reflected the peak of the metamorphism, it is necessary to study the available textural evidence.

The absence of muscovite and the presence of quartz + K-feldspar + sillimanite is an indication that the assemblage is above the reaction

muscovite + quartz → K-feldspar + sillimanite + H_2O

so that the temperature was above 700°C and the pressure about 5 kbar (Chatterjee & Johannes, 1974). As biotite, cordierite and sillimanite surround the garnets, with cordierite and biotite in direct contact with the garnet, it is likely that both cordierite and biotite grew at the expense of garnet, indicating a drop in pressure. It follows that pressure and temperature, calculated on basis of the Fe-Mg exchange reaction between garnet and cordierite, do not reflect the highest grade of metamorphism this rock suffered. As the formation of cordierite indicates a drop in pressure, the highest metamorphism may have differed from the calculated values in that a higher pressure existed, resulting from a thicker overburden or tectonic overpressure.

The inclusions of sillimanite needles in the garnets indicate two

stages of garnet growth, whereby the different orientations of the needles may indicate some rotation of the garnets before the second stage of garnet growth started. It is not possible to determine what the metamorphic conditions were, under which the first garnets were formed. Microprobe analyses did not show a difference in garnet composition between core and rim, contrary to what would be expected on basis of the pattern of sillimanite inclusions. As very few analyses were carried out however, this is no reliable evidence and no conclusions may be drawn on the basis of it.

The other assemblages formed during M_1 are not diagnostic assemblages in that they can be stable over vast pressure-temperature ranges. As a result they can only be used as general indications of the grade of metamorphism. Used in this manner they suggest medium grade of metamorphism.

Feldspar megacrysts

K-feldspar megacrysts occur at several places in the area and can be divided into two groups, namely a) the small feldspar concentrations of approximately 1 x 2 mm, as described in Section 2.4.1 and b) the less common larger concentrations, with a long axis of up to 10 cm, as described in sections 2.4.5 and 2.8.2. The latter group is situated in the direct vicinity of major shear zones (Kakamas Shear Zone and Cnydas Shear Zone) and it is thought that their formation is in some way related to the presence of the shear zones. One possible solution is the emplacement of granitic rocks along the existing zones of weakness. Phenocrysts could then have formed and subsequent deformation would have resulted in the situation as shown in Fig. 5.6. This possibility cannot be excluded as the biotite gneiss could be classified as an alkali feldspar granite, using the classification of Streckeisen (1976). This model however requires the formation of a granite of the same composition as the country rock in two different localities, situated some 60 km apart, hence it is thought to be more likely that one of the following metamorphic models produced the megacrysts in this rock.

An increase in temperature due to frictional heating (Yuen, *et al.*, 1978) could have been sufficient to cause secondary recrystallisation as described by Vernon (1976) and should be restricted to the surroundings of the shear zones only.

Another possibility is the circulation of fluids, made possible by a higher permeability along the shear zones (Annex.1, 2).

Winkler (1974, chapter 18) points out that for gneisses containing plagioclase between An_{10} and An_{35} (plagioclase in the study strip is oligoclase/andesine) the initial melt is a water-saturated cotectic mixture of An-Ab-Or-Qtz. As soon as one of these components has melted completely the temperature has to rise in order to melt the other components. It is also pointed out that plagioclase and K-feldspar will be molten before quartz will melt and quartz in turn melts before the ferromagnesian minerals, in the order:

biotite → hornblende → garnet → opaque minerals (Jackson, 1976; Winkler, 1974). In the unlikely event that $P_{H_2O} = P_{tot}$, as much as 70-95 vol % may be molten greywackes. If sufficient water is to be present it means that for saturation of a granitic melt about 12 weight % water at 5 kbar and about 665°C is required. With this in mind it becomes clear that the difference between the porphyroblasts of group A and group B can be explained by the accessability of water : at 5 kbar and about 670°C anatexis may have started, but under these conditions not much water is to be expected in the rock. Hence only a small amount of neosome formed. The larger amount of leucosome in the gneisses near the Hartbees River and in the north-east of the area indicate that a larger amount of H_2O may have been available when anatexis commenced. This could be explained by the presence of major shear zones in the direct vicinity of these rocks: respectively the Kakamas Shear Zone and the Cnydas Shear Zone.

Textural evidence for all megacrysts suggests that they formed pre- or syn-D_{n+2} or at the latest late-D_{n+2} (Fig. 5.6), as rounded megacrysts with melanosome wrapping around them coexist with more angular megacrysts that to some extent truncate the melanosome. As a result it is not possible to distinguish between the different mechanisms suggested above anymore.

When the conditions of the formation of the cordierite in the Venterskop Kinzigite are plotted on the graph in Fig. 5.7 it becomes clear that these conditions will only yield an appreciable melt if sufficient water is present, thus supporting the interpretation that the required H_2O was supplied due to the greater permeability of the rocks in the direct vicinity of the shear zones.

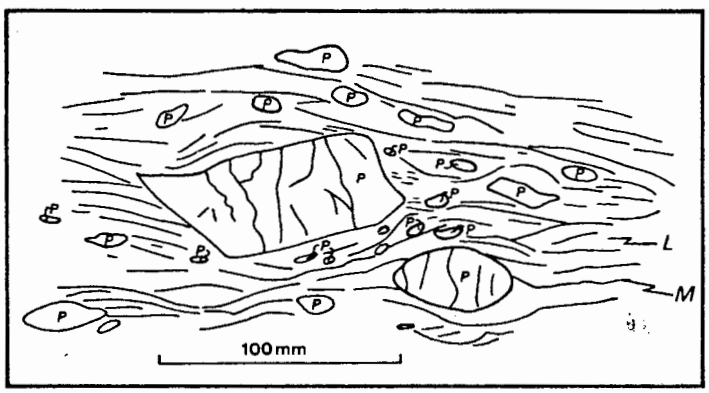

Fig. 5.6 Sketch showing the structural relationship between the feldspar megacrysts (P), the leucosome (L) and the melanosome (M).

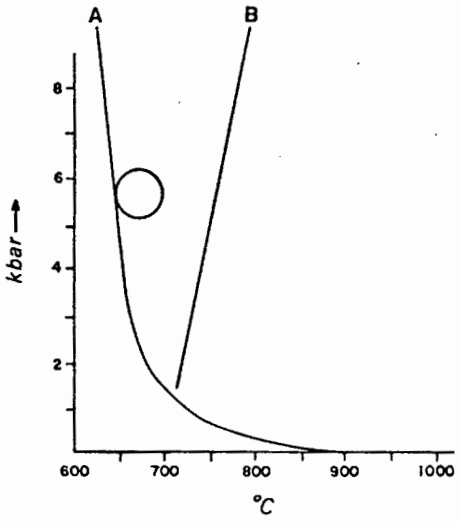

Fig. 5.7 Solidus and liquidus relations in granitic rock. See text for explanation.
A: solidus in Q-Ab-Or if water is present
B: solidus dry biotite granite circle represents P-T conditions of cordierite formation in kinzigite in the Central Dome (after Winkler, 1974, Fig. 18.8)

5.3 Contact metamorphism M_2

Contact metamorphism in the area is mainly related to the emplacement of the charnockitic adamellite and the Straussburg Granite and to a lesser extent to the emplacement of the Middel Post Mafic Rocks. In the northeastern part of the area rocks of kinzigitic composition developed due to emplacement of Straussburg Granite. The main criterion for the interpretation of the presence of contact metamorphism is the lack of a tectonic fabric in medium to high grade metamorphic rocks (Fig. 5.8).

Assemblage and texture

In these outcrops of the Venterskop Kinzigite the paragnesis garnet + cordierite + biotite + sillimanite + staurolite + chlorite + quartz is encountered. Of these minerals the garnet and the sillimanite appear to have grown progressively at the expense of the cordierite, because sillimanite needles with a random orientation are observed scattered throughout the rock and are often intergrown with the garnet. The garnet is always poikiloblastic and includes, apart from sillimanite, cordierite and opaque minerals.

Staurolite crystals are often overgrown by sillimanite and are not seen to overgrow any mineral themselves, hence they form one of the "oldest" constituents of the rock.

Biotite and chlorite are both randomly oriented and grow at the expense of garnet. Additionally, biotite is frequently observed growing from opaque minerals.

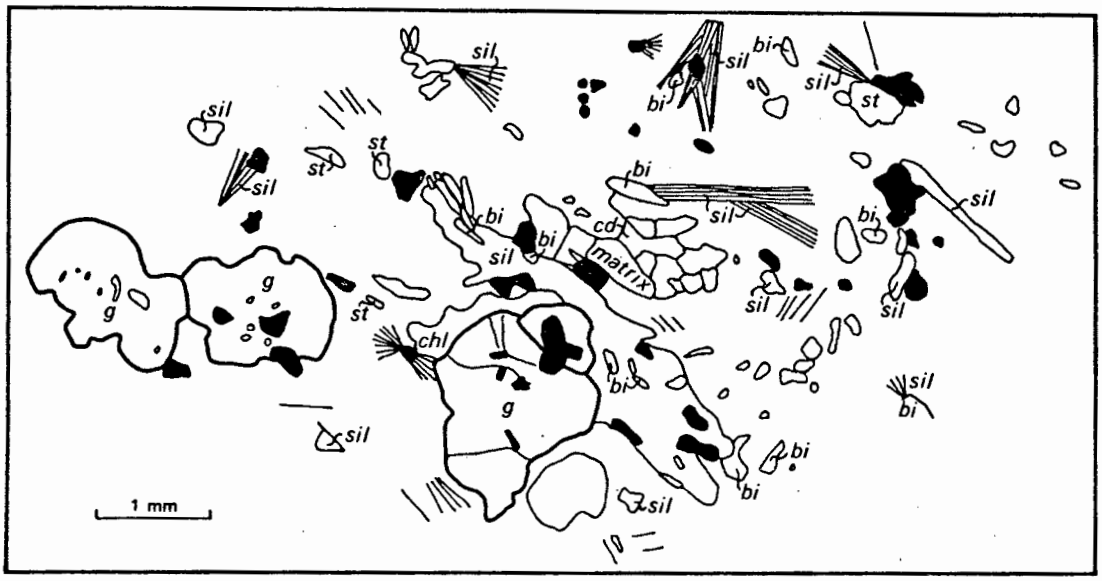

Fig. 5.8 Texture of the kinzigite as outcropping at station 944. Note the random orientation of sillimanite, biotite and chlorite and the poikiloblastic garnets. "Matrix" is an indication of the grain size of the matrix, mainly consisting of cordierite with some quartz.

Further to the south, in the tourmaline-staurolite schist at Zoovoorby (Section 2.6), the situation is different, as here the staurolite crystals are obviously late grown, poikiloblastic and euhedrally shaped. The paragenesis in this rock is

garnet + biotite + muscovite + staurolite + sillimanite + quartz

This implies that the metamorphic grade of these rocks was below the stability of staurolite, indicating a higher crustal level. This contradiction in crustal level is explained by the presence of the Cnydas Shear Zone running between the two outcrops concerned (see also Section 5.5).

Along strike in the calc-silicate rocks, sheafs of amphibole needles occur.

Other evidence for contact metamorphism is found in the Warm Zand Structure, where in the northern ridge the assemblage

cordierite + biotite + sillimanite

formed with randomly oriented sillimanite needles. In the southern ridge of the structure late grown, poikiloblastic garnet is encountered close to the contact with the charnockitic adamellite.

In the Koekoeb area large amounts of wollastonite formed in layers varying in thickness of a few centimetres to several tens of metres.

In the same area sillimanite grew, randomly oriented and mainly in the direct vicinity of the adamellite body. Also late grown, poikiloblastic garnets developed in this area.

Interpretation

On the basis of the evidence presented above, it is suggested that in the kinzigite in the northeast of the area garnet and sillimanite formed during M_2 according to either of or both the following reactions

staurolite + quartz → sillimanite + almandine + cordierite + H_2O (5.1)

cordierite → almandine + sillimanite + quartz (5.2)

On basis of textural evidence it is decided that reaction 5.2 took place rather than 5.1 as staurolite is not commonly observed as being in contact with garnet. Additionally, both garnet and sillimanite appear to overgrow the cordierite. It has been calculated from microprobe analyses that the temperature for the formation of garnet from cordierite was about 580°C (Table 5.2, 5.3; Fig. 5.4). The FeO/(FeO + MgO) ratio of the rock is calculated from the same probe data to be 0.73, so that when using the P-T diagram of coexisting cordierite + almandine + quartz + sillimanite for this FeO/(FeO+MgO) ratio (Fig. 5.9) a pressure of between 5 and 5.7 kbar follows.

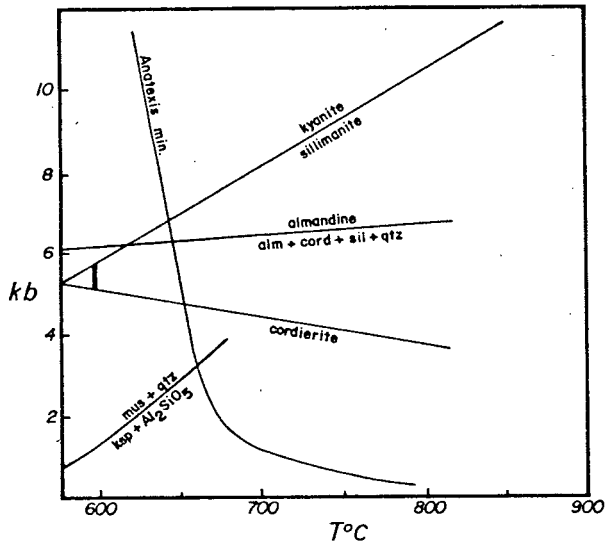

Fig. 5.9 P-T diagram for coexistance of garnet, cordierite, sillimanite and quartz for FeO/(FeO+MgO) = 0.73.
Thick bar is position of sample 944.
(After Winkler, 1974, Fig. 14-12)

ionic proportions - sample 96						ionic proportions - sample 944				
	Ga-1(12)	Ga-3(12)	Ga-2(12)	Bi(23)	Co(17)	Ga (12)	Bi-1(22)	Bi-2(22)	Co (17)	St (47)
Si	2.9677	2.9567	2.9646	5.5829	4.7088	2.9654	5.3061	5.2967	4.6882	7.6263
Ti	0.0017	0.0020	0.0018	0.4684	0.0002	0.0016	0.2025	0.2003	0.0001	0.0961
Al	2.0272	2.0363	2.0315	3.2572	3.8347	2.0332	3.7729	3.7309	3.8244	18.3725
Fe	2.2480	2.2313	2.2472	3.0170	0.6019	2.6003	3.0403	3.0117	0.7620	3.3941
Mn	0.0412	0.0401	0.0423	0.0033	0.0032	0.0347	0.0089	0.0088	0.0029	0.0142
Mg	0.5797	0.5930	0.5830	2.0111	1.1671	0.3707	1.4910	1.5568	1.1091	0.5841
Ca	0.1509	0.1635	0.1468	0.0009	0.0023	0.0099	0.0021	0.0021	0.0037	0.0034
Na				0.0183	0.0214		0.0223	0.0220	0.0168	
K				1.9389	0.0878		1.5397	1.6371		
Tot	8.0168	8.0232	8.0177	16.2985	10.4280	8.0162	15.3863	15.4669	10.4076	30.0911

Analyses Sample 96						Analyses Sample 944				
	GA-1	GA-2	GA-3	Bi	Co	Ga	Bi-1	Bi-2	Co	St
SiO_2	37.557	37.356	37.273	34.597	48.063	36.753	33.1421	33.473	47.839	26.583
TiO_2	0.029	0.030	0.033	3.850	0.004	0.027	1.6774	1.679	0.002	0.445
Al_2O_3	21.761	21.713	21.775	17.156	33.200	21.375	20.0308	20.040	33.101	54.322
FeO	34.017	33.859	33.635	22.329	7.346	38.536	22.6788	22.731	9.298	14.146
MnO	0.616	0.630	0.597	0.025	0.039	0.509	0.067	0.067	0.035	0.058
MgO	4.922	4.929	5.016	8.488	7.993	3.083	6.343	6.701	7.594	1.366
CaO	1.783	1.727	1.924	0.005	0.022	0.114	0.012	0.012	0.035	0.011
Na_2O				0.059	0.113		0.072	0.072	0.088	
K_2O				9.410	0.702		7.5318	8.102		
Tot	100.68	100.24	100.25	95.91	97.48	100.39	91.554	92.877	97.99	96.93

Table 5.3 Analysis and atomic proportions of samples 96 and 944.
Ga-garnet; Bi-biotite; Co-cordierite; St-staurolite

Like in the probe analysis for the kinzigite in the Central Dome (Sample 96) a discrepancy between the calculated temperature for the garnet-cordierite and garnet-biotite exchange reactions exists (580° and 690° C respectively). This is explained by the supposition that the biotite probed is not in equilibrium with the garnet, but rather with the opaque minerals.

It is concluded that the garnet and sillimanite formed at about 600°C and 5.5 kbar as a result from contact metamorphism generated by the emplacement of granites. The cordierite and staurolite formed at an earlier stage and they may represent medium grade conditions (Winkler, 1974) resulting from M_1.

The biotite and chlorite, appearing in the northeastern variety of the Venterskop Kinzigite, represent the third metamorphic event (see Section 5.4).

Other contact metamorphic assemblages occur on Curries Camp-Zoovoorby, where in the Zoovoorby Staurolite Schist metamorphic features indicative of a post-tectonic rise in temperature, such as poikiloblastic late grown staurolite crystals (section 2.6), are evident.

The paragenesis :

garnet + biotite + muscovite + staurolite + sillimanite + quartz

in a pelitic rock indicates almandine - medium grade. It is generally accepted that the beginning of medium grade metamorphism is indicated by the first appearance of staurolite and of cordierite (Winkler, 1974; Miyashiro, 1973). For staurolite to form instead of cordierite, the Mg/(Fe+Mg) ratio must have been rather low: less than 0.25 (Winkler, *op. cit.* p.213). The stability field for staurolite has been determined to be between 530° and 700°C and at pressures above 2 kbar (Richardson.1968). Sillimanite could place more constraints on the P-T conditions, but has been observed in one specimen only.

The minimum P-T conditions of this rock can thus be placed at 530°C and 2 kbar, the minimum P-T conditions for staurolite to form.

The appearance of randomly oriented amphibole needles at a similar distance to the intrusive body as the staurolite crystals along strike, is significant only in that they must have grown post-tectonically. No direct inference concerning temperature and pressure can be made.

The mineral parageneses discussed above are in good agreement and both indicate that temperatures and pressures of about 500-700°C and 5 kbar may have occurred during M_2. The pressure of 4-5 kbar suggests an overburden of 15-20 km. Because of a lack of a fabric, related to the time of growth of those minerals indicating the highest metamorphic grade, it is thought that these minerals grew as a result of contact metamorphism, due to the emplacement of granitic material at a medium pressure (3-5.5 kbar) yielding medium grade contact metamorphism (Winkler, 1974).

From the composition of the charnockitic adamellite (i.e. hyperstene) and the estimated pressure at the time of emplacement it is inferred that the temperature of the granitic magma must have been around 900°C. Using Turner's graphs (1968) to calculate the increase in temperature due to contact metamorphism, an increase at the contact (staurolite schist) of about 400°C should yield a temperature of the country rock at the time of intrusion of about 300°C, as the calculated temperature is about 700°C. This in turn would imply that a "normal" or somewhat higher geothermal gradient was in force in late-Precambrian times.

The western limit of these large intrusive bodies is formed by the northern, eastern and southern ridge of the Warm Zand Structure and the Koekoeb Area (Annex. 1). In the northern ridge the following assemblage has been formed:

cordierite + biotite + sillimanite

indicating that P-T conditions surpassed those required for the first formation of cordierite at temperature-pressure combinations of 505°C at 0,5 kbar up to 555° ± 10°C at 4kbar H_2O pressure (Hirschberg & Winkler, 1968).

Wollastonite in the presence of garnet, carbonate, plagioclase and quartz indicates P-T combinations ranging from 560° at 1 kbar up to 800°C at 6.5 kbar (Winkler, 1974; Krauskopf, 1967).

As sillimanite can form from about 1 kbar and 700°C up to 10 kbar and 750°C, with a minimum temperature of 600°C at 6 kbar (Althaus, 1967) it follows that the temperature and pressure of the contact metamorphism in this part of the study strip (Koekoeb area) are those marking the boundaries of the stability of sillimanite. Post-tectonically grown poikiloblastic garnet is not diagnostic for P-T conditions, as it can grow from 500°C upwards at a variety of pressures.

In summary it is not possible to pin the pressure-temperature conditions of contact metamorphism in the western part of the area more accurately than that the temperature is likely to have been between 500°C and 700°C and that the pressure has been between 1 and 6 kbar. More can be said of the P-T conditions in the eastern part of the area, as mineral parageneses indicate about 5.5 kbar and 600°C, with an intruding magma of about 900°C.

Timing of intrusion

In the geometrical analysis in Chapter 3 it has been shown that the Warm Zand Structure and the Curries Camp Structure formed as a result of D_{n+2}. This fact dates the intrusion as these structures have not formed as a result of the emplacement of the granites. The presence of numerous small shear zones in the granites indicate that they were present when D_{n+3} took place. The small effect D_{n+3} had east of the Neuspruit Lineament, combined with the presence of the small shear zones described

above, suggest that the granites had almost reached their maximum strength at the time of D_{n+3}. Because, had they still been plastic, no deformation would have shown and had they reached their final strength, the competence of the rock would have been too high for the low intensity D_{n+3} to have any effect at all. On this basis it is concluded that emplacement of the granites took place pre-syn-D_{n+3}.

5.4 Low grade metamorphism M_3

Parageneses

Mineral parageneses indicating low grade metamorphism exist throughout the area. Usually the presence of late grown biotite and chlorite, often randomly oriented and grown at the expense of e.g. garnet, provides ample evidence for retrogressive metamorphism, or a third, low grade peak of metamorphism. It is significant that these late grown minerals have also been encountered in the granitic rocks. Other minerals indicating low grade metamorphism are prehnite and pumpellyite, although not observed in the same thin section.

Interpretation

Apart from the obviously late grown low grade minerals occurring throughout the area, one specific part of the study-strip stands out because of the lack of medium grade minerals. In the Neusberg Formation the paragenesis

quartz + K-feldspar + biotite + muscovite + chlorite + plagioclase

occurs frequently. This specific paragenesis can be explained as a typical very low grade - low grade assemblage, where

microcline + chlorite + phengitic muscovite → biotite + less phengitic muscovite + quartz + H_2O (Mather, 1970)

as illustrated in Figure 5.10.

A prerequisite for this reaction to take place would be a sufficiently high phengite content in the white mica, which could not be proved. Additionally a very low grade - low grade assemblage is contradicted by the presence of occasional garnets in the rock and the local occurrence of sillimanite suggests that higher P-T conditions have prevailed. Supporting evidence is that the Baviaans Krantz Calc-silicate Quartzite in direct contact with the rocks of the Neusberg Formation generally indicates medium grade

metamorphism. It is concluded therefore that the composition of the rocks of the Neusberg Formation is not suitable for the formation of minerals such as biotite and garnet. Hence the apparent low grade assemblage is misleading and it is more likely that, like most of the area, the Neusberg Formation reached medium grade metamorphism.

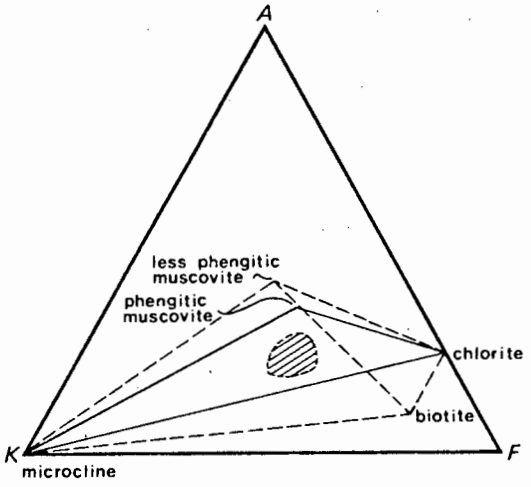

5.10 AKF diagram showing the breakdown of the assemblage microcline + chlorite + phengitic muscovite.

—— tie lines indicate lower grade assemblage

--- dotted tie lines indicate higher grade assemblage

▨ probable position of assemblage in Neuspoort Member of Neusberg Formation (after Mather, 1970)

5.5 Discussion

From the previous sections it becomes clear that two metamorphic highs have existed. The first of these encompassed the entire study-strip and is presently reflected by medium grade assemblages throughout the area. Two exceptions to this general pattern have been described: one area of apparent low grade metamorphism, where the chemistry is unsuitable to form Fe-Mg bearing minerals. Assemblages here are stable over a vast range of temperature-pressure conditions, from low grade up to high grade, when muscovite and quartz form sillimanite. The other exception is found in the Central Dome area, where a high grade assemblage crops out. It is in this area that the relationship between deformation and metamorphism can be determined adequately. One of the most striking features in the kinzigite is the sillimanite foliation wrapping around the garnet aggregates. This indicates that sillimanite and garnet were present when flattening took place. As no later events can be recognized, this flattening (at least part of it) probably reflects D_{n+3}. As pointed out in Section 5.2 it is likely

that cordierite formed at the expense of garnet, probably according to a reaction involving both garnet and sillimanite, e.g.

cordierite $\rightleftharpoons$ almandine + sillimanite + quartz + H_2O (Holdaway & Lee, 1977)

If this reaction did take place, the rimming of the garnets by cordierite cannot be dated relatively to the deformation of the sillimanite foliation, because it would be impossible to distinguish between cordierite formed pre-D_{n+3} which is subsequently deformed and cordierite formed syn-D_{n+3}, even though the cordierite may show undulose extinction. The decrease in pressure, reflected by the cordierite development, most likely resulted during the upward movement of the rocks. The lack of microstructures predating the sillimanite foliation, indicates that D_{n+2} took place under P-T conditions, suitable for sillimanite to form. Since the sillimanite foliation has been shown to have been formed during D_{n+2}, it is concluded that M_1 and D_{n+2} coincided. It is not possible to establish what caused the two periods of garnet growth, observed in the kinzigite.

The conclusion that M_1 and D_{n+2} coincided explains the transposition of pre-D_{n+2} features as recrystallisation must have taken place under those conditions.

From the paragenesis presented in Section 5.2 it becomes apparent that no diagnostic parageneses can be defined on the basis of the presented data outside the Central Dome. These parageneses may even be stable under P-T conditions favourable for the formation of the kinzigites, so that the vertical movement of the central dome block relative to the surrounding, need not have been large. The growth of cordierite in this case reflects the upward movement of a larger part than the limited area of the Central Dome: possibly even the entire block west of the Neusspruit Lineament. When combined with the staurolite-cordierite paragenesis in the northeast, where only at the direct contact with the granite the same assemblage as in the Central Dome developed, and the fact that sillimanite in the Neusberg Formation is only preserved in the direct vicinity of the granitic bodies, the important conclusion is drawn that the overall degree of metamorphism east of the Neusspruit Lineament has been lower than west of the Lineament: medium grade to the east and possible high grade to the west. This implies that west of the Lineament a deeper level of the crust is exposed than east of the Lineament.

These conclusions are in marked contrast to the picture presented in earlier publications (Von Backström, 1964) where an increasing grade of metamorphism from Neusberg to core of Central Dome was thought to range from greenschist facies to granulite facies.

Finally, low grade assemblages in the area have probably formed as a result of cooling and pressure release, rather than as the result of a late increase in pressure and temperature reaching very low - low grade conditions. This is mainly based on the understanding that in retrogressive metamorphism metastable parageneses form, whereas in later upsurge of pressure and

temperature such metastable parageneses could have been changed to stable parageneses. An example of such a metastable paragenesis may be found in the localized occurrance of prehnite and pumpellyite, whereas in a prograde sequence limiting assemblages containing these minerals could have been expected.

Summary of conclusions (See also Fig. 5.11)

1. Metamorphism M_1 throughout the area reached medium grade conditions and coincided with D_{n+2} and these conditions may have persisted from when the D_{n+1} event took place, although evidence to support this suggestion is not present.

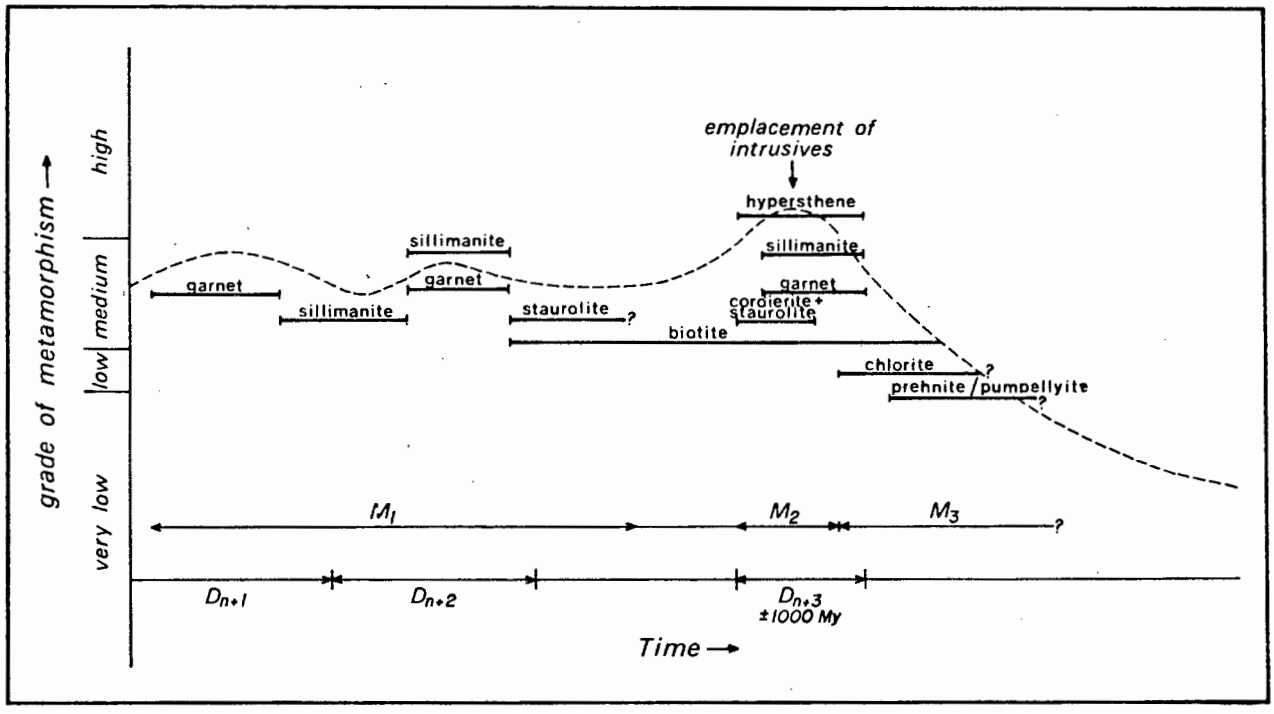

Fig. 5.11 Relationship deformation - metamorphism

2. Few diagnostic assemblages are present, but it has been shown that the difference in the degree of medium grade metamorphism between the areas to the east and to the west of the Neusspruit Lineament indicates a difference in crustal level.

3. Intrusion of the Straussburg Granite and the charnockitic adamellite locally raised the temperature during the M_2 event to form

garnet and sillimanite in the kinzigite, staurolite in the Staurolite-Tourmaline Schist of Zoovoorby, wollastonite in the calc-silicate rocks and sillimanite in the rocks of the Neusberg Formation.

4. In M_3, retrogressive metamorphism formed low grade minerals, such as chlorite, prehnite and pumpellyite.

6. CORRELATIONS

Correlating the geology of the area under consideration with the surrounding areas is attempted by reviewing the combined structural-metamorphic picture and comparing the main characteristics such as : which deformational event is responsible for the main penetrative foliation and when the main metamorphism took place. Temperature and pressure conditions of the main metamorphism are also taken into account.

This approach has the advantage that, assuming that Namaqualand acted as a homogeneous body on this scale, it can be shown whether differences between the different descriptions are indeed different geologies or merely nomenclature differences. In Table 6.1 the lithological units described in this report are compared with those of other areas used by other investigators.

From the structural and metamorphic analyses given in Sections 3 and 5, it has been possible to arrive at a sequence of events.

In Table 6.2 the relationship in time between the main deformational events and other important parameters (formation of main foliation, main metamorphism) is shown.

When compared with the larger area of eastern Namaqualand (Fig. 6.1, Table 6.3) there appears to be good agreement throughout the complex concerning the timing of the different events: a major deformational event resulted in a generally penetrative foliation, usually accompanied by the peak of the metamorphism. It follows that the n, used in the annotation D_{n+x}, is most probably 1. If that is the case the timing of the different events is fairly uniform in Namaqualand, except from Toogood's (1976) study. He shows that an early metamorphic event reached P-T conditions of 800-600°C and 8-9 kbar. Evidence for this high grade metamorphism is restricted to a small area only. In most of his area foliations appear to be related to the Velloorian event (M_2+M_3), during which P-T conditions of 650-700°C and 5-7 kbar occurred in the block north of the Pofadder Lineament. This took place during D_5-D_6 deformations. It is concluded therefore that the main metamorphism described in this study and other studies consulted, is the equivalent of Toogood's Velloorian event and that evidence for an equivalent of the Kumian event is not preserved. The discrepancy in the number of deformational events is probably a result of different terminology used.

This Report	Other Authors.
Straussburg Granite	Colston Granite (Geringer & Botha) Grey Gneiss (Von Backström, 1964)
Warm Zand Charnockitic Adamellite	Charnockitic Adamellite Porphyry (Von Backström, 1964, 1965)
Zwart Boois Berg Member of Neusberg Formation	Goede Hoop Formation (Geringer, 1973)
Neuspoort Member of Neusberg Formation	Quartzite and Quartz-sericite schist (Von Backström, 1964)
Baviaans Krantz Banded Calc-silicate Quartzite	Cafemic rocks (Von Backström & Poldervaart, 1949) Granulite, containing lenses of calc-silicate rocks (Von Backström, 1964) N'Rougas Formation (Botha *et al.*,1976) Umeis Formation (Beukes, 1973) Biesiepoort Formation (Geringer, 1973)
Kakamas Metamorphic Complex	Pink Gneiss Aasvogelkop Granulite (Von Backström,1964) Pink Gneiss (Joubert, 1971) Houmsrivier Formation (Beukes, 1973) Riemvasmaak Formation (Geringer, 1973) Austerlitz Formation (Toogood, 1976) Kokerberg Formation (Botha *et al.*,1976) Pink Gneiss (Moore, 1977)
Venterskop Kinzigite	Sillimanite Garnet Granulite (Von Backström, 1964)
Kakams Suid Leucogneiss	Granite Gneiss of Central Dome (von Backström, 1964)

Table 6.1 Main lithological units described in this report with their suggested equivalents of other areas.

Folding phase	D_{n+1}	D_{n+2}	D_{n+3}	uplift & cooling
	formation of penetrative foliation	Development of NW trending folds	open folding (NE trending)	
area affected	main evidence W of NL, some evidence E of NL	whole area affected	significantly only W of NL	all areas
metamorphism	? main	metamorphism	intrusion of granites → contact metam.	growth of low grade minerals
fracturing and shearing	Neusspruit Lineament?	Neusspruit L. Kakamas SZ	Brakfontein SZ Neusspruit L Kakamas SZ	formation of joints?
		Duivelsnek SZ Cnydas SZ	Duivelsnek SZ Cnydas SZ	continued movement along shear zones & NL?

Table 6.2 Summary of events showing the correlation between the folding phases and other events

NL = Neusspruit Lineament

SZ = Shear Zone

	T*	M	P	R	J	L	G	V
nº of folding phases	3	5	4	5	4	4	3	3
Development of penetrative foliation took place in	F_3	F_2	F_2	F_2	F_2	F_2	$F_{1,2}$	D_{n+1}
Development of large folds (no penetrative foliation)	F_4	F_3	F_3	F_3	F_3	F_3	F_3	D_{n+2}
Development of interference pattern	-	F_4	-	F_4	-	-	-	D_{n+3}
Timing of maximum metamorphism	early	2	3?	pre 2	2	2-3	3	D_{n+2}
ºC	800-860	650-750	amphi-bolite	630-670	gran/ amph.	low gran.	625-670	660-700
P kbar	8-9	5-7	"	2,8-4,5	"	"	3-3.5	5
charnockitic emplacement during	F_{5-6}	-	-	-	-	-	-	D_{n+3}
major shearing	F_{5-6}	-	F_5	F_5	$F_{5,6,7}$	F_3	-	D_{n+2} - D_{n+3}
faulting	-	F_5	F_6	-	$F_{8,9}$	-	post F_2	D_{n+3}

Table 6.3 Summary of major events in Namaqualand Metamorphic Complex as seen by various authors.
T = Toogood (1976); M = Moore (1977); P = Paizes (1975); R = Rozendaal (1975);
J = Joubert (1971, 1974); L = Lipson (1978); G = Geringer & Botha (1977, 1978);
V = this study.
F-numbers refer to deformational events (for location of these areas see Fig. 6.1).
* See text for explanation.

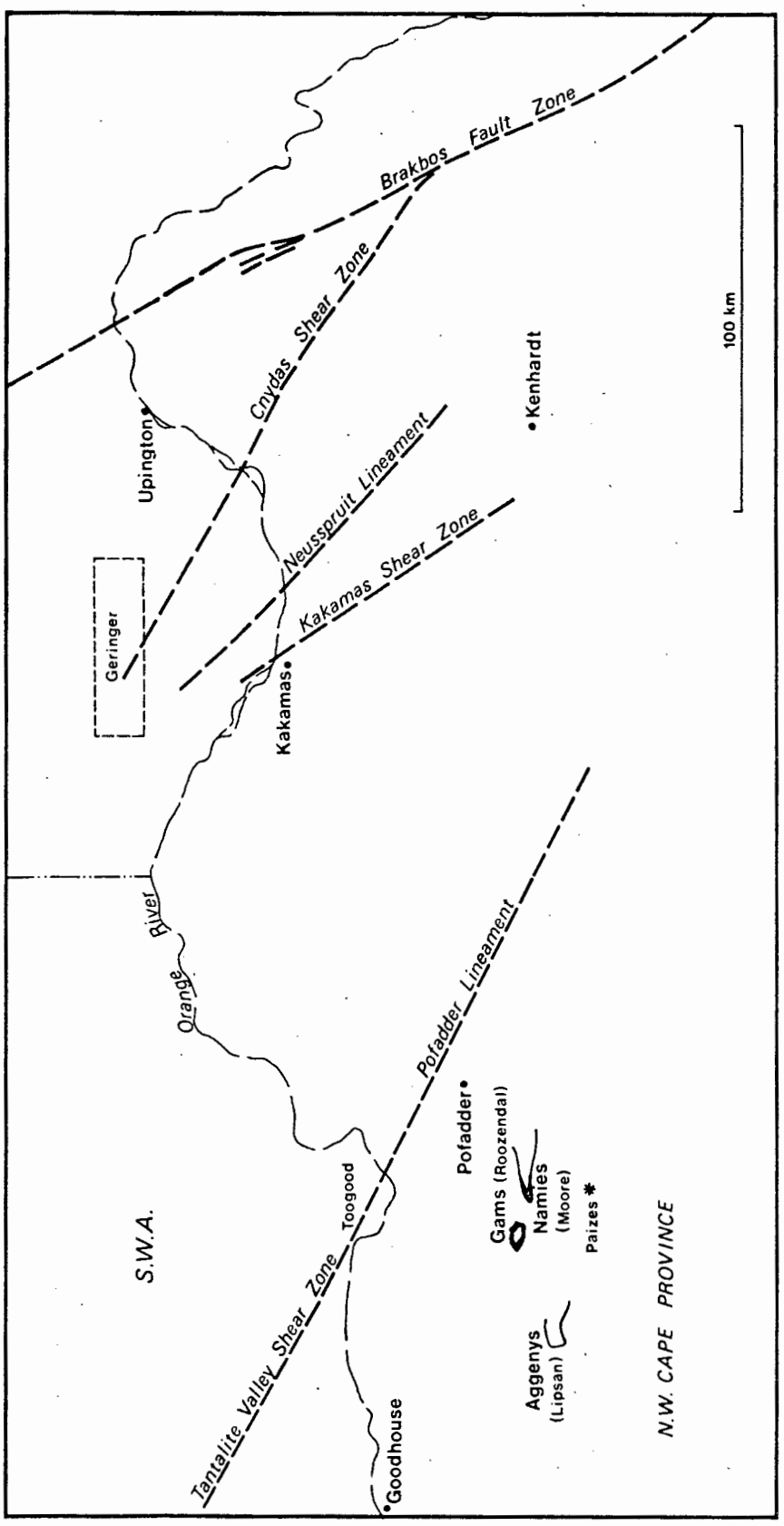

Fig. 6.1 Sketch map showing the position of the areas described by other workers, listed in Table 6.3.

7. KINEMATICS AND DYNAMICS

In the foregoing chapters the structure and metamorphism of the area have been described and analysed. These provide a basis for proposing a model to account for all the structural and metamorphic events recorded. In the following section the kinematics will be discussed first of all according to the geometrical analyses and strain analyses derived in Chapter 3. Subsequently a dynamic model will be proposed for the study-strip as seen in a wider context.

7.1 Kinematics

The reconstruction of the kinematic history of an area aims to present a picture of the magnitude and directions of movements of the various parts of the area in relation to time. As deformation is normally not homogeneous at the scale of the area, the state of strain differs through the area, as has been discussed in Sections 3.9 and 3.10. It appears that flattening, producing S-tectonites, was the major mechanism, as 5 out of the 6 areas plot in the field between $K_{fabric} = 1$ and $K_{fabric} = \infty$. In order to establish what the subsequent movements, leading to the pattern mentioned above, has been, each deformational event is to be examined separately.

Kinematics of the last deformational event (D_{n+3}).

From the descriptions in Chapter 3 it has become clear that no important fold structures of the last major deformational event have been recorded east of the Neusspruit Lineament.* West of the Lineament the situation is different and various interference patterns between folds of D_{n+2} and D_{n+3} have been recorded.

This striking difference across the lineament can be explained by a difference in plasticity, probably resulting from a difference

---

* "East of the Lineament" refers to the area bounded by Neusspruit Lineament and Cnydas Shear Zone.

in temperature. Griggs *et al.*, (1960) showed that plastic deformation in a specific rock type sets in at different levels of stress, depending on the temperature conditions. Assuming approximately equal stresses at equal depth, different degrees of plasticity in similar rocks reflect a different temperature.

Assuming a constant geothermal gradient over the area as a whole, it may be expected that approximately similar pressures and temperatures existed at the same depth at different places in the area. Consequently, plasticity will be the same too. It follow that at higher levels, where temperature is lower, plasticity will decrease. It is therefore suggested that the difference in plasticity reflects a different crustal level, resulting from uplift of the western block relatively to the eastern block before D_{n+3} took place. This is confirmed by the metamorphic record (see also Table 7.1).

West		Neusspruit Lineament		Cnydas Shear Zone	East
M_2	not recorded		T ∿300°C P ∿2 kbar D ∿8-13 km		T ∿600°C P ∿5.5 kbar D ∿18 km
M_1	T ∿ 660°C P ∿ 5 kbar D ∿ 18 km		T ∿495-565°C P ∿2 kbar D ∿8-13 km		T ∿ 515-530°C P ∿ 5.5 kbar D ∿ 18 km

Table 7.1 Summary of temperature and pressure differences across the major shear zones.

T = Temperature

P = Pressure

D = Depth

The D_{n+2} parageneses to the west of the lineament indicate temperatures higher than 660°C and pressures around 5 kbar (Section 5.2). Using the graph suggested by Winkler (1974, Fig. 1.1) to calculate the overburden, a depth of about 18 km follows.

Between Neusspruit Lineament and Cnydas Shear Zone, M_1 temperature and pressure were below the P-T conditions required to form staurolite : 495°-565°C and a pressure of about 2 kbar. The depth calculated on this basis is about 8 km, a depth one would expect for shallow contact

metamorphism. East of the Cnydas Shear Zone staurolite and cordierite were probably the M_1 minerals, indicating that P-T conditions were 515-530°C and at least 2 kbar H_2O pressure. This would result in a geothermal gradient of about 11° km^{-1}, which is unlikely as a considerably higher gradient existed west of the Neusspruit Lineament. Assuming the same gradient to the west of the Neusspruit Lineament as to the east of the Cnydas Shear Zone (about 30°km^{-1}), the depth following from the temperatures mentioned above (based on microprobe analyses) is about 17 km. On the basis of the evidence presented above vertical displacement along the Neusspruit Lineament and Cnydas Shear Zones can be calculated; between 5 and 10 km in both cases.

The geothermal gradient mentioned above of about 30° km^{-1} is close to the present-day world average (25°C/km) but almost double the present-day geothermal gradient for the Rhodesian Craton (Oxborough, 1977, unpublished report). Geothermal gradient in Hercynian times reached values as high as 150°C/km in the Pyrenees (Zwart, 1967) and 60°C/km in the Austrian Alps (Fritsch, 1962). Geothermal gradient in Alpine deformation was as low as 10-15° C/km (Zwart, *op.cit.*).

Yet another factor should be considered here : the possibility of higher heat flow and thus higher geothermal gradient during M_2. As the majority of granites exist east of the Neusspruit Lineament and across the Cnydas Shear Zone, higher heat flow is likely to occur in the eastern part. This would affect the interpretation of the vertical movement, in that displacement along Neusspruit Lineament would be closer to the maximum values obtained, whereas displacement along Cnydas Shear Zone would be closer to the minimum values obtained.

All D_{n+3} structures have approximately southwest-northeasterly-trending axial planes and fairly shallow plunging fold axes, apart from the Omkyk Structure, where the axial plane has quite a different strike and dip (Table 7.2). This could be explained by a different orientation of the XY plane of the strain ellipsoid of the area between Kakamas Shear Zone

STRUCTURE	STRIKE/DIP OF AXIAL PLANE	TREND/PLUNGE OF FOLD AXES
Vaalgras	210/54	3/33
Regt Kyk	-	-
Swartpad	220/68	17/33
Omkyk	80/42	83/36
North of Central Dome (7A)	255/80	40/33

Table 7.2 Strike and dip of D_{n+3} axial planes and trend and plunge of D_{n+3} fold axes of structures west of the Neusspruit Lineament.

and Duivelsnek Shear Zone. In this case the two shear zones should be regarded as the boundaries of a zone of intense deformation, where the variation in orientation of the axial plane indicates a variation in simple shear (Ramsay and Graham, 1970). However, in such an area a considerable amount of shearing would be expected between the boundaries, but has not been observed outside the shear zones mentioned above. Another, more likely possibility, is the rotation of the whole block containing the Omkyk Structure after D_{n+3} folding was completed, or perhaps towards the end of this deformational event. The evidence for this is found in the fact that D_{n+3} obviously deformed both the Kakamas and Duivelsnek Shear Zones (Annex.1,2) and the D_{n+2} axial plane of the Omkyk Structure. Continued right-lateral movement along Duivelsnek and Kakamas Shear Zones could have caused the rotation, as shown in Fig. 7.1.

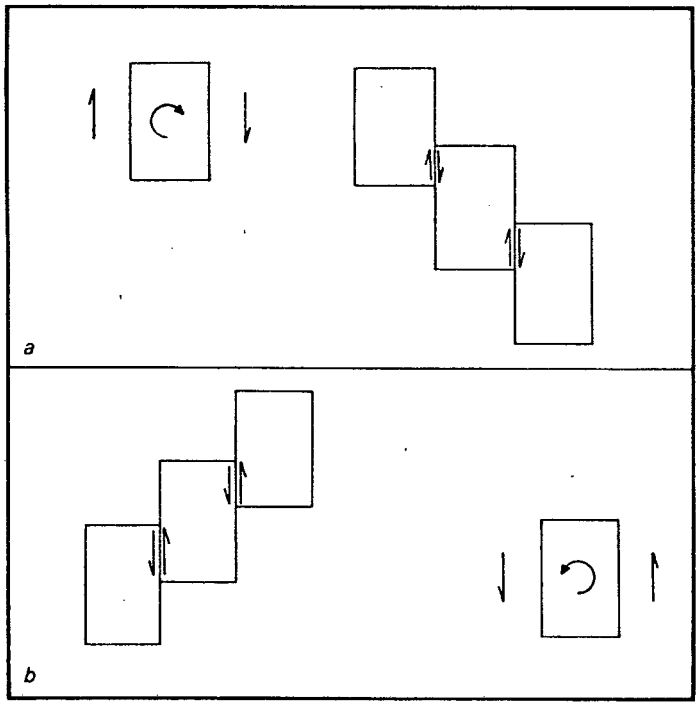

Fig. 7.1 Relative movement and resulting sense of rotation for right lateral (A) and left lateral (B) movement

Right-lateral shear zones should result in a step-wise movement, with the easternmost block most advanced. If three adjacent blocks are considered, the results of this movement shall be that, relatively to the central block, the left block moved northwards and the right-hand block moved southwards, resulting in a clockwise rotation of the middle block. The apparently undisturbed position of the hinge zone of the Omkyk Structure suggests that the rotation was mainly effective in the northern part of the block, because movement past the flexure point in the Duivelsnek Shear Zone may have been impossible as it is locked in the south (Annex. 1). Assuming

no shear took place, the minimum displacement between the shear zones can be calculated by using the indicated angle of maximum rotation (34°) of the central block. Assuming equal amounts of movements along both zones, the displacement is obtained by multiplying half the distance between the two shear zones measured along the axial plane, with the sine of the angle of rotation. With this technique it follows that displacements just under 1 km (986 m) took place on both shear zones. Alternatively, the maximum displacement along one of these shear zones has been about 2 km after D_{n+3} folding. How much movement took place earlier cannot be calculated as no displaced marker beds are available.

A similar situation exists east of the lineament, where the orientation of the traces of the D_{n+2} axial planes of zone D (Fig. 7.2) show a mismatch of about 40° with the neighbouring zone, suggesting an anti-clockwise rotation. This can be explained by the left-lateral movement along the Cnydas and Brakfontein Shear Zones, resulting in a relative northward movement of the block east of the Cnydas Shear Zone and a relative southward movement of the block west of the Brakfontein Shear Zone after the D_{n+2} (Fig. 7.1). Maximum displacement is calculated on the basis of a distance between the two shear zones of about 20 km (⊥ to the shear zones), which is subsequently multiplied by the tangent of the maximum rotation (40°). As a result a maximum post-D_{n+2} movement along one of the bordering shear zones of about 16,5 km is suggested. As very little movement could be established to have taken place along the Brakfontein Shear Zone, most of the abovementioned displacement is expected to have taken place along the Cnydas Shear Zone.

These figures of displacements are based on the assumption that D_{n+2} axial planes were oriented similarly throughout the area. Because of the different lithologies involved and the likelihood of the strain being heterogeneously distributed through the area, this assumption is bound to be incorrect. It follows that displacements can be either more or less than mentioned above, as the acute angle between the traces can become smaller or larger where an initial misfit existed.

In summary it is concluded that the kinematics of D_{n+3} resulted in a relatively small amount of buckling (about 8%) in the Omkyk - Central Dome area. It is likely that homogeneous strain took place as it is thought that these two processes occur simultaneously (Hobbs, 1971). Classification of the D_{n+3} structures according to the methods described by Ramsay (1967) and Huddleston (1973 a,b,c) has been attempted in order to arrive at an estimate of the λ_1/λ_2 ratio for homogeneous strain. However, as no complete wavelength is available and only one inflection point, where angles do not exceed 30°, the method yielded results that were too unreliable to be able to estimate λ_1/λ_2. As a result no estimate of the homogeneous strain can be given and the shortening of 8% is to be regarded as a minimum value. Rotation amounted to a maximum of 34° in a dextral sense to the west of the lineament and to a maximum of about 40° sinistral to the east of the lineament . These rotations are shown to have taken place post-D_{n+3} and post-D_{n+2} respectively. Displacement along

these shear zones was up to 2 km west of the lineament and up to 16,5 km east of the lineament.

Kinematics of the main deformational event D_{n+2}

In Fig. 7.2 the orientation of the XY plane of the D_{n+2} strain ellipsoids is shown (double lines) together with the orientation of the λ_1-λ_2 plane of the D_{n+2} fabric ellipsoid. From this figure it becomes clear that the area can be divided into several zones concerning the orientation of λ_1-λ_2, c.q. XY planes of the fabric and strain ellipsoids: A. the area west of the Kakamas Shear Zone, with roughly northwest-southeast striking λ_1-λ_2 planes ; B. the area between Kakamas and Duivelsnek Shear Zones with an average NNE-SSW strike; C. the area in the direct vicinity of the Neusspruit Lineament, with λ_1-λ_2 planes parallel or subparallel to the lineament; and D. the area east of the Brakfontein Shear Zone. Like the total bulk strain and the component of flattening of the total strain, this distribution illustrates the importance of the Neusspruit Lineament, and what is more, the orientation of planes in zone C shows that the Neusspruit Lineament is of the same generation as the fabric ellipsoids, which were shown to be mainly due to D_{n+2}. From Sections 5.5 and 7.1 it is concluded that the main kinematic event along the Neusspruit Lineament was the D_{n+2} deformational event. As a result it would seem that from the two possible interpretations given in Section 4.10 on electron microscopy, the first (Brakfontein Shear Zone accommodated movement, after movement along the Neusspruit Lineament ceased) is the correct interpretation. This is unlikely however, because as D_{n+3} or even post- D_{n+3} movement along all the other shear zones has been proven, the Neusspruit Lineament can not be expected to have remained static during D_{n+3} . Consequently the second possible solution (highest generation of frictional heat in the northern part of the Warm Zand Structure, intermediate heat generation near Neusberg South closure and less shear and hence less frictional heat near Brakfontein Shear Zone) must be the correct interpretation,especially since D_{n+3} movement along the Brakfontein Shear Zone is shown to be of minor importance. It is concluded therefore that the main deformation along the Neusspruit Lineament took place in D_{n+2} , but that movement continued during D_{n+3}.

In Section 3.4 it has been pointed out that the shape of the D_{n+2} fabric ellipsoids of the Omkyk Area has been influenced by considerable shearing in the direct vicinity of the Kakamas Shear Zone. It follows that this shear zone was already active during D_{n+2}. The sense of movement was in all probability dextral, like reported by Joubert (1976) from the continuation of the shear zone further south. It is not possible to assess the displacement during D_{n+2}, as no displaced marker beds are available. From the shape of the fabric ellipsoids it can be concluded that the amount of flattening, and therefore the importance of this shear zone, is of a lower magnitude than of the Neusspruit Lineament.

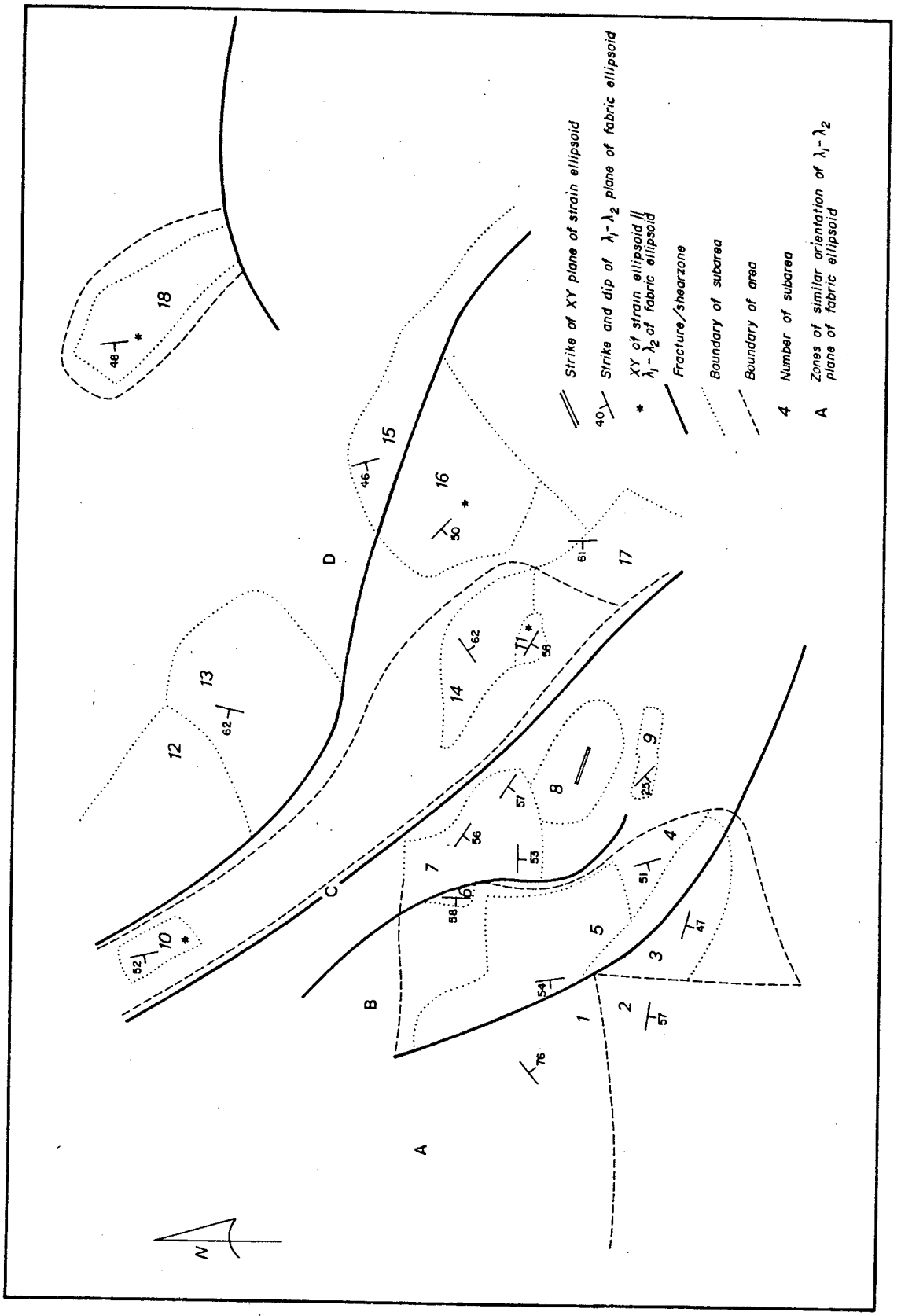

Fig. 7.2 Sketch map showing division into four zones, based on orientation of λ_1-λ_2 plane of fabric ellipsoid.

The difference in orientation of the λ_1-λ_2 planes in zone B is explained by post- or late- D_{n+3} rotation, as outlined in the previous section. Fig. 7.3B shows the position of axial plane traces after removal of this rotation.

East of the Neusspruit Lineament the λ_1-λ_2 planes show rather larger discrepancies when compared with those from west of the lineament. The discrepancy in the orientation of the λ_1-λ_2 plane in subarea 14 can be due to several factors, or combination of factors:

- sinistral rotation of the block between Neusspruit Lineament and Brakfontein Shear Zone due to sinistral movement along those shear zones during D_{n+3}. This is unlikely, as no significant movement along the latter zone is observed. It is possible however, that sinistral movement along the Neusspruit Lineament alone resulted in this misorientation. No proof for such a movement could be found however.
- The emplacement of the charnockitic adamellite. To what extent this factor influenced the orientation cannot be established, but some influence should not be excluded.
- Yet another possibility is that a strong homogeneous flattening strain imposed on the structure comprising subareas 11 and 14 caused the development of an elasticas fold in the extended subarea 11.

Mismatch in orientation of λ_1-λ_2 planes in zone D (Fig. 7.2) is explained by sinistral movement along the Cnydas Shear Zone, as described earlier. It is suggested here that this sinistral movement was in operation already during D_{n+2}, causing a sinistral movement of the block containing the Warm Zand Structure, resulting in the severe shortening in the northern part of this structure, described in Section 3.7.3. The imbrication is envisaged to have taken place as a result of this sinistral movement of the Warm Zand Structure against the rigid Neusspruit Lineament.

Evidence for vertical movement along the Neusspruit Lineament has been presented earlier in this section. It was shown that vertical movement resulted in the exposure of different crustal levels on both sides of the lineament. It is postulated that this vertical movement had already started in D_{n+2}, as the two Neusberg closures developed during D_{n+2} and probably formed as a result of drag along the vertical plane of movement.

In summary, it is concluded that during D_{n+2} shortening varied from 30 percent west of the Kakamas Shear Zone to 74 percent in the Neusberg area, with a minimum shortening of 20 percent measured in the Central Dome area. Close to the Cnydas Shear Zone shortening increases again to 66 percent (see also 3.10). These figures represent shortening due to buckling and homogeneous shortening during and after buckling. Homogeneous

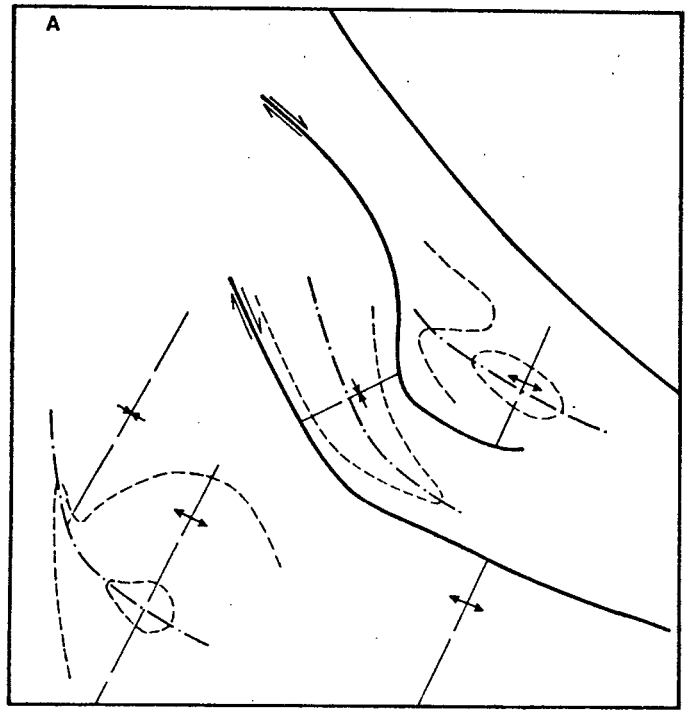

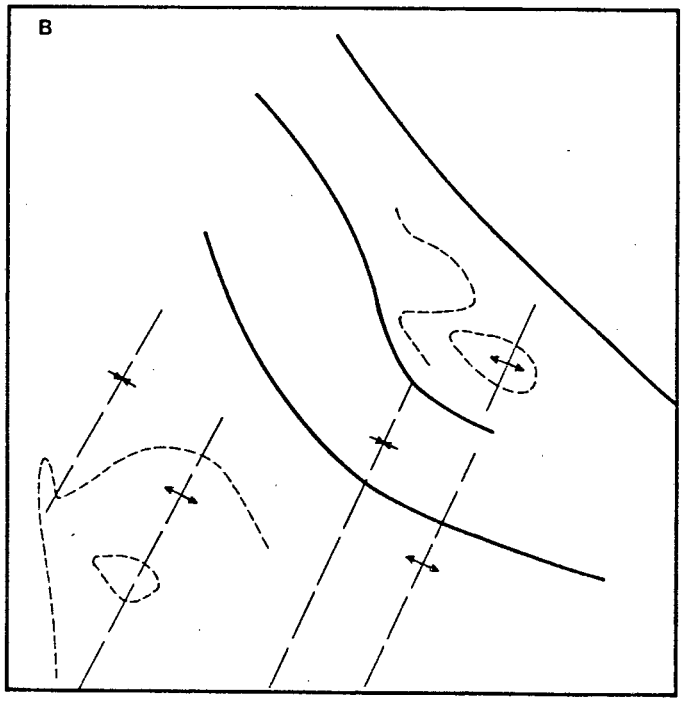

Fig. 7.3 Sketch maps showing the traces of D_{n+3} axial planes in the area west of the Neusspruit Lineament as at present (A) and after removal of rotational component (B).

shortening prior to folding has not been taken into account, as no proper strain markers exist. It is difficult to estimate D_{n+2} rotation from the orientation of λ_1-λ_2 planes of the fabric ellipsoid as, because of the strong flattening, the fabrics will in the end be more or less parallel throughout the area. A good indication of D_{n+2} rotation is the imbrication structure in the north of the Warm Zand Structure. It is suggested that this structure resulted from sinistral rotation, which in turn is the result of sinistral movement along the Cnydas Shear Zone. Horizontal movement along the Neusspruit Lineament could not be quantified, but vertical movement has been between 5 and 10 km. Likewise it has been possible to calculate that vertical movement along the Cnydas Shear Zone has also been between 5 and 10 km. The Duivelsnek and Kakamas Shear Zones existed already in D_{n+2}, as could be shown from metamorphic analyses and geometrical structural analyses, but only movements that took place during the last deformational event have been described quantitatively.

Kinematics of the first deformational event are extremely difficult to assess, as not enough evidence is available to warrant reliable results. The observed D_{n+1} structures do however, indicate that considerable buckling and homogeneous strain must have taken place.

7.2 Dynamics

Work carried out in the eastern part of the study-strip has revealed a stepwise increase in metamorphic grade from east to west, each step being marked by a shear zone (van Zyl, pers. comm.). This pattern is broken at the Cnydas Shear Zone, where an area of medium grade metamorphism starts. Confusing here is the presence of hyperstene-bearing granites. It has been shown however, that they do not reflect the regional metamorphism and have clear contact metamorphic aureoles. The area of lower grade metamorphism is bounded in the west by the Neusspruit Lineament, where again a high grade metamorphism is preserved. The high grade conditions described for the Central Dome area persist up to the Pofadder Lineament (c.q. Tantallite Valley Shear Zone) which, according to Toogood (1976), separates the high grade metamorphic area in the east from the lower grade metamorphic assemblages west of this lineament. These facts point to a stepwise upthrusting of a number of large blocks, whereby subsequent erosion exposed different crustal levels, the deepest being the block between Neusspruit and Pofadder Lineaments and the highest being the block between Neusspruit Lineament and Cnydas Shear Zone, bounded on both sides by "Lower -level blocks". The block east of the Neusspruit Lineament is thus a graben structure, due tc relatively less uplift than the neighbouring blocks.

It is suggested that the D_{n+2} structures resulted from strong SW-NE directed compressional stress. Due to this strong folding horizontal shortening and vertical thickening resulted and steep fold limbs developed along which shearing took place, thus forming the major shear zones of the area. Alternatively these shear zones predate the deposition of material and the folding. The solution of the Cnydas and Brakfontein Shear Zones representing $D_{n+2}\tau max$, oriented at about 30^{o} to the σ_{max} direction, has to be rejected as the sense of movement does not agree with this explanation. The last deformational event can be divided into two phases : a folding phase and a shortening phase. It is suggested that both took place as a result of a south-southeast - north-northwesterly directed compressional stress field. Evidence has been presented that this stress field was rather weak during the folding phase, as about 8 percent of shortening due to buckling combined with homogeneous strain is measured. The pre-buckling homogeneous strain is not recorded. When stress became too low to yield any buckling, shearing accommodated the deformation, resulting in late deformational rotation.

7.3 Synthesis

On the basis of dynamics and kinematics, given in the previous section, the following model is constructed (see also Fig. 7.4).

Granitic basement subsided to form a large basin of moderate depth. Whether fracturing occurred already during subsidence is not known. Deposition of pelitic sediments, followed by a thick sequence of greywackes with a decrease in the amount of pelitic material towards the top of the sequence, filled the basin. Amphibolites occurring in this sequence may represent sills or subaquous lava flows, emplaced in the deepest sections of the basin. It is suggested that at this stage isostatic adjustment started, resulting in upward movement, creating the shallow shelf conditions for the deposition of calc-silicate-rich quartzites. Once isostatic uplift had resulted in a regression, braided river systems deposited the cross-bedded feldspathic quartzites.

Horizontal shortening resulted in vertical thickening, during which the D_{n+2} structures developed. (It is thought that D_{n+1} consisted mainly of compaction and gravity-governed fold development, e.g. slumping). One aspect of this shortening is the formation of the imbrication in the Warm Zand Structure aided by sinistral rotation. An important factor of the vertical thickening was that vertical movement along the major shear zones occurred, possibly accentuated by the isostatic corrections. This type of block-faulting can be the result of crustal extensions where, due to a local tension in the crust, the block between the Neusspruit Lineament and Cnydas Shear Zone moved downwards. Alternatively crustal uplift can have caused normal faulting (Moore, 1960), resulting in the more or less symmetric

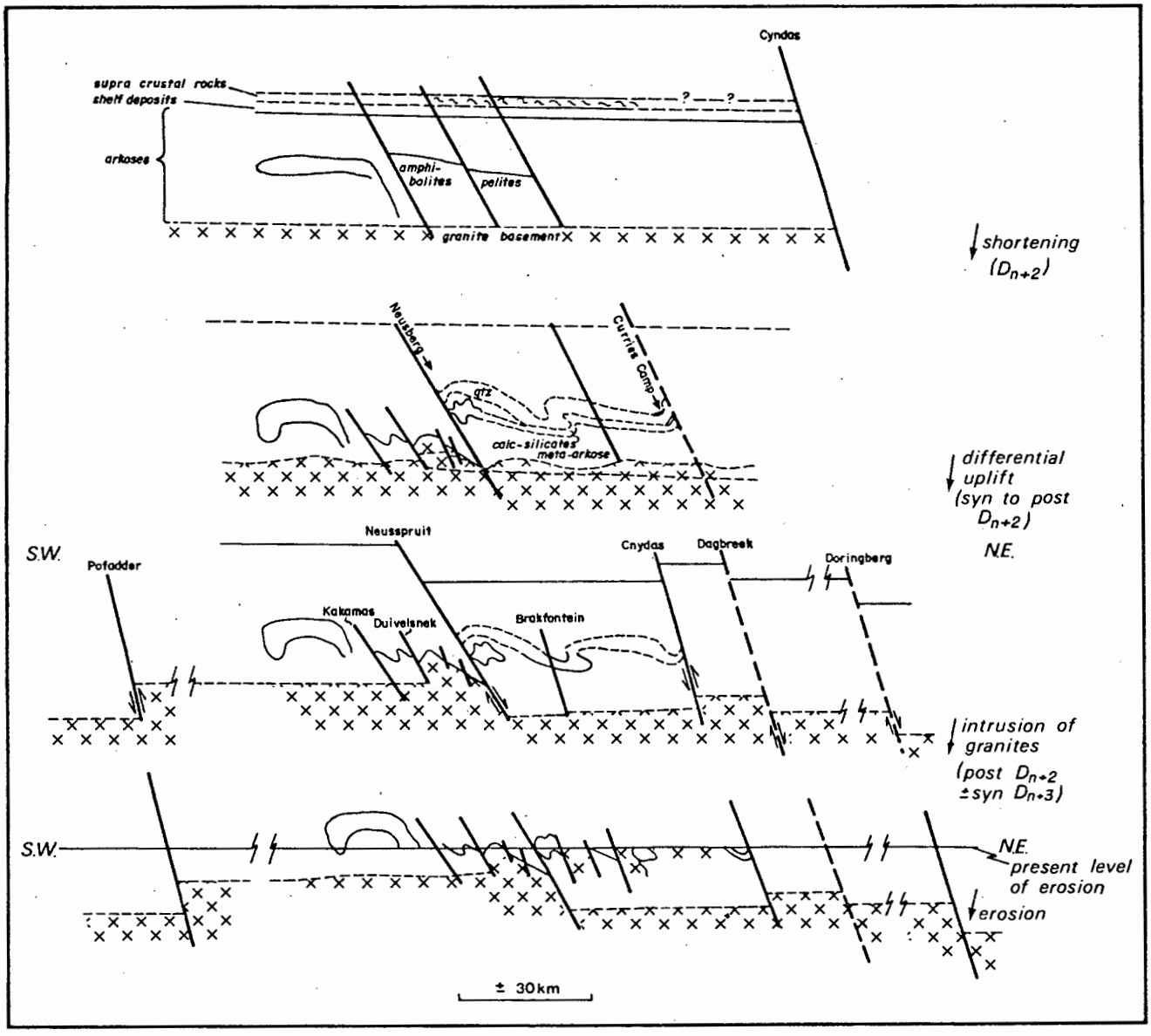

Fig. 7.4 Outline of structural evolution as described in text. Horizontal scale = vertical scale

pattern of exposures of different crustal levels, as encountered in Namaqualand. Joubert (1974) suggests wrench-fault tectonics to explain the pattern of shear zones and faults throughout Namaqualand. The pattern of fractures as shown in Fig. 3.2 is not uncommon in wrench-fault systems as shown by several authors (Hills, 1963; Moody & Hill, 1956; Hobbs *et al.*,1976). These authors also stress that while a young structure may accommodate mainly horizontal movement and to a smaller extent vertical movement, there may be no significant horizontal movement. Furthermore, Hobbs *et al.* (1976) quote from the work of Tchalenko (1970), who showed that a shear zone, resulting from wrench-faulting, becomes simpler as deformation continues during the same deformational event. When these results are combined with the results of this investigation, it becomes apparent that wrench-faulting did occur in the region. The Neusspruit Lineament may have been the original major fault, from which Duivelsnek and Kakamas Shear Zones are younger branches. The position of the Cnydas Shear Zone in this context is not very clear. It is possible however, that it forms the surface representation of an old wrench-fault, as both horizontal and vertical movement have been recorded.

The shear zones mentioned above played an important role in the emplacement of the granites. The position of the granites with respect to the shear zones strongly suggests that the shear zones penetrated deep enough to enable the granitic material to move upwards along them. The concentration of the granites in the block between Neusspruit Lineament and Cnydas Shear Zone confirms the postulated theory of block-faulting, as this block represents the most complete and therefore thickest part of the crust. Consequently, the possibility that lower levels of the crust were partial melts is strongest in this block. The timing of these intrusions has been late- or even post-D_{n+3}, as they obviously postdate D_{n+2}, but are related to and slightly affected by the late shear zones. As a result of the activities along these shear zones, rotation took place in the Omkyk Structure and in the block between Brakfontein and Cnydas Shear Zones, resulting in horizontal displacements of about 2 km and about 16 km respectively. Vertical displacement along the two major discontinuities was between 5 and 10 km. This represents post-D_{n+2} uplift as the different mineral parageneses, on the basis of which the different depths have been calculated, reflect the peak of the metamorphism, which has been shown to coincide with D_{n+2}. (Assuming that the area as a whole was affected by the same pressure and temperature conditions).

Continued isostatic uplift and erosion resulted in a relaxation of pressure and temperature, during which period low grade minerals formed.

8. CONCLUSIONS AND DISCUSSION

8.1 Summary of conclusions

(i) It has been shown that the bulk of the Kakamas Metamorphic Complex rocks in the area are of sedimentary origin, deposited on a granitic basement. Amphibolites now occurring in the Kakamas Metamorphic Complex probably were sills, emplaced in deep sections of the basin. Shallow shelf conditions probably formed the environment in which the calc-silicate rocks formed, followed by a fluviatile high energy environment in which the cross-bedded quartzites were deposited.

(ii) Three phases of folding have affected the deposits. An exception in this respect are the granites, which have only been slightly affected by the last deformational event.

The first event saw the formation of a penetrative foliation and large, isoclinal folds. This was followed by the second event during which the NNW-trending fold pattern, dominating the map, was formed. Folding, combined with post-folding homogeneous strain, resulted in a non-homogeneous shortening variable between 30 and 74 percent. The areas where this shortening reached its maximum are situated near the major shear zones : the Neusspruit Lineament and Cnydas Shear Zone.

The last folding phase is responsible for the development of interference patterns such as the Central Dome and its (D_{n+3}) shortening direction was almost perpendicular to the previous one. Shortening due to folding and the post-folding homogeneous strain (if present at all) amounted to at least 8 percent.

(iii) Metamorphism (M_1), accompanying these deformations, reached medium grade conditions (660°C and $\pm$ 5 kbar), but different levels of exposure resulted in different grades of metamorphism shown: 530°C and 2 kbar (minimum P-T conditions) in the Curries Camp Staurolite-Tourmaline Schist. Contact metamorphism (M_2) caused by the intrusion of the granites reached 600°C and 5.5 kbar east of the Cnydas Shear Zone. On the basis of these results it has been possible to calculate vertical displacement along the major shear zones : between 5 and 10 km along the Neusspruit Lineament and the same range of displacement along the Cnydas Shear Zone. Inaccuracy in this method does not allow the calculation of a more precise amount of vertical displacement, supporting the thesis that the relative uplift along the Neusspruit Lineament exceeded that along the Cnydas Shear Zone. This thesis is based on the fact that garnet and

sillimanite grew as a result of the intrusion of granites east of the Cnydas Shear Zone, in a rock containing staurolite and cordierite (thus prograde), whereas west of the Neusspruit Lineament the presence of cordierite indicates a drop in pressure while garnet and sillimanite were present (thus retrograde).

(iv) Late movement along the major shear zones resulted in dextral rotation of about 34° of the block containing the Omkyk Structure, with a maximum horizontal displacement of about 2 km along one of its bounding shear zones. Similarly sinistral movement of 40° of the block between Brakfontein and Cnydas Shear Zones has been shown to have taken place with a maximum post D_{n+2} lateral displacement of about 16,5 km, mainly along the Cnydas Shear Zone.

With the aid of information obtained from Transmission Electron Microscopy it is concluded that most intense D_{n+3} shearing took place in the northern part of the Warm Zand Structure and least along the Brakfontein Shear Zone.

Finally, a dynamic model is proposed, in which block-faulting and wrench-fault tectonics are suggested to have taken place.

8.2 Discussion

In terms of the purpose of this study as defined in Section 1.2 the major questions can now be answered. With respect to the processes taking place along the boundary between craton and mobile belt and the precise character and position of this boundary, it has been shown that the old granitic craton is possibly the basement to the gneissic rocks in Namaqualand. Stepwise upthrusting as suggested by Pretorius (1974) marks the transition from craton into mobile belt, exposing different crustal levels. The shear zones described in the study are vertical boundaries between the different crustal blocks, but all are in fact situated within the mobile belt. The fracture bounding the craton is probably the Brakbosch fault system, as this obviously important fault shows a strong lineament far into Botswana on the airborne magnetic record. It follows therefore, that the Neusspruit Lineament, although an important local boundary, does not represent the boundary between craton and mobile belt as initially suggested by Vajner and Jackson (1974). The importance of the Neusspruit Lineament lies in the strong flattening along its course due to horizontal shortening and in the accommodation of significant vertical movement (5-10 km). Both shortening and vertical movement took place during the main deformational event and continued into the last event and even after that. Horizontal movement continued until after D_{n+3}, but not in equal amounts along the various shear zones. As a result a rather irregular pattern developed:

little displacement between Duivelsnek and Kakamas Shear Zones (1-2 km) and no observed horizontal movement along the Neusspruit Lineament, although some horizontal movement has taken place. The Cnydas Shear Zone forms a sharp contrast with a horizontal movement of some 16 km . For the mechanisms involved in the two major shortening events during D_{n+2} and D_{n+3}, geotectonic processes involving plate tectonics are suggested. Recently it has been shown that some form of plate tectonic processes in Precambrian times are likely to have taken place (Mathews, 1972; Hartnady, 1978; Windley, 1977). This would imply that uniformitarianism applies, which has been opposed by Anhaeuser *et al.*, (1969) and several other authors. It is possible that the Limpopo mobile belt is a reworked portion of an originally large Rhodesian-Kaapvaal Craton , along which the strain was concentrated in one zone. It is also possible that the Namaqualand mobile belt is a similar area of intense deformation between two stable nuclei, one being the Kaapvaal Craton and one situated in Southern America. This process would then supply the driving force behind the large D_{n+2} crustal shortening. Mathews (1972) suggested that obduction took place in the Natal part of the Natal-Namaqualand mobile belt, roughly 1000 my. ago. Obduction in the proposed direction (towards the north) requires a compressive force in the same direction. As the relative late movement along the shear zones took place after D_{n+3}, which is placed at about 1000 my. and as the D_{n+3} shortening required a compressive stress operating in northerly directions, it is likely that both events are linked. Whether this compressive force was operating already during D_{n+2}, resulting in the relative movement, cannot be established with certainty. The possibility may not be rejected outright, because movement along the shear zones is likely to have taken place during an earlier stage of the deformation. As a different sense of movement occurred on the Cnydas Shear Zone and west of the Neusspruit Lineament, it is unlikely that they represent the maximum direction of shearing of the D_{n+2} stress field. It is possible however, that the different sense of movement originated along the same lines as the different sense of movement along transform faults in the oceanic regions, i.e. one block moving southwards relatively to the blocks on either sides, would yield an opposite sense of movement along its bounding shear zones. Such a system could result from a northerly directed compressive stress.

However, no firm evidence is available as yet to base these two postulations upon, so that, until considerably more research in the terrains concerned has been conducted, the question as to what the ultimate driving force behind the shortening along the two major directions was, will have to remain unanswered.

REFERENCES

ALTHAUS, E., 1967 - The triple point andalusite-kyanite-sillimanite. *Contr. Miner. Petrol. 16, 29-44.*

AMELINCKX, S., 1964 - *The direct observation of dislocations.* Solid state physics and Academic Press, N.Y., 487p.

ANHAEUSSER, C.R., MASON, R., VILJOEN, M.J. and VILJOEN, P.V., 1969 - A reappraisal of some aspects of Precambrian Shield geology. *Bull. geol. Soc. Am., 80, 2175-2200.*

ARDELL, A.J., CHRISTIE, J.M. and TULLIS, J.A., 1973 - Dislocation substructures in deformed quartz rocks. *Crystal Lattice Defects 4, 275-285.*

BALL, A. and WHITE, S., 1977 - An etching technique for revealing dislocation substructures in deformed quartz grains. *Tectonophysics 37/4 , T9-14.*

_____ 1978 - On the deformation of quartzite. *J. Phys. Chem. minerals 3, 163-172.*

BENEDICT, P.C., WIID, D. de N., CORNELISSEN, A.K. & STAFF, 1964 - Progress report on the geology of the O'okiep Copper District. *In:* Haughton, S.H., (Ed.)., *The geology of some ore deposits in Southern Africa.* Vol.II. Geol. Soc. S.Afr., Jhbg., 739p.

BEUKES, G.J., 1973 - *'n Geologiese ondersoek van die gebied suid van Warmbad, Suidwes-Afrika, met spesiale verwysing na die metamorf-magmatiese assosiasies van die Voorkambriese gesteentes.* Unpubl. D.Sc. thesis, Univ. Orange Free State, 333p.

BIOT, M.A. 1961a - Theory of folding of stratified visco-elastic media and its implications in tectonics and orogenesis. *Bull. geol. Soc. Am., 72, 1595-1620.*

_____ 1965 - *Mechanics of incremental deformations.* John Wiley & Sons, Inc.

_____ ODÉ, H. and DE ROEVER, W.L., 1961b - Experimental verification of the theory of folding of stratified visco-elastic media. *Bull. geol. Soc. Am., 72, 1621-1632.*

BOTHA, B.J.V., GROBLER, N.J., LINSTROM, W. and SMIT, C.A., 1976 - Stratigraphic correlation between the Kheis and Matsap formations and their relation to the Namaqualand Metamorphic Complex. *Trans. geol. Soc. S.Afr., 79, 304-311.*

_____ 1977 - Major structural features of the area between the Langeberg range and Kenhardt, N.Cape Province. *Trans. geol. Soc. S.Afr., 80, 101-109.*

CHATTERJEE, N.D. and JOHANNES, W., 1974 - Thermal stability and standard thermodynamic properties of synthetic $2M_1$ -muscovite, $KAl_2[AlSi_3O_{10}(OH)_2]$ *Contr. Miner. Petrol., 48, 89-114.*

CHRISTIE, J.M. and ARDELL, A.J., 1974 - Substructures of deformation lamellae in quartz. *Geology 2, 405-408.*

CLOOS, E., 1947 - Oolite deformation in the South Mountain Fold, Maryland. *Bull. geol. Soc. Am., 58, 843-918.*

CORNELL, D.N., 1975 - *Petrology of the Marydale metabasites.* Unpubl. Ph.D. thesis, Univ. Camb., 216p.

DEER, W.A., HOWIE, R.A. and ZUSSMAN, J., 1966 - *An introduction to the rock-forming minerals.* Longman, London. 528p.

DIETZE, H.D., 1952 - Versetzungsstrukturen in kubisch-flächenzentrierten kristallen. II. *Z. Phys. 131, 156-169.*

ESKOLA, P., 1915 - On the relations between chemical and mineralogical composition in metamorphic rocks of Orijärvi region. *Bull. Comm. geol. Finl. 44.*

ETHERIDGE, M.A., 1977 - Guidelines for the stratigraphic nomenclature of metamorphic rocks - Proposed addendum to the International Stratigraphic Guide. *Australian Geologist 16, p 9.*

ETHIER, V.G. and CAMPBELL, F.A., 1977 - Tourmaline concentrations in Proterozoic sediments of the southern Cordillera of Canada and their economic significance. *Can. J. Earth. Sci. 14, 2348-2363.*

FITCH, A.A., 1932 - Contact metamorphism in southeastern Dartmoor. *Q. Jl. geol. Soc. Lond., 576-609.*

FLINN, D., 1962 - On folding during three-dimensional progressive deformation. *Q. Jl. geol. Soc. Lond., 385-433.*

_____ 1978 - Construction and computation of three-dimensional progressive deformations. *J. geol. Soc. 135/3, 291-307.*

FRISCHAT, G.M., 1970 - Sodium diffusion in natural quartz crystals. *J. Am. Ceram. Soc., 53, p 357.*

FRITSCH, W., 1962 - Von der "Anchi" zur katazone im kristallinen Grundbebirge Ostkärntens. *Geol. Rdsch., 52, 202-210.*

GAY, S. PARKER, Jnr., 1972 - *"The new basement tectonics". Fundamental characteristics of aeromagnetic lineaments, their geological significance and their significance to geology.* American Stereo Map Co., Salt Lake City, Utah. 94p.

GERINGER, G.J., 1973 - *Die geologie van die Argeiese gesteentes en jongere formasies in die gebied wes van Upington met spesiale verwysing na die verskillende granietvoorkomstes.* Ph.D. thesis. U.O.F., 203p.

GERINGER, G.J. and BOTHA, B.J.V., 1977A - Anatektiese graniete in die mobile gordel Namakwaland, wes van Upington. *Bull. geol. Surv. Div., S.Afr., 61, 36p.*

_____1977B - The gneisses and regional structural pattern of the Namaqualand Mobile Belt in part of the Gordonia district, northwest Cape. *Trans. geol. Soc. S.Afr., 80, 93-95.*

_____ 1978 - Metamorfose in die Mobile Gordel Namakwaland, wes van Upington. *Ann. geol. Surv. Dep. Min. S.Afr., 11, 205-219.*

GILLESPIE, P., MCLAREN, A.C. and BOLAND, J.N., 1971 - Operating characteristics of an ion-bombardment apparatus for thinning non-metals for transmission electron microscopy. *J. Materials Sci. 6, 87-89.*

GRIGGS, D.T., 1967 - Hydrolytic weakening of quartz and other silicates. *Geophys. J. Roy. Astron. Soc., 14, 19-31.*

_____ and BLACIC, J.D., 1965 - Quartz : anomalous weakness of synthetic crystals. *Science 147, 292-295.*

GRIGGS, D.T., TURNER, F.J. and HEARD, H.C., 1960 - Deformation of rocks at 500° to 800° C. *In:* Griggs and Handin (Eds.). Rock Deformation, 39-104. *Mem. geol. Soc. Am., 382p.*

GYULAI, Z. and HARTLY, D., 1928 - Elektrische leitfähigkeit verformter steinsalzkristalle. *Z. Phys., 51, 378-387.*

HARTNADY, C.J.H., 1978 - *The structural geology of the Naukluft nappe complex and its relationship to the Damara Orogenic Belt, S.W.A., Namibia.* Unpubl. Ph.D. thesis. U.C.T. 290p.

HEARD, H.C., 1976 - Comparison of the flow properties of rocks at crustal conditions. *Phil. Trans. R. Soc. Lond., A283, 173-186.*

HEDBERG, H.D., 1970 - Preliminary report on lithostratigraphic units. *Internat. Subcomm. Stratigr. Classif. Rept. 3, Montreal, 30p.*

HEINRICH, E. Wm., 1965 - *Microscopic identification of minerals.* Mc Graw-Hill, New York. 414p.

HEUER, A.H., FIRESTONE, R.F., SNOW, J.D., GREEN, H.W., HOWE, R.G. and CHRISTIE, J.M., 1971 - An improved ion-thinning device. *Sci., Instrum. Rev., 42, 1177-1184.*

HILLS, E.S., 1963 - *Elements of structural geology.* Methuen & Co., Ltd., London. 483p.

HIRSCH, P.B., HOWIE, A., NICHOLSON, R.B., PASHLEY, D.W. and WHELAN, M.J., - 1965 - *Electron microscopy of thin crystals.* Butterworths, London. 549p.

HIRSCHBERG, A. and WINKLER, H.G.F., 1968 - Stabilitätsbeziehungen zwischen chlorit, cordierit und Almandin bei der metamorphose. *Contr. Miner. Petrol. 18, 17-42.*

HOBBS, B.E., 1968 - Recrystallisation of single crystals of quartz. *Tectonophysics, 6, 353-401.*

_____1971 - The analysis of strain in folded layers. *Tectonophysics, 11, 39-375.*

_____ MCLAREN, A.C. and PATERSON, M.S., 1972 - Plasticity of single crystals of synthetic quartz. "The Griggs Volume". *Geophys. Monogr. Ser. Am. Geophys. Union, Washington, D.C., 16, 29-53.*

_____ MEANS, W.D. and WILLIAMS, P.F., 1978 - *An outline of structural geology.* Wiley and Sons, 571p.

HOLDAWAY, M.J. and LEE, SANG MAN, 1977 - Fe-Mg cordierite stability in high-grade pelitic rocks based on experimental, theoretical and natural observations. *Contr. Miner. Petrol., 63, 175-198.*

HOSSACK, J.R., 1968 - Pebble deformation and thrusting in the Bygdir area (S.Norway). *Tectonophysics 5(4), 315-339.*

HUDLESTON, P.J., 1973a - Fold morphology and some geometrical implications of theories of fold development. *Tectonophysics, 16, 1-46.*

_____ 1973b - An analysis of single layer folds developed experimentally in viscous layers. *Tectonophysics 16, 189-214.*

_____ 1973c - The analysis and interpretation of minor folds developed in the Moine rocks of Monar, Scotland. *Tectonophysics, 17, 89-132.*

HUGO,P.J., 1969- The pegmatites of the Kenhardt and Gordonia districts, C.P. *Mem. geol. Surv. S.Afr., 58, 94p.*

HULL, D., 1965 - *Introduction to dislocations.* Pergamon Press, London, 259p.

HYNDMAN, D.W., 1972 - *Petrology of igneous and metamorphic rocks.* McGraw-Hill, New York, 533p.

JACKSON, M.P.A., 1976 - High-grade metamorphism and migmatization of the Namaqua Metamorphic Complex around Aus in the southern Namib desert, South West Africa. *Bull. Precambr. Res. Unit, Univ. Cape Town, 18, 299p.*

JANSEN, H., 1960 - The geology of the Bitterfontein area, Cape Province. *Geol. Surv. S.Afr., Explanation of sheet 253.*

JOUBERT, P., 1971 - The regional tectonism of the gneisses of part of Namaqualand. *Bull. Precambr. Res. Unit, Univ. Cape Town. 10, 220p.*

_____ 1974 - Wrench-fault tectonics in the Namaqualand metamorphic complex. *Bull. Precambr. Res. Unit, Univ. Cape Town, 15, 17-28.*

_____ 1975 - The fault pattern south of Kakamas. *In:* Abstracts of papers XVI Geokongress 75, 71p.

KNIPE, R.J. and WHITE, S.H., 1978 - On the deformation of quartz containing bubbles. *J. geol. Soc., 135/3: 313-317.*

KRAUSKOPF, K.B., 1967 - *Introduction to geochemistry.* McGraw-Hill Book Company, New York, 721p.

KRÖNER, A., 1968 - The gneiss-sediment relationships N.W. of Vanrhynsdorp, Cape Province. *Bull. Precambr. Res. Unit, Univ. Cape Town , 3, 233p.*

_____ 1971 - The origin of the southern Namaqualand Gneiss Complex, S.A., in the light of geochemical data. *Lithos 4, 325-344.*

LEIBFRIED, G. and DIETZE, H.D., 1951 - Versetzungsstrukturen in Kubisch-flächenzentrierten kristallen I. *Z. Phys., 131, 113-129.*

LIPSON, R.D., 1978 - *Some aspects of the geology of part of the Aggeneysberge and surrounding gneisses, Namaqualand.* Unpubl. M.Sc. thesis. Univ. Witwatersrand, Jhbg., 100p.

LISLE, R.J., 1977 - The evaluation of Laxfordian deformation in the Carloway area, Isle of Lewis, Scotland. *Tectonophysics 42, 183-209.*

MATHER, J. D., 1970 - The biotite isograde and the lower greenschist facies in the Dalradian rocks of Scotland. *J. Petrol. 11/2, 253-273.*

MATHEWS, P.E., 1972 - Possible Precambrian obduction and plate tectonics in southeast Africa. *Nat. Phys. Sci., 240, 98, 37-39.*

MCLAREN, A.C. and PHAKEY, P.P., 1965 - Dislocations in quartz observed by T.E.M. *J. Applied Phys., 36, 3244-3246.*

MIALL, A.D., 1977 - A review of the braided river depositional environment. *Earth-Sc. Rev., 13, 1-62.*

MIYASHIRO, A., 1973 - *Metamorphism and metamorphic belts.* George Allen and Unwin Ltd., 492p.

MOODY, J.D. and HILL,M.J., 1956- Wrench-fault tectonics. *Bull. geol. Soc. Am., 67, 1207-1246.*

MOORE, J.G., 1960 - Curvature of normal faults in the Basin and Range Province of western United States. *In:* Short papers in the geol. Sciences U.S. Geol. Survey Prof. paper 400 B. 409-411.

MOORE, J.M., 1977 - The geology of Namiesberg, Northern Cape. *Bull. Precambr. Res. Unit. Univ. Cape Town, 20, 69p.*

NABARRO, F.R.N., 1967 - *Theory of crystal dislocations.* Oxford at the Clarendon press, 821p.

NADAI, A., 1963 - *Theory of flow and fracture of solids Vol.2. Engineering Societies Monographs.* McGraw-Hill, New York, 705p.

OXBOROUGH, A., 1977 - *Temperatures in various Rhodesian gold mines.* Unpublished report.

PAIZES, P.E., 1975 - *The geology of an area between Vaalkop and Aggeneys in the vicinity of Pofadder, Northwestern Cape Province.* Unpubl. M.Sc. thesis, Univ. Witwatersrand.

PARKER, R.B., 1961 - Petrology and structural geometry of pre-granitic rocks in the Sierra Nevada, Alpine County, California. *Bull. geol. Soc. Am., 72, 1789-1806.*

POLDERVAART, A., 1966 - Archaean charnockitic adamellite phacoliths in the Keimoes-Kakamas region, C.P. South Africa. *Trans. geol. Soc. S.Afr., 69, 139-154.*

_____ and VON BACKSTRÖM, J.W., 1949 - Study of an area at Kakamas. *Trans. geol. Soc. S.Afr., 52, 433-495.*

PRETORIUS, D.A., 1974 - The structural boundary between the Kaapvaal and Sonama crustal Provinces. *Bull. Ec. Res. Un. information circular 88, 26p.*

PRICE, N.J., 1975 - Rates of deformation. *Jl. geol. Soc. Lond. Vol. 131, 553-575.*

RAMBERG, H., 1970a - Folding of laterally compressed multilayers in the field of gravity. I : Theory. *Phys. Earth. Planet Int. 2, 203-232.*

_____ 1970b - Folding of laterally compressed multilayers in the field of gravity. II : Numerical examples. *Phys. Earth. Planet Int. 4, 83-120.*

_____ and STRÖMGÅRD, K.E., 1971 - Experimental tests of modern buckling theory applied on multilayered media. *Tectonophysics 11, 461-472.*

RAMSAY, J.G., 1967 - *Folding and fracturing of rocks.* Mc Graw-Hill, New York, 568p.

_____ and GRAHAM, R.H., 1970 - Strain variation in shear belts. *Can. J. Earth. Sci., 7, 786-813.*

REINHARDT, E.W., 1968 - Phase relations in cordierite bearing gneisses from the Garanoque area, Ontario. *Can. J. Earth Sci., 5, 455-482.*

RICHARDSON, S.W., 1968 - Staurolite stability in a part of the system Fe-Al-Si-O-H. *J. Petrol., 9, 468-488.*

ROZENDAAL, A., 1975 - *The geology of Gamsberg.* Unpubl. M.Sc. thesis, Univ. of Stellenbosch, 109p.

RUTTER, E.H., 1976 - The kinetics of rock deformation by pressure solution. *Phil. Trans. R. Soc. Lond.A. 283, 203-219.*

SANDER, B., 1948 - *An introduction to the study of fabrics of geological bodies.* Pergamon Press (translation, 1970), 641p.

SCHULTZ, R., 1977 - Origin of the so-called charnockitic adamellite porphyry from the Upington Geotraverse, South Africa. *Ann. Rep., Precambr. Res. Unit, Univ. Cape Town, 14, 48-83.*

SCHWERDTNER, W.M., 1970 - Hornblende lineations in Trout Lake area, Lac La Ronge map sheet, Saskatchewan. *Can. J. Earth Sci., 7, 884-899.*

_____ 1973 - Schistosity and penetrative mineral lineation as indicators of paleostrain directions. *Can. J. Earth Sci., 10, 1233-1243.*

_____ SHEEHAN, P.M. and RUCKLIDGE, J.C., 1971 - Variation in degree of hornblende grain alignments within two boudinage structures. *Can. J. Earth Sci., 8, 144-149.*

SOUTH AFRICAN CODE OF STRATIGRAPHIC TERMINOLOGY AND NOMENCLATURE, 1971 - *Trans. Geol. Soc. S.Afr., 74, 111-133.*

STRECKEISEN, A., 1976 - To each plutonic rock its proper name. *Earth-Sc. Rev., 12, 1-33.*

TAYLOR, G.I., 1938 - Plastic strain in metals. *J. Inst. Met., 62, 307-324.*

TCHALENKO, J.S., 1970 - Similarities between shear zones of different magnitudes. *Bull. geol. Soc. Am., 81, 1625-1640.*

THAKUR, V.C. and TANDON, S.K., 1976 - Significance of pebble and mineral lineation in Chamba syncline of Punjab, Himalaya, Himachal Pradesh, India. *Geol. Mag. 113(2), 141-149.*

THOMPSON, J.B., 1976 - Mineral reactions in pelitic rocks. II : calculation of some P-T-X (Fe-Mg) phase relations. *Am. J. Sci. , 276, 425-454.*

TOOGOOD, D.J., 1976 - Structural and metamorphic evolution of a gneiss terrain in the Namaqua belt near Onseepkans, S.W.A. *Bull. Precambr. Res. Unit, Univ. Cape Town, 19, 189p.*

TULLIS,J., CHRISTIE, J.M. and GRIGGS, D.T., 1973 - Microstructure and preferred orientations of experimentally deformed quartzites. *Bull. geol. Soc. Am., 64, 297-314.*

TURNER, F. J. and WEISS, L.E., 1963 - *Structural analysis of metamorphic tectonites.* Mc. Graw-Hill, 545p.

TWISS, R.J., 1977 - Theory and applicability of a paleo piezometer. *Pure & Appl. Geophys., 115, 229-244.*

VAJNER, V., 1974 - Crustal evolution of the Namaqua Mobile Belt and its foreland in parts of the N.Cape. *Bull. Precambr. Res. Unit. Univ. Cape Town, 15, 1-17.*

_____ and JACKSON, M.P.A., 1974 - Brief report on a field trip to the area between Kakamas, Kenhardt, Marydale and Upington. *Ann. Reps. Precambr. Res. Unit, Univ. Cape Town, 10 & 11, 56-57.*

VAN BEVER DONKER, J.M., 1974 - *Experimentele deformatie van plasticine-plasticine modellen en plasticine-welpasta modellen.* Unpubl. M.Sc. thesis, Univ. Leiden, 87p.

_____ 1977 - Estimating strain rate in naturally deformed rocks; an application of T.E.M. in geology. *Proc. El. Micr. Soc., S.Afr., 7, 39-40.*

VERHOOGEN, J., TURNER,F.J., WEISS,L.E. and WAHRHAFTIG,C., 1970 - The earth, an introduction to physical geology. *Holt, Rinehart & Winston, New York,748p.*

VERNON, R., 1976 - *Metamorphic reactions and microstructural processes.* George Allen & Unwin, London, 247p.

VON BACKSTRÖM, J.W., 1950 - Notes on a Tungsten-Tin deposit near Upington, Gordonia district. *Trans. geol. Soc. S.Afr., L111, 35-51.*

_____ 1962 - The geology along the lower reaches of the Molopo River and a note on the Riemvasmaak thermal spring, Gordonia district, C.P. *Ann. geol. Surv., Dep. Min. S.Afr., 1, 57-66.*

_____ 1964 - The geology of an area around Keimoes, Cape Province, with special reference to phacoliths of charnockitic adamellite-porphyry. *Mem. geol. Surv., S.Afr., 53, 218p.*

_____ 1965 - Deuteric alteration in the charnockitic adamellite-porphyry of the N.W. Cape Province. *Ann. geol Surv., Dep . Min. S.Afr., 4(2), 99-107.*

_____ 1967 - The geology and mineral deposits of the Riemvasmaak area, N.W. Cape Province. *Ann. geol. Surv., Dep. Min. S.Afr., 6, 43-53.*

_____ and POLDERVAART, A., 1953 - Phacoliths of charnockitic adamellite porphyry at Keimoes, C.P., South Africa. *Bull. geol. Soc. Am., 64, (12,2) p 1486.*

VON MISES, R., 1928 - Mechanik der plastischen Formänderung von kristallen. *Z. Angew. Math. Mech. 8, 161-185.*

WATSON, G.S., 1966 - The statistics of orientation data. *J. Geol., 74, 786-797.*

WHITE, S., 1970 - Ionic diffusion in quartz. *Nature, 225, 375-376.*

_____ 1971 - Electrical conductivity in quartz, a reply. *Nature Phys., Sci., 233, 63-64.*

_____1973a - Syntectonic recrystallisation and texture development in quartz. *Nature, 244, 276-278.*

_____ 1973b - Deformation lamellae in naturally deformed quartz. *Nature Phys. Sci., 245, 26-28.*

_____ 1973c - The dislocation structures responsible for the optical effects in some naturally deformed quartzes. *J. Mat. Sci., 8, 490-499.*

WHITE, S., 1976c - The effects of strain on the microstructures, fabrics and deformation mechanisms in quartz. *Phil. Trans. R. Soc. Lond., A.283, 69-86.*

_____ 1977 - Geological significance of recovery and recrystallization processes in quartz. *Tectonophysics 39, (1-3), 143-169.*

WILLIAMS, P.F., 1970 - A criticism of the use of style in the study of deformed rocks. *Bull. geol. Soc. Am., 81, 3283-3296.*

WILSON, C.J.L., 1973 - The prograde microfabric in a deformed quartzite sequence, Mount Isa, Australia. *Tectonophysics 19, 39-81.*

WINDLEY, B.F., 1977 - Timing of continental growth and emergence. *Nature, 270, 426-427.*

WINKLER, H.G.F., 1974 - *Petrogenesis of metamorphic rocks.* Springer Verlag, New York, Heidelberg, Berlin, 320p.

WOOD, D.S., 1973 - Patterns and magnitudes of natural strain in rocks. *Phil. Trans. R. Soc. Lond. A274, 373-382.*

WOODCOCK, N.H., 1977 - Specification of fabric shapes using an eigenvalue method. *Bull. geol. Soc. Am., 88, 1231-1236.*

WORST, B.G., 1960 - The great dyke of Southern Rhodesia. *Southern Rhodesia Geol. Surv. Bull. 47, 234p.*

YUEN, D.A., FLEITOUT, L. and SCHUBERT, G., 1978 - Shear deformation zones along major transform faults and subducting slabs. *Geophys. J. 54.*

ZWART, H.J., 1963 - The structural evolution of the paleozoic of the Pyrenees. *Geol. Rdsch., 53, 170-205.*

_____ 1967 - The duality of orogenic belts. *Geologie Mijnb. 46e/9/283-309.*

APPENDIX A

Fig. A.1 Simplified topographical map showing farm names and station numbers referred to in the text. (see also list of stations)

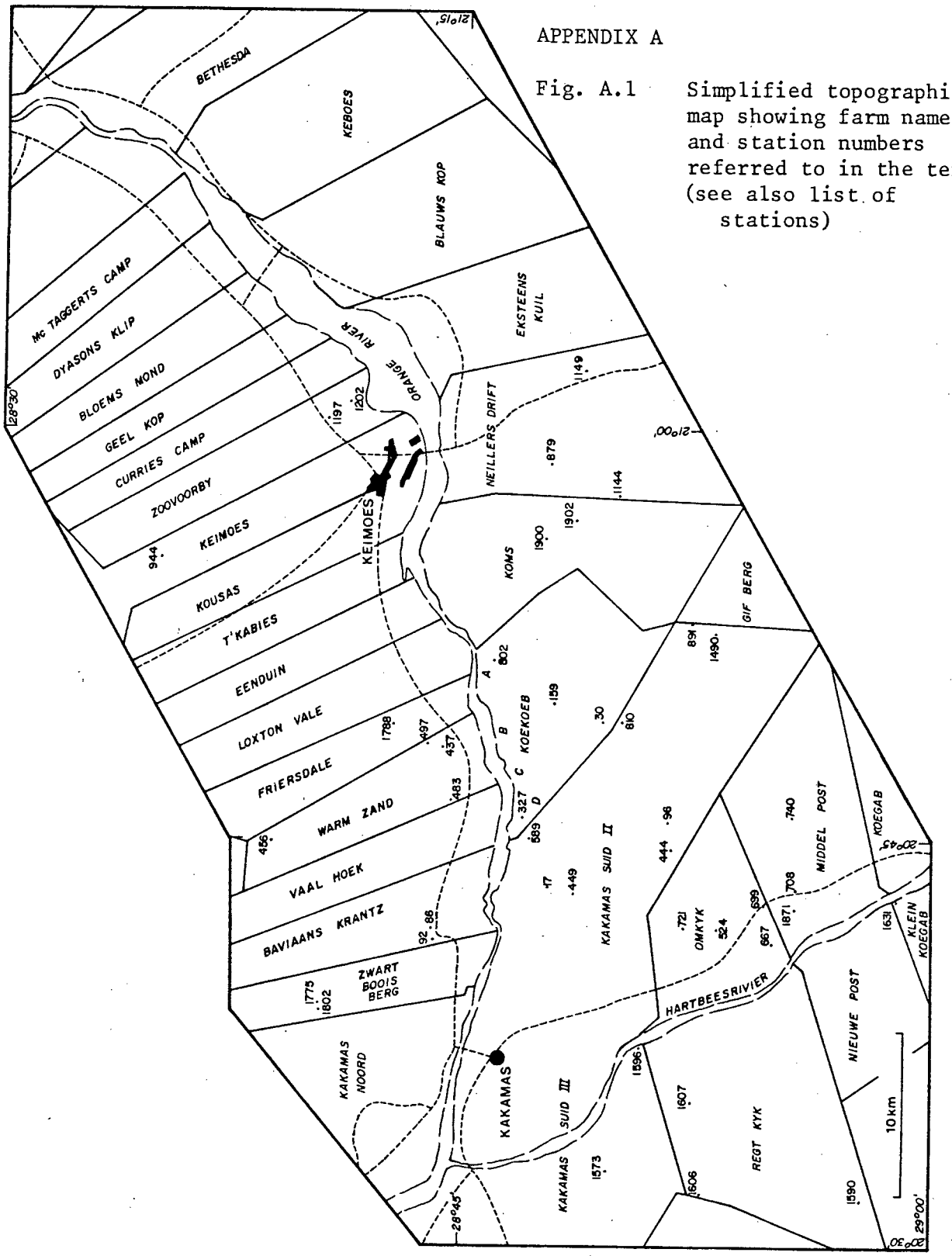

APPENDIX A

List of Stations
(See also Fig.A.1)

	X	Y	Z	Sheet
17	3188250	28875.00	705.0000	2820 DC
30	3189400	17250.00	750.0000	2820 DD
86	3179100	28450.00	730.0000	2820 DA
92	3180000	30725.00	710.0000	2820 DA
96	3194200	23750.00	772.0000	2820 DD
159	3186975	16400.00	795.0000	2820 DD
327	3185050	22950.00	730.0000	2820 DD
439	3180700	22500.00	715.0000	2820 DB
444	3193300	25250.00	765.0000	2820 DC
449	3189900	26550.00	760.0000	2820 DC
456	3170950	24900.00	838.0000	2820 DA
483	3180400	22300.00	730.0000	2820 DB
497	3179650	18350.00	745.0000	2820 DB
524	3197600	28650.00	745.0000	2820 DC
589	3186250	16650.00	715.0000	2820 DD
667	3199500	30850.00	740.0000	2820 DC
699	3199500	28300.00	760.0000	2820 DC
708	3201350	28000.00	750.0000	2820 DC
721	3195200	28500.00	730.0000	2820 DC
740	3201850	21300.00	810.0000	2820 DD
802	3183550	13700.00	735.0000	2820 DD
810	3190400	17100.00	835.0000	2820 DD
879	3187950	3600.000	805.0000	2820 DD
891	3195400	11500.00	860.0000	2820 DD
944	3164400	8600.000	850.0000	2820 DB
1144	3193250	7600.000	850.0000	2820 DD
1149	3188750	-4400.000	825.0000	2821 CC
1197	3172550	-750.0000	785.0000	2821 CA
1202	3173250	-2350.000	765.0000	2821 CA
1490	3196650	11600.00	825.0000	2820 DD
1500	3185300	7750.000	795.0000	2820 DD
1502	3187300	6600.000	795.0000	2820 DD
1573	3189400	46250.00	705.0000	2820 DC
1590	3204000	46500.00	825.0000	2820 DC
1596	3193350	35400.00	680.0000	2820 DC
1606	3195150	45650.00	765.0000	2820 DC
1607	3195200	38900.00	735.0000	2820 DC
1631	3206700	27500.00	710.0000	2820 DC
1775	3172100	34000.00	790.0000	2820 DA
1788	3177550	26575.00	820.0000	2820 DB
1802	3171350	34600.00	800.0000	2820 DA
1871	3201200	29250.00	776.0000	2820 DC

X Y Z coordinates refer to grid lines of the South African Co-ordinate System,as indicated(in metres) in the margins of the topographical maps.

APPENDIX B

Index of Farms quoted in this report

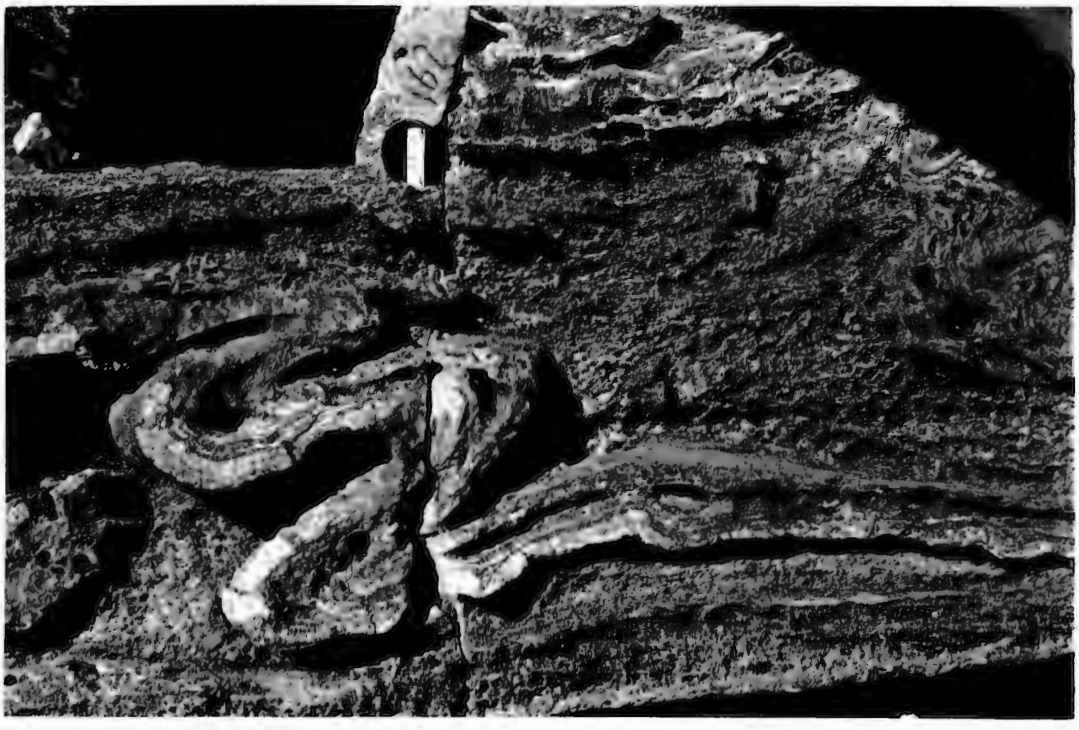

Plate 1 Strongly folded calc-silicate quartzite in wollastonite rock.

Plate 2. Xenolith of Baviaans Krantz Banded Calc-silicate Quartzite in Straussburg granite.

Plate 3 Crossbedding in Zwart Boois Berg Member of Neusberg Formation. Younging upwards. Scale mark 55 mm across.

Plate 4 Block of folded kinzigite, surrounded by undeformed kinzigite .

Plate 5 Left-lateral shear zone in feldspathic quartzite of Neusberg Formation. (Brakfontein Shear Zone). The plane of the photograph is the horizontal plane.

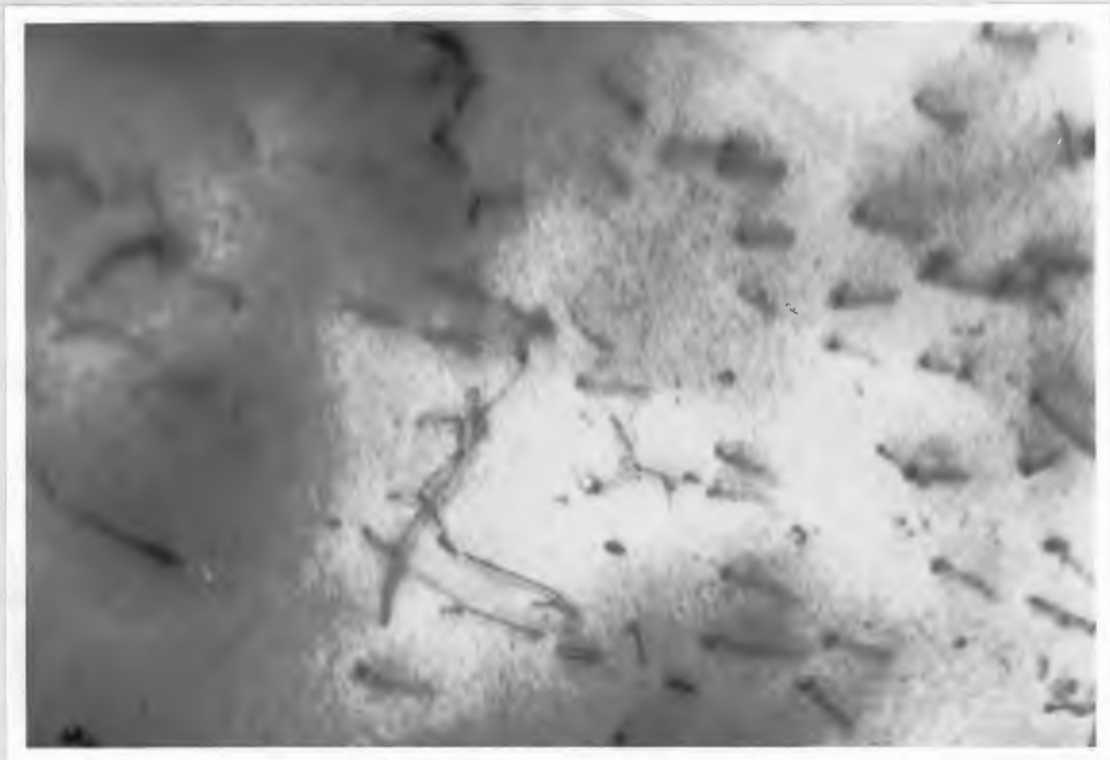

Plate 6 Electron micrograph showing dislocations pinned to impurities. Note the parallel lines representing stacking faults.

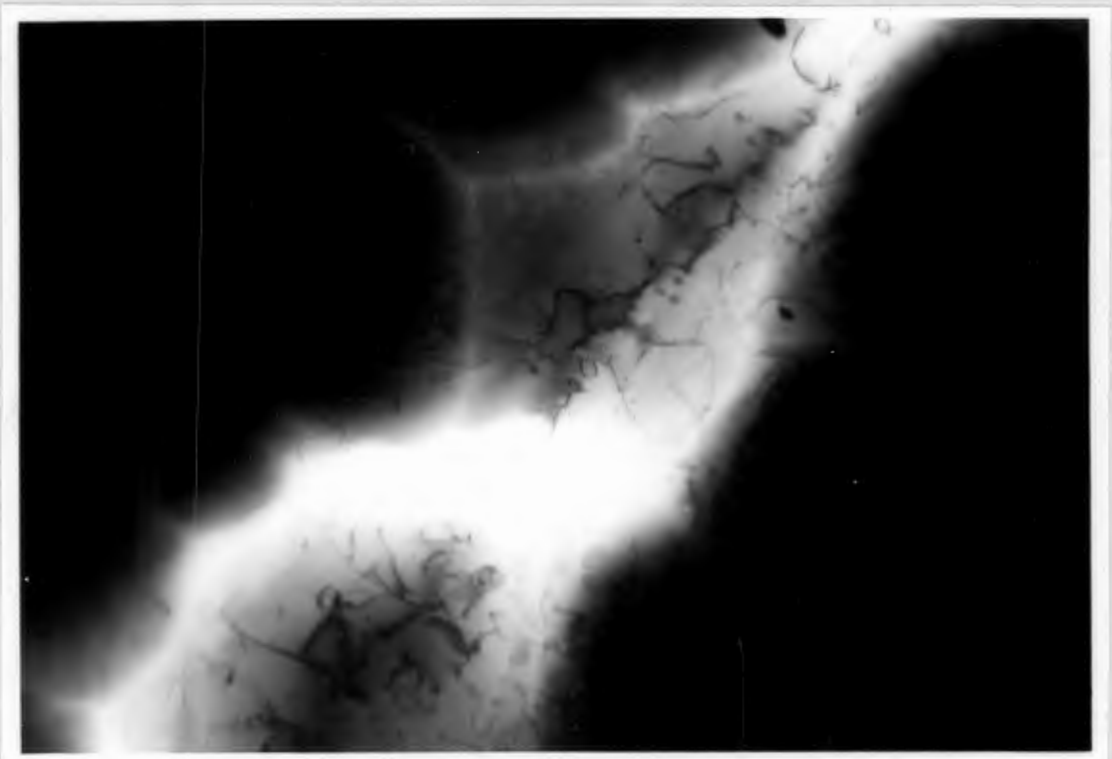

Plate 7 Electron micrograph taken with the goniometer stage at a randomly chosen orientation.

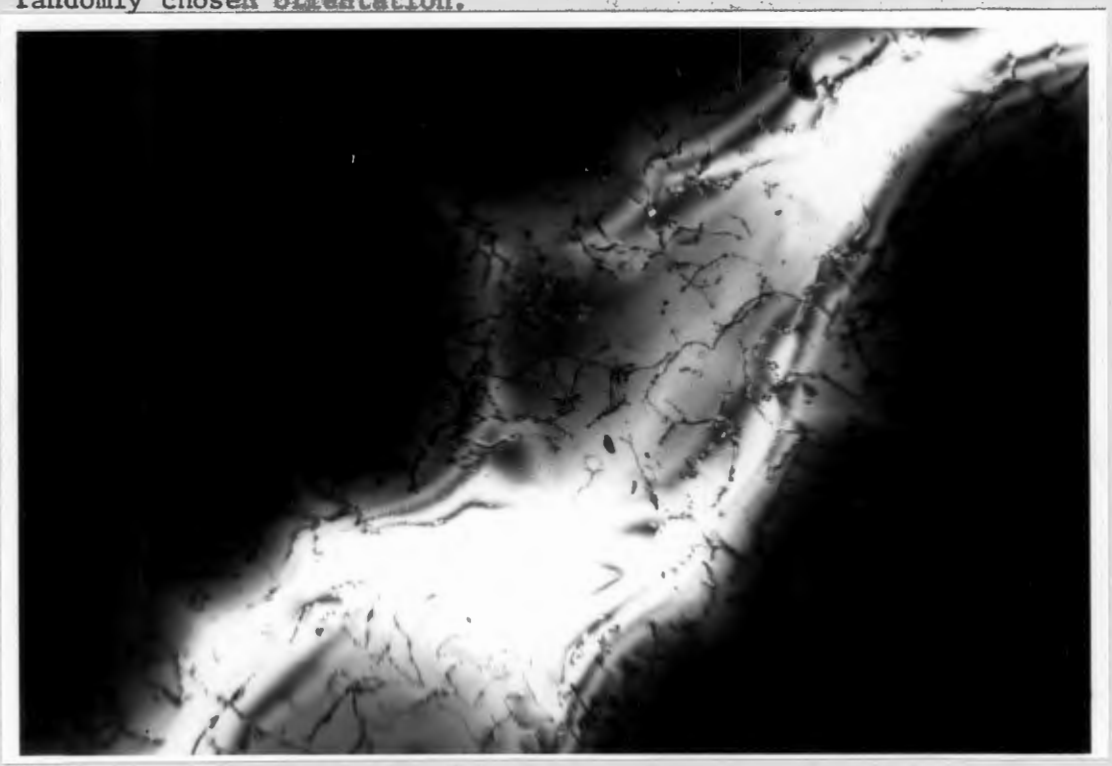

Plate 8 Electron micrograph taken with the specimen orientated in zone-axis position. Note the difference in number of visible dislocations compared with plate 7.

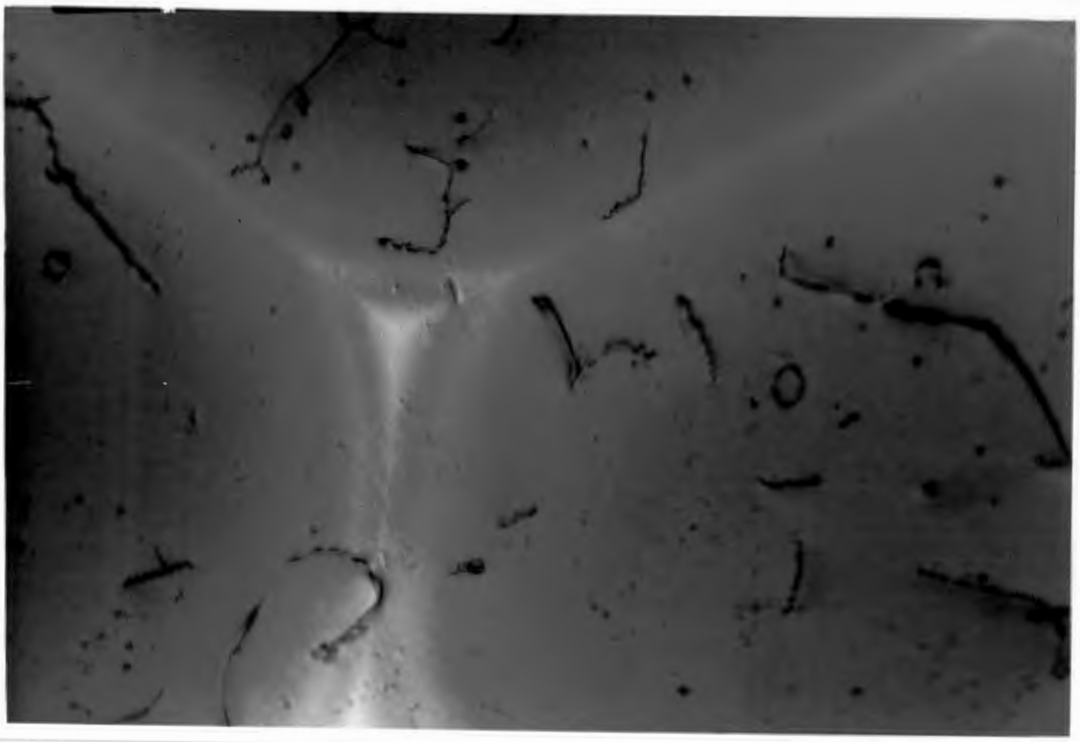

Plate 9 Electron micrograph showing mobile dislocations. Circular shapes are loops. Zig-zag pattern is a result of the periodicity and a reflection of the thickness of the sample.

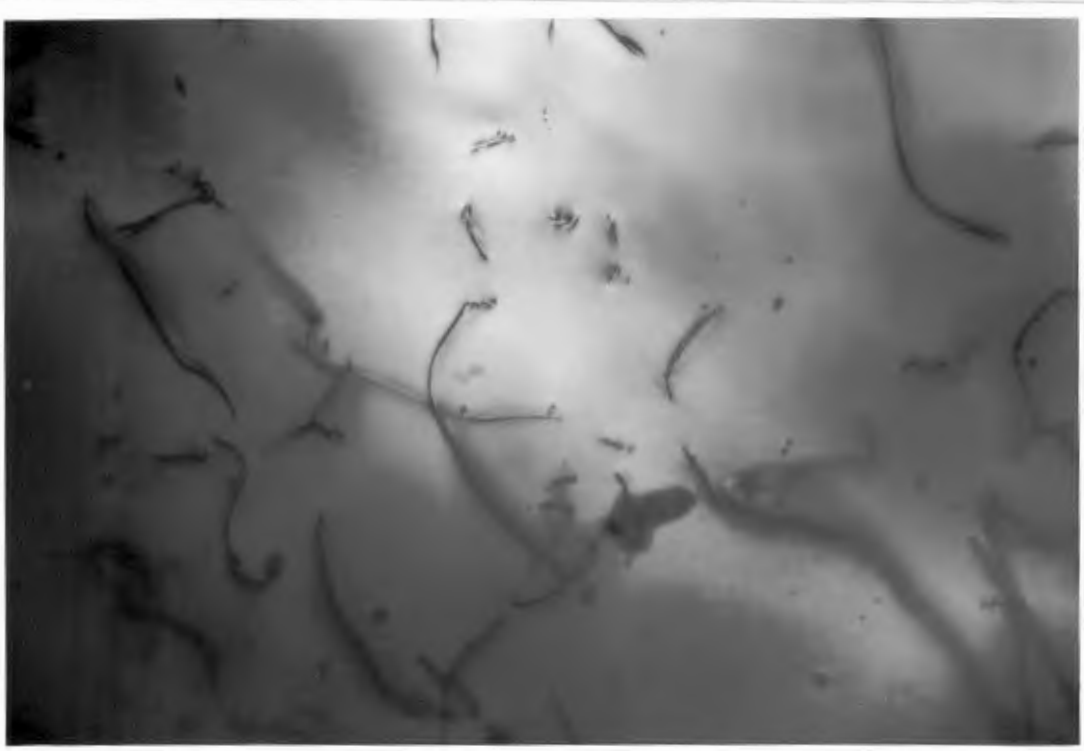

Plate 10 Electron micrograph showing dislocations, pinning one another.

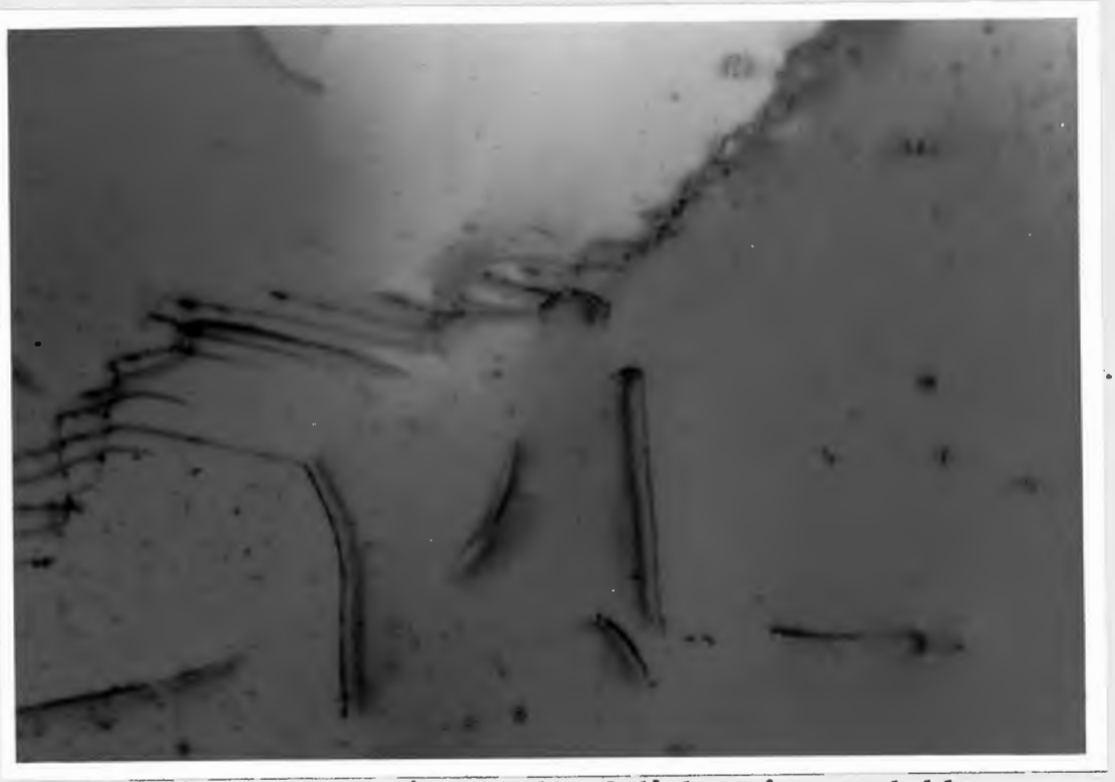

Plate 11 Electron micrograph showing a wall of dislocations probably representing a subgrain boundary. Small spots are the result of electron-beam damage.

Plate 12 Electron micrograph showing mats of dislocations in Sample 1775.